The University Of Sheffield.

Novel Transfer Printing Techniques for Semiconductor Device Fabrication

Henry Thomas Worthy

A thesis submitted in partial fulfilment of the requirements for the degree of Doctor of Philosophy

The University of Sheffield
Faculty of Engineering
Department of Electronic and Electrical Engineering

24th of April 2022

Acknowledgements

There are many people who deserve thanks for the support they have given me throughout my PhD. Unfortunately there is not the space to thank everyone, but please know that this would not have been possible without you. Firstly I would like to thank my supervisor, Dr Rick Smith, for giving me the opportunity to explore transfer printing and for the support and guidance he has provided throughout my PhD. I would also like to thank all of the members of our research group: Philippe Bantsi, Si Chen, Yilun Zhou, and Xuefei Yang for the many discussions that were had which were of great help. Additionally I would like to thank Stephen Atkins, Jon Wall, Jon Milner, and Paul Haines for their technical advice and support throughout my PhD.

Thank you to all my friends for the many discussion we have had, and advice you have given me without which I would not have achieved as much as I have. Also it would be remiss of me to fail to mention the many coffee meetings we have had which have been an excellent pick me up during this PhD.

And finally, a big thank you to my family and Emma, for always being there and supporting me. This would not have been achievable without the support and encouragement everyone has given to me.

Abstract

In this report, novel transfer printing techniques for semiconductor device fabrication have been presented. It has been found that Sylgard 182 and Sylgard 170 are potential alternatives for Sylgard 184, the most commonly used PDMS for transfer printing stamps. Sylgard 182 displays a similar adhesion to Sylgard 184 while Sylgard 170 however shows a lower maximum adhesive force of 0.553 mN compared to an identical stamp made from Sylgard 184 which achieved 1.107 mN. A third alternative PDMS was also tested, Silcoset 105, which displayed no adhesion to a Si(100) substrate.

A novel method of performing PDMS double casting has been developed using ultraviolet/ozone treatment of a PDMS sub-master mould. This method requires basic laboratory equipment and facilities and has been successful in achieving PDMS double casting of Sylgard 184, Sylgard 182, and Sylgard 170, showing good replication of structures after 4 castings for Sylgard 184 and Sylgard 182, and 2 castings for Sylgard 170.

Widening the operating window of a PDMS transfer printing stamp enables a greater range of semiconductor device and substrate combinations to be achievable. A novel method of heating the surface of a PDMS stamp in order to modify its adhesive properties has been developed, using embedded fluidic channels inside the PDMS stamp, through which heated water could be pumped. This resulted in a temperature increase of 19°C which reduced the adhesion of a PDMS stamp by 56% at 700 $\mu m.s^{-1}$.

Another novel method of expanding the operating window of a PDMS stamp has been demonstrated, using embedded carbon nanotubes to create an electrically conductive PDMS stamp which can be electrostatically charged to achieve an increased adhesive force of ~25 μN to a Si(100) substrate at 20V bias, compared to no bias.

Table of Contents

List of Tables

List of Figures

Declaration

I, the author, confirm that the Thesis is my own work. I am aware of the University's Guidance on the Use of Unfair Means (www.sheffield.ac.uk/ssid/unfair-means). This work has not been previously been presented for an award at this, or any other, university.

SEM images included in this thesis were taken by Philippe Bantsi. SU-8 2050 development and processing was performed by Si Chen.

Chapter 1

Introduction

1.1 Introduction and Motivation

This chapter will establish the context of this thesis as well as introduce the motivation behind the work conducted. The process of transfer printing will be discussed as well as recent developments and current limitations of transfer printing. This thesis will be focussed primarily on transfer printing, a process by which semiconductor materials and devices can be manipulated and transferred between substrates and methods of expanding the process window which enables a wider range of materials to be printed.

We have seen an increase in abnormal weather events such as the wildfires in the USA in 2020 and severe flooding in India in the same year. It is widely believed that these events are largely due to climate change primarily caused by increased greenhouse gas concentrations in our planet's atmosphere. Global atmospheric CO_2 levels have risen significantly in the past 50 years [1] as can be seen in Figure 1.1. This drastic change taking place to our planet's environment has been the motivation and driving force for a number of technological developments. Much of the electricity consumed in the UK in 2020 is non-renewable and produced large quantities of CO2 and other greenhouse gasses [2] contributing to climate change.

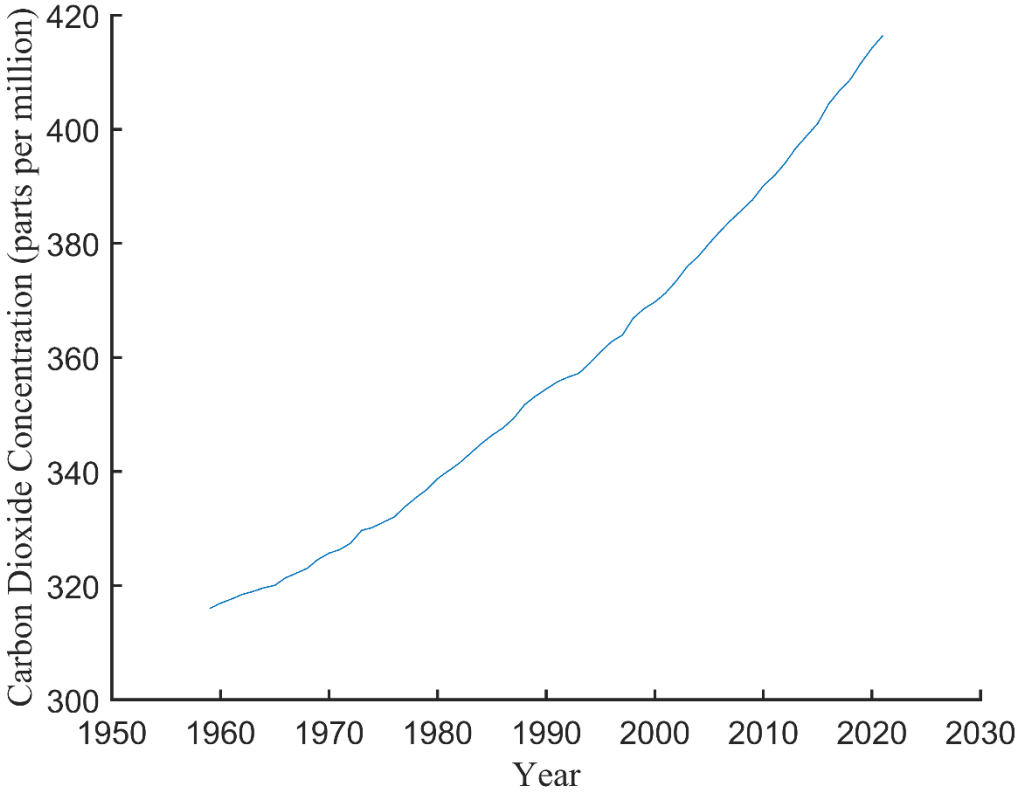

Figure 1.1: Graph of global atmospheric CO2 levels. Reproduced from [1].

By signing the Kyoto Protocol in 1997, which the UK signed in 1997, the UK pledged to reduce greenhouse gas emissions to 80% of the levels in 1990 by 2050 [3]. One way that can reduce energy consumption, thereby reducing greenhouse gas emissions is the replacement of traditional lighting methods with low energy consumption alternatives.

1.2 Semiconductors

The technological advances seen in recent years are testament to the developments made in the semiconductor field. Many aspects of modern life simply would not be possible without

semiconductors, from the smartphones that we all have in their pockets, to the solar cells that help to reduce our carbon footprints, to the MRI machines that help us if we fall ill. Few people on this planet go a day in their lives without making some use of semiconductors.

We have also seen a shift in methods of lighting as the effects of climate change have become more apparent. It is estimated that 15% of the global energy consumption is used for lighting [4]. Our energy consumption, especially of energy generated through non-renewable sources like fossil fuels contributes to greenhouse gas emissions. The replacement of traditional lighting methods with light emitting diode (LED) lighting has been appealing due to high efficiency [5] with LED lighting being around 10 times more efficient (lumen per watt) than traditional incandescent lighting.

There are a wide range of semiconductor materials, each with different characteristics and properties, which can be used to create a number of different devices and components. One of the key areas of development is integration of these devices into existing systems and processes to enable new technologies.

1.3 Flexible Electronics and Displays

One area that has been of particular interest recently has been applications and use of flexible electronics. The creation of flexible electronics is a complex feat, requiring multidisciplinary techniques from many fields such as chemistry, physics, electrical and electronic engineering, and material science. There is also specific research and knowledge needed for specific applications of these flexible devices. Once this has been overcome however, the opportunities for opening up new and novel areas of research are numerous.

There are many applications for flexible electronic devices across a range of fields, such as for use in biosensors [6] whereby a flexible substrate is used to mount electrical components to in order to create biocompatible sensors for applications like glucose monitoring through analysis of external bodily fluids [7] or for the analysis of urine through the use of woven organic electrochemical transistors on nylon fibres [8]. Another area that has increasingly shown promise lately has been flexible screens and displays such as those used by Samsung for their Galaxy Z Flip3/Fold3 smartphones which use organic LEDs which are mounted onto a flexible substrate in order to bridge the gap between the two rigid displays to create the foldable smartphone.

Often these flexible electronics use a flexible substrate, sometime materials like polyethylene terephthalate (PET) [9] or an elastomer like PDMS [10], upon which, circuitry is patterned [11] and electronic devices can be mounted. The material from which flexible substrates are made can be selected to meet the bespoke requirements of the application, whether that be transparency, how lightweight the substrate is, or biocompatibility, to name but a few. In the case of flexible displays, substrates like polyimide films [12] are often used

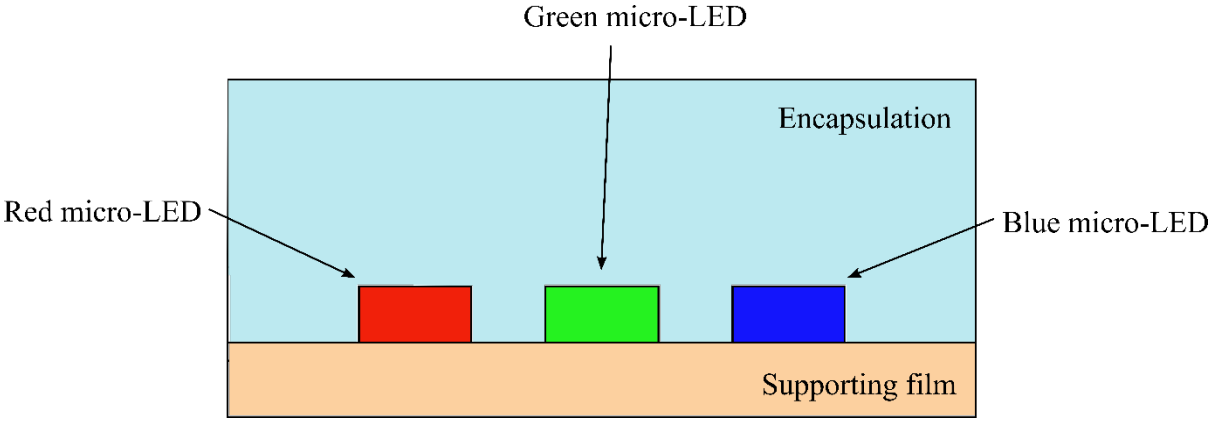

Figure 1.2: Diagram showing the encapsulation of 3 micro-LEDs, red, green, and blue, on a supporting flexible film. Reproduced from [15].

and organic LEDs (OLED) have been the most widely used due to the ability to produce high brightness and efficiency displays [13] and are compatible with flexible substrates and manufacturing technologies.

While flexible screens currently make use of OLEDs in order to produce a small scale displays (in fact, this is still the primary type of LED used to produce LED displays for smartphones), larger TV scale displays predominantly use inorganic LEDs in the form of backlights, using traditional packaged inorganic devices which are suitable for rigid and bulky displays. For Samsung's The Wall display however, micro-LEDs are used to create large, high resolution displays. This is a demonstration of an inorganic emissive pixel display which has the potentially a suitable for the creation of large scale flexible displays and require a form of transfer printing (a scalable pick and place process which will be discussed in section 1.5) to be produced. Micro-LEDs are comprised of a small array of red, green and blue inorganic LEDs, each of which is individually controlled, which make up one pixel of the display screen [14]. Combining these two technologies of flexible electronics, which have previously been used with OLEDs, with inorganic LED displays has been achieved [15] which can be seen in Figure 1.2, yet currently these kinds of displays are yet to be widely available in commercial applications.

One of the greatest obstacles to flexible inorganic LED displays is the need for flexible compatible semiconductor devices. OLED flexible displays have become commercially viable, despite the lower comparable performance of OLED displays [15], as typical inorganic materials are not directly compatible with flexible electronics, largely due to current methods of manufacturing.

1.4 Semiconductor Device Fabrication

Semiconductor devices have enabled many modern technologies which most people around the world rely on, such as computers. The term semiconductor device is a broad term, encompassing a host of different materials and structures, each of which provide a vital but different function. The growth and fabrication methods for these different materials vary wildly in the specifics of the processes, however these methods involve the use of rigid, inflexible wafers upon which further processing takes place, such as the deposition or growth of additional layers, or etching through layers through processes like reactive ion etching (RIE) [16].

These essential thick wafer substrates can be detrimental to the final applications of the devices grown on the surfaces. In some cases these substrates could be electrically insulating or may have poor thermal properties. Often this leads to methods of transferring the devices or materials from the substrate they are fabricated on, or grown on, onto a usable substrate being implemented. Methods of removing the material from the substrate can include processes such as laser induced transfer [17] or wafer bonding [18].

These methods limit the fabrication or growth processes that are available as these need to be compatible with these substrate removal processes. These methods of substrate removal can also be highly damaging, resulting in rough undersides of devices or damage the devices [19][20].

1.5 Transfer Printing

Instead of these other substrate removal processes, another method that has shown potential is transfer printing. There are many different types of transfer printing, wet transfer printing, where the transferred material is suspended on a liquid before bringing the target substrate into contact [21], or micro-transfer printing, where semiconductor materials are transferred onto a receiving substrate [22]. Micro-transfer printing, often just referred to as transfer printing, uses an adhesive stamp in a similar process to that of a rubber stamp and ink pad, where the ink in this case is semiconductor devices and materials which are still referred to as an 'ink'. The adhesive stamp is brought into contact with semiconductor material ink on a donor substrate in order to selectively pick up the ink. Once the stamp has been inked, it is brought into contact with a receiving substrate, and the ink is deposited. This process is shown in Figure 1.3.

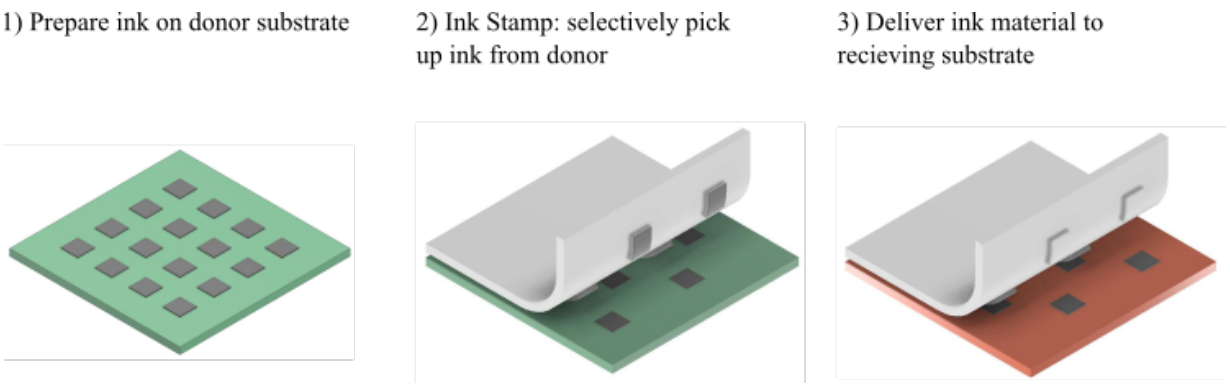

Figure 1.3: Schematic showing the transfer printing process using a PDMS stamp. 1) shows the donor substrate with an array of prepared ink material. In 2) the Stamp has been brought into contact and retracted at high speeds to selectively pick up ink material from the donor substrate. In 3) this inked stamp is then brought into contact with a receiving substrate and retracted slowly in order to leave the ink material behind on the receiving substrate.

For transfer printing using an adhesive stamp, poly(dimethylsiloxane) (PDMS) has becomes a widely used material. PDMS is a soft elastomer silicone which had already been established as an attractive material in other fields like microfluidics and MEMS. The greatest appeal of PDMS to these fields lies in the ability to create patterned PDMS structures through soft lithography, the process of casting soft polymers against a ridged structured mould.

Not only does PDMS have the capability to quickly and easily fabricate structured stamps, it had also been shown to have viscoelastic properties, where the adhesion between the stamp surface and the surface of a substrate is dependent on the retraction speed, with high retraction speeds leading to greater levels of adhesion, while low retraction speeds give a much lower adhesion [23]. This was greatly advantageous for transfer printing, as a successful printing process relies upon control over the adhesion of the stamp, with the pick-up of the ink material, known as the 'inking' process, requiring a high adhesion, and the printing of the ink requiring a low adhesion [24]. This can be seen in Figure 1.4.

The use of PDMS as a material for transfer printing stamps began with the Rogers Research Group, initially with the investigations identifying kinetic control of the adhesion of PDMS. Since then, transfer printing has evolved to use a structured PDMS stamp or integration into other systems, which can be designed to be bespoke to the particular ink layout or adhesive requirements. Examples can include an inflatable PDMS structure where the contact area between the stamp and ink could be modified in-situ by inflating the surface [25] and laser driven micro transfer printing [26].

A commercial transfer printing system has been developed by X-Celeprint, a spin-out company co-founded by Professor John Rogers, the founder of the Rogers Research group. This commercial system has shown to achieve a print yield of 99.96% of over 690,000 devices that were printed [27]. The high success rate of this commercial system has enabled transfer

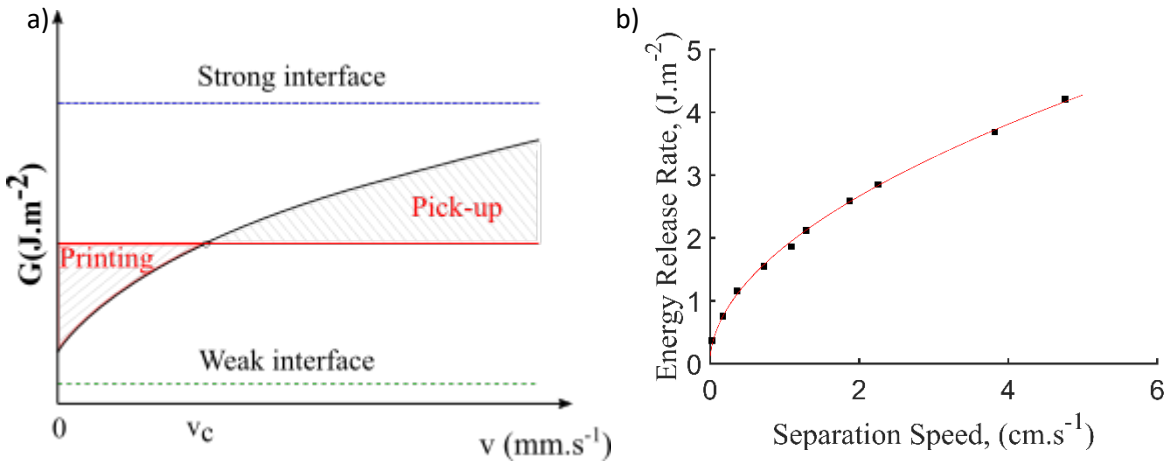

Figure 1.4: Diagrams illustrating the velocity dependant adhesion of PDMS. Part a) shows that below the critical velocity v_c a PDMS stamp is in a low adhesion state suitable for printing while above that critical velocity it is in a high adhesion state which is suitable for pick-up of material and devices. Reproduced from [24]. Part b) shows the velocity dependant adhesion displayed from the Rogers Research Group during the initial testing of the velocity dependant adhesion where a steel roller was rolled down an inclined PDMS slope. Reproduced from [23].

printing to become a more widely available and X Display, a spin-off company from X-Celeprint was established, with a focus on manufacturing transfer printed micro-led displays. X Display now have over 500 patents related to transfer printing.

The process of creating structured PDMS, a process called soft lithography, has been well documented [28][29][30]. PDMS is an attractive material in a range of fields for its biocompatibility [31], flexibility [10], optical transparency [32], and its ability to be rapidly cast into high resolution structures [33]. Soft lithography is the process by which an uncured PDMS silicone can be cast against a solid structured mould face and when released, maintains that structure.

1.6 Benefits of Transfer Printing

The use of transfer printing as a method of semiconductor device fabrication has enabled the use of a range of unusual substrates that previously were unavailable to be used as a receiving substrate. Through the use of PDMS, the ability of reducing the adhesion of the stamp to the ink when printing means that even low adhesion substrates can still be printed onto [34].This ability to print semiconductor devices onto a substrate without the need for adhesion promotion layers enables devices to be integrated into a wider range of new or existing applications.

By using a transfer printing process, the underlying substrate the devices are grown on which may not be thermally or electrically compatible with the application of the device, or which may be a limiting factor in creating thinner and smaller devices can be removed. By using a structured adhesive PDMS stamp, it is possible to selectively pick up semiconductor devices from a donor substrate and print onto a wide range of receiving substrates. This ability to print semiconductor devices onto many different surfaces opens avenues to integrate devices and materials into heterogeneous devices by growing components of the final device separately and once all processing has taken place, assembling the components [35].

What really makes transfer printing stand out as an attractive process however, is the scalability of the entire transfer printing process. The limiting factor for the scalability of transfer printing is predominantly based on the wafer size of the donor substrate. Every aspect of transfer printing is a parallel process, a printing process for a single device can be simultaneously performed for hundreds if not thousands of devices [23].

1.7 Limitations of Transfer Printing

While transfer printing has been shown to be a useful technique for the selective manipulation and transfer of semiconductor devices and materials, there are still areas that have not seen as much development. One of the mechanisms that underpins most transfer printing processes is that of switchable adhesion, the process by which an adhesive stamp can be placed into a high adhesion state to pick up devices and materials, and a low adhesion state when it comes to printing the picked up devices.

There is still a greater need for a greater range of switchable adhesion for a PDMS transfer printing stamp, where a stamp with a very high adhesion state can be used to pick up devices and materials that are well adhered to the donor substrate, yet can also be switched to a very low adhesion state in order to print the devices onto a substrate to which the printed devices may have poor adhesion to, maybe due to a rough interface caused by an undercutting process.

The ability to switch a PDMS stamp from a high adhesion state to a low adhesion state is often achieved through exploitation of the viscoelastic nature of PDMS, where low retraction speeds result in lower adhesion and high retraction speeds result in higher adhesion. This is not the only method of switching a PDMS stamp from a low adhesion to a high adhesion state, other methods have been demonstrated [36].

By developing transfer printing processes that utilised both the viscoelastic nature of PDMS as well as other methods of switching between high and low adhesion states, a PDMS stamp could achieve higher levels of adhesion, as well as achieving much lower adhesion levels, without significant modification being necessary to the transfer printing process. By developing this, novel devices and applications may become achievable.

1.8 Conclusion

This chapter introduced the broader field of transfer printing as well as establishing where transfer printing as a process fits and the some of the challenges that this technique faces. This thesis will go into further details about the transfer printing process, the mechanisms that drive it and the developments that have already been made.

An investigation into alternative PDMS silicones will be detailed to determine what characteristics they have, and whether they are suitable as a material to create transfer printing stamps.

A novel casting method will then be detailed, allowing for the double casting of PDMS stamps through the use of ultraviolet ozone treatment of a PDMS mould. This will include an investigation into the impact this double casting method has on the adhesive properties of a PDMS transfer printing stamp cast from a treated PDMS mould.

A method of expanding the operating window of a PDMS stamp in-situ is given. This is achieved through a novel process that exploits both the viscoelastic nature of PDMS and the temperature dependency of the adhesive properties through the use of thermally controlled embedded water channels to achieve lower level of adhesion than would otherwise be achievable with an identical.

Finally, a method of using a PDMS stamp, made conductive through the use of embedded carbon nanotubes, to electrostatically charge the stamp surface, increasing the adhesion to a substrate will be included.

1.9 References

[1] R. Keeling and P. Tans, “Mauna Loa CO2 records.” [Online]. Available: https://gml.noaa.gov/ccgg/trends/data.html.

[2] “UK Energy Brief in 2021,” *Dep. Business, Energy Ind. Strateg.*, 2021.

[3] Office of National Statisitics, “Net zero and the different official measures of the UK’s greenhouse gas emissions,” 2019. [Online]. Available: https://www.ons.gov.uk/economy/environmentalaccounts/articles/netzeroandthedifferentofficialmeasuresoftheuksgreenhousegasemissions/2019-07-24#:~:text=Estimates on this basis were,the Climate Change Act 2008.

[4] A. Kimble, C. Gallinat, H. Alarcon, and P. Bennich, “Global Lighting Challenge : Changing the world through public-private partnerships,” *eceee Summer Study Proc.*, pp. 1671–1675, 2017.

[5] P. Morgan Pattison, M. Hansen, and J. Y. Tsao, “LED lighting efficacy: Status and directions,” *Comptes Rendus Phys.*, vol. 19, no. 3, pp. 134–145, 2018.

[6] A. Yang and F. Yan, “Flexible electrochemical biosensors for health monitoring,” *ACS Appl. Electron. Mater.*, vol. 3, no. 1, pp. 53–67, 2021.

[7] Q. Liu *et al.*, “Highly Sensitive and Wearable In2O3 Nanoribbon Transistor Biosensors with Integrated On-Chip Gate for Glucose Monitoring in Body Fluids,” *ACS Nano*, vol. 12, no. 2, pp. 1170–1178, 2018.

[8] A. Yang *et al.*, “Fabric Organic Electrochemical Transistors for Biosensors,” *Adv. Mater.*, vol. 30, no. 23, pp. 1–8, 2018.

[9] S. De Mulatier, M. Ramuz, D. Coulon, S. Blayac, and R. Delattre, "Mechanical characterization of soft substrates for wearable and washable electronic systems," *APL Mater.*, vol. 7, no. 3, 2019.

[10] W. Y. Wu, X. Zhong, W. Wang, Q. Miao, and J. J. Zhu, "Flexible PDMS-based three-electrode sensor," *Electrochem. commun.*, vol. 12, no. 11, pp. 1600–1604, 2010.

[11] J. Van Den Brand *et al.*, "Flexible and stretchable electronics for wearable health devices," *Solid. State. Electron.*, vol. 113, pp. 116–120, 2015.

[12] L. Chen *et al.*, "Highly Transparent and Colorless Nanocellulose/Polyimide Substrates with Enhanced Thermal and Mechanical Properties for Flexible OLED Displays," *Adv. Mater. Interfaces*, vol. 7, no. 20, pp. 1–11, 2020.

[13] A. Sugimoto, H. Ochi, S. Fujimura, A. Yoshida, T. Miyadera, and M. Tsuchida, "Flexible OLED displays using plastic substrates," *IEEE J. Sel. Top. Quantum Electron.*, vol. 10, no. 1, pp. 107–114, 2004.

[14] C. A. Bower *et al.*, "High-brightness displays made with micro-transfer printed flip-chip microLEDs," *Proc. - Electron. Components Technol. Conf.*, vol. 2020-June, pp. 175–181, 2020.

[15] S. L. Lee, C. C. Cheng, C. J. Liu, C. N. Yeh, and Y. C. Lin, "9.4-inch 228-ppi flexible micro-LED display," *J. Soc. Inf. Disp.*, vol. 29, no. 5, pp. 360–369, 2021.

[16] M. E. A. Samsudin *et al.*, "Limiting factors of GaN-on-GaN LED," *Semicond. Sci. Technol.*, vol. 36, no. 9, 2021.

[17] P. Serra and A. Piqué, "Laser-Induced Forward Transfer: Fundamentals and Applications," *Adv. Mater. Technol.*, vol. 4, no. 1, pp. 1–33, 2019.

[18] H. Moriceau *et al.*, "Overview of recent direct wafer bonding advances and applications," *Adv. Nat. Sci. Nanosci. Nanotechnol.*, vol. 1, no. 4, 2010.

[19] D. Banks, K. Kaur, C. Grivas, and R. Fardel, "Femtosecond laser induced forward transfer for the deposition of nanoscale transparent and solid-phase materials," *Proc. LAMP*, pp. 1–9, 2009.

[20] A. Kawan and S. J. Yu, "Laser Lift-Off of the Sapphire Substrate for Fabricating Through-AlN-Via Wafer Bonded Absorption Layer Removed Thin Film Ultraviolet Flip Chip LED," *Trans. Electr. Electron. Mater.*, vol. 22, no. 2, pp. 128–132, 2021.

[21] S. Xiong *et al.*, "Water Transfer Printing of Multilayered Near-Infrared Organic Photodetectors," *Adv. Opt. Mater.*, vol. 10, no. 1, pp. 1–7, 2022.

[22] N. Ahmed, A. Carlson, J. A. Rogers, and P. M. Ferreira, "Automated micro-transfer printing with cantilevered stamps," *J. Manuf. Process.*, vol. 14, no. 2, pp. 90–97, 2012.

[23] M. A. Meitl *et al.*, "Transfer printing by kinetic control of adhesion to an elastomeric stamp," *Nat. Mater.*, vol. 5, no. 1, pp. 33–38, 2006.

[24] X. Feng, M. A. Meitl, A. M. Bowen, Y. Huang, R. G. Nuzzo, and J. A. Rogers, "Competing fracture in kinetically controlled transfer printing," *Langmuir*, vol. 23, no. 25, pp. 12555–12560, 2007.

[25] A. Carlson, S. Wang, P. Elvikis, P. M. Ferreira, Y. Huang, and J. A. Rogers, "Active, programmable elastomeric surfaces with tunable adhesion for deterministic assembly by transfer printing," *Adv. Funct. Mater.*, vol. 22, no. 21, pp. 4476–4484, 2012.

[26] R. Saeidpourazar *et al.*, "Laser-driven micro transfer placement of prefabricated microstructures," *J. Microelectromechanical Syst.*, vol. 21, no. 5, pp. 1049–1058,

2012.

[27] X-Celeprint, “Micro-Transfer Printing with x-Chips.”

[28] D. J. Gargas, O. Muresan, D. J. Sirbuly, and S. K. Buratto, “Micropatterned porous-silicon bragg mirrors by dry-removal soft lithography,” *Adv. Mater.*, vol. 18, no. 23, pp. 3164–3168, 2006.

[29] Y. Y. Huang *et al.*, “Stamp collapse in soft lithography,” *Langmuir*, vol. 21, no. 17, pp. 8058–8068, 2005.

[30] T. W. Odom, J. C. Love, D. B. Wolfe, K. E. Paul, and G. M. Whitesides, “Improved Pattern Transfer in Soft Lithography Using Composite Stamps,” *Langmuir*, no. 9, pp. 5314–5320, 2002.

[31] M. Ionescu *et al.*, “Enhanced biocompatibility of PDMS (polydimethylsiloxane) polymer films by ion irradiation,” *Nucl. Instruments Methods Phys. Res. Sect. B Beam Interact. with Mater. Atoms*, vol. 273, pp. 161–163, 2012.

[32] A. Shakeri, S. Khan, and T. F. Didar, “Conventional and emerging strategies for the fabrication and functionalization of PDMS-based microfluidic devices,” *Lab Chip*, vol. 21, no. 16, pp. 3053–3075, 2021.

[33] J. A. Rogers and R. G. Nuzzo, “Recent progress in soft lithography,” *Mater. Today*, vol. 8, no. 2, pp. 50–56, 2005.

[34] J. Justice, C. Bower, M. Meitl, M. B. Mooney, M. A. Gubbins, and B. Corbett, “Wafer-scale integration of group III-V lasers on silicon using transfer printing of epitaxial layers,” *Nat. Photonics*, vol. 6, no. 9, pp. 610–614, 2012.

[35] J. Yoon, S. M. Lee, D. Kang, M. A. Meitl, C. A. Bower, and J. A. Rogers,

"Heterogeneously Integrated Optoelectronic Devices Enabled by Micro-Transfer Printing," *Adv. Opt. Mater.*, vol. 3, no. 10, pp. 1313–1335, 2015.

[36] R. Li *et al.*, "Axisymmetric thermo-mechanical analysis of laser-driven non-contact transfer printing," *Int. J. Fract.*, vol. 176, no. 2, pp. 189–194, 2012.

Chapter 2

Transfer Printing Processes and Applications

This chapter will introduce the technique of transfer printing and will discuss the different types of transfer printing, additive transfer, subtractive transfer, and deterministic assembly. A look into key considerations when performing these different transfer printing types will also be included along with a discussion about the required additional stages necessary when selecting and preparing a particular target material for transfer printing.

Poly(dimethylsiloxane) (PDMS) will be introduced as an attractive material from which to create transfer printing stamps and the stages of development made in order to achieve successful kinetic control over the adhesion of a PDMS stamp.

Finally, major developments to the transfer printing technique will be looked at, including using transfer printing alongside other processing techniques, and modifications to the transfer printing stamp structure in order to widen the process window available, potentially enabling the pick-up and printing of a wider range of new materials.

2.1 Transfer Printing: An Overview

In recent years, methods of assembly for solid material structures based on a transfer printing process have seen a rise in popularity in a wide range of applications most prominently within the semiconductor field. The ability to heterogeneously integrate semiconductor materials and devices such as the integration of InP lasers into SOI (silicon on insulator) substrates with polymer waveguides [1], and the capability to be scaled up to enable integration of entire circuits of crystalline silicon chiplets with OLED (organic light emitting diode) displays [2] shows the diversity in applications that transfer printing has. The increase in popularity of transfer printing as a semiconductor fabrication process has been largely due to its ability to manipulate materials and transfer them easily between two substrates, which might have been impossible using older, more established techniques, and the scalability of the entire transfer printing process, allowing for parallel processing from individual devices, to full wafer scale transfer of thousands of individual devices in a single pick-up and print cycle [3]. X-Celeprint, suppliers of commercial transfer printing systems, which achieve a mean print yield of 99.96% across over 690,000 printed devices [4].

The transfer printing process is a micro and nano scale fabrication method appropriate for a wide range of materials that utilises an adhesive stamp to pick up, deposit, or otherwise manipulate the desired materials, or "ink", using a collection of parallel processes and procedures. One of the key benefits of transfer printing is that the inks involved can be fabricated using existing processes and techniques as the transfer printing process can takes place after the fabrication process has been completed.

The use of transfer printing can be valuable due to its ability to heterogeneously integrate materials and devices that might otherwise not be achievable by conventional methods. By using transfer printing to heterogeneously integrate materials, it allows for mature

and well developed processes to be used in conjunction with other techniques and materials. Unlike during homogenous integration, by using transfer printing to heterogeneously integrate materials and devices, well established techniques can be used without compromise as each technique can be used independently of other necessary techniques. An example of this would be the heterogeneous integration of GaN HEMTs onto CMOS circuits while being separately processed in dedicated conditions and environments in order to minimise restrictions or potential damage to either component [5].

Usually, in order to fabricate devices or materials, a homogeneous monolithic fabrication process is used, whereby layers of a composite device are fabricated, or grown, on top of a previous layer [6]. By using transfer printing to facilitate the ability to process components of a heterogeneous device separately before assembling, more possibilities are opened up. This is due to some of the processing methods and techniques necessary for the fabrication stages may be incompatible with certain other materials, which could lead to flaws or damage being caused, or in some cases, the destruction of previously deposited material layers. Transfer printing allows for each component to be fabricated entirely separately, ensuring there is no damage occurring to other components as only once all potentially damaging processing has taken placed, are the components assembled [7].

The ability to accurately, and precisely, manipulate a wide range of materials, which transfer printing excels at, can be crucial for integrating multiple shapes and structures of a material, however, pick and place technologies did not start with transfer printing. Microgrippers have been used previously, and often still are, used to manipulate individual devices [8]. These micro-grippers can be manufactured and designed in a variety of methods depending on the application. Some designs use a small probe like device with a small hole in the tip that can be used to suck a material to the tip using a vacuum. One of the major drawbacks

to a method like this is that it can be difficult to manipulate multiple inks at once and is often done in series.

Other methods of manipulating and transferring materials existed too, such as laser induced transfer, where a pulsed laser beam is used to vaporise or decompose a backing layer beneath the target material, projecting the target material on an awaiting receiver substrate [9], and wafer bonding, a process whereby two polished semiconductor wafers of any materials bond using van der Waals forces [10] or sometimes with the aid of adhesives [11].

Not only can transfer printing help to achieve device structures and material combinations that might otherwise be impossible to create, but it also has the potential to be used in an industrial scope by allowing for devices grown in a high-density array to be distributed onto a receiving substrate in a much lower density without having to individually manipulate each device into position such as processes with use micro-grippers.

There are some applications that are only achievable through the use of transfer printing processes, such as flexible displays and electronics. Flexible displays have been a highly focused on area due to the inherent challenge in integrating inorganic semiconductor devices and other inflexible materials with soft, flexible substrates, commonly made from organic polymer films. There have been demonstrations of transfer printing enabling the creation of devices printed onto a flexible substrates by using overlapping tokens, reminiscent of designs found in nature, such as fish or snake scales [12]. Further examples of successful printing of materials onto flexible substrates include GaAs solar cells on a PET substrate [13] and transfer printed electrical connections onto a Polyethylene Naphthalate (PEN) substrate topped with a spin coated epoxy layer [14].

2.2 Fundamentals of Transfer Printing

The term transfer printing covers a range of different techniques used for the manipulation of materials. This section will look at some different transfer printing processes and suitable materials that can be processed with these methods. Also discussed will a look at how control of adhesion plays a crucial role in transfer printing and why PDMS has become a popular material to create stamps for transfer printing.

2.2.1 Transfer Printing Types

Fundamentally transfer printing involves the movement of a material from one substrate to another. This can be achieved in different ways however any transfer printing process often comprises of two essential components, the material being transferred, referred to as an “ink”, and some form of adhesive component, dubbed a “stamp”. In all cases of transfer printing, a moulded adhesive stamp, or a stamp with a surface that has been made adhesive by chemical treatments is used to manipulate material.

Although there are multiple ways of performing transfer printing, these all rely on these two components, each having their own challenges and properties that must be considered when being used. Most techniques fall within three categories of transfer printings: additive transfer, subtractive transfer, and deterministic assembly [15], each of which is visually shown below in Figure 2.1.

Additive transfer uses a structured stamp upon which an ink has been deposited across the entire surface using methods such as spin coating [16] that is then brought into contact with a receiving substrate. After a retraction process, the ink that was on the raised features of the stamp is left behind on the receiving substrate[17] [18].

Subtractive transfer uses a donor substrate which has the ink already deposited or grown on the surface in an unstructured, continuous layer. A structured stamp is brought into contact to selectively retrieve ink and remove this ink from the donor substrate. The ink is then used either on the structured stamp or the now structured donor substrate[19][20].

Deterministic assembly on the other hand is a transfer printing process where both the ink and the stamp are structured. The structured stamp is then aligned to the selected ink and brought into contact. Once the structured stamp is retracted from the surface of the donor substrate, the selected ink is removed along with the stamp. The structured, and now inked, stamp, is repositioned over the receiving substrate. Then by making contact between the underside of the ink and the receiving substrate, the ink is transferred onto the new substrate.

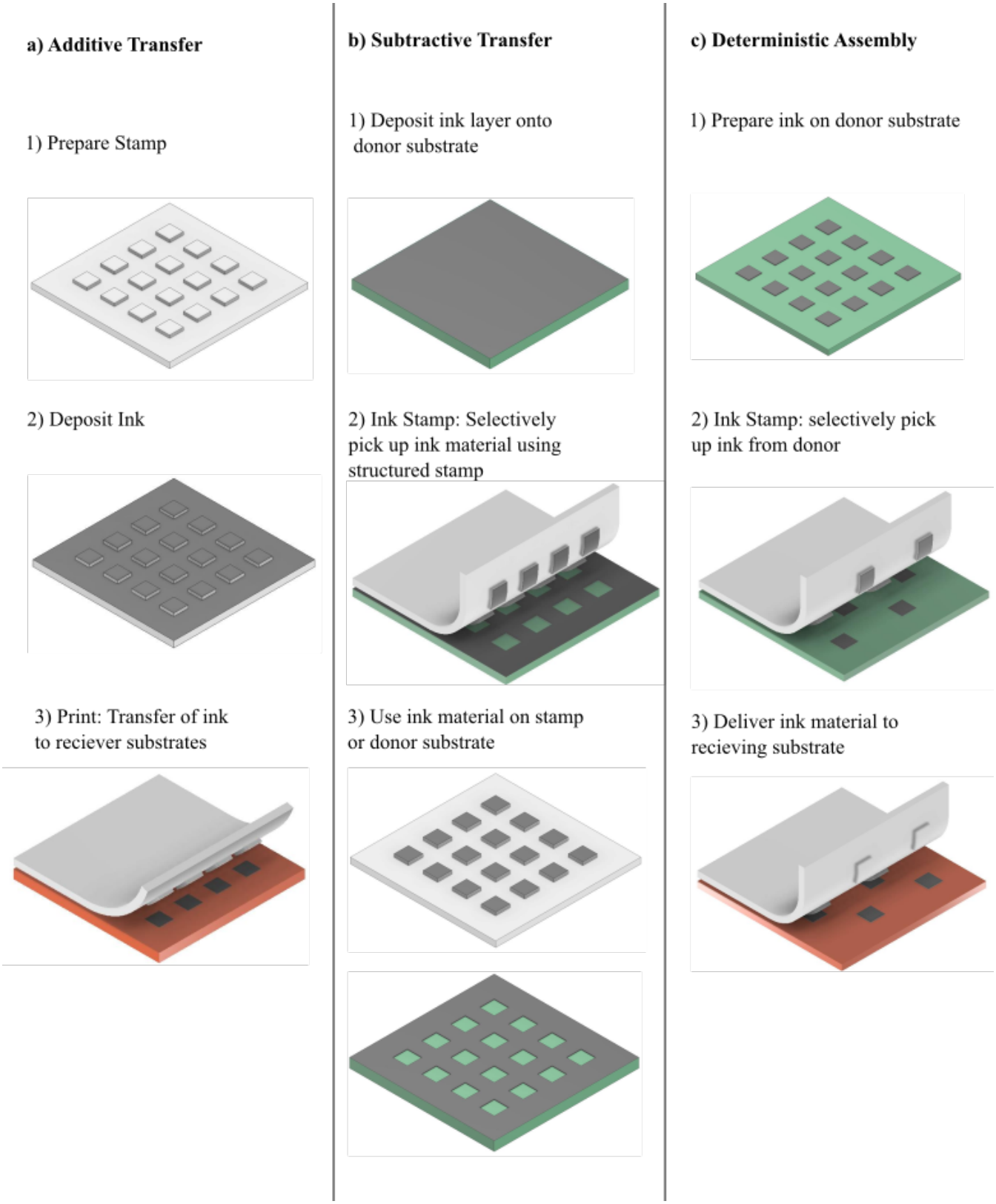

Figure 2.1: Visual representation of the different forms of transfer printing a) additive transfer, b) subtractive transfer, and c) deterministic assembly. Adapted from [15].

2.2.1.1 Comparison of Transfer Printing Methods

One of the fundamental differences between the first two categories of transfer printing, additive and subtractive, and the third, deterministic, is that during additive or subtractive transfer printing, the stamp is the method of structuring the ink which is being transferred. This mean that it has the potential to be a more simplified process than using deterministic assemble, which involves a greater number of components and fabrication stages.

In additive transfer printing, because the ink is deposited directly onto the stamp, a receiving substrate can be selected which has specific properties that might otherwise not be suitable for deposition, or further processing. A structured stamp is often quick and easy to fabricate, providing a disposable substrate upon which to deposit material. In many cases, the deposited material onto a structured stamp through processes such as evaporation deposition can provide a quick way to achieve structured thin films of material. To aid the successful transfer of the ink from the stamp to the receiving substrate, the addition of an adhesion promoter can be added to the receiving substrate, as is displayed by Felmet et al [21] who used 1,8-Octanedithiol onto the surface of a freshly etched GaAs substrate in order to promote adhesion between the Cu surface of a Cu coated PDMS (poly(dimethylsiloxane)) structured stamp. Alternatively, reducing the adhesion between the structured stamp and the ink can be achieved to enable more successful printing of the ink. One example [22] uses oxidisation to create a PDMS stamp surface that is less hydrophobic which enabled better whetting of the ink (a solution of ligands in ethanol) onto the surface but also forms a silica-like crust on the treated surface [23] which would have the effect of reducing the adhesion of the PDMS stamp to the ink.

Subtractive transfer printing however uses a flat layer on a donor substrate which when a structured adhesive stamp is brought into contact and retracted, removes sections of the ink,

leaving behind the remainder of the ink. This method could be used for different purposes, either to structure material on a substrate by removing the surrounding material using a stamp as shown by Wang et al [24] whereby a stamp made from partially cured epoxy was lowered onto a flat small-molecule microcrystalline film which was then heated to bond the partially cured epoxy to the unwanted material before being removed or this method could be used to ink a stamp with desired material for later use such as in [25] where a PDMS stamp was used to selectively pick up porous silicon microstructures from a donor wafer. Once the stamp was inked, a polymer (poly[(vinyl butyral)- co -(vinyl alcohol)- co -(vinyl acetate)] (PVB)) was drop cast and cured on the surface. Once peeled from the stamp surface, the silicon structures were removed, ready for use in optical devices [26].

Unlike the previous two transfer printing methods, deterministic assembly uses a structured stamp to selectively pick up prepatterned material from a donor substrate, then deposit that material onto a receiving substrate. This method relies either on a stamp with controllable adhesion, or the donor or receiving substrates adhesion must be modified to allow for printing of the material to occur. By undercutting the ink by removing the underlying material either in its entirety, or in specific locations [27], the adhesion between the ink and the donor substrate is drastically reduced which allows for a less adhesive stamp to be used which can make printing the picked up ink easier. Deterministic assembly has the benefit of allowing for the ink to be fabricated on any substrate, and be printed onto any receiving substrate meaning that this transfer printing method requires the least change to the standard fabrication process that probably is highly developed and well established.

2.2.1.2 Adhesion and Adhesive Stamps

Each of these different transfer printing methods rely on control of the adhesion, either on a single surface or multiple surfaces to facilitate successful transfer of material. During the transfer printing process it becomes necessary to control where the ink is transferred too, in the case of additive manufacturing, the adhesive quality of the stamp surface is less important, and instead, the adhesive properties of the receiving substrate become more critical. The force of adhesion of the receiving substrate to the ink face needs to be greater than that of the stamp to ink interface. Sometimes this could be as simple as using an inherently adhesive substrate such as a PMMA substrate or by using an adhesive layer of an epoxy on top of a less adhesive substrate as shown in [14].

Control over both of the aforementioned interfaces (substrate/ink interface and ink/stamp interface) is crucial for all different processes of transfer printing, however with subtractive printing, this is slightly more complicated than in additive transfer as the force of adhesion between the ink layer deposited onto the donor substrate must be strong enough so that when the stamp is brought into contact and retracted, the materials breaks at the desired places and is not just lifted off in one sheet. Because of this, the stamp must be even more adhesive than in additive transfer.

Deterministic assembly requires the most control over all the interfaces present as it uses both a pickup stage, like in subtractive transfer, and then a printing process, like during additive transfer. It is common for stamps used for deterministic assembly to have switchable adhesion, so that a single stamp can be changed from a state of high adhesion to low adhesion depending on what is needed.

2.2.1.3 Energy Release Rates

Each of the three methods of transfer printing rely on the control of adhesion and fracture mechanics at the various interfaces in the system, such as the ink/substrate interface, or the stamp/ink interface, to achieve successful printing. In additive and subtractive transfer printing the process is simpler due to a reduced number of stages involved in the transfer printing process. In these cases the ink is grown or made on the surface of the stamp, or in the case of subtractive transfer the stamp is the receiving substrate. During additive transfer, so long as the adhesion between the stamp and the ink is lower than that of the ink/substrate interface, a successful printing will take place. In comparison, when performing subtractive transfer, if the adhesion between the stamp and the ink is greater than the ink/substrate interface then the material will be successfully picked up. Controlling the adhesion in these cases can be achieved by selecting a stamp or substrate with the desired properties.

Deterministic assembly, however, is more complicated. This is because the stamp must be adhesive enough to selectively pick up the ink from the donor substrate but it must also be less adhesive than the receiving substrate in order to successfully print the ink. There are ways to create a stamp that would be suitable for both the inking and printing such as this process shown by Sim el al [28] who use a highly adhesive tape to achieve a successful inking of the stamp, then use an acetone treatment to modify the adhesion of the tape, and reducing the adhesion sufficiently so that a successful printing onto a silicon on insulator (SOI) substrate was achieved.

Despite the success of techniques such as this, one material that has been used widely in transfer printing, specifically in deterministic transfer, has been poly(dimethylsiloxane) (PDMS), a soft, transparent, and versatile silicone elastomer. PDMS silicone elastomers are most commonly associated with the term silicones, however this class of material can include

many other types of material composed of Si-O chains [29]. The reason for the appeal of this material is that PDMS displays kinetically controlled adhesive properties meaning that depending on the speed at which the stamp is retracted from the target substrate, the adhesive properties of the stamp can be increased or decreased. The cause of this velocity dependant adhesive property of PDMS lies in the viscoelastic nature of the stamp which impacts the van der Waals interactions between the stamp surface and the target substrate. This means that by just controlling the speed of the stamp, a stamp could be switched from a high adhesion state required for ink pickup, to a low adhesion state necessary for printing with no additional processing required, opening up potential routes for printing of different materials that may be incompatible with other process, such as using acetone to modify adhesion. Figure 2.2 displays the velocity dependant adhesion of PDMS. This shows an adhesion curve of PDMS at different retraction velocities. Below the red line the adhesion of a PDMS stamp is suitable for printing, where the adhesion of the stamp surface to the ink surface is lower than the adhesion between the ink and a receiving substrate. Above this line and the stamp is more suited to pick up, as

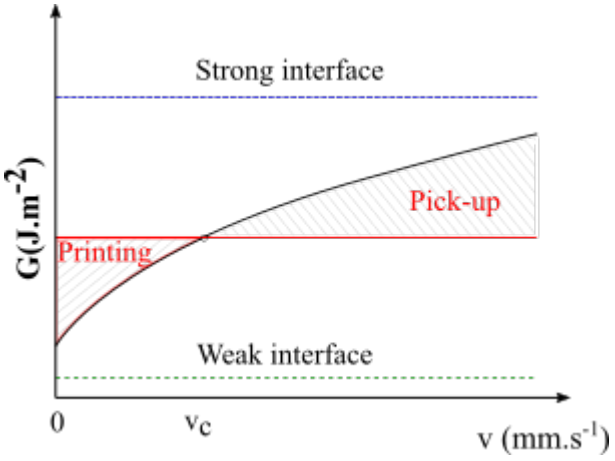

Figure 2.2: Diagram illustrating the velocity dependant energy release rate of a PDMS stamp. At the critical velocity, v_c, there is a switch between a printing condition (when the adhesion between the adhesion between the ink and substrate is higher than that of the ink and stamp) and a pick-up condition (when the adhesion between the ink and stamp is higher than that of the ink and substrate). Adapted from [37].

the reverse is true. The position of this line is dependent on a wide variety of factors, from the substrate being used (the surface of a piece of silicon wafer is much less adhesive than a soft polymer surface such as polymethyl-methacrylate (PMMA)) to the adhesive nature of the stamp (different PDMS silicones have different properties as well as PDMS silicones often can be mixed in different ratios to alter the physical properties of the final cured material).

2.2.2 Ink Fabrication for Transfer Printing

There are plenty of different materials that could be used as inks for transfer printing depending on the applications and needs of the user. For a demonstration of the far-reaching uses of transfer printing, a grain of pollen was even printed onto the surface of a silicon wafer [30].

For the purposes of this work, the main types of materials being considered as most relevant as transfer printing inks can be broken down into two main categories, organic and inorganic materials. Organic materials are materials such as polymers, whereas inorganic materials include materials such as gold and silicon. Both of these categories of materials come with their own set of challenges when looking for appropriate transfer printing methods and processes. Alongside these challenges come restrictions of what processing, fabrication, or deposition methods can be used to create these materials.

A common method for deposition of organic materials is spin coating, a process which involves placing droplets of a liquid material or a material suspended in a solution onto a flat substrate and then spinning at high speeds to give a uniformly thick layer over the entire surface. It has been shown many times that by creating thin uniform films of organic materials

using methods such as spin coating, transfer printing can be a simple and reliable way of patterning and transferring these materials between the substrate they are deposited on to a new substrate.

Due to the spin coating method often used to create these thin organic layers, one transfer printing method stands out as being the most suited to this process, this is subtractive transfer. Due to the nature of the subtractive transfer method, a flat uniform film is already desired, and the subsequent patterning comes from the use of a structured stamp. This stamp could be made from any material that can be made adhesive enough to remove sections of the organic film from the donor substrate.

However, spin coating is not the only method of depositing organic materials, Fukuda et al [31] show a method whereby an organic material is deposited onto a roller which then rotates, coming into contact with a structured glass surface and deposits the ink. This process is, in a manner, very similar to that of subtractive assembly, in that there is a single flat film that is structured by a stamp that is brought into contact.

Like with some organic materials, inorganic materials can sometimes be deposited onto substrates using spin coating as well such as the method shown in [32] where quantum dots are placed into a suspension which allowed them to be spin coated onto a treated silicon substrate then a flat PDMS stamp is used to pick up large sections of the quantum dots in a process similar to that of subtractive transfer. This process was then followed by a further printing process to pattern the quantum dot layer further in an additive transfer process.

Not all inorganic materials can be deposited in this way, some, such as metals, are commonly deposited using thermal evaporation deposition. In processes such as these, small quantities of the desired metals heated under vacuum to evaporate the metal and coat the inside of the vacuum chamber, as well as the desired surface. Processes like this are widely used in

the semiconductor field in order to fabricate devices. Normally, a semiconductor surface would be patterned with a thin photoresist layer prior to metal deposition which can be removed later, leaving metal only in the exposed areas. An alternative method of transfer printing has been demonstrated by transferring a patterned metal film onto a semiconductor surface [33] where an intermediary layer of Parylene C, a polymer with the capability to be deposited onto surfaces using chemical vapour deposition (CVD), was coated over a silicon wafer prior to the photoresist spin coating. This layer was essential to reduce the adhesion between the metal film and the silicon substrate. Once the desired metals, in this case aluminium, copper, gold, silver, and nickel were investigated, had been deposited and patterned appropriately, the metal surface was brought into contact with a treated polymer substrate and both substrates were heated for 3 minutes at 175°C and at 500psi before separating leading to a transfer of the metal pattern from the Parylene coated silicon to the polymer substrate.

In the case of semiconductor materials, there are many different processes that can be suitable for device fabrication and further integration, depending on the materials involved and the target application, however, in this section the most relevant process for transfer printing will be discussed. One such process is undercutting. In order to successfully pick up materials from the surface of the donor substrate, it must be possible to fabricate a stamp that is adhesive enough to overcome any adhesion between the ink and the donor substrate. For semiconductors that are epitaxially bonded to the donor substrate, it would be highly challenging to achieve a successful pick-up without additional processing. By removing large amounts of the supporting material underneath the ink using an undercutting process, it becomes easier to successfully pick up using an adhesive PDMS stamp [7]. An example of an undercut ink array can be seen in Figure 2.3, in which the tethers, the means by which to hold the undercut ink in place, can clearly be seen suspending undercut SiO_2/SiN stacks.

Picking up epitaxially bonded materials from the donor substrate is the key challenge that must be overcome for any transfer printing process, as the lower the adhesion of the ink to the donor substrate, the lower the adhesion required by the PDMS stamp needed to overcome this and achieve a successful pickup. By enabling a lower adhesion stamp to be used, the subsequent printing process becomes easier. The wide range of transfer printing inks and target materials, as well as the range of potential receiving substrates show that precise control over the operating window of the transfer printing process is essential. This control could range from exploiting the velocity dependant adhesion of a PDMS stamp, however there are a range of options available to expand that further.

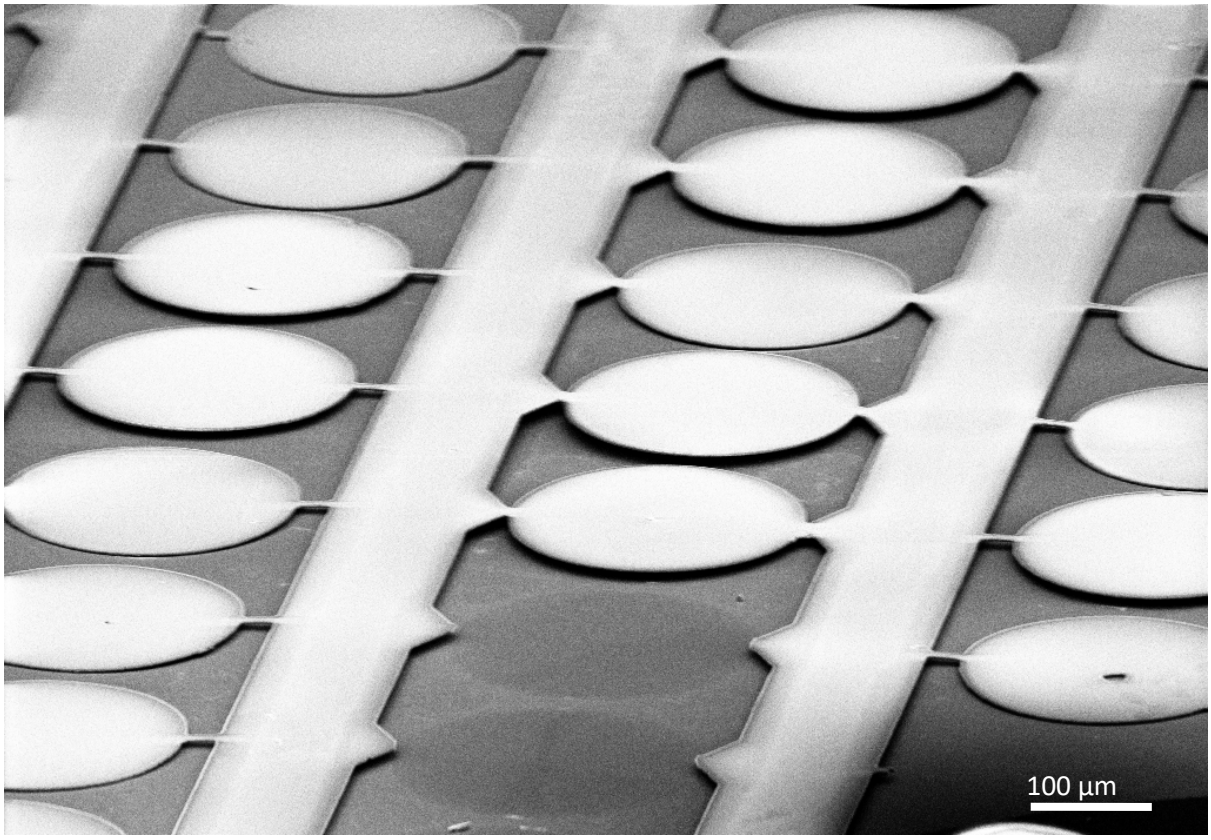

Figure 2.3: SEM image showing undercut SiO_2/SiN stacks held in place by tethers.

2.3 Transfer Printing Stamps

One of the most widely used materials for creating transfer printing stamps is the soft elastomer poly(dimethylsiloxane) (PDMS). The method of using a stamp made from this material has become such a dominant technology due to the ability to utilise the velocity dependant adhesive properties of PDMS in order to control the adhesion of the stamp simply by modifying the retraction speed. PDMS has become a very attractive as a material in many different fields for its biocompatibility [34] and the ability use soft lithographic techniques to rapidly create small, high-definition patterns by casting the uncured liquid polymer over a patterned mould [35].

When the viscoelastic properties of the PDMS were initially studied for a potential application as a method of performing transfer printing, a steel cylinder was rolled down an inclined surface coated with PDMS in a process in a manner similar to that described by Barquins [36] in 1992 when the rolling resistance of a PMMA coated roller was investigated. However, for a PDMS coated roller, the Rogers Research Group found that by increasing the

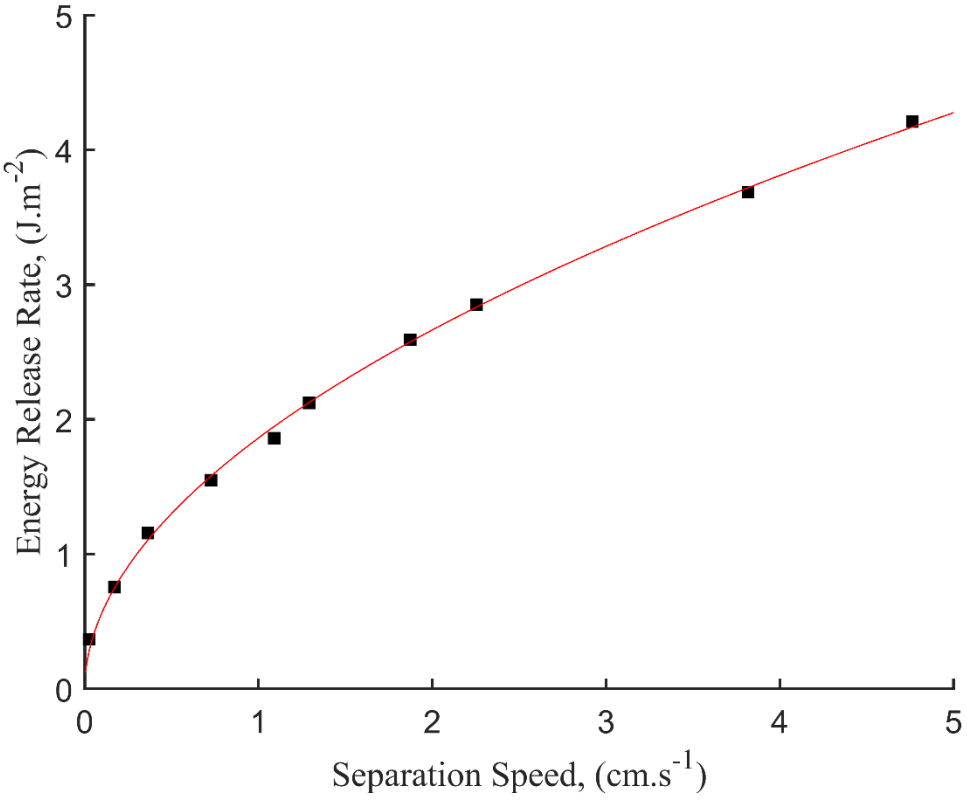

Figure 2.4: Energy release rate of a PDMS coated roller down an inclined plane at varied speeds. Recreated from data taken from [30].

angle of the inclined slope, the roller would move at an increased speed and the faster the roller moved down the inclined PDMS ramp, the greater the adhesion of the PDMS seemed to be [30]. Their results are recreated in Figure 2.4.

The first progression from a cylindrical roller was flat unstructured stamps that were capable of picking up large areas of material [37]. These stamps were fabricated using two flat polycarbonate plates separated by 1mm. PDMS was cast between them and once these sheets had cured, smaller stamps were cut, washed with IPA and dried, ready for use. Once clean, these were pressed against a glass slide surface coated a 100nm thick Au film (deposited using electron beam evaporation) and left in contact for 3 minutes. The glass slide and PDMS stamp

were then turned upside down and weights were attached to the PDMS stamp, allowing for a rudimentary control over the peeling speed.

The next stage of the development of PDMS stamps was to be able to selectively pick up material, either for particular assembly stages as part of a larger fabrication process, or to move specific materials from a high density array where they are created, to a low density application such as for use in LED displays where particular devices are used in conjunction with other materials and devices for example, using different LEDs that emit in different wavelengths in order to fabricate an RGB (Red Green Blue) light source [38]. Other LED applications include use of the commercial X-Celeprint transfer printing system (a spin-out company from the Rogers Research Group) in order to fabricate microLEDs, arrays of inorganic LED devices connected to electronic circuitry in order to control light emission from each LED independently [39]. Samsung have used micro-LEDs in order to create the product, The Wall, a modular display system that can be built in order to achieve an 8k resolution display [40].

This required the stamps that had previously been flat, to have features that could pick up individual coupons of ink, rather than large, unstructured areas like the Au films in the previous experiments. These features, often referred to as pedestals, were often square or rectangular patterns in the PDMS that corresponded to the size, shape, and positioning of the desired ink material. Each stamp would be designed to match a particular layout of ink. By using pedestals, the PDMS could come into contact with desired areas, while never touching the unwanted areas allowing for a greater control and selectivity of which material was picked up. By using a structured PDMS surface, it would also be possible to selectively pick up devices in an easily scalable manner, from the pickup of a single device, to a wafer scale pickup process providing a method of area multiplication, where devices can be transferred from their high

density ‘as grown’ state to a lower density, more dispersed state more suitable for application purposes which can be seen in Figure 2.5.

In order to create these patterned moulds, layers of photoresists (photosensitive polymers commonly used in the semiconductor industry as well as MEMS applications) could be spin coated onto the surface of a range of substrates, commonly silicon, then patterned by exposing certain areas to ultraviolet light which can then be removed by submerging the whole silicon and photoresist sample in a designated developer. Depending on the photoresist used, pedestals of different heights could be made. The liquid, uncured PDMS polymer could then be poured over the mould and, once cured, be peeled off, leaving a piece of PDMS with a small pedestal, or pedestal array, which could then be used for transfer printing. Patterning a PDMS surface in this manner has become a common method of mould creation which can provide feature sizes down to 100nm [41] which is dependant both on the photolithography accuracy as well as the processing method of the PDMS casting. However, these resolution limits are more a result of the limitations involved in creating the PDMS mould, not necessarily the PDMS itself. There have been reports of PDMS replication of patterns much smaller than 100nm, such as this report by Rogers et al [42] where replication of a 0.5-5 nm diameter single walled carbon nanotube pattern was presented. It was suggested that at these scale, the molecular structure of the PDMS as well as the crosslinking played a part in the success of the replication.

The commonly used photoresist for mould creation is SU-8, a negative photoresist that can be spun to achieve a much larger thicknesses than other resists can be and is known for its physical longevity which makes it suitable for a casting mould.

When referring to PDMS, the silicone in question is usually the product Sylgard 184. This particular silicone has been commonly used for most transfer printing applications due to

its versatility, robust nature, viscoelastic properties as well as the ability to cure either at elevated temperatures or at room temperature.

With the use of pedestalled stamps, it became possible to selectively pick up and place entire arrays of devices and materials at the same time as well as the ability to move ink from their high density growth layout to a less densely populated receiving substrate which is more appropriate for practical applications [43].

Another property of PDMS that was utilised to great effect, was that if PDMS is mixed in different ratios to those stated by the manufacturer (10:1 base to curing agent) the rigidity and adhesion can be modified. At 20:1, as there is much more base polymer to curing agent the stamp created is much more flexible and significantly more adhesive, while at a ratio of 5:1 the PDMS is more rigid and much less adhesive as the amount of curing agent to base is larger [44].

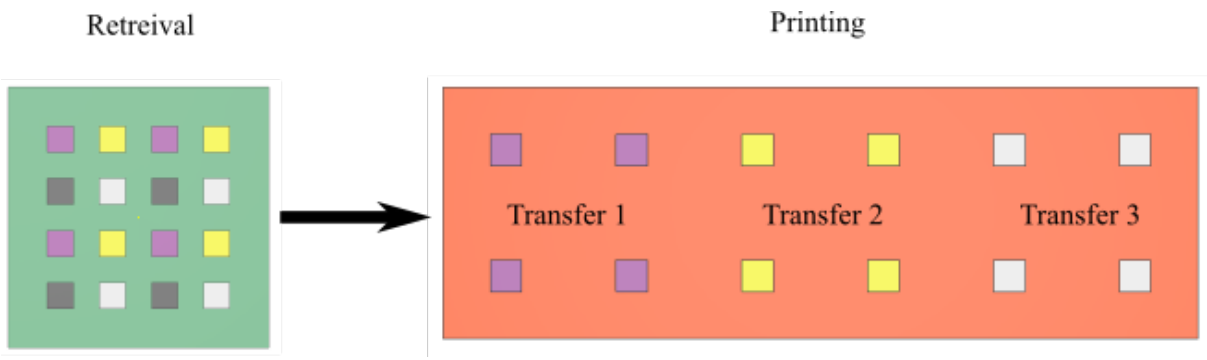

Figure 2.5: Visual representation of the transfer of ink from a high density 'as grown' state to a low density application state. Adapted from [43].

2.4 Developments in Transfer Printing

Transfer printing is not an isolated process, but most often used in conjunction with other techniques and processes, commonly as a way to facilitate fabrication methods that might have been challenging or impossible using other methods. Often this will be in order to pick and place materials and devices that could not be moved using more conventional methods. This has led to the original transfer printing process being modified, increasing the applicability of transfer printing to other applications or enhancing existing processes.

2.4.1.1 Thermally Dependant Adhesion of PDMS

One of the other properties of the Sylgard 184 PDMS is a temperature dependence of its adhesion curve, a well-known property for many viscoelastic processes [45][46], but described in a transfer printing context by the Rogers Research Group, by increasing the temperature of the stamp, a reduction in the adhesion becomes noticeable [37]. This is displayed in Figure 2.6.

By controlling the temperature of the stamp this allows the user to reduce the adhesion of a stamp without changing the retraction speed or with a different design of stamp. This would also increase the operating window at which a particular stamp can be used, potentially allowing for a wider range of materials to be used as inks. In order to modify the stamp temperature, stamps were heated in an oven and once the target temperature had been reached, the stamp was removed and adhesion testing was performed.

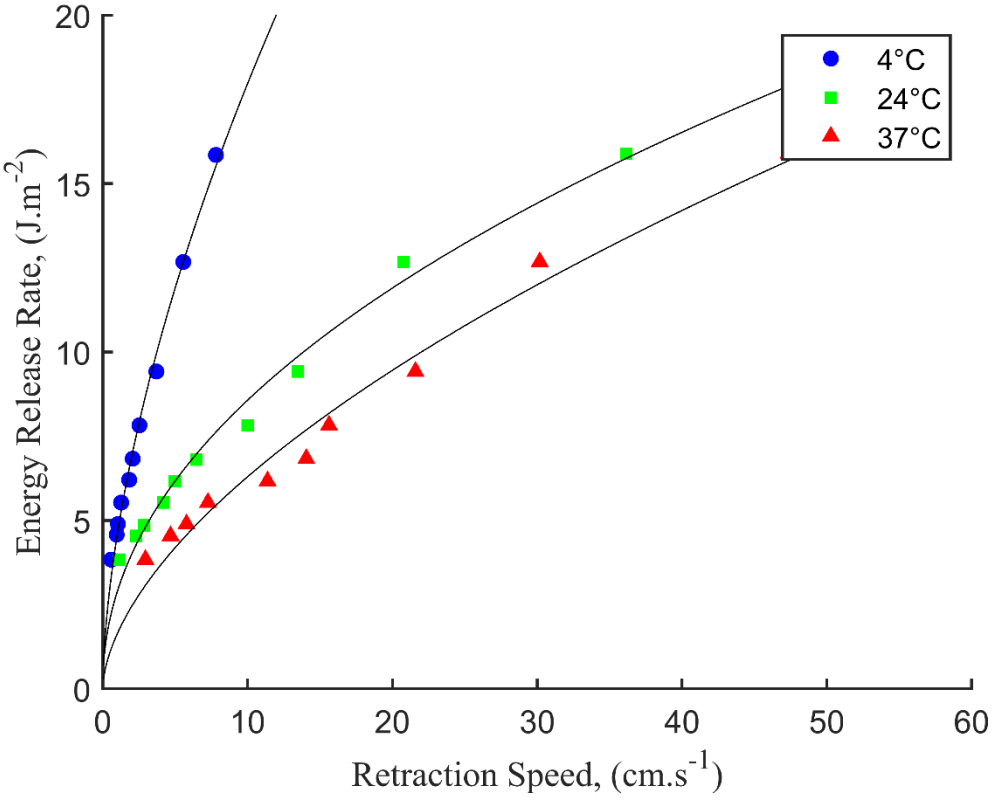

Figure 2.6: Energy release rate for a PDMS stamp at 4°C, 24°C, and 37°C, showing the temperature dependence of the adhesive properties of PDMS. Replotted using data from [37].

2.4.1.2 Laser Driven Transfer Printing

The Rogers Research Group then performed further experimentation exploiting this temperature dependent adhesive property of the Sylgard 184 [47] through the use of a pulsed near infrared laser diode (30W 805 nm) to heat the surface of the ink. This then led to a change in temperature at the stamp/ink interface which reduced the adhesion of the stamp and facilitating easy printing. The wavelength of the laser was chosen so that the stamp material was transparent, but the ink was highly absorbing, ensuring heating occurred at the ink surface.

The heating of the PDMS in the immediate vicinity of the ink uses both the temperature dependence of the adhesive nature of PDMS but also exploitation of the thermal expansion coefficient difference between PDMS and the ink. As the ink is under compression between the stamp and the receiving substrate, this change in thermal expansion coefficient causes a curvature of the ink material which stresses the interface promoting the propagation of a crack between the ink surface and the stamp that would occur during the printing stage of a transfer printing process. A schematic diagram of this process is shown in Figure 2.7.

The use of a laser to facilitate crack propagation leaves the stamp undamaged and it was suggested that this laser driven transfer printing could be the basis of a new pick and place assembly process without the necessary use of the velocity dependant adhesion often used. This report only describes the thermal expansion coefficient mismatch of the PDMS stamp and the ink as playing a part in the printing process, however the significant increase in temperature that takes place at the PDMS/ink interface (approximately an increase of 250°C), it is impossible that the temperature dependency of the adhesive properties of PDMS does not play any part in facilitating the printing of the ink.

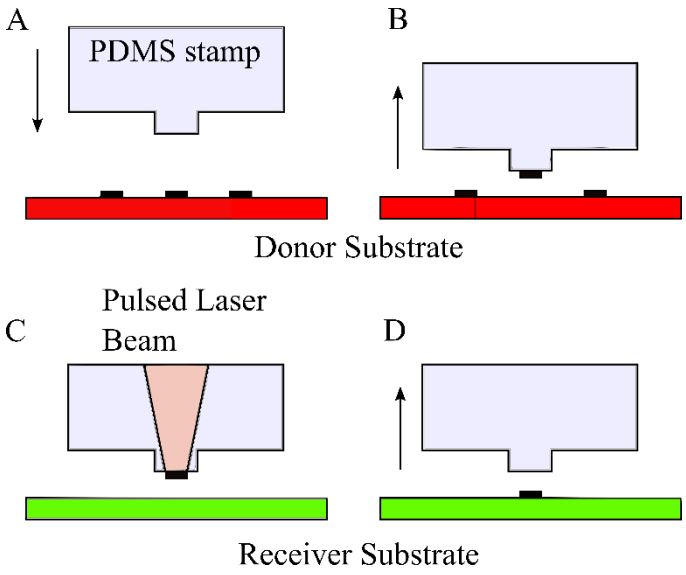

Figure 2.7: Stages of laser driven transfer printing A) PDMS stamp aligned with ink on the donor substrate and brought into contact. B) Stamp is retracted, picking up selected ink. C) PDMS stamp is aligned with receiver substrate and a pulse from the laser is used to heat the ink/stamp interface. D) Ink is transferred to the receiver substrate. Adapted from [47].

2.4.2 Structural Changes to Stamps

Stamp design is not limited to the creation of arrays of pedestals, it can also include additional methods to add control measures for switchable adhesion that is not limited only to retraction speed or temperature. By changing this structure of the stamp, the operating window can be modified allowing for higher adhesion, lower adhesion, or a combination of both. This can be useful for situations where a simple structured stamp cannot achieve the high level of adhesion required to pick up a desired ink while still having the ability to achieve a low enough adhesion to print said ink onto a receiving substrate.

2.4.2.1 Inflatable Pedestals

A simple way to modify the adhesion between a stamp and an ink is to either increase or decrease the contact area, depending on the desired outcome. Carlson et al [48] describe a method of creating a PDMS stamp with a hollow pedestal, upon which a thin flexible PDMS film over the top. By inflating, or deflating the stamp surface, the contact area between the ink and stamp is modified, allowing for a stamp surface to have a mode of high adhesion and low adhesion, with easy switchablity. This is shown in Figure 2.8.

This method allowed for the pedestal to be deflated during pickup, creating a flat surface which increased the contact area between the pedestal and the ink surface putting the stamp into a high adhesion state, where pickup of the ink is easier and requires a lower retraction speed in order to achieve a successful pickup.

When it comes to printing the picked up ink, the pedestal can be inflated, causing the flexible film covering to pedestal to become rounded, reducing the contact area between the pedestal and the ink surface, hence putting the stamp into a low adhesion state meaning that printing can be achieved using a higher retraction speed. This process also means that printing onto low adhesion substrates is also possible, such as those demonstrated by Carlson et al [48], silicon plates, PET plastic sheets, glossy card stock and a leaf, without the need for an adhesion layer.

In order to produce this structured stamp, solid moulds of photoresist on silicon were fabricated and a series of casting and bonding stages were performed with individual components. By producing parts of the stamp in different steps, different mixing ratio of PDMS were able to be used to create a composite stamp so that the properties of each could be best

utilized. Once the stamp body was partially cured, circular holes were manually punched into the PDMS in order to provide connections to the microchannels. To create the film covering the internal reservoir, a 20:1 mixture of PDMS was spin coated onto a treated silicon surface (silicon surfaces were treated with FOTCS (tridecafluoro-1,1,2,2-tetrahydrooctyl) trichlorosilane) anti-adhesion layers) and partially cured on a hot plate. After this, the two parts of the stamp (the 5-1 base and the 20:1 film) were aligned and brought into contact before finishing the curing process, permanently bonding the two components together.

This method uses PDMS of different mixing ratios to create the stamp. By doing this, the most desirable properties of each ratio can be utilised, the rigidity of the 5:1 (base to curing agent) allowing for a pedestal that is much more rigid than the standard 10:1 ratio suggested by the manufacturer which lead to less deformation of the side walls of the pedestal during inflation of the stamp, while the 20:1 (base to curing agent) PDMS is a lot more flexible, meaning that when pressure is increased inside the reservoir, the surface of the pedestal has a more pronounced ballooning.

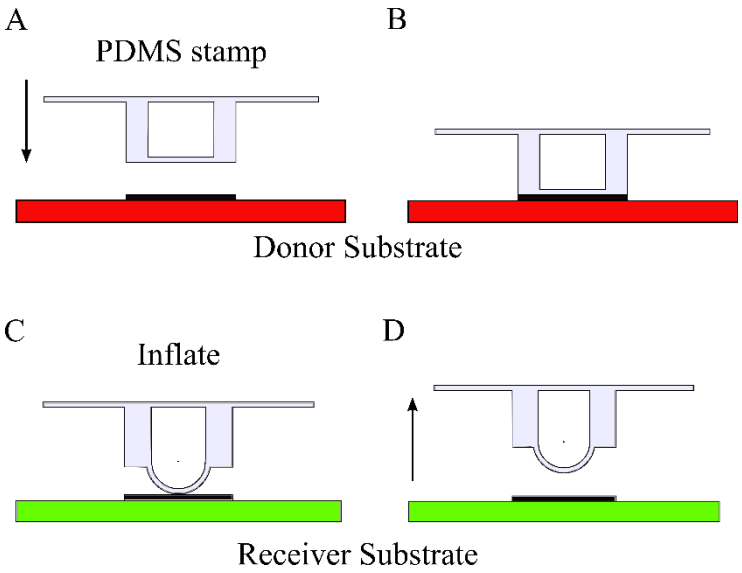

Figure 2.8: Programmable inking and printing of ink using the stamp at its uninflated state to create a high adhesion state for inking, then printing with the stamp inflated, providing a smaller contact area and putting the stamp into a low adhesion state. Adapted from [48].

2.4.2.2 Micro-tip Stamps

Instead of controlling the contact area by inflating and deflating a stamp, Kim et al [49] created a structured PDMS pedestal surface by KOH etching selected areas of the surface of a silicon (100) wafer masked with SiN in order to create pyramidal pits. By casting a 5:1 (base to curing agent) PDMS against the pitted Si surface and curing, the pyramidal structure pattern was transferred to the PDMS stamp surface.

When in use, by compressing the stamp to differing degrees while picking up and printing, these pyramidal structures become more squashed, so for low adhesion states, the stamp would be compressed only slightly, meaning the tips of the pyramids would make contact with the ink surface but not the majority of the flat pedestal surface. If a higher adhesion state was needed, then the stamp could be compressed to a greater extent, collapsing the pyramids entirely and bringing the full surface of the pedestal into contact. This can be seen in Figure 2.9.

The process of pickup and print can be achieved by lowering the pedestal surface of the desired ink, then compressing until the majority of the pedestal surface makes good contact,

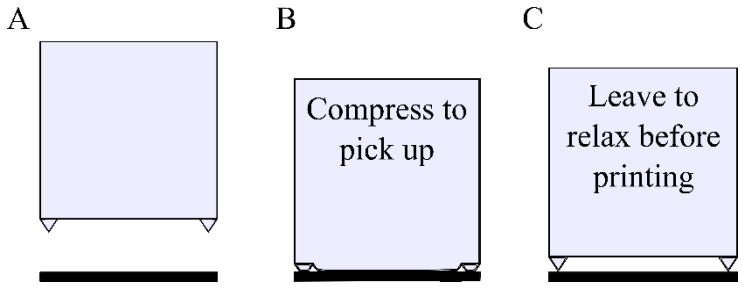

Figure 2.9: Using a micro-tip stamp A) approaching the ink. B) Compressing the stamp, collapsing the micro-tips and making full contact between the stamp and the ink. C) Leaving the stamp to relax and reduce the contact area in preparation for printing. Adapted from [49].

then retracting at high speed. This will ink the stamp in preparation for printing. First however, the stamp is left to relax. Due to the elastomeric nature of PDMS, during that relaxation time, the pyramid structures will slowly force the ink away from the flat underside of the stamp leaving the ink connected to the stamp by only the tips of the pyramid structures. This can then carefully be brought into contact with the receiving substrate and retracted slowly.

2.4.2.3 Pedestal with Stem

Sometimes modification of the surface of a stamp in order to achieve different adhesion capabilities from a material is not possible. This could be due to restraints with fabrication methods needed for inks, designs of the ink, or limitations with equipment access. Kim and Carlson et al [50] suggest a method of increasing the adhesion of a PDMS stamp by modifying the structure of the stamp pedestal itself, rather than any surface modification. This process involves fabricating a pedestal with a stem (50 μm tall and between 100 μm-50 μm^2 in cross section) supporting a larger (100 μm^2), flat pad which has the effect of, during retraction, limiting the crack propagation occurring at the edges, and instead, the crack initiates from the centre region of the ink. This can be seen in Figure 2.10.

The fabrication process of this stamp involves casting the stamp into SU-8 and silicon moulds in two parts, the first being the bulk of the stamp with a rectangular stem protruding from the surface, the second being the pad. PDMS of a 5:1 (base to curing agent) mixture was used to cast both parts. Once the bulk of the stamp was cured, and the pad was partially cured, these two pieces were carefully aligned before being fully cured which bonded the two components permanently.

The effect of using this stamp to pick up material showed that when the stem was reduced to 50 μm^2, at sub 100 $\mu m.s^{-1}$ retraction speeds, the pull-off force was near to 15 mN compared to a 100 μm^2 stem which achieved under 2 mN. This drastic increase in low retraction speed adhesion could have a use in enabling pick-up of particularly well bonded materials to their donor substrate which would otherwise be incompatible with a regular transfer printing process.

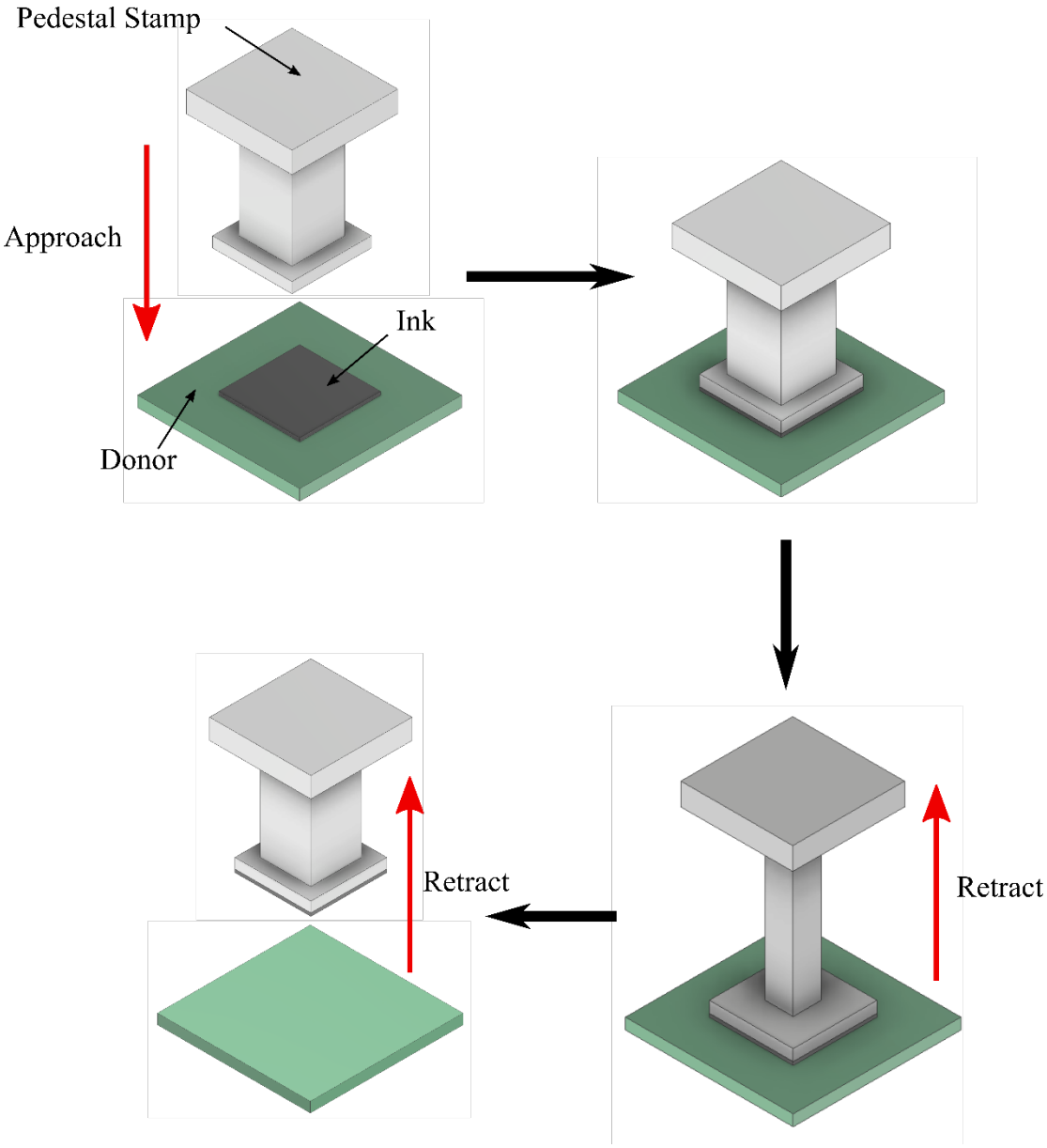

Figure 2.10: Illustration depicting the process of transfer printing using a stem pedestal shaped stamp. Adapted from [50].

2.5 Conclusion

In this chapter, the process of transfer printing in a range of forms has been discussed and the form of transfer printing with the greatest potential for further development has been identified, deterministic assembly, the process whereby a desired material (ink) is selectively picked up from a donor substrate, and is printed onto the surface of a receiving substrate. After this, a range of potential ink materials have been reviewed along with potential fabrication methods. Key developments in the transfer printing process have also been investigated and it is clear that an adhesive stamp, made from a viscoelastic material such as PDMS enables the transfer of a wide range of semiconductor materials which is an enabling process for device fabrication and a fundamental part of integration of semiconductor devices.

Different methods of modifying the adhesion of a PDMS stamp have also been investigated, from laser induced transfer printing, to modification of the PDMS stamp surface in order to give greater selectivity of the contact area made between the stamp and the ink. These different techniques are summarised and listed in Table 2.1.

From these developments to the transfer printing process it is evident that widening the process window for switchable adhesion is key in order to enable the transfer printing of new devices and for new applications. It is also clear that there is commercial interest in transfer printing with the company X-Celeprint supplying commercial transfer printing systems and there is also potential for industry interest as well, with large companies showing interest in inorganic microLEDs such as Samsung's The Wall.

Table 2.1: Summary of transfer printing techniques discussed in this chapter

Transfer Printing Process/Stamp Design	**Energy Release Rate**	**Substrate/Ink Materials**	**Notes**
Temperature Controlled Stamp [37]	16 $J.m^{-2}$ achieved at a retraction speed of: 7.8 $cm.s^{-1}$ (4°C), 36 $cm.s^{-1}$ (24°C), 47 $cm.s^{-1}$ (34°C)	-	Increasing PDMS temperature led to decrease in adhesion.
Laser induced transfer Printing [47]	-	Silicon	250°C temperature increase
Pneumatically inflated Pedestal Stamps[48]	Un-inflated: 4mN pull-off force Inflated: Approx. 2mN pull-off force	Silicon Plates	PDMS ratio at contact interface was 20:1 giving a more flexible and more adhesive PDMS.
Micro-tip Pedestal Stamps [49]	Full contact: 0.8 mN pull-off force at 800 $\mu m.s^{-1}$ Tip Contact: No measurable pull off force	Silicon(100)	

Stem Pedestal Stamp [50]	Stem 50% width: 10mN at 700 $\mu m.s^{-1}$ Stem 100% width: Approx. 1mN at 700 $\mu m.s^{-1}$	Silicon	Opposite observed effect at 50% stem width, at high retraction speeds the adhesion reduced. PDMS stamp fabricated from 5:1 ratio PDMS

2.6 References

[1] R. Loi *et al.*, "Edge-Coupling of O-Band InP Etched-Facet Lasers to Polymer Waveguides on SOI by Micro-Transfer-Printing," *IEEE J. Quantum Electron.*, vol. 56, no. 1, 2020.

[2] R. S. Cok, J. W. Hamer, C. A. Bower, E. Menard, and S. Bonafede, "AMOLED displays with transfer-printed integrated circuits," *J. Soc. Inf. Disp.*, vol. 19, no. 4, p. 335, 2011.

[3] J. Justice, C. Bower, M. Meitl, M. B. Mooney, M. A. Gubbins, and B. Corbett, "Wafer-scale integration of group III-V lasers on silicon using transfer printing of epitaxial layers," *Nat. Photonics*, vol. 6, no. 9, pp. 610–614, 2012.

[4] X-Celeprint, “Micro-Transfer Printing with x-Chips.”

[5] R. Lerner *et al.*, “Flexible and Scalable Heterogeneous Integration of GaN HEMTs on Si-CMOS by Micro-Transfer-Printing,” *Phys. Status Solidi Appl. Mater. Sci.*, vol. 215, no. 8, pp. 1–7, 2018.

[6] Y. M. Xie *et al.*, “Homogeneous Grain Boundary Passivation in Wide-Bandgap Perovskite Films Enables Fabrication of Monolithic Perovskite/Organic Tandem Solar Cells with over 21% Efficiency,” *Adv. Funct. Mater.*, vol. 2112126, pp. 1–12, 2022.

[7] H. Keum *et al.*, “Microassembly of heterogeneous materials using transfer printing and thermal processing,” *Sci. Rep.*, vol. 6, no. July, pp. 1–9, 2016.

[8] N. Dechev, W. L. Cleghorn, and J. K. Mills, “Microassembly of 3-D microstructures using a compliant, passive microgripper,” *J. Microelectromechanical Syst.*, vol. 13, no. 2, pp. 176–189, 2004.

[9] P. Serra and A. Piqué, “Laser-Induced Forward Transfer: Fundamentals and Applications,” *Adv. Mater. Technol.*, vol. 4, no. 1, pp. 1–33, 2019.

[10] H. Moriceau *et al.*, “Overview of recent direct wafer bonding advances and applications,” *Adv. Nat. Sci. Nanosci. Nanotechnol.*, vol. 1, no. 4, 2010.

[11] Y. Xu, S. K. Wang, P. Yao, Y. Wang, and D. Chen, “An air-plasma enhanced low-temperature wafer bonding method using high-concentration water glass adhesive layer,” *Appl. Surf. Sci.*, vol. 500, no. April 2019, p. 144007, 2020.

[12] S. Kim *et al.*, “Imbricate scales as a design construct for microsystem technologies,” *Small*, vol. 8, no. 6, pp. 901–906, 2012.

[13] J. Yoon *et al.*, “GaAs photovoltaics and optoelectronics using releasable multilayer

epitaxial assemblies," *Nature*, vol. 465, no. 7296, pp. 329–333, 2010.

[14] C. Prevatte *et al.*, "Pressure activated interconnection of micro transfer printed components," *Appl. Phys. Lett.*, vol. 108, no. 20, 2016.

[15] A. Carlson, A. M. Bowen, Y. Huang, R. G. Nuzzo, and J. A. Rogers, "Transfer printing techniques for materials assembly and micro/nanodevice fabrication," *Adv. Mater.*, vol. 24, no. 39, pp. 5284–5318, 2012.

[16] V. Vohra, T. Anzai, S. Inaba, W. Porzio, and L. Barba, "Transfer-printing of active layers to achieve high quality interfaces in sequentially deposited multilayer inverted polymer solar cells fabricated in air," *Sci. Technol. Adv. Mater.*, vol. 17, no. 1, pp. 530–540, 2016.

[17] Y. L. Loo, R. L. Willett, K. W. Baldwin, and J. A. Rogers, "Additive, nanoscale patterning of metal films with a stamp and a surface chemistry mediated transfer process: Applications in plastic electronics," *Appl. Phys. Lett.*, vol. 81, no. 3, pp. 562–564, 2002.

[18] D. Suh, S. J. Choi, and H. H. Lee, "Rigiflex lithography for nanostructure transfer," *Adv. Mater.*, vol. 17, no. 12, pp. 1554–1560, 2005.

[19] J. K. Kim, J. W. Park, H. Yang, M. Choi, J. H. Choi, and K. Y. Suh, "Low-pressure detachment nanolithography," *Nanotechnology*, vol. 17, no. 4, pp. 940–946, 2006.

[20] L. Gao *et al.*, "Nanoimprinting techniques for large-area three-dimensional negative index metamaterials with operation in the visible and telecom bands," *ACS Nano*, vol. 8, no. 6, pp. 5535–5542, 2014.

[21] K. Felmet, Y. L. Loo, and Y. Sun, "Patterning conductive copper by nanotransfer

printing," *Appl. Phys. Lett.*, vol. 85, no. 15, pp. 3316–3318, 2004.

[22] J. Lahiri, E. Ostuni, and G. M. Whitesides, "Patterning ligands on reactive SAMs by microcontact printing," *Langmuir*, vol. 15, no. 6, pp. 2055–2060, 1999.

[23] T. Ohishi, H. Noda, T. S. Matsui, H. Jile, and S. Deguchi, "Tensile strength of oxygen plasma-created surface layer of PDMS," *J. Micromechanics Microengineering*, vol. 27, no. 1, 2017.

[24] Z. Wang, J. Zhang, R. Xing, J. Yuan, D. Yan, and Y. Han, "Micropatterning of Organic Semiconductor Microcrystalline Materials and OFET Fabrication by 'Hot Lift Off,'" *J. Am. Chem. Soc.*, vol. 125, no. 50, pp. 15278–15279, 2003.

[25] D. J. Sirbuly, G. M. Lowman, B. Scott, G. D. Stucky, and S. K. Buratto, "Patterned microstructures of porous silicon by dry-removal soft lithography," *Adv. Mater.*, vol. 15, no. 2, pp. 149–152, 2003.

[26] D. J. Gargas, O. Muresan, D. J. Sirbuly, and S. K. Buratto, "Micropatterned porous-silicon bragg mirrors by dry-removal soft lithography," *Adv. Mater.*, vol. 18, no. 23, pp. 3164–3168, 2006.

[27] E. Menard, K. J. Lee, D. Y. Khang, R. G. Nuzzo, and J. A. Rogers, "A printable form of silicon for high performance thin film transistors on plastic substrates," *Appl. Phys. Lett.*, vol. 84, no. 26, pp. 5398–5400, 2004.

[28] K. Sim *et al.*, "High Fidelity Tape Transfer Printing Based On Chemically Induced Adhesive Strength Modulation," *Sci. Rep.*, vol. 5, pp. 1–9, 2015.

[29] B. Jiang, X. Shi, T. Zhang, and Y. Huang, "Recent advances in UV/thermal curing silicone polymers," *Chem. Eng. J.*, vol. 435, no. P1, p. 134843, 2022.

[30] M. A. Meitl *et al.*, “Transfer printing by kinetic control of adhesion to an elastomeric stamp,” *Nat. Mater.*, vol. 5, no. 1, pp. 33–38, 2006.

[31] K. Fukuda *et al.*, “Reverse-Offset Printing Optimized for Scalable Organic Thin-Film Transistors with Submicrometer Channel Lengths,” *Adv. Electron. Mater.*, vol. 1, no. 8, pp. 1–6, 2015.

[32] M. K. Choi *et al.*, “Wearable red-green-blue quantum dot light-emitting diode array using high-resolution intaglio transfer printing,” *Nat. Commun.*, vol. 6, no. May, pp. 1–8, 2015.

[33] J. Bavier, J. Cumings, and D. R. Hines, “Transfer printing of patterned metal films using parylene C coated surfaces,” *Microelectron. Eng.*, vol. 104, pp. 18–21, 2013.

[34] P. J. Wipff, H. Majd, C. Acharya, L. Buscemi, J. J. Meister, and B. Hinz, “The covalent attachment of adhesion molecules to silicone membranes for cell stretching applications,” *Biomaterials*, vol. 30, no. 9, pp. 1781–1789, 2009.

[35] T. W. Odom, J. C. Love, D. B. Wolfe, K. E. Paul, and G. M. Whitesides, “Improved Pattern Transfer in Soft Lithography Using Composite Stamps,” *Langmuir*, no. 9, pp. 5314–5320, 2002.

[36] M. Barquins, “Adherence, friction and wear of rubber-like materials,” *Wear*, vol. 158, no. 1–2, pp. 87–117, Oct. 1992.

[37] X. Feng, M. A. Meitl, A. M. Bowen, Y. Huang, R. G. Nuzzo, and J. A. Rogers, “Competing fracture in kinetically controlled transfer printing,” *Langmuir*, vol. 23, no. 25, pp. 12555–12560, 2007.

[38] H. S. Kim *et al.*, “Unusual strategies for using indium gallium nitride grown on silicon

(111) for solid-state lighting," *Proc. Natl. Acad. Sci. U. S. A.*, vol. 108, no. 25, pp. 10072–10077, 2011.

[39] C. A. Bower *et al.*, "High-brightness displays made with micro-transfer printed flip-chip microLEDs," *Proc. - Electron. Components Technol. Conf.*, vol. 2020-June, pp. 175–181, 2020.

[40] Samsung, "The Wall Datasheet," vol. 399, no. 10320, pp. 136–137, 2022.

[41] M. Bender *et al.*, "High resolution lithography with PDMS molds," *J. Vac. Sci. Technol. B Microelectron. Nanom. Struct.*, vol. 22, no. 6, p. 3229, 2004.

[42] J. A. Rogers and R. G. Nuzzo, "Recent progress in soft lithography," *Mater. Today*, vol. 8, no. 2, pp. 50–56, 2005.

[43] R. Saeidpourazar, M. D. Sangid, J. A. Rogers, and P. M. Ferreira, "A prototype printer for laser driven micro-transfer printing," *J. Manuf. Process.*, vol. 14, no. 4, pp. 416–424, 2012.

[44] W. Megone, N. Roohpour, and J. E. Gautrot, "Impact of surface adhesion and sample heterogeneity on the multiscale mechanical characterisation of soft biomaterials," *Sci. Rep.*, vol. 8, no. 1, pp. 1–10, 2018.

[45] A. N. Gent, "Adhesion and Strength of Viscoelastic Solids. Is There a Relationship between Adhesion and Bulk Properties? †," *Langmuir*, vol. 12, no. 19, pp. 4492–4496, 1996.

[46] W. G. Knauss, "Delayed failure - the Griffith problem for linearly viscoelastic materials," *Int. J. Fract. Mech.*, vol. 6, no. 1, pp. 7–20, 1970.

[47] R. Saeidpourazar *et al.*, "Laser-driven micro transfer placement of prefabricated

microstructures," *J. Microelectromechanical Syst.*, vol. 21, no. 5, pp. 1049–1058, 2012.

[48] A. Carlson, S. Wang, P. Elvikis, P. M. Ferreira, Y. Huang, and J. A. Rogers, "Active, programmable elastomeric surfaces with tunable adhesion for deterministic assembly by transfer printing," *Adv. Funct. Mater.*, vol. 22, no. 21, pp. 4476–4484, 2012.

[49] S. Kim *et al.*, "Microstructured elastomeric surfaces with reversible adhesion and examples of their use in deterministic assembly by transfer printing," *Proc. Natl. Acad. Sci.*, vol. 107, no. 40, pp. 17095–17100, 2010.

[50] S. Kim *et al.*, "Enhanced adhesion with pedestal-shaped elastomeric stamps for transfer printing," *Appl. Phys. Lett.*, vol. 100, no. 17, 2012.

Chapter 3

Experimental Techniques

In this chapter, the techniques and processes that are the foundation of this PhD will be detailed. Most of these processes have been established for this PhD specifically but will be used by future projects and research. Initially the processes involved fabricating PDMS stamps for transfer printing will be described such as preparing the PDMS silicone in preparation for casting, different casting methods, and creating composite stamps.

This will then be followed by the transfer printing system. The components that make up the transfer printing system will be described as well as modifications that were made in order to improve the results that were obtained.

Finally the code that was written to automate the transfer printing system will be shown and sections will be explained in order to describe the purpose of key sections of the script.

3.1 PDMS Casting

The ability to cast PDMS silicones into functional stamps and to fabricate structured surfaces is essential to achieve successful transfer printing [1][2][3]. In this section the process of PDMS casting established during this PhD will be explained and detailed including stages of development and potential considerations necessary in order to achieve high quality and high definition PDMS stamps for use in transfer printing.

3.1.1 PDMS Preparation and Casting

The term PDMS refers to a wider range of silicones composed of Si-O chains [4] however the PDMS that has been the focus of development of the casting process during this report has been Sylgard 184, an addition cure PDMS which has been used extensively for casting transfer printing stamps [5][2][6][7] which comprises of a bulk base PDMS and a curing agent containing a platinum catalyst which instigates the crosslinking process [8] of the siloxane chains in the base to form the liquid PDMS base to a solid elastomer. This can be seen in Figure 3.1.

The process for preparing this PDMS silicone involved pouring a measured quantity of the Sylgard 184 base into an aluminium tray. Then, using a pipette, an appropriate quantity of the curing agent was added (10:1 ratio of base to curing agent is recommended by the manufacturer). A plastic spoon was then used to thoroughly combine the two components. The

Sylgard 184 mixture now had a working time of 1 hour and 30 minutes and was ready to be poured into a mould and cured.

Complete casting of PDMS silicones is a necessary part of many applications in order to fully utilise the physical properties of PDMS silicones. Initially during this project, Sylgard 184 was the primary PDMS that was of interest. Sylgard 184 has the capability to be cured at room temperature over a 48 hour period. This long curing time had some benefits. Any bubbles

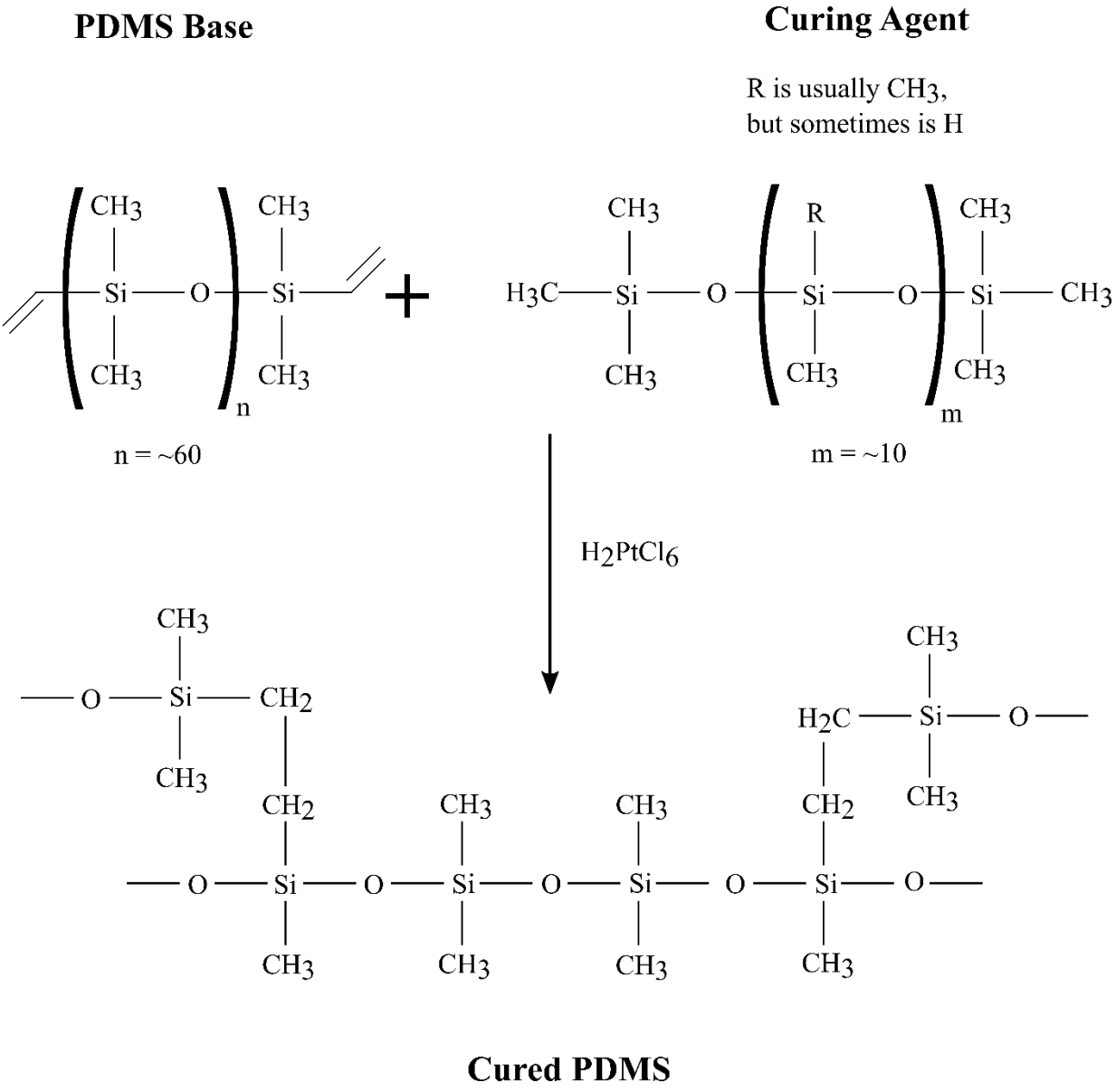

Figure 3.1: Diagram showing the chemical structure and curing process of PDMS. Replicated from [8]

that were formed during mixing of the two components (base and curing agent) rose to the surface of the PDMS and burst. As well as this, at room temperature castings, many materials of casting moulds were available, such as the use of cheap and disposable polystyrene Petri dishes, which could provide a very uniform and flat surface. These moulds could then be placed onto a levelled optical bench in order to achieve a PDMS stamp with parallel top and bottom surfaces, minimising any further alignment of equipment at later stages of the transfer printing process.

This process of casting at room temperature was suitable for most applications initially during the development of this process. However, the curing time of Sylgard 184 has a temperature dependency with the curing time decreasing with elevated temperatures, this is shown in Figure 3.2. At room temperature, Sylgard 184 cured in 48 hours, but at 150°C that

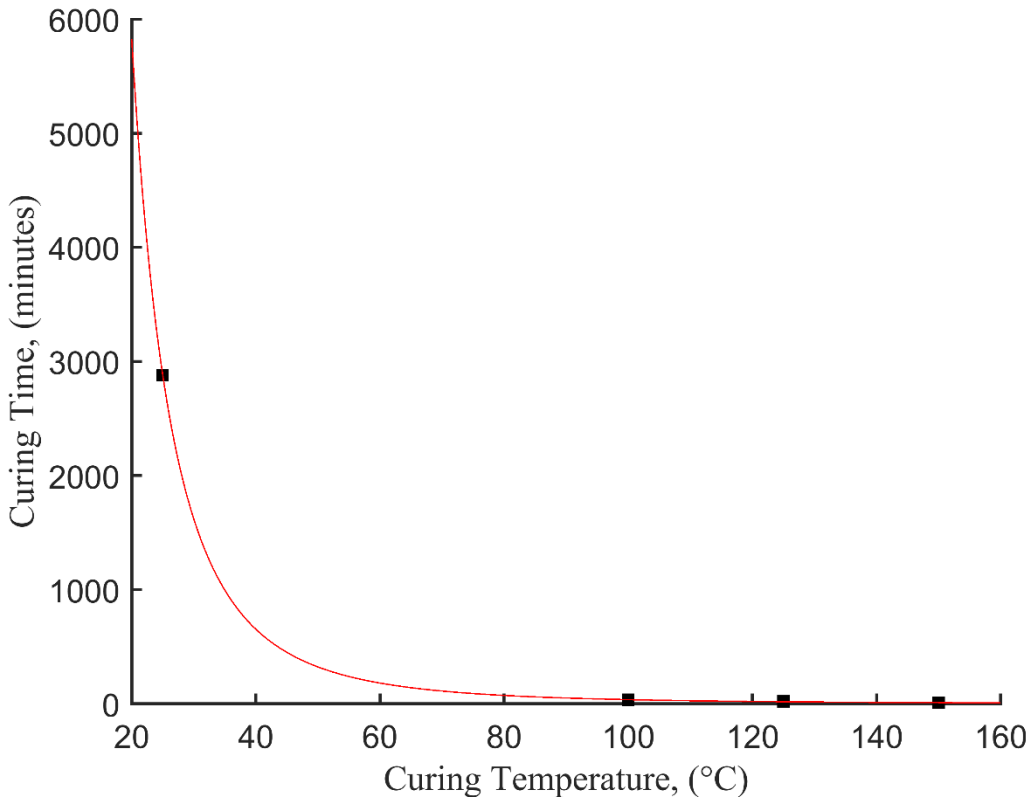

Figure 3.2: Graph showing the curing time of Sylgard 184 at different temperatures, reproduced from data from [9]

curing time is reduced to 10 minutes [9]. The most appropriate temperature was determined be 100°C, which would cure the Sylgard 184 PDMS in 35 minutes and could be heated using a laboratory oven. A time that was deemed to accelerate the curing time sufficiently, but also mitigated the effects of variations in either the curing temperature, or the curing time.

As a side effect, curing at elevated temperatures meant that the use of a flat and level surface, like that of the optical bench used in room temperature castings, was not available. Another effect of using an accelerating curing time, is that bubbles trapped in the PDMS did not have time to burst before the PDMS fully cured. To overcome this, an extra stage was necessary in the preparation of the PDMS. Once the PDMS mixture had been thoroughly mixed and combined, it was placed into a vacuum desiccator for 10 minute intervals until the mixture is free of bubbles. The PDMS mixture was then ready to be cast at an elevated temperature.

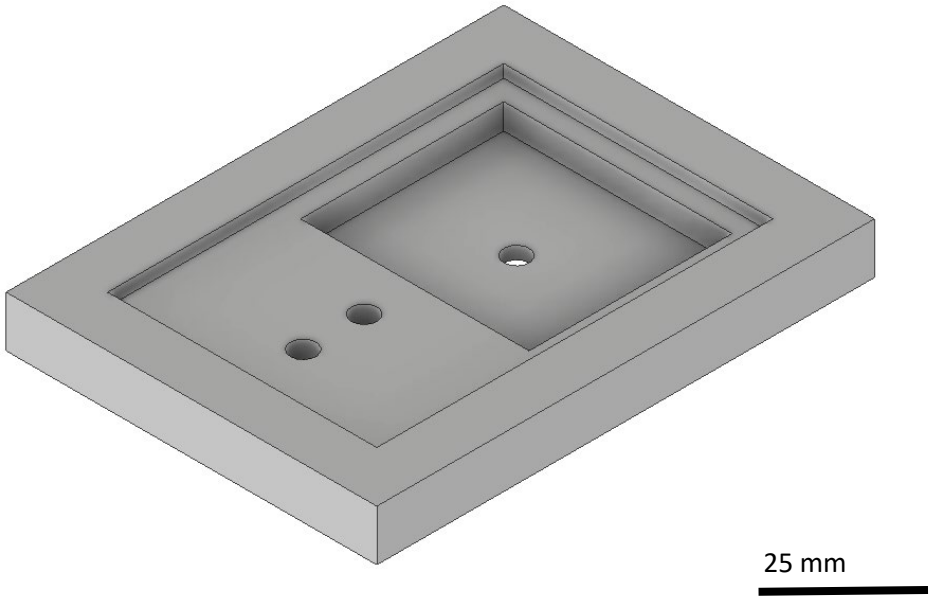

Figure 3.3: Schematic diagram showing the first iteration of the casting process using a milled aluminium block. The deep recessed area could house the structured face of the mould, either through patterned aluminium plates, or using a photoresist and silicon mould. The small ridge around the edge supported a glass slide, ensuring both faces of the PDMS stamp were parallel.

The use of elevated curing temperatures limited the potential range of mould materials to those thermally compatible. At 100°C polystyrene becomes malleable and loses its rigidity which would have a lasting impact on any castings. A new method of casting was necessary.

The initial solution was an aluminium mould, formed from a block of aluminium and milled out in the centre so that PDMS could be poured into it and a glass slide could be adhered to the back side of the stamp, a schematic of this design can be seen in Figure 3.3 and Figure 3.4.

This design was introduced in order to achieve flat castings despite potentially angled oven racks, however it had a major flaw. Any PDMS that seeped between the glass slide and the aluminium mould, formed an excellent seal and adhered the glass and aluminium. The method of separation for this mould used screws to gently lift the glass slide away from the aluminium releasing it from the mould along with the PDMS stamp. However, once liquid PDMS seeped between the glass and the aluminium faces and cured, separation became impossible and any attempt to separate these two pieces led to the glass cracking. Removal of the PDMS stamp after curing without causing damage to the stamp was also challenging due to the high sides of the mould which limited access to the stamp.

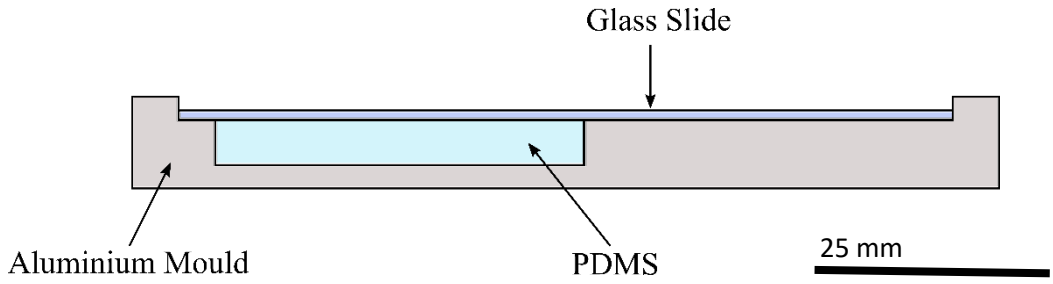

Figure 3.4: Schematic diagram showing the PDMS casting with suing the aluminium mould and a glass slide backing.

The next iteration of the mould was a simplified approach, by using an aluminium plate with a 40 mm by 40 mm square milled out, the height of the stamp could be selected with some accuracy. This plate was then clamped to a larger flat aluminium plate, which would act as the flat face of the mould. During castings performed with the previous version of the mould, it was found that Sylgard 184 does not bond very well with a smooth aluminium surface. This mould design had no back cover to ensure a flat top layer, as this had been the primary issue with the previous design, instead, a larger aluminium plate was placed into the oven when cool, and using a spirit level, was positioned so that a flat surface was achieved. This design was an important step in developing the final moulding process as it led to an understanding of the PDMS casting process and considerations that were needed when developing a new process. The first consideration was that any amount of PDMS that seeps between two solid pieces, such as the aluminium plate and the glass slide used in this design, will stick the two together and are challenging to separate. The second being that, while this method did create a flat stamp, in order to fabricate any high resolution structured surface such as those used by Ruben

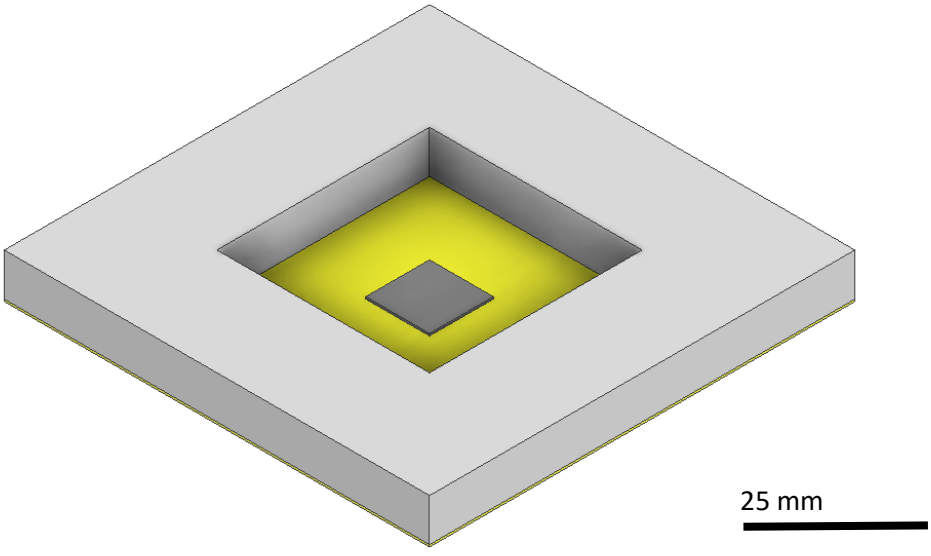

Figure 3.5: Schematic diagram of the final casting method, with the aluminium frame, the thickness of which determines the thickness of the final PDMS stamp, an adhesive backing of polyimide tape and a silicon and photoresist structured mould face.

et al [10], this design was not easily adapted to include additional mould components that were necessary.

By taking the aluminium frames with the 40 mm^2 milled hole and using adhesive tape on the back, it was possible to create an adhesive backing to which structured components could be adhered, like those in [11] where patterned SU-8 on silicon was used as a rigid mould surface upon which PDMS was cast. The process of creating these SU-8 structured moulds is included in the following section. Figure 3.5 and Figure 3.6 shows the casting process using a silicon and SU-8 mould.

This led to the creation of a mould that was modular, where the thickness can be changed easily by replacing the aluminium frame, and the structured face can be easily modified by replacing the structured silicon and SU-8 mould. The first few adhesive tapes selected led to failed castings. The solvent based rubber and resin adhesive used on the electrical tape [12] that was tested as well as the water based acrylic adhesive used in the Arco Glass Protection Film [13] appeared to inhibit the curing of Sylgard 184. However, the silicone adhesive on polyimide tape [14] appeared to not impact the curing and removal of polyimide tape from the back of a silicon substrate and aluminium plate was easily achieved.

3.1.2 SU-8 Mould Fabrication

Creating the structured SU-8 mould from which PDMS could be cast is a crucial aspect of soft lithography and the process of creating a PDMS stamp for transfer printing. The process of creating these moulds revolves around a 100 μm thick SU-8 photoresist (SU-8 2050,

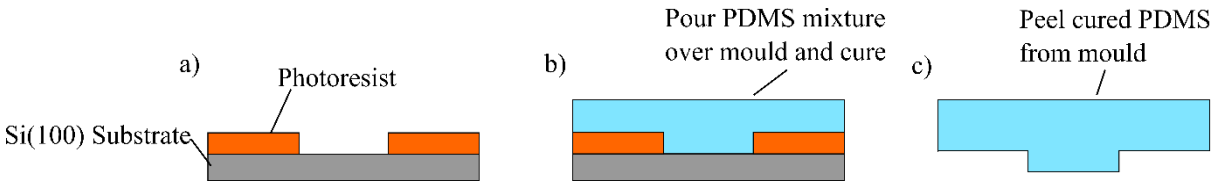

Figure 3.6: Schematic diagram showing the PDMS casting process using a structured photoresist pattern on a Si(100) substrate in order to achieve a structured PDMS surface.

MicroChem) which was spun onto a piece of Si(100) wafer. And patterned using photolithography in order to create a patterned surface upon which PDMS can be cast.

A Si(100) wafer was cleaved into 1.5 cm by 1.5 cm pieces. In order to remove and contaminants on the surface of these pieces, each one was cleaned using n-Butyl acetate (Fisher Chemical), acetone (99% acetone, Fisher Chemical), and isopropyl alcohol (99.8% isopropyl alcohol, Fisher Chemical). The Si(100) substrate was baked at 100°C for 1 minute on a hot plate in order to remove any surface water or condensation which might interfere with the photolithography process.

The Si(100) substrate was then mounted on a programmable spin coater and, in order to ensure that no dust had settled on the surface during the dehydration baking process, the sample was spun while blowing the surface with nitrogen for a few seconds. Once this was complete, SU-8 2050 was deposited onto the surface of the substrate which, due to the viscosity of this particular SU-8 (12900 cSt [15]), had to cover the entire substrate surface before spinning to ensure that no sections of the substrate were left uncovered by the SU-8. Once the SU-8 had been deposited onto the Si(100) surface, it was left for between 30 seconds and 60 seconds so that any bubbles trapped in the SU-8 can burst. One this time had elapsed, any large bubbles left were removed using a pipette and any smaller bubbles were removed in following steps.

Once the bubbles had been removed the SU-8 covered Si(100) substrate was then accelerated to 500 rpm at a rate of 100 rpm/s for 15 after which this was increased to a spin

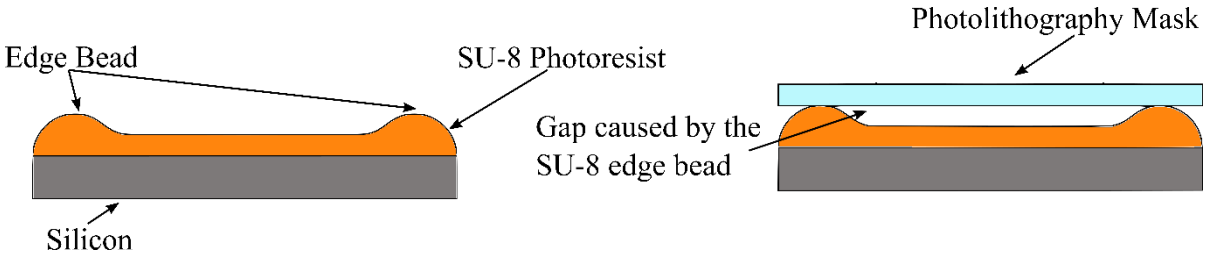

Figure 3.7: Diagram showing the effect that the presence of an edge bead has when making contact with the SU-8 to the mask.

speed of 1700 rpm for 30 seconds with a 300 rpm/s acceleration. The edge bead formed during spinning was great enough that it would prevent good contact being made with the mask during the exposure stage, this is shown in Figure 3.7. To reduce or remove the edge bead, an edge bead removal process was performed using 0.5 ml of an edge bead remover (EBR PG, MicroChem) which was sprayed onto the SU-8 film, after which the Si(100) and SU-8 mould was covered with a plastic cover with a small 1mm hole drilled into the top. This ensured that the rate at which the edge bead remover would evaporate, helping to ensure that the SU-8 had time to become flat. After this had been left for 24 hours at room temperature the SU-8 surface was inspected. The edge bead removal process was repeated until the surface of the SU-8 was flat and free of bubbles.

The now bubble free and flat SU-8 coated Si(100) was baked at 65°C for 5 minutes on a hot plate, followed by a 95°C bake for 16 minutes to remove most of the solvent within the SU-8 before being aligned to the quartz and titanium mask using a UV400 mask aligner and exposed for 48 seconds. The SU-8 was then baked at 65°C for 4 minutes then for 9 minutes at 95°C.

To remove the unexposed SU-8 a development process was performed with the aid of an ultrasonic bath (UT8031/EUK Ultrasonic Cleaner, Shesto). The SU-8 coated Si(100) was first submerged in SU-8 developer (SU-8 Developer, MicroChem) and lowered into the ultrasonic

bath for 6 minutes on delicate mode. Every two minutes however the process was paused in order to visually inspect the SU-8 film to check the development progress. Once all of the unexposed SU-8 had been removed, the sample was then rinsed and dried with de-ionised water and nitrogen to remove any remaining developer. At this stage small crack were often seen on the SU-8 surface which would be replicated in any PDMS cast off of this mould. In order to repair the surface, the mould was placed onto a hotplate at 180°C for 30 seconds. This caused the SU-8 to re-flow and 'heal' any minor surface cracks. Once the mould was fully exposed, developed, cleaned and crack free, it was flood exposed with the UV400 mask aligner for 5 minutes. The process of SU-8 patterning is shown in Figure 3.8.

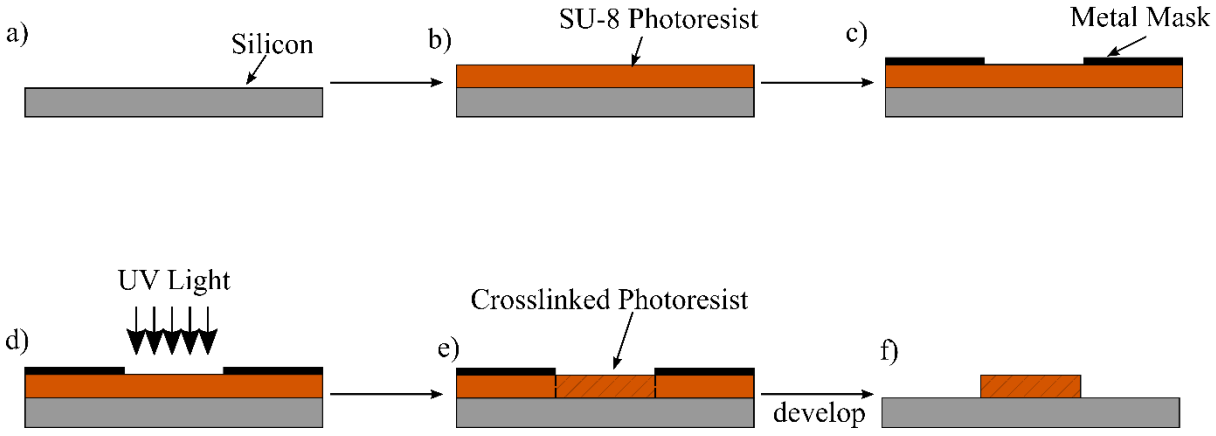

Figure 3.8: Schematic showing the process of patterning SU-8 photoresist starting with a) a clean silicon substrates followed by b) spin coating the SU-8 onto the surface giving a photoresist thickness of 100 um and then performing the edge bead removal. In c) the photoresist coated silicon is brought into contact with the patterned metal mask and in d) and e) the exposed areas of the SU-8 are exposed to UV light which crosslinks the exposed SU-8. F)The uncrosslinked SU-8 is then removed using SU-8 Developer.

3.1.3 Injection Moulding

Injection moulding is a technique that offers the potential to completely replicate the inverse pattern of a three dimensional mould. Despite the success in enabling successful castings in an oven using an aluminium plate, perfectly flat stamps were not always guaranteed, as the surface tension of the PDMS mixture could lead to raised PDMS at the edges of the mould. For some applications, it was necessary to have a uniformly flat surface without trimming and cutting away the non-flat edges of the finished PDMS stamp. In order to improve the casting process to ensure that PDMS castings were uniformly flat, an injection moulding process was developed.

By creating a two part mould, one side made from PTFE (a polymer with excellent non-stick properties [16]) and the other made from polycarbonate it would be possible to achieve a regularly flat PDMS stamp, photographs of this mould are shown in Figure 3.9. The polycarbonate top section, being transparent, means that any bubbles introduced during the injection process can be identified and removed. The injection process uses a syringe filled with bubble free PDMS to manually fill the mould. An outlet hole ensures that any air inside

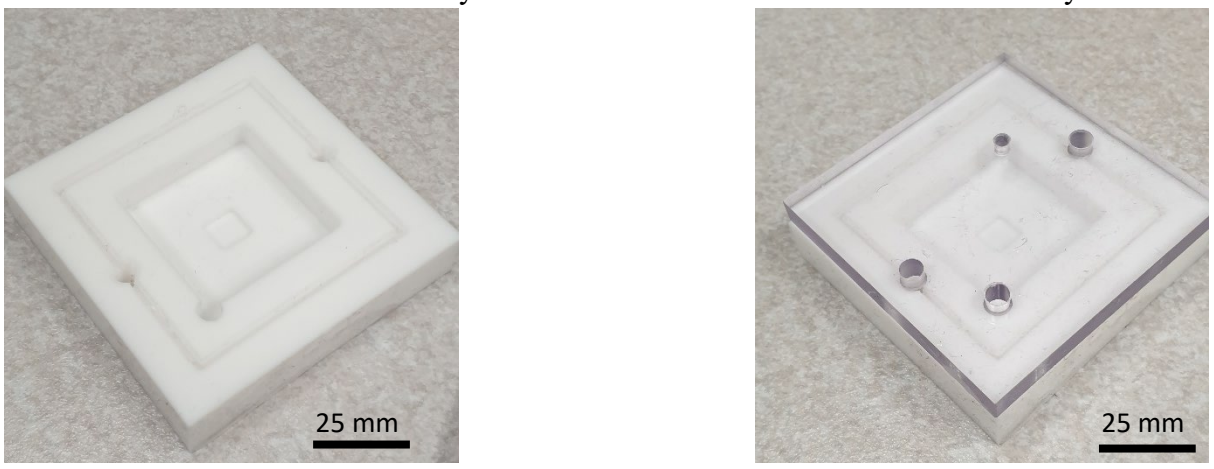

Figure 3.9: Photographs displaying the PTFE injection moulding component (left) and the PFTE component combined with the polycarbonate top (right).

the mould has somewhere to escape but it also allows excess PDMS to leave via that hole. The major challenge while developing this mould was finding a way to create a structured surface on the cast PDMS stamp. PTFE has low adhesive properties which is beneficial for release of cured PDMS from the mould. When integrating a structured mould face to this mould, like a patterned SU-8 mould, there were limited methods of adhering these structured components to the low adhesion PTFE mould surface.

The initial method of adhering the silicon and SU-8 mould to the base of the PTFE injection moulding component was to use Sylgard 184 in a 20:1 mixing ratio (which has a greater adhesion PDMS) as a bonding material between the silicon mould to the PTFE base. Once this was cured, the Sylgard 184 PDMS stamp mixture could then be cast and cured. A diagram showing the use of a PDMS adhesive to adhere a structured mould to a PTFE mould is shown in Figure 3.10

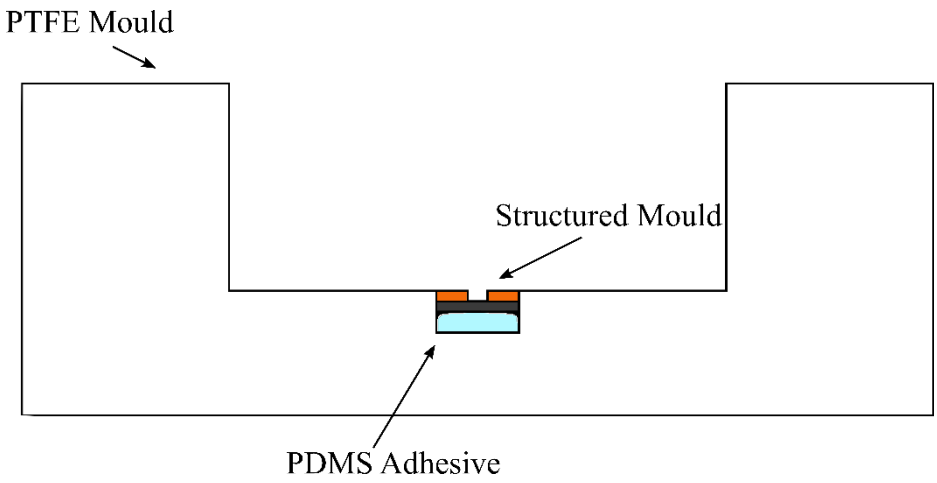

Figure 3.10: Diagram showing the method of using PDMS as an adhesive in order to stick a structured silicon and SU-8 photoresist to the lower PTFE component of the injection moulding mould.

3.1.4 PDMS Bonding

In order to fabricate PDMS stamps made from different components that are made individually and assembled together, it was necessary to develop a reliable process for PDMS bonding. There are a range of methods of PDMS bonding [17] [18] [19] however the two that were most applicable and suitable were the following: Using a PDMS as an adhesive layer, and Ultraviolet/ozone (UVO) bonding.

The UVO treatment of PDMS is commonly used to modify the hydrophobic nature of PDMS for microfluidic applications and involves using an ultraviolet ozone cleaner which emits ultraviolet light in 185 nm and 254 nm wavelengths [20]. The 185 nm emitted UV light is absorbed by the O_2 in the air, creating O_3, which, in the presence of 254 nm UV light, reacts with the organic components on the PDMs surface forming CO_2 gas and H_2O. On PDMS, the CH_3 methyl group making up parts of the siloxane chains that make up the PDMS react with

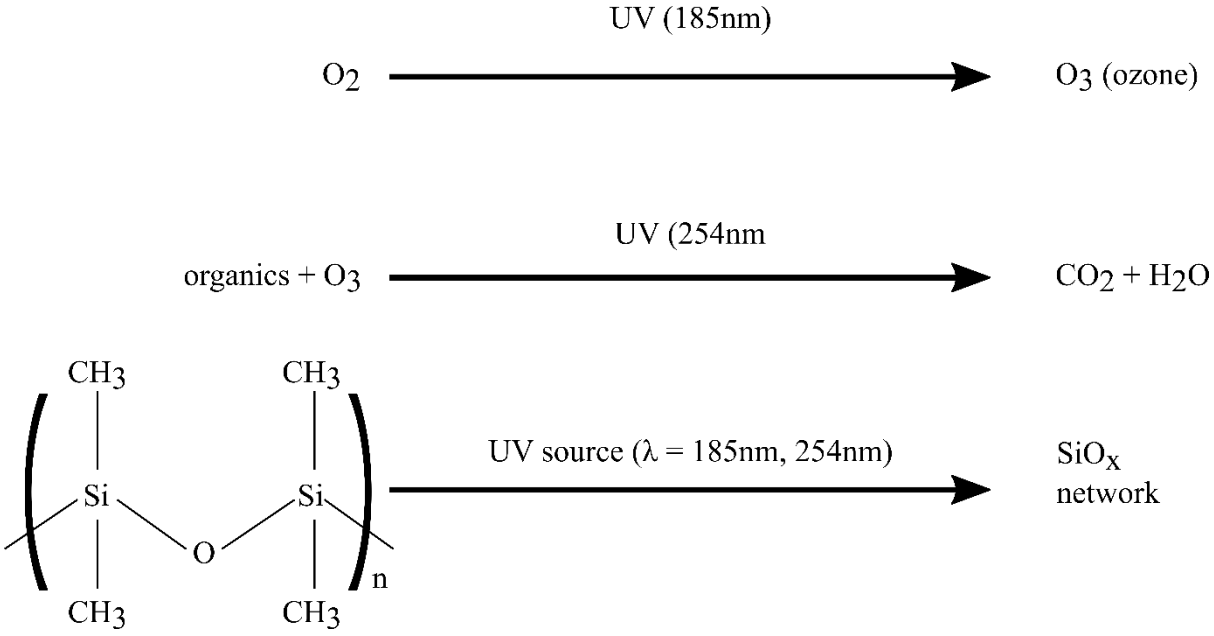

Figure 3.11: Diagram of the proposed chemistry of UVO treatment of a PDMS surface. Adapted from [21].

the O_3 as well, leaving a SiO_x crust-like surface behind [21]. Figure 3.11 shows the reaction that takes place when UVO treating a PDMS surface. The resulting PDMS surface also has Si-OH groups present which react chemically to other functional groups resulting in an effective bonding to other PDMS surfaces treated with UVO [22]. Each technique for bonding two different PDMS components together had their own merits and drawbacks, so the most appropriate particular technique was selected for each application.

There are numerous benefits to creating a composite stamp. Firstly, it can be an easy way to fabricate a structured piece of PDMS that has features on two sides. Instead of having to focus on an injection moulding technique, which can be costly and time consuming to establish, two thinner pieces of PDMS can be cast, each with a feature on one side. This process is relatively simple to establish and can have a fast turnaround with low upfront costs. Once the two structured components are fabricated, a PDMS adhesive could then be used to bond the two together.

Secondly, by fabricating parts of a PDMS stamp separately, it allows for bespoke curing ratios, or combinations of PDMS silicones, to be exploited without complicated casting processed. This has been shown to be effective in the fabrication of inflated pedestals [23] where different mixing ratios of Sylgard 184 were combined into a single stamp, to use the rigidity of a 5:1 PDMS mixing ratio, and the increased adhesion and flexibility of a 20:1 mixing ratio.

Bonding PDMS components in order to make a composite stamps also opens avenues of fabricating PDMS stamp components separately, and combining once all components are fully fabricated. Kim et al [24] used a method like this in order to create a pedestal shaped structures on a PDMS stamp which would not have been achievable without a bonding method

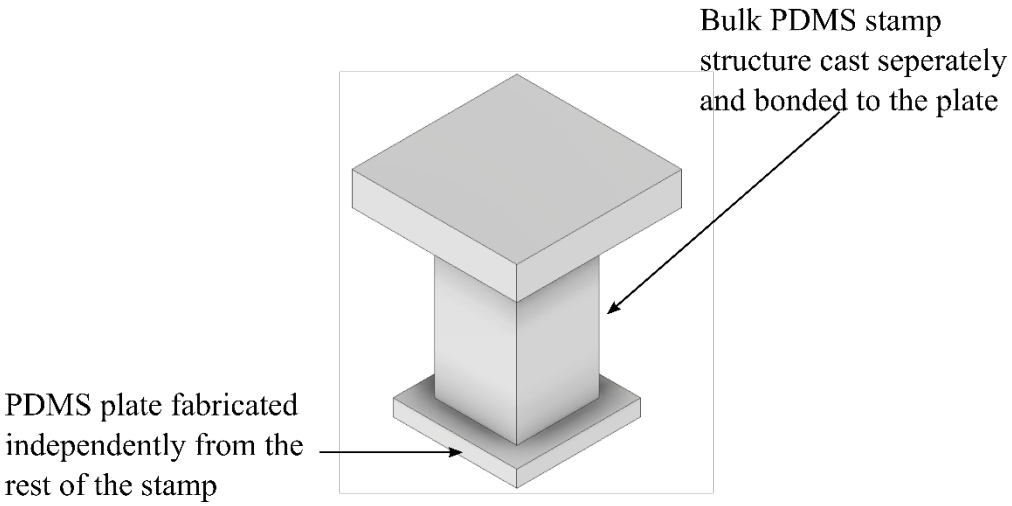

Figure 3.12: Diagram showing the structured pedestal PDMS stamp fabricated from individual components in order to achieve a casting that would not have been achievable with conventional casting methods. Reproduced from [24].

being used. Figure 3.12 shows the PDMS stamp structure and shows which components were bonded.

By fabricating the two components of a PDMS stamp separately, then bringing them together, it opens the possibility of creating a stamp with entirely embedded features. This has been incredibly useful to those in the microfluidic community, as McDonald et al who used an air plasma to bond section of a PDMS microfluidic device by oxidising the surface of a PDMS base, allowing for a water tight bond to be made [25].

3.1.4.1 PDMS Adhesive

For PDMS stamp components that had a particularly rough surface, such as those components moulded in a 3D printed mould, or required a faster turnaround, a PDMS adhesive was often

used. This used pre-prepared PDMS stamp components, that were fully cured and cleaned, and a small amount of uncured PDMS mixture was spread evenly over one surface. The easiest method for achieving repeatable results was to use a dip coater (Dip Coater, Ossila) to coat a PDMS stamp with fresh uncured PDMS, the thickness of which could be determined by the dip coater retraction speed. For using the dip coater to coat PDMS components in liquid PDMS to act as an adhesive, a withdrawal speed from the liquid PDMS bath was 0.1 $mm.s^{-1}$ or for surfaces that were particularly rough, a withdrawal speed of 0.3 $mm.s^{-1}$ was used, as this provided a thicker layer of the liquid PDMS. Once one side of a component stamp was coated in uncured PDMS, the opposite part could then be brought into contact, and the PDMS sandwiched between the two parts of the composite stamp could be cured.

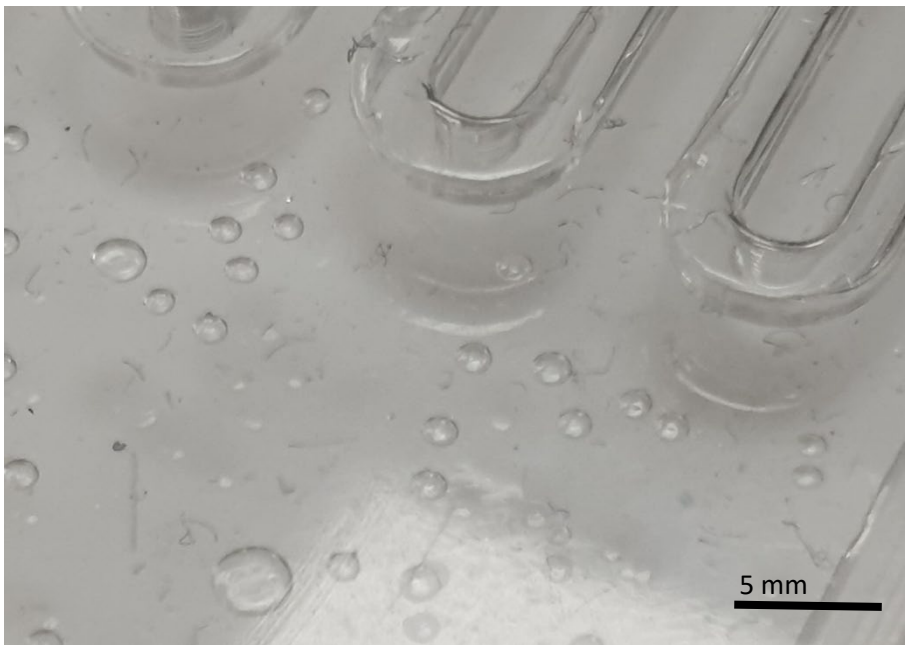

Figure 3.13: Photograph showing trapped bubbled in the PDMS adhesive used to bond a PDMS stamp with a fluidic channel to a PDMS backing stamp. The smaller bubbles like these may not have a major impact to most stamps, but larger bubbles could become areas where cracks can start, causing delamination of the two components.

The process of using PDMS as an adhesive had various complications which required multiple levels of modification to the process in order to bypass. One of the initial challenges encountered was the introduction of small bubbles during the bringing together of the two stamp components as shown in Figure 3.13. This appeared to be only a small inconvenience until the high temperature curing took place, during which, the bubbles expanded and repeatedly provided an interface upon which a crack could propagate between the two pieces. To reduce the chance of this happening, additional PDMS was applied so that, when bringing together the two components of the PDMS stamp, most of the liquid PDMS adhesive would be squeezed out, minimising the introduction of small air pockets.

As well as the introduction of air pockets, it was often found that during the room temperature curing of the PDMS adhesive, the PDMS components were likely to slide and become misaligned due to the PDMS adhesive acting as a lubricant, until it began to cure. By performing room temperature curing of the PDMS adhesive, it avoided over-curing, or thermally degrading the already cured PDMS components, which could impact the adhesive properties [26]. However, it was sometimes necessary to take that risk and use a high temperature curing. The high temperature curing enable the stamp to be cured faster, reducing the chance of misalignment occurring, although this did not entirely remove the possibility altogether. In order to minimise the chance of misalignment further, the use of clamps or side plates was often necessary during curing. These would hold the two components in place during the curing at high temperature but could lead to stamp damage when attempting to remove them. Due to leakage occurring over the 48hr curing period of Sylgard 184, this clamping method was not appropriate for room temperature castings.

The major challenge with this process of composite stamp fabrication was attempting to use this process in order to create PDMS stamp with fully embedded microchannel features for use in Chapter 6: Thermally Modified PDMS Transfer Printing Stamps Using Embedded

Fluidic Channels. The first issue was that this stamp needed to be water tight, and able to withstand a small amount of water pressure without bursting. This mean that any bubbles in the PDMS adhesive that was used, could potentially introduce either a leak, or a weak spot where a leak was likely to occur. The solution, as mentioned before, to removing the chances of bubbles in the PDMS adhesive was to use a thicker layer of PDMS adhesive, and, to ensure there was no slipping or misalignment, clamps were a solution. Together these two solutions were liable to flood the internal fluidic channels with uncured PDMS adhesive which when cured, would destroy the stamp. This meant that fine tuning of both the thickness of the liquid PDMS adhesive layer was necessary, along with the addition of delicate clamping.

3.1.4.2 Ultraviolet/Ozone Bonding

As a solution to the issues of misalignment that could occur when using a PDMS adhesive, another PDMS bonding process was established. By treating the two sides of the PDMS stamp that are to be bonded with an ultraviolet/ozone (UVO) cleaner, it is possibly to create a permanent bond between the two pieces as described in section 3.1.4.

In order to achieve a successful bond using UVO treatment, the two interfaces were cleaned thoroughly by leaving them to soak in a beaker of isopropyl alcohol (IPA) (99.8% isopropyl alcohol, Fisher Chemical) for 3 minutes, then removing from the beaker, drying with nitrogen, then repeating the process again. Once the two pieces were cleaned and dry, they were placed into the bed of the ultraviolet ozone cleaner (UV Ozone Cleaner, Ossila) as shown in Figure 3.14. After exposure to UVO for 40 minutes, the two components were immediately

brought into contact and left for up to 24 hours. This period of time is necessary in order to form the bond between the two components.

A more in-depth look at how UVO effects the surface of PDMS is presented in Chapter 5: Double Casting PDMS Silicones Facilitated by Ultraviolet/Ozone Surface Treatments, however, it can be summarised that the UVO process forms a silicon oxide crust and over time free siloxane chains can migrate to the surface [27]. This is used in the process of UVO bonding by bringing the two treated surface into contact, then, over the next 24 hours, free siloxanes have time to migrate to the surface and cure, forming a permanent bond between the two components.

Figure 3.14: Photograph showing two cleaned Sylgard 184 PDMS components before UVO treatment in order to bond together.

This process in an effective way of bonding together two flat and smooth PDMS surfaces. If one, or both, of the surfaces that have been treated with UVO are not flat, or have a rough surface, possibly due to the method of casting such as 3D printed moulds, good contact between the components cannot be made causing the bonding process to fail.

3.1.4.3 Dip Coating

In order to achieve thin films of a liquid onto a solid surface, dip coating is often used [28][29][30] whereby the solid surface is entirely submerged into a bath of the target liquid. The speed at which the substrate is retracted from the liquid is controlled so that the thickness of the liquid film created can be selected. This layer thickness is dependent both on the properties of the liquid, and the substrate retraction speed. Generally liquids with a higher viscosity, or substrates with a greater retraction speed, can achieve a thicker film for a given retraction speed than that of lower retraction speeds, or less viscous liquids [31].

In order to perform dip coating of PDMS in this report, an Osilla dip coater (Dip Coater, Ossila) as seen in Figure 3.15 was used, and a 3D printed PLA bath was designed to act as a bath, which can be seen in Figure 3.16. In order to avoid wasting excessive quantities of PDMS, the bath was designed to be deep enough to submerge a substrate and was narrow in width so that the volume of PDMS needed in order to successfully dip coat was minimised.

The substrates used in this report were glass slides and PDMS. To prepare these substrates for dip coating, each was washed with IPA to remove surface contaminants and dried using nitrogen. The substrates were then mounted in the clamp on the vertical arm of the dip

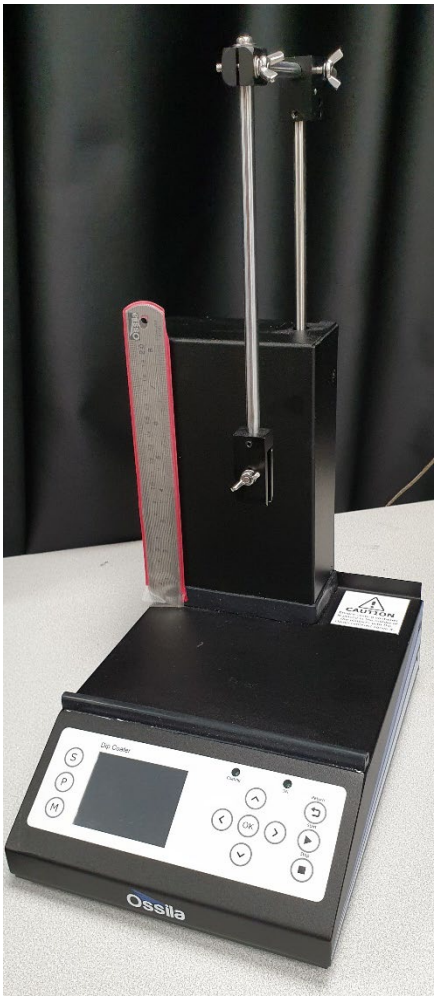

Figure 3.15: Photograph of the Ossila Dip Coater.

coater and the PDMS bath was positioned underneath. Once the bath and substrate were in position, the dip coater was set up, with the coating length and retraction speed being selected. For the purpose of coating a substrate with PDMS as an adhesive layer to bond PDMS stamps, a retraction speed on 0.3 $mm.s^{-1}$ was found to provide the most appropriate layer thickness.

The PDMS used as an adhesive which was applied by dip coating was 10:1 mixing ratio (base to curing agent) which provided sufficient adhesion for a composite stamp. Once the PDMS adhesive layer had been deposited, and the composite stamp had been assembled, the PDMS adhesive layer was cured in an oven at 100°C for 35 minutes.

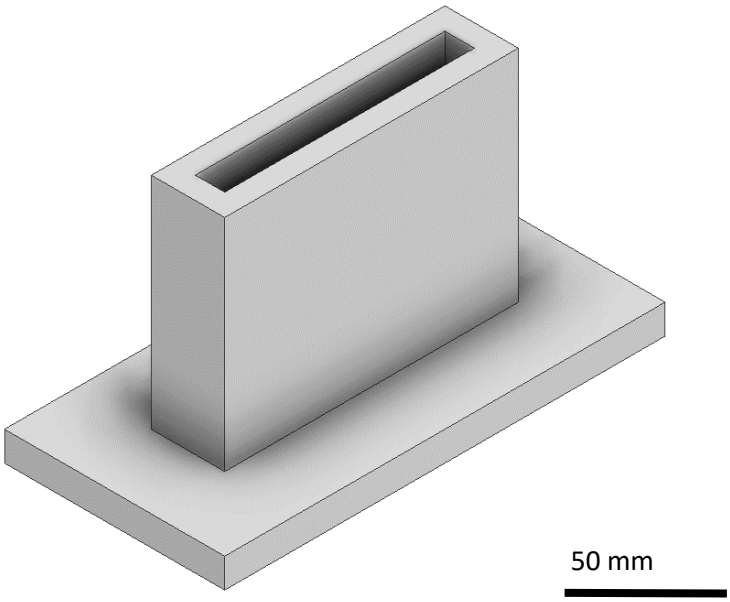

Figure 3.16: Diagram of the 3D printable file used to create the PDMS bath for dip coating. The large base provides stability while the raised thin vessel provides space for the substrate to be submersed without wasting large quantities of PDMS.

3.1.5 Contact Angle Goniometry

Studying the surface energies of materials can be an important for many processes [32][33][34][35]. Contact angle goniometry, the process by which measuring the angle made by a droplet of a liquid when in contact with a surface, can be used to quickly, and easily, achieve an understanding of the surface energy of a material.

The surface energy of a material determines the angle the droplet makes with the surface. This droplet could be a liquids such as oil [36], or, as was the case in this report, de-

ionised water can also be used [32]. If the surface has a surface energy that is greater than the surface tension of the droplet liquid, the droplet spreads on the surface, however, if the surface energy is lower than the surface tension of the liquid, then the droplet beads on the surface [37].

In order to perform these measurements, a contact angle goniometer is used, which uses a light source and a high resolution camera with a sample mounted in between. In this report, an Ossila Contact Angle Goniometer (Contact Angle Goniometer, Ossila) was used which can be seen in Figure 3.17. A syringe is used to drop a small droplet of de-ionised onto the sample

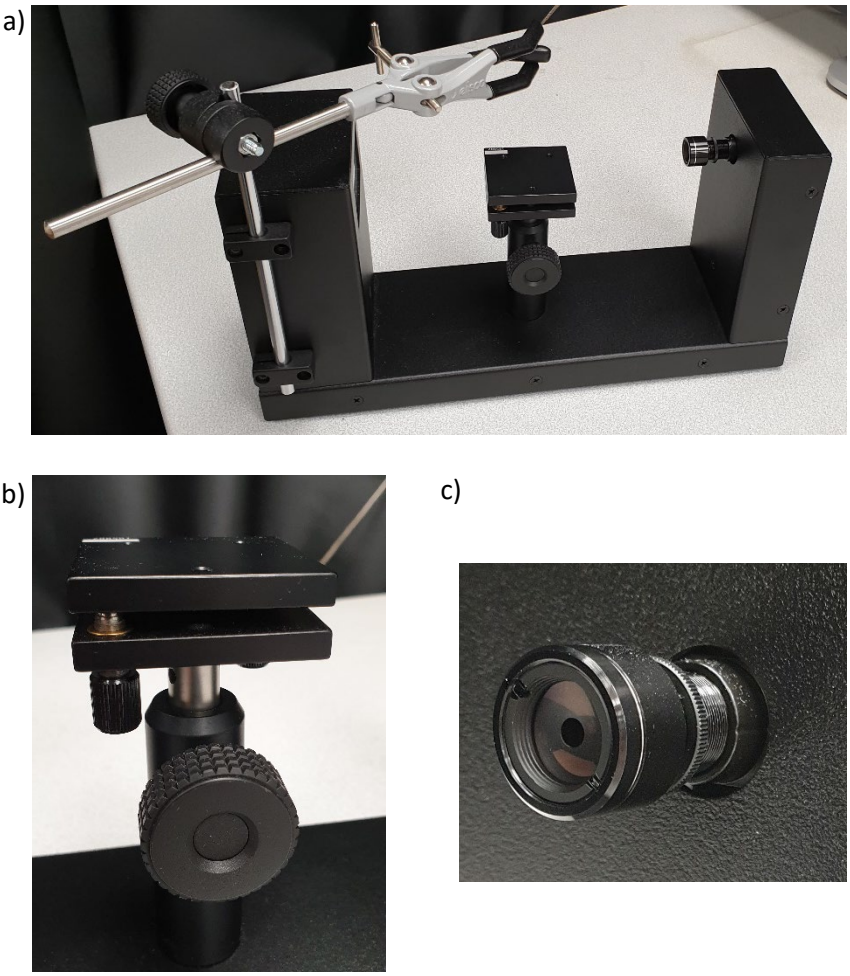

Figure 3.17: Photographs of the Ossila Contact Angle Goniometer showing b) the raised central platform upon which a sample can be mounted and levelled, and the high resolution camera c) used to take the image of the liquid droplet on the sample surface.

surface, and the camera takes an image. The Ossila Contact Angle software was then used to calculate the contact angle made by the droplet to the sample surface.

3.2 Transfer Printing

This section will cover the transfer printing process used throughout this PhD from the setup of the transfer printing system, to the considerations needed when performing measurements. After this there will be a section discussing the Aerobasic script that was written in order to automate the transfer printing process, giving greater control over particular parameters.

3.2.1 Transfer Printing System

In order to develop and test transfer printing processes a system was constructed that consisted of a vertical stage upon which a PDMS stamp could be mounted that was controlled to lower and raise at a set retraction speed in order to exploit the velocity dependant adhesion properties of the Sylgard 184 PDMS. A photograph of the system can be seen in Figure 3.18.

The precise control over the position of the z-stage as well as control over the adhesion and other parameters is crucial to achieve transfer printing. In order to have this control, an Ensemble Motion Controller (Ensemble HLe Controller and Linear Digital Drive, Aerotech) was used to control a vertical z-stage (ANT130LZ Single-Axis Z Nanopositioning Stage,

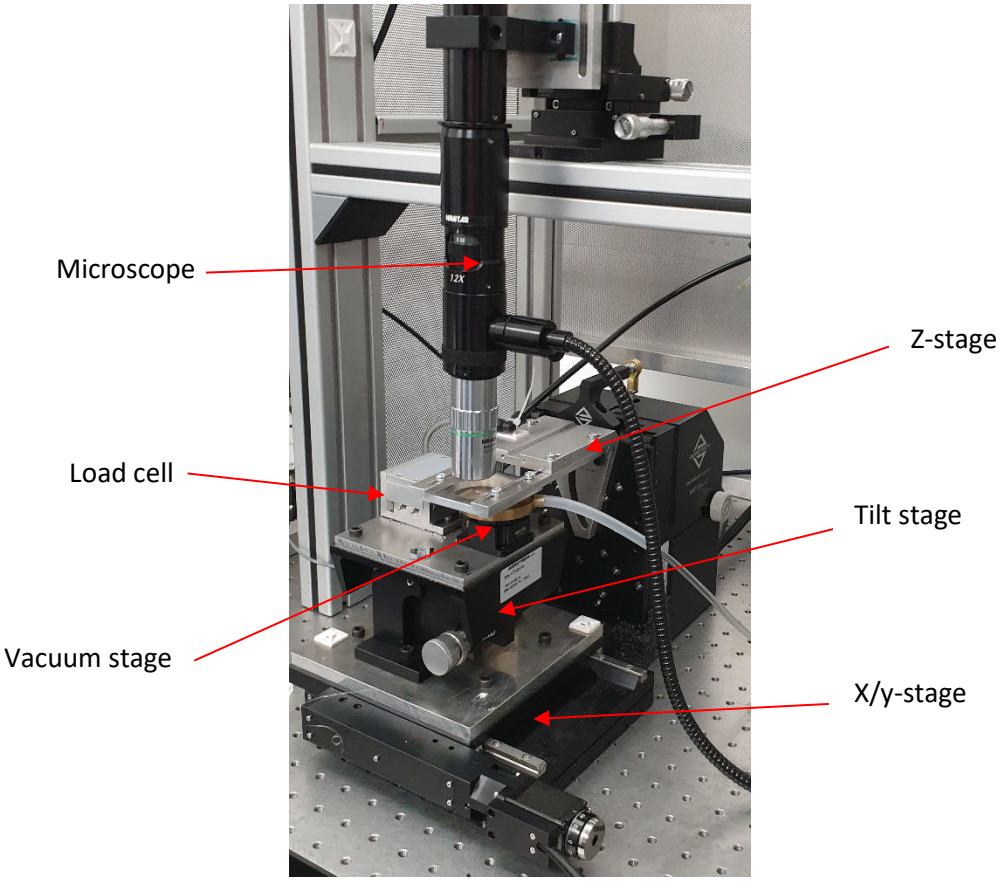

Figure 3.18: Photograph of the transfer printing system showing the microscope setup, the z-stage, and a load cell and vacuum stage mounted onto a tilt stage on an x/y-stage.

Aerotech). This allowed for control of the stage with a 2nm resolution with a repeatability of ±75nm. The specifications of the vertical z-stage are show in Table 3.1.

Table 3.1: Table showing the specifications of the Aerotech ANT130LZ Single-Axis Z Nanopositioning Stage used in the transfer printing system build in this PhD.

Accuracy	±300nm
Repeatability	±75nm
Resolution (Minimum Incremental Motion)	2nm
Maximum Speed	200mm/s
Maximum Acceleration (No Load)	1g

Attached to the z-stage was a vacuum chuck on an L-bracket connected to a horizontal stamp holder with a vacuum line attached which was specifically designed to fit with the 2" x 3" glass slides that were used as a method of mounting the PDMS stamp.

The z-stage had no method of alignment in any other direction than the z-direction to a substrate so an x/y-stage was introduced, on top of which was mounted a tilt stage. The introduction of these stages had a dual purpose, the first was to allow for fine control and alignment so that small features, such a 100 μm^2 pedestals could be aligned to the ink material, the second purpose was so that two substrates could be held at once, one donor, on receiver substrate. This would allow the entire transfer printing process to take place on one machine and setup, without the need to move to other setups. On top of this x/y-stage were slots to allow for the attaching of two mounts. These were modular and could be changed out with ease depending on the experimentation taking place. Two vacuum chuck holders were integrated, each with a range of compatible vacuum chucks that could be mounted which gave the ability to rotate each of the vacuum chucks, so that good rotational alignment between the pedestal on

the stamp surface and the donor or receiving substrates could be achieved. Each vacuum chuck had a different sized hole in which to secure a substrate ready for transfer printing. The user would select the maximum available size that would fit their sample, achieving the greatest adhesion possible to the vacuum chuck.

The third component option that could be mounted to the sample stage is a load cell (GSO-10, Transducer Techniques). Details about this load cell are included in Table 3.2 and an image of the load cell in used can be seen in Figure 3.19. This load cell was essential to carry out analysis of transfer printing stamp as it allows for the force of adhesion to be measured as well as allowing finer control over the compression of the pedestal on the stamp surface. It also could provide interesting information about the nature of PDMS stamps when under compression and during retraction. This load cell was connected via a shielded cable to the Ensemble Motion Controller which allowed the in-built software to read and record the data transmitted by the load cell.

Table 3.2: Table of the specifications of the Transducer Techniques GSO-10 load cell which was mounted on the x/y stage of the transfer printing system built in this report.

Hysteresis	0.05% of rated output
Accuracy	±0.005g
Capacity	10g
Safe Overload	150% of rated output
Calibration	Compression and Tension

A high magnification microscope setup was also an essential part of the transfer printing system as by enabling observation of the pedestal structure and the surface of the substrate on

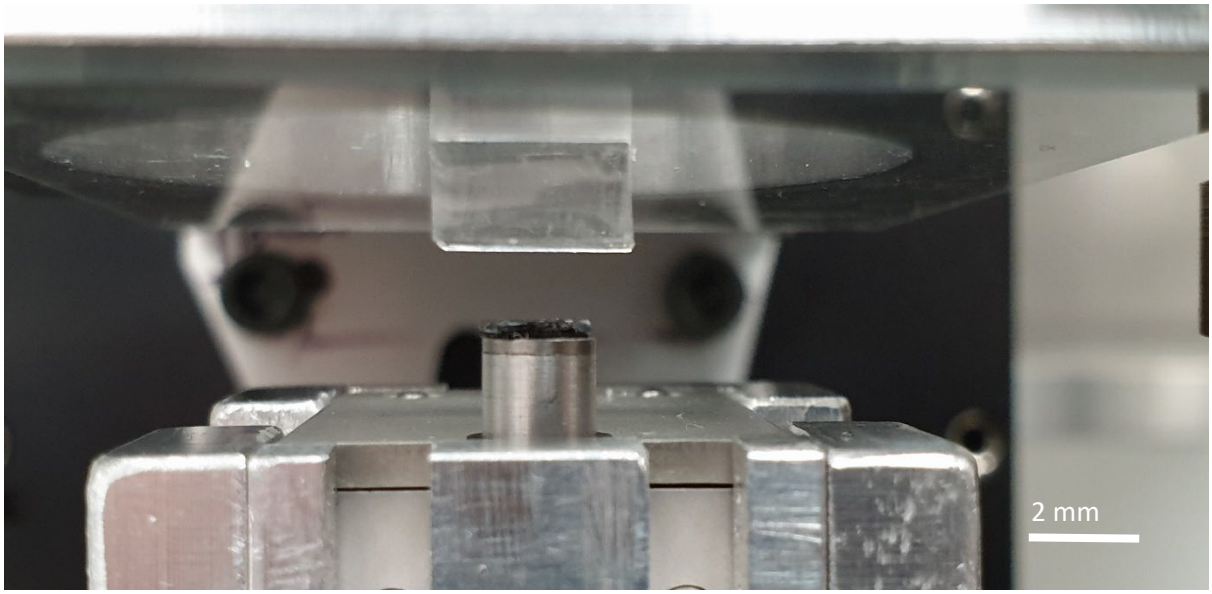

Figure 3.19: Diagram showing a Si(100) substrate mounted onto the load cell load stem using an adhesive carbon pad. A PDMS stamp, adhered to a glass slide, and mounted to the z-stage using a vacuum chuck can be seen approaching the Si(100) surface.

the x/y stage, careful alignment of them was achieved. This microscope setup comprised of a Navitar 12x Zoom Lens System giving a range of magnifications from 0.58-7x. This microscope system was invaluable when compressing the pedestal on the stamp surface, as it would provide immediate feedback when initial contact was made between the pedestal and the substrate, but also if complete pedestal collapse occurred and contact was made with the substrate surface in areas surrounding the pedestal.

3.2.2 Considerations and Adjustments to the Transfer Printing System

It was found that due to the sensitive nature of the load cell, both from physical interference but also electrical, further protections and considerations were necessary in order to collect meaningful results. A particular and immediate area causing disruption and interference to the results was physical vibrations in the laboratory. The sensitivity of the load cell was such that laboratory users walking nearby, or the laboratory door being opened could cause spikes in the readings, masking the signal that was expected. This was overcome by moving the transfer printing system entirely from an optical bench, with little vibration isolation, to a floating optical bench (Newport VH3030W-0PT) plumbed into the laboratory nitrogen line. This ensured that any vibrations that occurred outside of the floating optical bench, would not interfere with the load cell readings.

Secondly, the building that the transfer printing system was located in housed large amount of equipment, such as pumps and chillers. The proximity to these pieces of equipment caused noticeable quantities of induced EMI that would again mask any reading from the load

Figure 3.20: Photograph of the cable connecting the load cell to the Ensemble Motion Controller after the introduction of a twisted pair wire and a ferrite core.

cell. By building a Faraday cage around the transfer printing system, it was possible to shield the load cell, ensuring that there would be no EMI to interfere with any readings. This Faraday cage had a dual purpose, not only did it shield the load cell from induced EMI, but it also protected the load cell from the movement of air in the laboratory sue to the air conditioning system which could be seen on the load cell reading at times.

As well as EMI, it was also noticed that due to an electrical issue in the building, there was a large amount of noise coming through the electrical power lines. Again, at times this could cause issues with load cell readings, such as spikes in the load cell reading. By introducing a UPS (uninterruptable power supply) to both the PC and the Motion controlled,

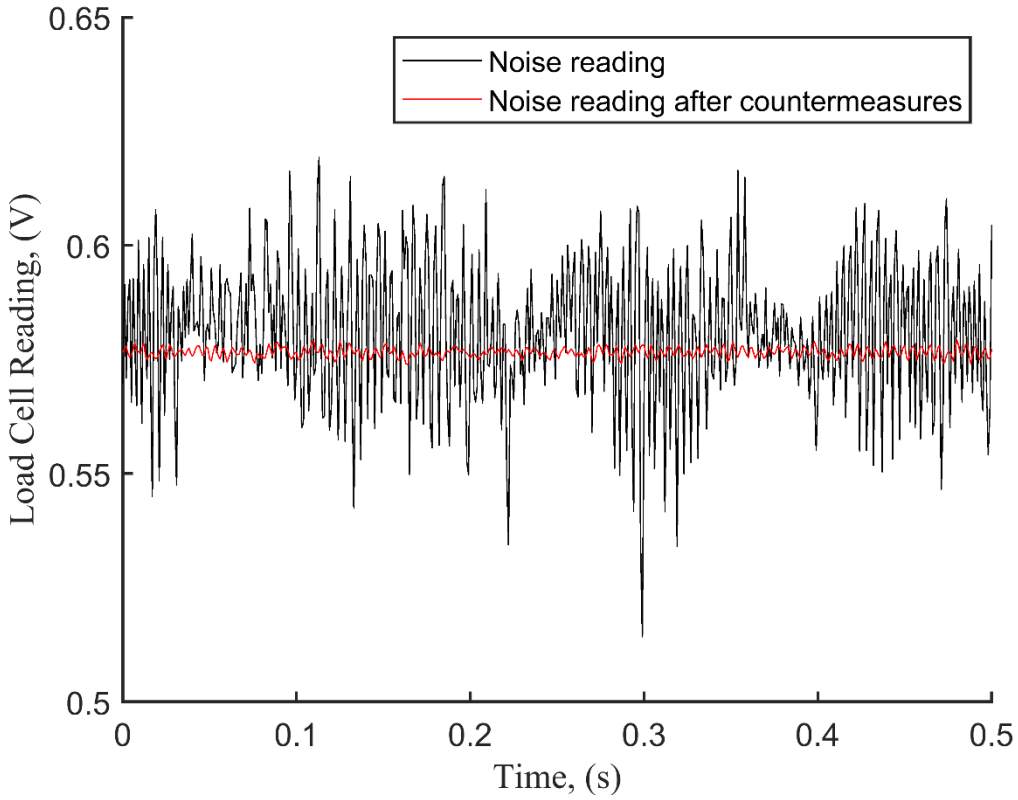

Figure 3.21: Graph showing the noise picked up by the load cell before and after the countermeasures, such as the vibration isolation bench, Faraday cage, and UPS, were implemented.

which in turn powered the load cell, the load cell could be protected from any fluctuations in the mains power cables.

As a further modification the transfer printing system in response to excessive noise, the cable connecting the load cell to the Ensemble Motion Controller was replaced. A twisted pair cable was made and replaced the individual wired used initially, this had the effect of improving the compatibility of these wires when surrounded by electromagnetic interference. Further to this, the twisted pair cable was wrapped around a ferrite ring in an effort to further reduce the impact of any electromagnetic interference. Finally, any exposed cabling from the load cell that left the Faraday cage that the transfer printing system was housed in, was run through a shielded cable. This can be seen in Figure 3.20. The impact of these noise countermeasures can be seen in Figure 3.21.

3.3 Transfer Printing System Control

The ability to control and manipulate a stage during a process as sensitive as transfer printing especially while using a PDMS stamp that has a velocity dependant adhesion to a substrate is essential. In this section, the basic control over the transfer printing system using the software's user interface is discussed, followed by a discussion of the use of a script that the Ensemble Motion Composer can use in order to manipulate the stage with a greater level of control. Then a more in depth look at this script and what it achieves will be included.

3.3.1 Software and Manual Control

The Ensemble motion controller was controllable through the Ensemble Motion Composer, a computer programme supplied with the Ensemble Motion Controller which allows for direct control of the connected z-stage using the programmes user interface (UI). This UI has inputs to allow the user to manually move the vertical stage a certain distance and at a certain velocity. This user input is adequate for rudimentary testing, but in order to perform accurate and repeatable testing and experimentation, it was necessary to write a script that could be run by the Ensemble Motion Composer. The script that was written will be described in greater detail in the next section, but a summary of the script is as follows:

1) Manual alignment of the stamp to any features on the substrate, such as any ink that was to be picked up.
2) The stage would then lower until a pre-selected load cell reading was met, followed by a relaxation period in order to ensure the PDMS pedestal obtained good contact to the substrate.
3) After this wait period, the stage was then retracted at a set velocity, acceleration and acceleration profile, in order to obtain the desired effect (e.g. pick-up or printing of ink). The stage would retract a desired distance and then stop and wait, ready for realignment to a receiving substrate, or for further testing.

3.3.2 Aerobasic Code

The code written to automatically control the z-stage is included in full in the Appendix however in this section key sections of the code will be included and discussed in order to provide an understanding of the different stages of the transfer process as well as to identify the additional control measures provided by the use of this code.

The first step was a function to set a variable for the load cell within the script. In order to do this, the software would have to collect a set of data in order to know which data inputs would be associated with which variable. The use of the commands SCOPEBUFFER and SCOPETRIGPERIOD determine the rate of data collection and the time duration that data would be collected for. In this case, the minimum rate of data collection and data collection time was required as only one data point was necessary. After that, the command SCOPETRIG initiated the collection of this reading and SCOPETRIG STOP was used to cancel the data collection after 0.2 seconds to bypass the minimum SCOPETRIGPERIOD of one second. There was then a short waiting time that pauses the script giving time for the data collection software to process the data before attributing the Load Cell input as the data being input through the Analog Input 1 channel. This section of code can be seen below as:

```
Setting LoadCellOutput Variable

Setting the number of data points that are collected.
     SCOPEBUFFER 1
     SCOPETRIGPERIOD 1

Triggering the scope to collect data.
     SCOPETRIG

Pauses the code for a given time in seconds. This gives the
software time to collect enough data points.
```

```
     DWELL 0.2

Cancels the scope data collection.
     SCOPETRIG STOP

Pauses the code to give the digital scope time to process the
data.
     DWELL 2

Defines the variable LoadCellOutput using the SCOPEDATA
function.
<return> = SCOPEDATA (<DataType>, <DataIndex>)
DataIndex refers to the data point that is returned.
     LoadCellOutput = SCOPEDATA (AnalogInput0, 1)
```

Once the zero value of the load cell was set, the variables controlling the motion of the stage were set. These used two variables to select the retraction distance, how far the stage would retract once contact had been made, and the retraction speed, the desired velocity achieved by the stage when retracting from the target substrate. These two variables enables users to define the retraction distance, which would ensure that any collisions with other surrounding equipment could be avoided, such as the microscope positioned above the stage. In this case, a retraction distance of 0.3 mm was suitable, as it was large enough for any PDMS pedestals to elongate full and break contact with the substrate during the retraction but without risking damage to the microscope or the stage hitting the upper limits. The ability to determine the retraction speed was also crucial as it allowed for exploitation of the PDMSs tamps velocity dependant properties, which are so commonly used in order to achieve transfer printing. The code section for defining the retraction distance and speed can be seen below:

```
Defining Retraction Distance and Retraction Speed

Setting the distance (mm) that the stage will retract once the
approach has been completed and the stamp has been compressed.
```

```
     RetractionDistance = -0.3

Setting the speed at which the stage will retract (mm/s).
     RetractionSpeed = 0.7
```

The greatest benefit of using a code such as this to control the stage, other than control over the retraction speed and distance, is that it provides greater control over other properties of the stage, such as this next section which allows the user to set the acceleration profile used during retraction. This profile includes the acceleration achieved by the stage during retraction but also the curve factor of the acceleration. By manually selecting the acceleration profile and speed, it ensured that each transfer printing process that was performed used identical settings to improve repeatability. The code section that determines the acceleration profile can be seen below:

```
ACCELERATION PROFILE SETUP

Set the curve factor.
This value ranges anywhere from 0 to 100. Any value outside
this range is a runtime error. If the S-curve is zero, the ramp
up and ramp down is linear. If the value is 100, the ramp up
and ramp down is parabolic. Any value between these values is
the percentage of the ramp up and ramp down that is parabolic.
     SCURVE 0

Declares that the acceleration desired will be set by the
user.
     RAMP MODE RATE

Setting acceleration (mm/s^2) (1000 mm/s^2 = 1 m/s^2)
     RAMP RATE 3000
```

Now that the stage was set up and programmed, it was time to activate the stage so that the software could control the z-stage. In order to control the approach of the stage, and the stamp attached to it, a WHILE loop was used which would automatically take a snapshot of the load cell readings, read the load cell output, and so long as this output value was lower than the user determined force, the stage would lower by 0.01 mm. This command of reading the load cell output and lowering was repeated until the load cell reading reached above the determined value which would compress the pedestal on the PDMS stamp surface sufficiently so that good contact could be made. Due to the nature of the PDMS materials and different casting ratios, selecting the appropriate compression value was more intuition than using precise values as the mixing ratio of PDMS determines how flexible and malleable the pedestal would be, so a 20:1 PDMS would require a lower load cell reading in order to compress the pedestal by 20 µm compared to a 5:1 mixing ratio of PDMS which would require a higher load cell reading. The section of code that establishes the loop and approach method can be seen below:

```
Creating a WHILE loop stating that while the load cell reading
is less than a given value (in volts (which is equivalent to
grams with the GSO-10 load cell) the stage is to lower by 0.01
mm at 0.1 mm/s.
     WHILE LoadCellOutput < 0.56

Triggers the digital scope to start collecting data.
     SCOPETRIG

Commands the stage to move down at 0.01 mm at a speed of 0.1
mm/s.
LINEAR <Axis> <Distance> F <CoordinateSpeed)
     Linear X 0.001 F 0.1

Cancels the digital scope data collection.
     SCOPETRIG STOP

Updates the value of the LoadCellOutput variable which will be
used in the next iteration of the WHILE loop.
     LoadCellOutput = SCOPEDATA (AnalogInput0, 1)
```

```
Ends the WHILE loop
     WEND
```

After the stamp has made contact with the mounted substrate, there was a relaxation period of 5 seconds which enables the stamp to relax and make better contact to the substrate. After this, the Digital Scope (the data collection software of the Ensemble Motion Controller) is set up again. This time however, unlike for the initial data collection, high frequency load cell measurements are required as well as a greater number of measurements. After scope is prepared, the data collection begins and the stage retracts at the preselected retracting speed for the distance that was selected previously.

3.4 General Adhesion Measurements and Data Processing

Each time an adhesion test was performed, the Ensemble Digital Scope would present a range of data sets, including the velocity profile, acceleration profile, and, most importantly, the load cell data. From this data, the minimum value is determined as well as the zero value of the load cell. An example of the data collected during an adhesion test is shown in Figure 3.22. The point at which the PDMS pedestal surface separated from the substrate corresponded to this minimum point. For example, for a stamp with no adhesive properties, the load cell reading would never be reduced to below the zero readings but for an adhesive stamp, such as a PDMS stamp made from Sylgard 184, the force of adhesion would raise up the load cell stem upward, providing a lower reading. Once this force is measured and recorded, the next adhesion test can be performed by modifying the code discussed in the previous section to change the

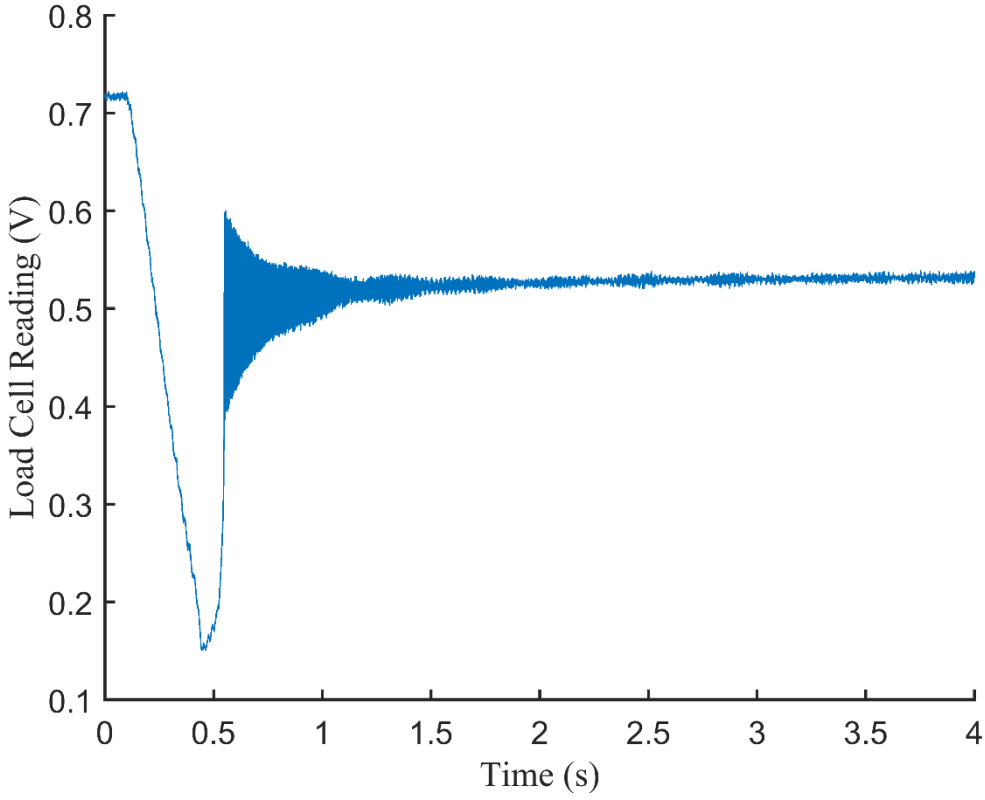

Figure 3.22: Graph showing an example of the data outputted by the load cell during a typical retraction process. The minimum point is the time that the stamp achieves the maximum adhesion before a crack is propagated along the stamp/substrate interface.

retraction speed. This was then performed for a range of velocities, usually between 35 $\mu m.s^{-1}$ and 700 $\mu m.s^{-1}$. These points were then plotted in order to obtain a graph showing the velocity dependant nature of any PDMS material.

3.5 References

[1] K. Felmet, Y. L. Loo, and Y. Sun, "Patterning conductive copper by nanotransfer printing," *Appl. Phys. Lett.*, vol. 85, no. 15, pp. 3316–3318, 2004.

[2] T. W. Odom, J. C. Love, D. B. Wolfe, K. E. Paul, and G. M. Whitesides, "Improved Pattern Transfer in Soft Lithography Using Composite Stamps," *Langmuir*, no. 9, pp. 5314–5320, 2002.

[3] H. Schmid *et al.*, "Preparation of metallic films on elastomeric stamps and their application for contact processing and contact printing," *Adv. Funct. Mater.*, vol. 13, no. 2, pp. 145–153, 2003.

[4] B. Jiang, X. Shi, T. Zhang, and Y. Huang, "Recent advances in UV/thermal curing silicone polymers," *Chem. Eng. J.*, vol. 435, no. P1, p. 134843, 2022.

[5] J. Wu, Q. Dan, and S. Liu, "Effect of viscoelasticity of PDMS on transfer printing," *16th Int. Conf. Electron. Packag. Technol. ICEPT 2015*, pp. 759–764, 2015.

[6] M. A. Meitl *et al.*, "Transfer printing by kinetic control of adhesion to an elastomeric stamp," *Nat. Mater.*, vol. 5, no. 1, pp. 33–38, 2006.

[7] V. Vohra, T. Anzai, S. Inaba, W. Porzio, and L. Barba, "Transfer-printing of active layers to achieve high quality interfaces in sequentially deposited multilayer inverted polymer solar cells fabricated in air," *Sci. Technol. Adv. Mater.*, vol. 17, no. 1, pp. 530–540, 2016.

[8] M. W. Lee, S. S. Yoon, and A. L. Yarin, "Release of Self-Healing Agents in a Material: What Happens Next?," *ACS Appl. Mater. Interfaces*, vol. 9, no. 20, pp. 17449–17455, 2017.

[9] The Dow CompanyChemical., "SYLGARD ™ 184 Silicone Elastomer Technical Datasheet," *Silicone Elastomer Tech. Data Sheet*, no. 11-3184–01 C, pp. 1–4, 2017.

[10] B. Ruben *et al.*, "Oxygen plasma treatments of polydimethylsiloxane surfaces: Effect of the atomic oxygen on capillary flow in the microchannels," *Micro Nano Lett.*, vol. 12, no. 10, pp. 754–757, 2017.

[11] S. Wang, D. Feng, C. Hu, and P. Rezai, "The simple two-step polydimethylsiloxane transferring process for high aspect ratio microstructures," *J. Semicond.*, vol. 39, no. 8, p. 086001, 2018.

[12] "Datasheet RS Pro PVC Harnessing Tape."

[13] UltraTape, "Arco Glass prtection Film Datasheet."

[14] "Kapton Tapes Datasheet." [Online]. Available: https://www.kaptontape.com/1_Mil_Kapton_Tapes_Datasheet.php.

[15] MicroChem, "Su-8 2025-75 Datasheet," pp. 1–5, 2006.

[16] Y. Ohkubo, K. Endo, and K. Yamamura, "Adhesive-free adhesion between heat-assisted plasma-treated fluoropolymers (PTFE, PFA) and plasma-jet-treated

polydimethylsiloxane (PDMS) and its application," *Sci. Rep.*, vol. 8, no. 1, pp. 1–11, 2018.

[17] S. Bhattacharya, A. Datta, J. M. Berg, and S. Gangopadhyay, "Studies on Surface Wettability of Poly(Dimethyl) Siloxane (PDMS) and Glass Under Oxygen-Plasma Treatment and Correlation With Bond Strength," *J. Microelectromechanical Syst.*, vol. 14, no. 3, pp. 590–597, 2005.

[18] M. A. Eddings, M. A. Johnson, and B. K. Gale, "Determining the optimal PDMS-PDMS bonding technique for microfluidic devices," *J. Micromechanics Microengineering*, vol. 18, no. 6, 2008.

[19] R. W. R. L. Gajasinghe *et al.*, "Experimental study of PDMS bonding to various substrates for monolithic microfluidic applications," *J. Micromechanics Microengineering*, vol. 24, no. 7, 2014.

[20] Ossila, "Ossila UV Ozone Cleaner Manual," pp. 1–22, 2020.

[21] Y. Berdichevsky, J. Khandurina, A. Guttman, and Y. H. Lo, "UV/ozone modification of poly(dimethylsiloxane) microfluidic channels," *Sensors Actuators, B Chem.*, vol. 97, no. 2–3, pp. 402–408, 2004.

[22] C. M. Yousuff, M. Danish, E. T. W. Ho, I. H. K. Basha, and N. H. B. Hamid, "Study on the optimum cutting parameters of an aluminum mold for effective bonding strength of a PDMS microfluidic device," *Micromachines*, vol. 8, no. 8, 2017.

[23] A. Carlson, S. Wang, P. Elvikis, P. M. Ferreira, Y. Huang, and J. A. Rogers, "Active, programmable elastomeric surfaces with tunable adhesion for deterministic assembly by transfer printing," *Adv. Funct. Mater.*, vol. 22, no. 21, pp. 4476–4484, 2012.

[24] S. Kim *et al.*, "Enhanced adhesion with pedestal-shaped elastomeric stamps for transfer printing," *Appl. Phys. Lett.*, vol. 100, no. 17, 2012.

[25] J. C. McDonald and G. M. Whitesides, "Poly(dimethylsiloxane) as a material for fabricating microfluidic devices," *Acc. Chem. Res.*, vol. 35, no. 7, pp. 491–499, 2002.

[26] Z. Brounstein, J. Zhao, D. Geller, N. Gupta, and A. Labouriau, "Long-term thermal aging of modified sylgard 184 formulations," *Polymers (Basel).*, vol. 13, no. 18, 2021.

[27] K. Ma, J. Rivera, G. J. Hirasaki, and S. L. Biswal, "Wettability control and patterning of PDMS using UV-ozone and water immersion," *J. Colloid Interface Sci.*, vol. 363, no. 1, pp. 371–378, 2011.

[28] O. T. Zaremba, A. E. Goldt, E. M. Khabushev, A. S. Anisimov, and A. G. Nasibulin, "Highly efficient doping of carbon nanotube films with chloroauric acid by dip-coating," *Mater. Sci. Eng. B Solid-State Mater. Adv. Technol.*, vol. 278, no. May 2021, p. 115648, 2022.

[29] Y. Chen *et al.*, "Controllable β-phase formation in poly(9,9-dioctylfluorene) by dip-coating for blue polymer light-emitting diodes," *Thin Solid Films*, vol. 746, no. January, p. 139118, 2022.

[30] M. Niazmand, A. Maghsoudipour, M. Alizadeh, Z. Khakpour, and A. Kariminejad, "Effect of dip coating parameters on microstructure and thickness of 8YSZ electrolyte

coated on NiO-YSZ by sol-gel process for SOFCs applications," *Ceram. Int.*, no. December 2021, 2022.

[31] H. K. Zhang, Y. R. Yin, X. M. Zhang, S. C. Chen, W. X. Chen, and G. H. Hu, "Numerical simulation of the hydrodynamics of yield stress fluids during dip coating," *J. Nonnewton. Fluid Mech.*, vol. 298, no. September, p. 104675, 2021.

[32] A. Kozbial *et al.*, "Study on the surface energy of graphene by contact angle measurements," *Langmuir*, vol. 30, no. 28, pp. 8598–8606, 2014.

[33] A. W. Hefer, A. Bhasin, and D. N. Little, "Bitumen Surface Energy Characterization Using a Contact Angle Approach," *J. Mater. Civ. Eng.*, vol. 18, no. 6, pp. 759–767, 2006.

[34] M. Gindl, G. Sinn, W. Gindl, A. Reiterer, and S. Tschegg, "A comparison of different methods to calculate the surface free energy of wood using contact angle measurements," *Colloids Surfaces A Physicochem. Eng. Asp.*, vol. 181, no. 1–3, pp. 279–287, 2001.

[35] J. S. Kim, R. H. Friend, and F. Cacialli, "Surface energy and polarity of treated indium-tin-oxide anodes for polymer light-emitting diodes studied by contact-angle measurements," *J. Appl. Phys.*, vol. 86, no. 5, pp. 2774–2778, 1999.

[36] M. Kalin and M. Polajnar, "The correlation between the surface energy, the contact angle and the spreading parameter, and their relevance for the wetting behaviour of DLC with lubricating oils," *Tribol. Int.*, vol. 66, pp. 225–233, 2013.

[37] M. E. Schrader, "Young-Dupre Revisited," *Langmuir*, vol. 9, no. 6, pp. 3585–3589, 1995.

Chapter 4

Comparison of Transfer Printing Compatibility of Different PDMS Silicones

This chapter will present and describe a comparison between a selection of commercially available PDMS silicones, Sylgard 184 (Dow), Sylgard 182 (Dow), Sylgard 170 (Dow), and Silcoset 105 (CHT) to determine compatibility of each for use as a material from which to create transfer printing stamps. An overview of Sylgard 184, the most commonly used PDMS silicone for the fabrication of transfer printing stamps, will be presented, followed by a look at some potential alternative silicones.

Following a discussion of alternative silicones, the curing conditions and processing for the selected alternatives will be detailed, followed by the data from adhesion tests performed in order to compare the adhesive nature of each PDMS silicone.

Finally the chapter will conclude with the results of adhesion testing performed with each PDMS as well as determining which PDMS material is most appropriate as a material to fabricate transfer printing stamps.

4.1 Introduction

4.1.1 PDMS Silicones

The most widely used PDMS silicone for use in the transfer printing field as a material to fabricate adhesive stamps from is Sylgard 184 [1][2][3][4]. It has become the default choice when creating transfer printing stamps dependant on adhesion control and switchable adhesion due to the viscoelastic nature of PDMS [5]. Other PDMS silicones are available and are often used in other fields, therefore a review has been carried out to determine the comparative performance of alternative silicones in transfer printing applications.

In regards to the physical properties, Sylgard 184 is a transparent and flexible silicone with a high electrical resistivity (2.9 x 10^{14} Ω.cm) [6] and a Young's Modulus of 1.32-2.97 MPa (depending on the curing conditions) [7] which has been shown to have a peel velocity dependant adhesive nature [8], allowing for easy switchability between a high adhesion state and a low adhesion state. This high and low adhesive state is a highly exploited property of Sylgard 184 when used for transfer printing as it enables the pickup and printing of material, also referred to as an ink, from the donor substrate upon which the material or devices have been deposited or grown, onto a receiving target substrate. By being able to change the adhesive nature of the stamp in-situ, potential substrates and ink that were previously unavailable can be used by using a high adhesive state to selectively pick up ink from the donor substrate and a low adhesive state to print onto a receiving substrate, this process is detailed

For a PDMS silicone to be suitable for fabrication of a transfer printing stamp, it often is necessary to structure the surface in order to create pedestals, small raised areas which allow for contact to be made between the stamp surface and the desired ink only. Often this is

achieved by casting the uncured PDMS mixture against a patterned solid mould in order to create a structured and patterned surface through a process called soft lithography [9]. This method has been used extensively in a range of fields such as microfluidics [10], and MEMS applications [11] and can yield high accuracy and precise castings of features down to 100 nm [12].

PDMS are a type of silicone with a backbone of Si-O chains [13]. Sylgard 184 is an addition cure PDMS where a curing agent is added to a base PDMS, the chemical structure and curing process for PDMS can be seen in Figure 3.1 in Chapter 3. In order to cure Sylgard 184, it must be mixed with a curing agent at a suggested ratio of 10:1 (base : curing agent) and left to cure for 48 hours at room temperature or at an elevated temperature, reducing its curing time to 35 minutes at 100°C. As a result of this wide curing temperature range, a wide range of moulds and mould materials are compatible, such as Polylactic acid (PLA), a polymer common as a 3D printing filament material which can deform or melt at high temperatures [14], silicon [15], or photoresists [16]. This diversity in curing conditions potentially opens up Sylgard 184 as a PDMS silicone to a wider range of applications.

4.1.2 Alternative PDMS Silicones

Sylgard 184 is but one type of PDMS silicone. It is a variant of another product produced by Dow, Sylgard 182. The properties of these two PDMS silicones are similar with both being a transparent and flexible PDMS which has a Young's Modulus of 0.935 Mpa [17], slightly lower than that of Sylgard 184 (~1.3 Mpa [7]), a tensile strength of 7.6 Mpa [18] compared to

the tensile strength of Sylgard 184 which is 6.7 Mpa [6], and a Shore hardness of 51 [18] to Sylgard 184s 43 [6]. The similarities in physical properties between Sylgard 184 and Sylgard 182 make Sylgard 182 a potential alternative PDMS for use as a transfer printing stamp material while the difference in Young's modulus could increase the maximum adhesion achieved by a stamp made from this material [19].

Sylgard 182 however has a significant difference in curing conditions compared to Sylgard 184. Unlike Sylgard 184 which can be cured at room temperature and at elevated temperatures, Sylgard 182 can only be cured at elevated temperatures [20], this has the effect of limiting the applications where Sylgard 182 is a suitable casting material due to additional factors such as a mould material that cannot be heated, or the inclusion of low boiling point additives to the PDMS otherwise the cast PDMS may become porous as shown by Kwak et al [21] who intentionally mixed a range of solvents including isopropyl alcohol, ethanol, and acetone into the Sylgard 184 base in order to achieve microporous PDMS.

As a result of the Sylgard 182 curing only at high temperatures, the working time of this PDMS is substantially increased, from 90 minutes, the working time for Sylgard 184, to 8 hours. This increased working time can provide a greater operating window during which further stages in the casting process can be performed, such as outgassing, an important stage during PDMS casting which removes trapped air bubbles which occur while mixing. This would also assist in the repeated casting using the same exact mixing ratios or with precise quantities of additives, such as in [22] where carbon dots, a potential substitute for inorganic quantum dots, are embedded within a PDMS stamp. When performing repeat and successive castings using a shorter working time PDMS like Sylgard 184, it is often necessary to mix new PDMS for each casting. When performing castings that involve the addition of material, like the carbon dots mentioned previously, this may be inefficient as the addition process takes

time. By mixing a larger quantity of longer working time PDMS initially, future mixings would be avoidable.

Another PDMS that is a part of the Sylgard product line is Sylgard 170, primarily designed as a thermally conductive elastomer encapuslant and potting material for electrical components [23]. Unlike the previous two Sylgard PDMS silicones the two components of Sylgard 170 contain larger quantities of additives, 44% quartz and 0.84% zinc oxide in Component A, and 45% quartz in Component B [24] which modify the properties to allow for better performance in a plotting application. However, these additive could impact the adhesion achievable by a transfer printing stamp made from Sylgard 170. Sylgard 170 is an opaque grey PDMS which is significantly less flexible than Sylgard 184 and Sylgard 182 and has a Young's modulus of 0.65 Mpa [25]. Composed of equal quantities of 2 components, Sylgard 170 has a much shorter working time of 15 minutes and a rapid high temperature curing time of 10 minutes at 100°C but is curable at room temperature, giving flexibility to the casting conditions.

An additional encapuslant PDMS silicone is Silcoset 105, an opaque white silicone with a high electrical resistivity of 5.8×10^{13} Ω.cm [26] and a high operating temperature range of between -60°C and 200°C. Like with Sylgard 170, Silcoset 105 contains an additive that might have a significant impact on the adhesive properties it exhibits. The primary additive in Silcoset 105 is calcium carbonate (16-17.5%), with small quantities of partially hydrolysed ethylsilicates (2.5-3%), dodecamethyl cyclohexasiloxane (0.1-0.2%), and decamethylcyclopentasiloxane (0.1-0.2%) [27]. The primary application of this PDMS silicone is as a potting or embedding material for delicate electrical equipment but also as a mould materials for surface detail reproduction. These additives, as well as the low tensile strength could lead to a low adhesive alternate PDMS to Sylgard 184, which could be advantageous when attempting to pick up ink that is not well adhered to a donor substrate, as a highly adhesive PDMS stamp may struggle to print the ink onto a receiving substrate without an

adhesion promoting layer being first deposited onto a receiving substrate. A summary of the physical properties of Sylgard 184, Sylgard 182, Sylgard 170, and Silcoset 105 are summarised in Table 4.1.

Table 4.1: Comparison of some of the physical properties of Sylgard 184, Sylgard 182, Sylgard 170, and Silcoset 105.

	Sylgard 184	Sylgard 182	Sylgard 170	Silcoset 105
Young's Modulus	1.32-2.97 Mpa (depending on curing conditions) [7]	0.935 Mpa [17]	0.65 Mpa [25]	-
Tensile Strength	6.7 MPa [6]	7.6 MPa [18]	2.9 MPa [23]	1.1 MPa [26]
Shore Hardness	43 [6]	51 [18]	50 [23]	45 [26]

4.1.3 Adhesion Testing

For transfer printing in particular, it is crucial to have an understanding of how the adhesive nature of a stamp can change depending on the velocity of the retraction from a surface. Sylgard 184 in particular has shown to have a strong velocity dependant adhesion (a 4-fold increase from 10 $\mu m.s^{-1}$ to 750 $\mu m.s^{-1}$ [28] which has enabled transfer printing to become so adaptable and useful for applications such as the pickup and print of semiconductor devices from a native substrate to a receiver substrate. In order for these other silicones to be considered as a potential replacement, or as an alternative, it is important to characterise the properties and retraction

velocity dependant adhesion in order to understand the behaviour of these silicones in a transfer printing application.

4.2 Casting Methods

For this study, four PDMS silicones were selected, Sylgard 184, Sylgard 182, Sylgard 170 and Silcoset 105. In order to provide repeatable and comparable PDMS stamps with precisely controlled dimensions and structures it was necessary to develop a moulding and casting process. This section will describe the stamp fabrication process for these four PDMS silicones along with the specific mould fabrication process.

4.2.1 Mould Creation

SU-8 photoresist (SU-8 2050, MicroChem) was used to create the structured master moulds, spun to a thickness of 100μm onto a piece of Si(100) wafer. A Si(100) wafer was cleaved into 1.5cm by 1.5cm pieces then cleaned using n-Butyl acetate (Fisher Chemical), acetone (99% acetone, Fisher Chemical), and isopropyl alcohol (99.8% isopropyl alcohol, Fisher Chemical) to remove any dust, particulates, or other surface contaminants. A dehydration baking stage was then performed on the Si(100) substrate by baking the substrate on a hotplate set to 100°C for 1 minute which removed any moisture from the surface which could impact the photolithography process.

After the dehydration bake, the substrate was mounted onto a programmable spinner and spun for a few seconds while blowing the surface with nitrogen. This helped to remove any dust from the surface which may have settled during the dehydration bake. Once the substrate was free from dust, moisture and other contaminants, SU-8 2050 was deposited onto the surface of the substrate. Due to the viscosity of SU-8 2050 (12900 cSt [29]), the entire substrate surface had to be covered with SU-8 before spinning to avoid gaps in the SU-8 film left after spinning. The deposition of the SU-8 often left bubbles trapped in the SU-8 coating which could destroy the final SU-8 and Si(100) mould. To remove these the sample was left for between 30 seconds and 60 seconds after the SU-8 was deposited allowing any bubbles that were trapped in the SU-8 during deposition to burst. Any remaining bubbles were either removed using a pipette if they were large enough or, if only very small bubbles remained, these were often removed by later processing stages.

Once the SU-8 layer was free of most of the bubbles, the sample was spun at 500 rpm for 15 seconds with an acceleration of 100 rpm/s increasing to a spin speed of 1700 rpm for 30 seconds with a 300 rpm/s ramp rate. The resulting SU-8 layer was found to have large edge beads which would inhibited good contact with the mask during the exposure step. An edge bead removal process was performed, using 0.5 ml of an edge bead remover (EBR PG, MicroChem) which was sprayed onto the SU-8 layer. Once coated in the edge bead remover, the sample was placed onto a levelled plate and covered with a plastic cover with a small 1mm hole drilled into the top, restricting the rate at which the edge bead remover would evaporate. Visual inspections were performed after 24 hours at room temperature and if the surface did not appear to be flat or bubble free, the edge bead removal process was repeated.

A soft bake was then performed by placing the SU-8 coated Si(100) onto a hotplate at 65°C for 5 minutes followed by a 95°C bake for 16 minutes. The soft baked sample was then aligned to the mask made from quartz glass and titanium using a UV400 mask aligner and

exposed for 48 seconds. After the exposure the SU-8 was then baked at 65°C for 4 minutes then for 9 minutes at 95°C.

Unexposed SU-8 was then removed with the use of an ultrasonic bath (UT8031/EUK Ultrasonic Cleaner, Shesto) by submerging the sample in a beaker of SU-8 developer and placing into the ultrasonic bath for 6 minutes on delicate mode with visual checks being performed every 2 minutes to check the development progress. Once all unexposed SU-8 was removed, the sample was rinsed with de-ionised water and dried with nitrogen. Small cracks in the SU-8 surface were common at this stage and were repaired by performing a 30 second bake at 180°C causing the SU-8 to re-flow and 'heal' the cracks. The final stage was to flood expose the entire SU-8 surface with the UV400 mask aligner for 5 minutes.

For high temperature casting, an aluminium frame was used backed with adhesive tape. There were multiple iterations of this mould before a reliable mould was developed. Castings that relied upon mould components clamped together encountered the issue that small quantities of PDMS that leaked between the two parts which led to difficulty separating the mould parts. To bypass this, an aluminium frame was selected, the thickness of which would determine the thickness of the final PDMS stamp. By using an adhesive tape across the back of the frame, the mould is sealed on 5 sides and a structured facet of the mould can be introduced, such as by using a silicon wafer and SU-8 mould. Polyimide tape was selected as an adhesive tape backing as the silicone adhesive used would not impact the curing of the PDMS and its high temperature stability (up to 260°C [30]) , as well as due to the silicone adhesive used in the tape, it does not interfere with the curing of PDMS silicones. This can be seen in Figure 4.1.

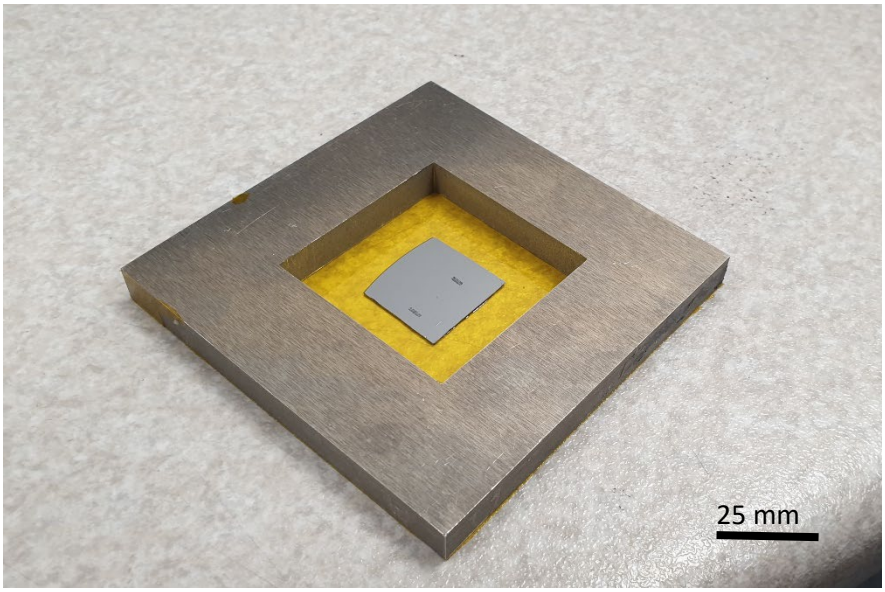

Figure 4.1: Photograph showing the aluminium frame backed with polyimide tape and an SU-8 photoresist on Si mould is adhered inside.

When curing a PDMS silicone at room temperature the mould used was a silicon and patterned and baked SU-8 photoresist in order to achieve a structured surface, which was placed into a polystyrene Petri dish as shown in Figure 4.2. Prolonged contact to adhesive tape, such

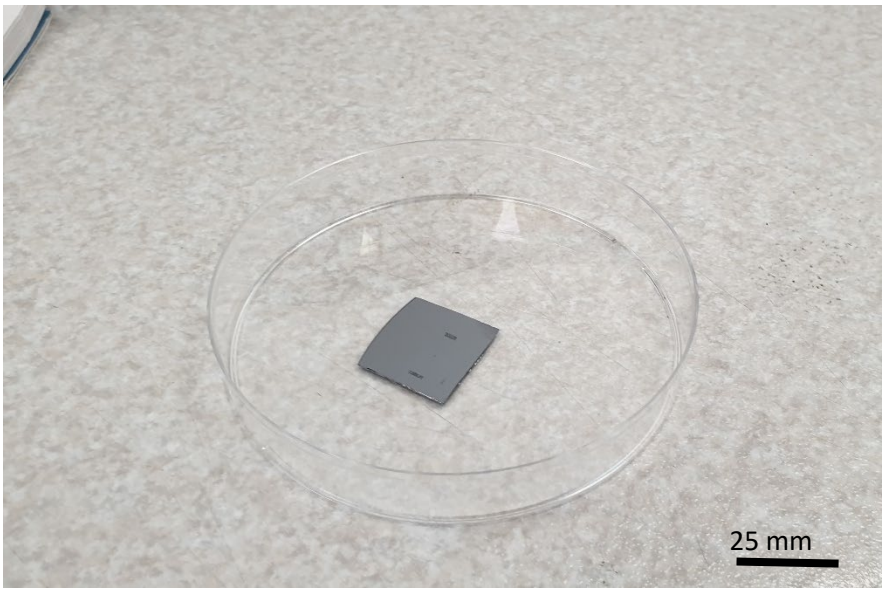

Figure 4.2: Photograph showing the mould setup for room temperature castings. An SU-8 photoresist on Si mould can be seen located inside the polystyrene Petri dish.

as those used for the high temperature casting process led to either inhibited curing of the PDMS or permanent bonding to the tape. One challenge that had to be overcome was to ensure that the silicon and SU-8 mould was flat during casting. Often, once the PDMS was poured, the silicon and SU-8 mould would begin to float, leading to a casting that is not flat. A way around this was to use small pieces of polyimide tape to adhere the mould to the base of the Petri dish.

4.2.2 Sylgard 184 and Sylgard 182

Sylgard 182 and Sylgard 184 both have the same processing method, with the only difference occurring when curing. The base silicone was weighed out into an aluminium tin and weighed using a mass balance before being mixed with the relevant curing agent in a 10:1 ratio of base to curing agent by mass. This was then thoroughly mixed using a plastic spoon for 5 minutes to ensure a complete and even mixture of the two parts. The Sylgard 184 and Sylgard 182 slurries were then placed into a vacuum desiccator and outgassed for 10 minutes, before being brought back to atmospheric pressure. This was then repeated typically between two and three times until the mixture slurries appeared bubble free. The number of outgassing repetitions required depended on the quantity of PDMS in the aluminium tin. Figure 4.3 shows the importance of the outgassing stages and Figure 4.4 shows what impact bubbles can have on the final cast PDMS

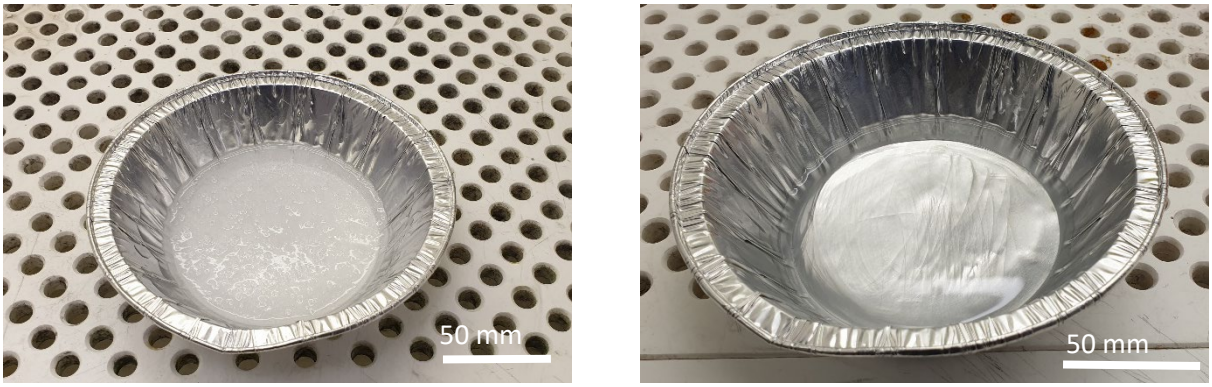

Figure 4.3: Mixed Sylgard 182 mixture before outgassing (left) and after 20 minutes of outgassing (right).

The bubble free mixtures were then poured from a low height into the mould to ensure minimal introduction of new bubbles. Once the mould was full, it was left for 5 minutes to allow any newly introduced bubble to rise to the surface. Once at the surface, these could then be burst manually using a pair of tweezers, or by gently blowing the surface of the PDMS with a nitrogen gun. Once the mould was full and the PDMS mixture inside was bubble free, the entire mould was placed into a laboratory oven set to 100°C. As stated previously, the Sylgard 184 required 35 minutes (detailed in Chapter 3: Experimental Techniques) in the oven to full cure, while the Sylgard 182 was left in the oven for 75 minutes to fully cure. These were then immediately removed from the oven once the time had elapsed and removed from the mould. Once released from the mould and left to cool, the stamp was trimmed using a scalpel to remove the excess material.

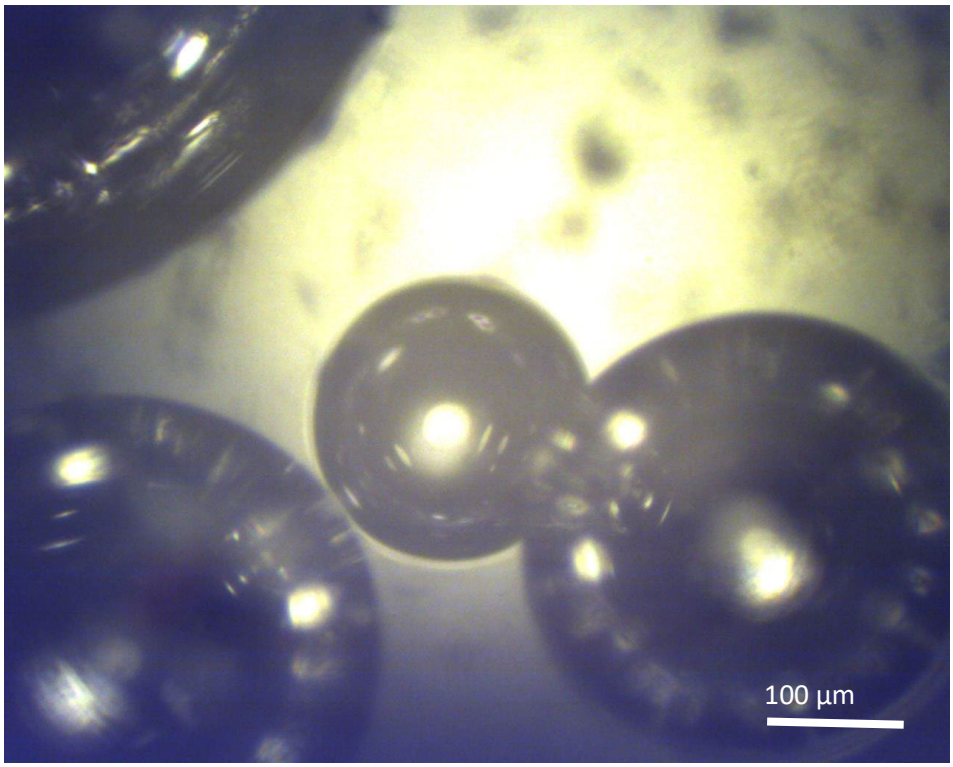

Figure 4.4: Microscope image of bubbles formed on the surface of Sylgard 184 when not fully outgassed. The central bubble is approximately 200µm in diameter which would be large enough to completely engulf any features that were to be cast onto the PDMS stamp.

4.2.3 Sylgard 170

In order to fabricate the stamp made from Sylgard 170, the process differs slightly from the other Sylgard PDMS silicones in this report. Firstly, equal quantities of the Sylgard 170 Part A and Part B are poured into separate aluminium tins and measured on a mass balance. Part B was poured into the tin containing the Part A and mixed with a plastic spoon thoroughly. Sylgard 170 has a very short working time of 15 minutes so the mixing was done thoroughly but quickly. Unlike with Sylgard 184 and 182 where both the curing agent and the base are a transparent colourless liquid, Part A of the Sylgard 170 is an opaque dark grey and Part B

is an opaque white, so it is visually obvious once the two parts are mixed thoroughly. Once the Sylgard 170 mixture was mixed, it was outgassed for 5 to 10 minutes. Sylgard 170 is much less viscous than the other silicones tested in this report, so outgassing occurs quickly.

Once the outgassed and mixed Sylgard 170 is ready, it is carefully poured from a low height into the prepared mould. As this PDMS is opaque, it is impossible to see if there are any trapped bubbles in the poured PDMS, so the remaining working time was spent gently agitating the mould in an attempt to release any trapped bubbles. Any that rose to the top were popped with tweezers or a nitrogen gun, in the same manner as for the other Sylgard products previously discussed. The filled mould was then placed into a laboratory oven set to 100°C for 10 minutes. Due to the short curing time, any minor temperature changes, such as opening the oven door, can have a noticeable impact on the curing time and can extend the duration of time in the oven up to 12 minutes depending on the oven.

When the Sylgard 170 had completely cured, it was removed from the oven and immediately peeled from the mould. If the Sylgard 170 was left to cool before removal from the mould, it was liable to adhere to the adhesive polyimide tape, damaging the stamp. This

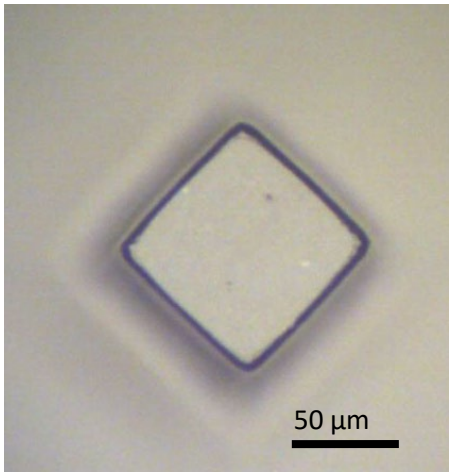

Figure 4.5: Sylgard 170 casting of a 100µm^3 pedestal design to be used to measure the adhesion of the Sylgard 170 stamp surface to a Si(100) substrate.

was then trimmed with a scalpel to remove excess material. Extra care was taken when removing stamps made from Sylgard 170 from the mould as it is less flexible than Sylgard 184 and 182, and was prone to tearing or splitting. A microscope image of the finished Sylgard 170 pedestal stamp can be seen in Figure 4.5.

4.2.4 Silcoset 105

The casting process for a transfer printing stamp made from Silcoset 105 starts in a similar way to the other silicones, by pouring some of the base Silcoset 105 into an aluminium tin and measuring the mass on a mass balance. The CA28 curing agent was added to the base in a ratio of 100:1 base to curing agent, due to this, it was typically easier to mix a single large batch of Silcoset 105 and performing multiple castings with it in order to accurately add the correct quantity of curing agent.

Once the curing agent was added, the Silcoset 105 mixture was thoroughly combined with a plastic spoon and outgassed in a desiccator for 10 minutes, before returning to atmospheric pressure. This outgassing process was repeated until there were no longer bubbles present. Silcoset 105 has a higher viscosity and often took longer to outgas than the other silicones, so three outgassing cycles were often necessary to achieve a bubble free mixture. Once bubble free, the Silcoset 105 mixture was poured slowly over the prepared mould and cured at room temperature for 7 hours. Once cured, the stamp was peeled from the mould and trimmed down with a scalpel to remove excess material. This PDMS silicone adhered more firmly to the silicon and SU-8 mould, so additional care was taken when peeling the stamp from the mould in order to ensure no damage occurred to the structured mould or to the Silcoset 105 stamp.

4.3 Adhesion Testing and Results

4.3.1 Transfer Printing System and Equipment

In order to obtain the velocity dependant adhesion properties of the PDMS silicones being investigated, the transfer printing system previously described was used. The details of the system used are described in more detail in Chapter 3: Experimental Techniques. A Si(100) wafer was used as a representative surface to which the adhesion of the PDMS was tested.

Each PDMS stamp under investigation was adhered to a clean glass slide by placing the back of the PDMS stamp in contact with a clean glass slide and attached to the z-axis stage using the vacuum chuck and vacuum pump. Once secured in place, the x/y-stage was used to position the silicon wafer on the load cell under the pedestal on the PDMS stamp surface. Using the tilt stage on the x/y-stage, the silicon surface was adjusted to ensure it was parallel to the stamp surface (this stage was usually only necessary if there was an uneven rack in the curing oven, causing a slightly angled PDMS surface).

Once the stamp was in the correct position and aligned to the silicon test wafer surface, the Aerobasic code (this is discussed in more detail in the Chapter 3: Experimental Techniques) was used to control the z-stage to lower the stamp into contact with the substrate surface and gently compressing the pedestal slightly (10-20 μm). Figure 4.6 shows the transfer printing setup in action while performing an approach process to the load cell. Once compressed the stage had a relaxation period of 5 seconds to ensure the stamp had time to flow (due to PDMS being a viscoelastic material [31] it has the capability to flow when undergoing deformation) and reduce any internal strain before retracting with a desired retraction speed (ranging from

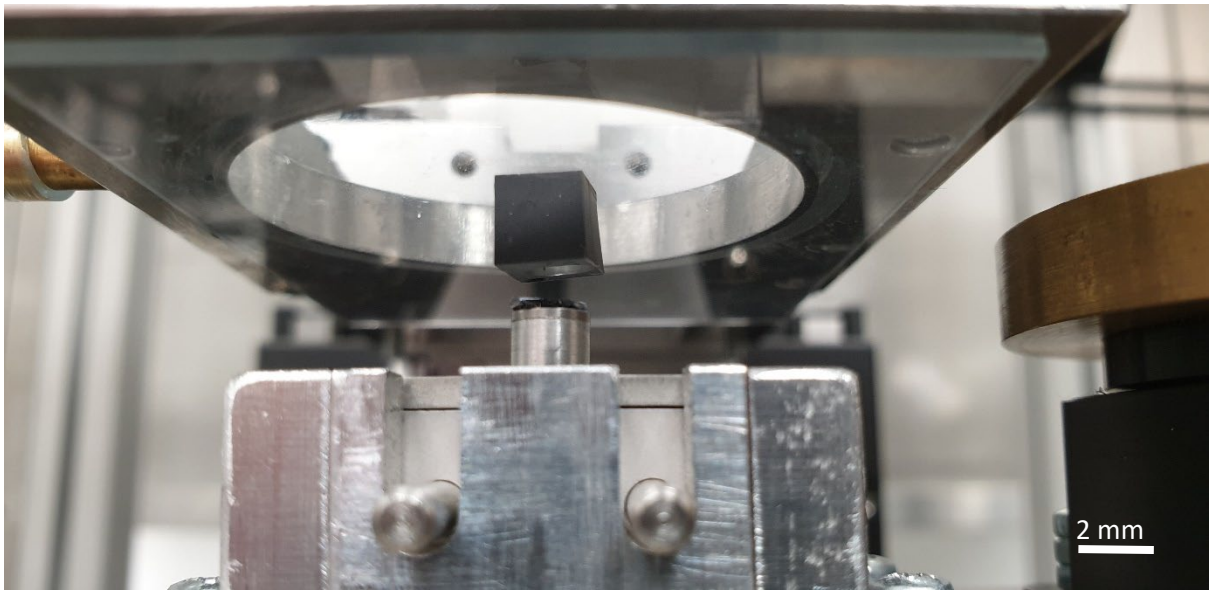

Figure 4.6: Sylgard 170 pedestal stamp during manual approach to the load cell. The purpose of this manual approach is to bring the PDMS stamp surface close to the substrate mounted onto the load cell quickly, without the need of the approaching Aerobasic code which can be very slow.

35 μm.s^{-1} to 700 μm.s^{-1}). These last steps using the Aerobasic code were then repeated for a range of retraction speeds.

There were a major challenges that were encountered while performing initial adhesion measurements which led to modification to the transfer printing system. Before the SU-8 patterning process was established, flat PDMS stamps were used to obtain adhesion data. These stamps, due to being completely flat, made contact with the entire surface of the substrate that was mounted onto the load cell. The effect of this was to provide a larger magnitude of the force of adhesion data that was collected. However, at higher retraction speeds, the force of adhesion began to approach the maximum force that the load cell was able to measure (±10g). Passing this value could cause damage to the load cell, or in some cases, complete destruction

of the load cell. In order to prevent this, the SU-8 patterning process was developed, enabling the fabrication of pedestal structured stamps, which would reduce the contact area between the stamp surface and the substrate surface. This drastically reduced the magnitude of the adhesion measurements taken, protecting the load cell.

The reduction in the magnitude of the load cell readings was necessary to prevent damage occurring to the load cell, however, previously negligible levels of background noise now began to interfere with the load cell readings, and in the case of low retraction speed adhesion test results, which yielded a much smaller force of adhesion, which could completely mask any useful adhesion data. To attempt to remove or at least reduce the noise that was picked up by the load cell a range of modifications were made to the transfer printing system.

Firstly the entire transfer printing system was transferred from an optical bench, onto an optical bench with a floating bench top. By moving onto this bench, any physical vibrations would not impact the load cell readings. It was noted previously that even vibrations caused by other laboratory users walking nearby could be detected by the load cell. This had the effect of reducing the background noise present in the load cell readings, however a particular noise artefact was still present at irregular times throughout the day which was not removed by the vibration isolation of the load cell.

In an attempt to remove this noise artefact, a Faraday cage was designed and built specifically to surround the transfer printing system which would shield the load cell from any induced EMI that was present. See Figure 4.7 for a photograph of the transfer printing system with the Faraday cage installed. The floating optical bench that the transfer printing system was previously moved onto was smaller than the original optical bench it was designed for. This meant that when a Faraday cage was installed, the microscope rig had to be redesigned in order to accommodate the cage. This cage provided a complete enclosure to the transfer printing

system with the exception of small holes in the sides and back that enabled nitrogen gas lines and power cables to be fed to the transfer printing system. A by-product of this shielding was also protection against air movement throughout the laboratory, caused by air conditioning units in the ceiling, which could have introduced some background noise due to vibrations in the air.

The Faraday cage and the vibration isolation was not sufficient to remove the noise artefact that remained present in load cell readings. Although the load cell was shielded by the Faraday cage, the wire connecting it to the motion controller, which also acted as a method of data collection, was not. This wire was replaced with a twisted pair wire, wrapped around a ferrite core which was then connected to a shielded cable outside of the Faraday cage which led out of the Faraday cage, and into the motion controller.

This had the effect of reducing much of the background noise, however, the noise artefact persisted. A final addition to the transfer printing station was the introduction of an uninterruptable power supply (UPS). A UPS is often used in order to protect a piece of equipment in case of a power cut or power failure. When connected to a mains power supply, an internal battery is charged. If the mains power is switched off for any reason, this battery takes over, supplying mains power for a short period of time (around 24 hour depending on the power draw of the connected equipment) to any connected equipment. However, a UPS also acts as a filter to the mains power due to this charging of the battery. The building in which the laboratory where the transfer printing station is housed, also contains a large quantity of pumps and chillers that could introduce noise along mains power lines. A UPS was hoped to reduce the impact of this and, along with the other measures taken to reduce noise, the overall effect was a reduction in noise which was sufficient to allow low velocity retraction speed adhesion measurements to be taken.

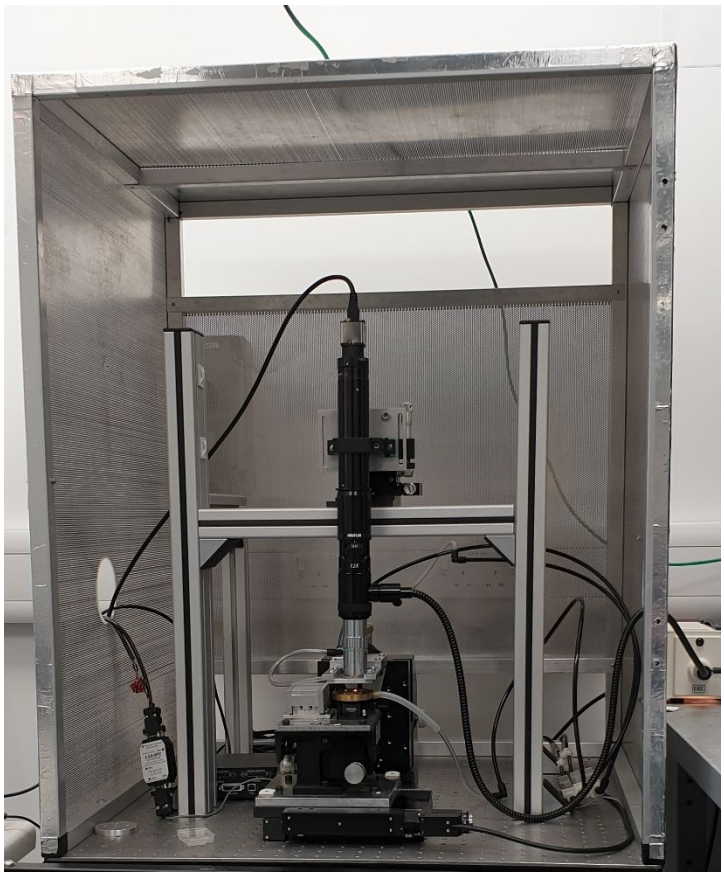

Figure 4.7: Photo of the transfer printing system used throughout this report. In this configuration a vacuum chuck and a load cell are mounted upon the x/y stage. Note: in this photograph the door covering the front of the Faraday cage has been removed to enable ease of access.

4.3.2 Sylgard 182

As discussed earlier in this chapter, Sylgard 182 has a similar appearance and physical properties to the Sylgard 184 PDMS silicone that is most commonly used as a transfer printing stamp. Figure 4.6 shows a comparison between the velocity dependant adhesion of a 100 μm^2 contact area of a Sylgard 182 stamp and a Sylgard 184 stamp across a range of velocities between 35$\mu m.s^{-1}$ and 700 $\mu m.s^{-1}$. An example of the data outputted by the load cell during

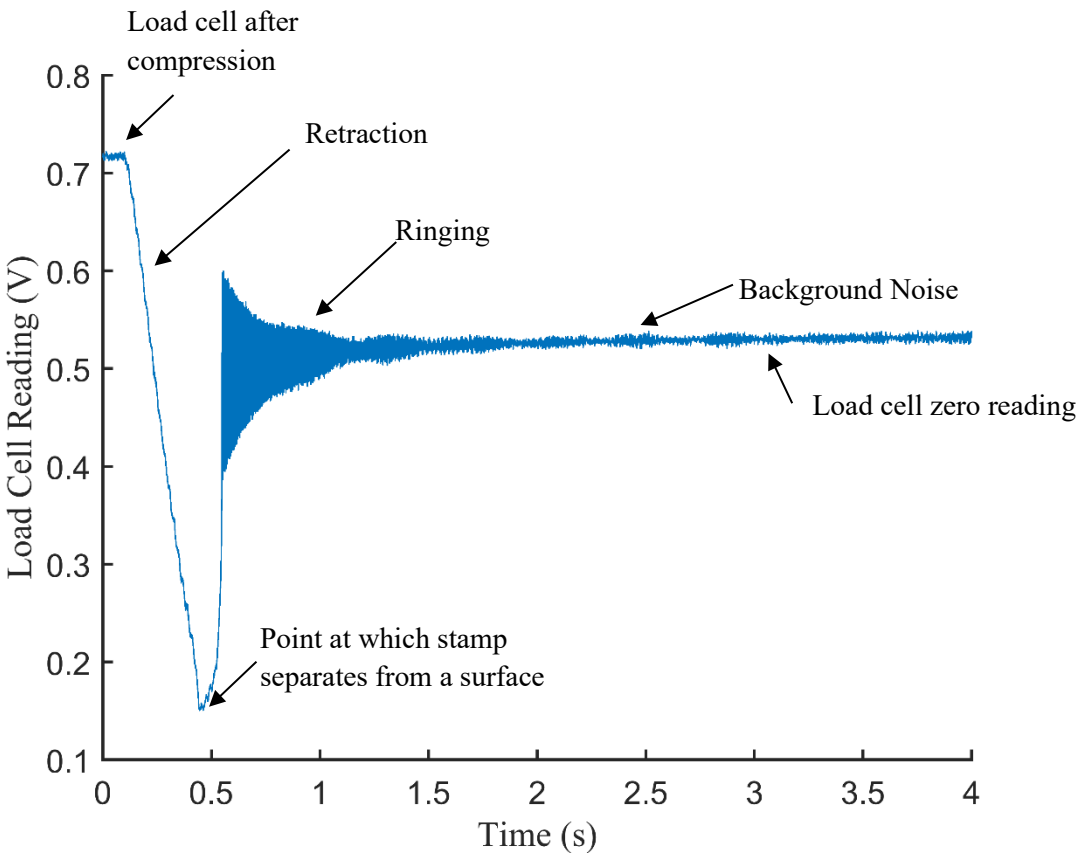

Figure 4.8: An annotated graph of an example data set collected by the load cell during a typical retraction process. Initially the data set starts with the load cell having been compressed, then the stamp surface being retracted away from the sample surface. The lowest point is when the stamp separated from the load cell surface and the load cell returns to its zero position after some ringing.

each of these retraction processes is included in Figure 4.8 along with annotations identifying the different aspects of the data.

As can be seen in Figure 4.9 Sylgard 182 displays a similar velocity dependant adhesion to Sylgard 184. A curve has been fitted with a power fitting [28] to guide the eye and the error bars are ±5%. At sub 200 $\mu m.s^{-1}$ retraction speed, Sylgard 182 displayed a slightly lower force of adhesion than Sylgard 184. Above 200 $\mu m.s^{-1}$ retraction speed however, Sylgard 182 displayed a slightly higher level of adhesion to the silicon substrate than Sylgard 184 achieving

a maximum adhesion force of 1.2 mN at 700 µm.s^{-1} compared to 1.1 mN at a retraction speed of 700 µm.s^{-1} which was achieved by a comparable Sylgard 184 stamp.

The slight differences in the adhesion could be due to the curing time differences and potential inaccuracies in the temperature control of the laboratory oven. As Sylgard 182 takes much longer to cure at 100°C than Sylgard 184, the impact of over and under curing would be much reduced as opposed to Sylgard 184. As shown in [32], the thermal degradation or thermal aging of Sylgard 184, which would also apply for Sylgard 182 as well, shows that at elevated temperatures, such as those used during high temperature curing, reduce the tensile elongation during prolonged exposure to elevated temperatures. Although the effects of

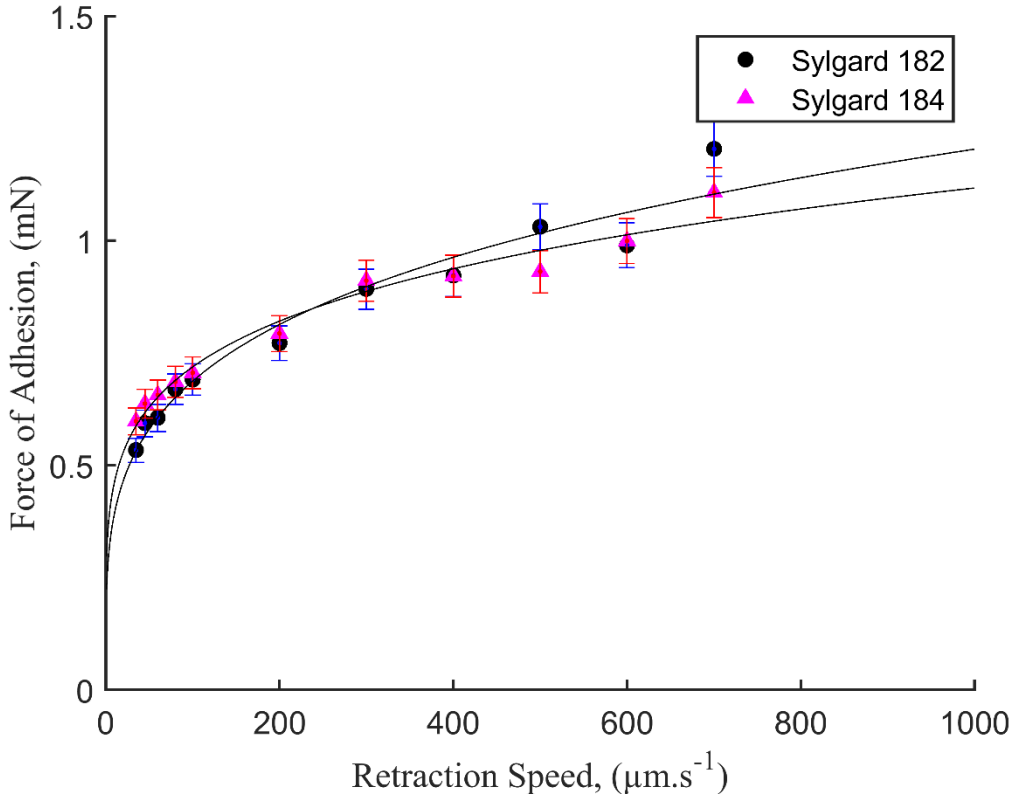

Figure 4.9: Graph showing the retraction velocity dependant adhesion for a Sylgard 184 stamp and a Sylgard 182 stamp with a 100 µm^2 contact area when brought into contact and retracted from a clean Si(100) surface.

thermal degradation take significantly longer (~25 hours) to impact the physical characteristics of PDMS than the time that the castings here were performed [32], on the much smaller scale and more sensitive adhesion measurements taken, these could have an impact similar to the differences seen in the adhesion data in Figure 4.9.

4.3.3 Sylgard 170

Unlike with the Sylgard 182, Sylgard 170 has very different physical properties as described earlier. As well as these differences in physical characteristics and properties, the adhesion of the Sylgard 170 stamp displayed a significantly lower overall adhesion which can be seen in Figure 4.10. A curve has been fitted with a power fitting [28] to guide the eye and the error bars are ±5%. At 700μm.s^{-1} the force of adhesion of the Sylgard 170 stamp to a Si(100) substrate was only 0.55 mN, in comparison, a Sylgard 184 stamp at that retraction speed achieved 1.1 mN. At 35μm.s^{-1}, the lowest retraction speed investigated in this report, Sylgard 184 displayed an adhesive force of 0.6 mN, higher even than the maximum value achieved by a Sylgard 170 stamp.

Like with the Sylgard 184 and Sylgard 182 where the curing conditions may have accounted for some of the variations in the adhesion, the curing conditions may also have impacted the adhesive nature of the Sylgard 170. Due to the much shorter curing time needed for Sylgard

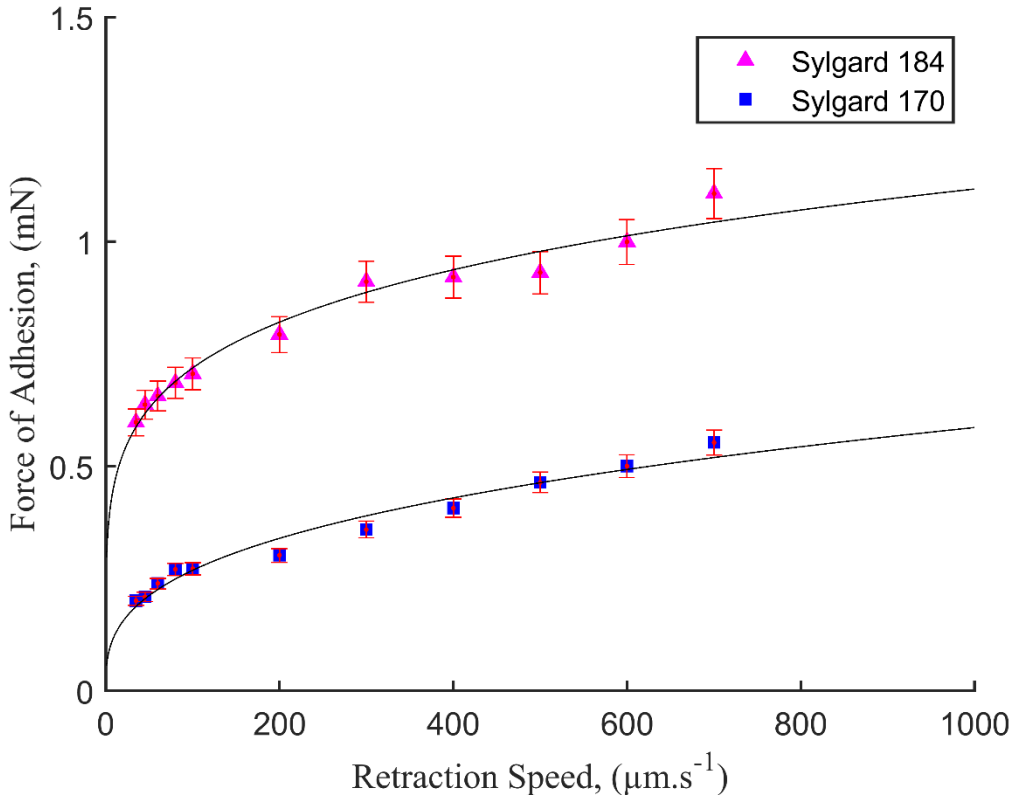

Figure 4.10: Graph showing the retraction velocity dependant adhesion for a Sylgard 184 stamp and a Sylgard 170 stamp with a 100µm^2 contact area when brought into contact and retracted from a clean Si(100) surface.

170 (10 minutes at 100ºC) it is possible that minor variations in the curing temperature could have a proportionally larger impact on the final PDMS silicone.

However, the significant difference between the adhesion curves of Sylgard 184 and Sylgard 170 is more likely down to a difference in the Young's modulus of each material and the additives in Sylgard 170. Sylgard 170 has a much lower Young's modulus than Sylgard 184 and Sylgard 182 which has been shown to have an impact on the adhesion of a stamp [5]. Not only does Sylgard 170 have a lower Young's modulus than Sylgard 184, but it also contains a large quantity of additives (44% in Component A and 45% in Component B) which may also have an impact on the adhesion achieved by a stamp made from Sylgard 170.

4.3.4 Silcoset 105

Experimentation using Silcoset 105 showed that within the retraction speed range of 35-3000 $\mu m.s^{-1}$, a 100 μm^2 pedestal contact area displayed no notable adhesive nature, velocity dependant, or otherwise, as can be seen in Figure 4.11. The reason for this apparent lack of adhesion could be due to the following reasons. Firstly, as is seen with Sylgard 170, the velocity dependant adhesion of a PDMS stamp seems to be, to some degree, dependant on the viscoelasticity of the PDMS itself. This would mean that a less flexible PDMS silicone such as Sylgard 170 and Silcoset 105 would see a lower adhesion to those that are more viscoelastic, like Sylgard 184 and Sylgard 182. We see that in the adhesion results in Figure 4.6 and Figure 4.7 where Sylgard 184 and 182 are very similar in their velocity dependant adhesion and Sylgard 170 and Silcoset 105 are significantly lower. The reason that Silcoset 105 may see absolutely no adhesion could be a result of the additives present in the base PDMS. The base Silcoset 105 contains, in addition to the siloxane chains, 16-17.5% calcium carbonate [27]. Sylgard 170 also contains a large percentage of additives, however a transfer printing stamp made from this PDMS silicone still displays adhesive properties with a peel velocity dependency. The impact these different additives may have on the final PDMS may depend on the size, shape, or material properties of the particular additive which could impact the smooth and flat surface that is necessary for a PDMS stamp to achieve good contact between the stamp surface and the substrate.

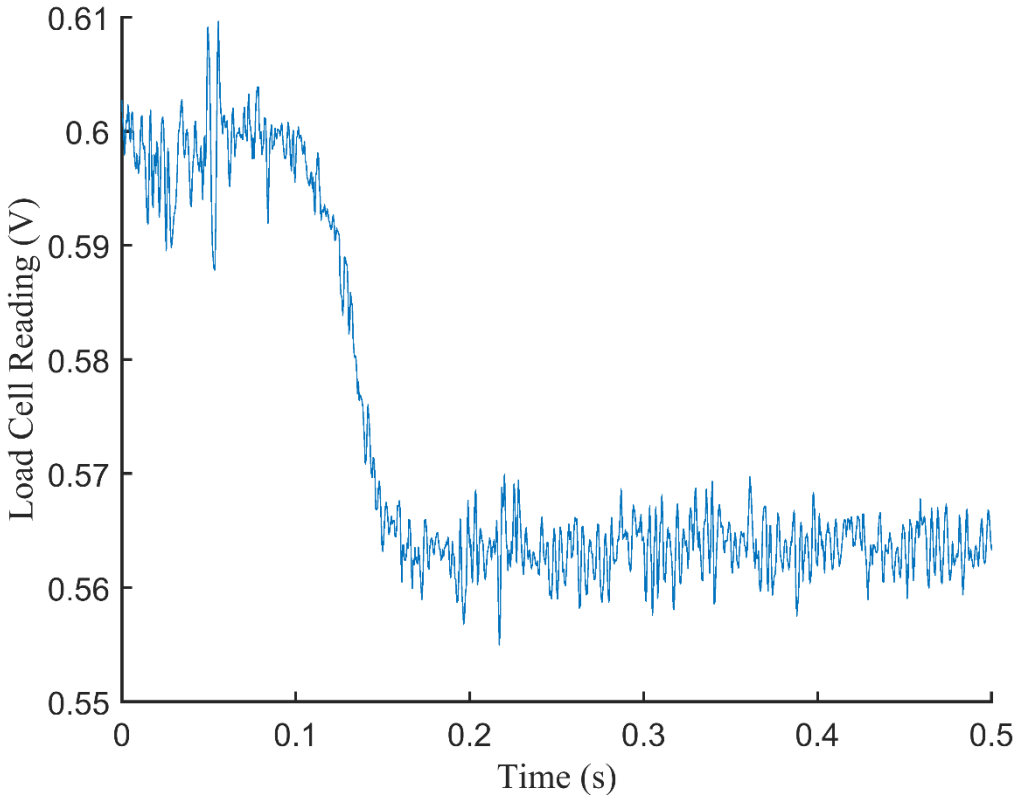

Figure 4.11: Graph showing the load cell data collected while retracting a 100 µm² Silcoset 105 stamp at 600 µm.s⁻¹ from a Si(100) surface.

4.3.5 Contact Angle

In order to ensure that the difference in adhesion seen for each of these PDMS silicones was not due to any significant difference in the surface energies contact angle measurements were taken. For these results, flat, unstructured surfaces of each of the PDMS silicones were investigated, following the same casting process as is previously described and droplets of de-ionised water were dropped onto the surface for the contact angle to be measured. As shown in Figure 4.12, the contact angles of Sylgard 184 and Sylgard 182 are 106 °±0.37° and 100° ±0.39° respectively indicating that the surface energy of the surfaces of each of these PDMS silicones was similar.

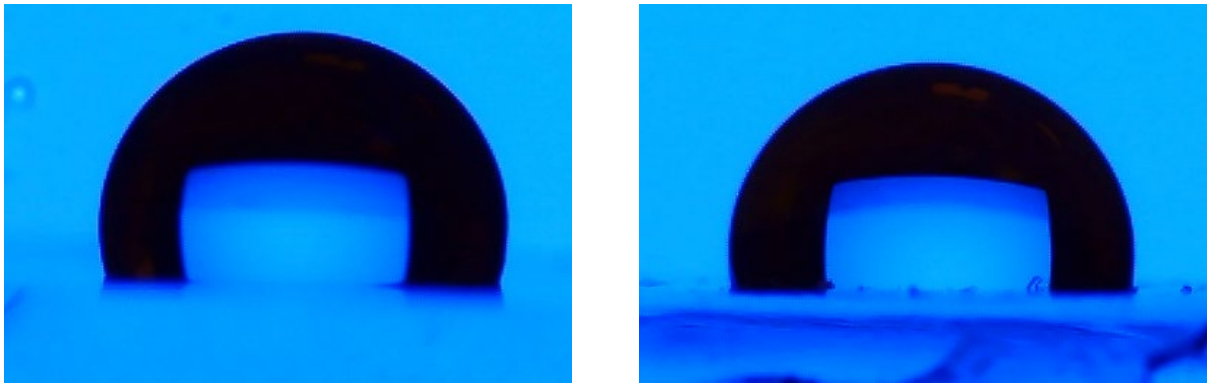

Figure 4.12: Contact angle images of deionised water on Sylgard 184 (left) and Sylgard 182 (right) surfaces using an Ossila Contact Angle Goniometer. Contact angle measurements for the Sylgard 184 surface and Sylgard 182 were 106°±0.37° and 100° ±0.39° respectively.

Looking at the two PDMS silicones that have shown to have a lower adhesion than Sylgard 184 (Sylgard 170 and Silcoset 105) it can be seen in Figure 4.13 that the contact angle goniometer measurements show a similar surface energy for Sylgard 170 and Silcoset 105, 99°±0.36° and 97°±0.36° respectively, as was seen for Sylgard 184 and Sylgard 182. This supports the argument that the adhesive nature of a PDMS stamp, regardless of the type, is not dependant entirely on just the surface energy, but is more likely dependant on the viscoelastic nature of each material. This can be concluded due to the similarities between each of the contact angle measurements taken for every PDMS silicone tested in this report, regardless of their adhesive nature. Table 4.2 shows all of the contact angle results for each of the four silicones studied in this

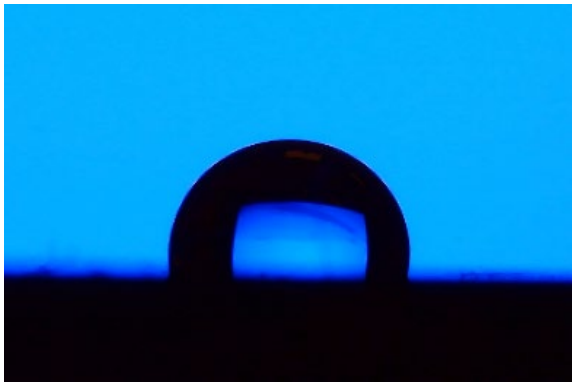
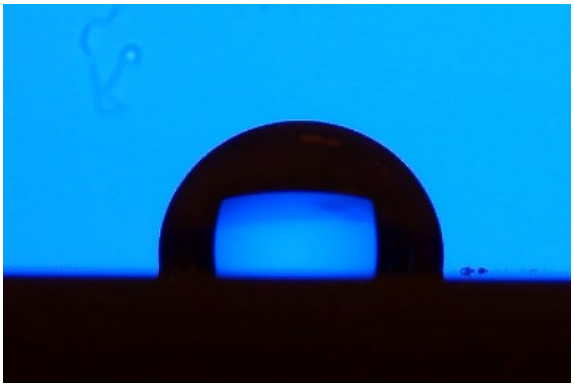

Figure 4.13: Contact angle images of deionised water on Sylgard 170 (left) and Silcoset 105 (right) surfaces using an Ossila Contact Angle Goniometer. Contact angle measurements for the Sylgard 170 surface and Silcoset 105 were 99°±0.36° and 97°±0.36° respectively.

Table 4.2: Table comparing the contact angle and maximum adhesion results obtained for each of the four PDMS silicones tested in this report, Sylgard 184. Sylgard 182, Sylgard 170, and Silcoset 105.

PDMS Material	**Contact angle**	**Adhesion at 700 µm.s^{-1}**
Sylgard 184	106°±0.37°	1.107 mN
Sylgard 182	100°±0.39°	1.204 mN
Sylgard 170	99°±0.36°	0.553 mN
Silcoset 105	97°±0.36°	0 mN

4.4 Conclusion

In this chapter, four different PDMS silicones have been compared in terms of their application to transfer printing, Sylgard 184, the most commonly used PDMS for the fabrication of transfer printing stamps, Sylgard 182, Sylgard 170, and Silcoset 105. Of these PDMS silicones, Sylgard 182 and Sylgard 170 both displayed peel velocity dependant adhesion to a Si (100) wafer substrate, while Silcoset 105 displayed no adhesion at all. It was possible for each silicone to be cast onto a structured silicon and SU-8 photoresist mould, patterned with a flat area with a central 100 μm^3 raised pedestal. Particular care was needed when peeling Sylgard 170 and Silcoset 105 due to the lower flexibility of the PDMS silicones as they were prone to split, and in the case of Silcoset 105, adhere strongly to the mould, leading to a destroyed stamp and on occasion, the mould as well was damaged. This capability to be cast and be formed into high definition micrometre scale features indicates that each of these PDMS silicones could be a potential substitute for Sylgard 184.

The capability of a PDMS silicone to be cast into a structured stamp, is not the sole characteristic that is necessary in a transfer printing stamp. Silcoset 105 was the only PDMS silicone in this study that displayed absolutely no adhesion to the Si(100) wafer at all, between a retraction speed of 35 $\mu m.s^{-1}$ up to 3000 $\mu m.s^{-1}$. This is thought to be due to an additive present in the Silcoset 105 base combined with the physical properties of Silcoset 105. It can be seen that the viscoelastic nature of a PDMS silicone has a large impact on the adhesion achievable as both Silcoset 105 and Sylgard 170 are much less flexible and viscoelastic. Both of these PDMS silicones have a much lower adhesion to the more flexible Sylgard 184 and Sylgard 182.

Despite the lower adhesion seen for a stamp made from Sylgard 170, it does display a velocity dependant adhesion that follows a power law fitting as seen for Sylgard 184 and

Sylgard 182. Due to the lower maximum adhesion possible, Sylgard 170 might be better suited to an application where pickup of an ink is easily achieved at a lower adhesive state, while printing onto a very low adhesion substrate. By having greater control over the lower adhesion necessary for printing and greater precision in retraction speeds, a stamp made from Sylgard 170 might be beneficial compared to the use of a Sylgard 184 stamp. The main challenge with using a stamp made from Sylgard 170 is the opaque grey colour which would lead to difficulties in aligning stamp features with a patterned donor or receiving substrate. This challenge however is not insurmountable. By creating a composite stamp, using Sylgard 170 alongside another PDMS silicone which was transparent, alignment of a structured stamp could be achieved.

Sylgard 182 and Sylgard 184 are almost identical in their physical properties and both have a similar velocity dependant adhesion to a Si(100) substrate. There are some variations however, but this is probably due to inconsistencies in curing temperature, leading to the Sylgard 184 stamp to be slightly over-cured, while the Sylgard 182 stamp, with the much longer curing time, was less affected by this. This prolonged curing time also gives a much longer working time as well, which could be beneficial if performing a series of castings, or if a more involved casting was being performed, such as injection moulding, where the additional time could be used.

Each of the Sylgard PDMS silicones investigated in this report are suitable as a material from which to fabricate transfer printing stamps and each could be selected to exploit a particular property, depending on the application and limitations of the process. The PDMS silicones that contained additives, Sylgard 170 and Silcoset 105 displayed a much lower adhesion than Sylgard 184 and Sylgard 182, which did not have such additives. The reduced adhesion seen for stamps made from Sylgard 170 meant that could be tailored to precisely control the adhesive properties of a PDMS transfer printing stamp. Further investigation

would be required to understand how the size, shape and material properties of the additives in Sylgard 170 impact the behaviour of a transfer printing stamp made from this PDMS.

4.5 References

[1] T. H. Kim *et al.*, "Kinetically controlled, adhesiveless transfer printing using microstructured stamps," *Appl. Phys. Lett.*, vol. 94, no. 11, 2009.

[2] S. Lee *et al.*, "Heterogeneously Assembled Metamaterials and Metadevices via 3D Modular Transfer Printing," *Sci. Rep.*, vol. 6, no. 1, p. 27621, 2016.

[3] V. Vohra, T. Anzai, S. Inaba, W. Porzio, and L. Barba, "Transfer-printing of active layers to achieve high quality interfaces in sequentially deposited multilayer inverted polymer solar cells fabricated in air," *Sci. Technol. Adv. Mater.*, vol. 17, no. 1, pp. 530–540, 2016.

[4] Y. L. Loo, R. L. Willett, K. W. Baldwin, and J. A. Rogers, "Interfacial chemistries for nanoscale transfer printing," *J. Am. Chem. Soc.*, vol. 124, no. 26, pp. 7654–7655, 2002.

[5] J. Wu, Q. Dan, and S. Liu, "Effect of viscoelasticity of PDMS on transfer printing," *16th Int. Conf. Electron. Packag. Technol. ICEPT 2015*, pp. 759–764, 2015.

[6] The Dow CompanyChemical., "SYLGARD ™ 184 Silicone Elastomer Technical Datasheet," *Silicone Elastomer Tech. Data Sheet*, no. 11-3184–01 C, pp. 1–4, 2017.

[7] I. D. Johnston, D. K. McCluskey, C. K. L. Tan, and M. C. Tracey, "Mechanical characterization of bulk Sylgard 184 for microfluidics and microengineering," *J.*

Micromechanics Microengineering, vol. 24, no. 3, 2014.

[8] X. Feng, M. A. Meitl, A. M. Bowen, Y. Huang, R. G. Nuzzo, and J. A. Rogers, "Competing fracture in kinetically controlled transfer printing," *Langmuir*, vol. 23, no. 25, pp. 12555–12560, 2007.

[9] Y. N. Xia and G. M. Whitesides, "Soft lithography," *Annu. Rev. Mater. Sci.*, vol. 37, no. 5, pp. 551–575, 1998.

[10] G. Kaur, M. Tomar, and V. Gupta, "Development of a microfluidic electrochemical biosensor: Prospect for point-of-care cholesterol monitoring," *Sensors Actuators, B Chem.*, vol. 261, pp. 460–466, 2018.

[11] F. Schneider, J. Draheim, R. Kamberger, and U. Wallrabe, "Process and material properties of polydimethylsiloxane (PDMS) for Optical MEMS," *Sensors Actuators, A Phys.*, vol. 151, no. 2, pp. 95–99, 2009.

[12] M. Bender *et al.*, "High resolution lithography with PDMS molds," *J. Vac. Sci. Technol. B Microelectron. Nanom. Struct.*, vol. 22, no. 6, p. 3229, 2004.

[13] B. Jiang, X. Shi, T. Zhang, and Y. Huang, "Recent advances in UV/thermal curing silicone polymers," *Chem. Eng. J.*, vol. 435, no. P1, p. 134843, 2022.

[14] H. Gunaydin, Kadir & S. Türkmen, "Common FDM 3D Printing Defects," *Int. Congr. 3D Print. (Additive Manuf. Technol. Digit. Ind.*, no. April, pp. 1–8, 2018.

[15] L. Gitlin, P. Schulze, and D. Belder, "Rapid replication of master structures by double casting with PDMS," *Lab Chip*, vol. 9, no. 20, pp. 3000–3002, 2009.

[16] K. Zhou, X. G. Zhu, Y. Li, and J. Liu, "Fabrication of PDMS micro through-holes using micromolding in open capillaries," *RSC Adv.*, vol. 4, no. 60, pp. 31988–31993,

2014.

[17] A. Brinkmeyer, M. Santer, A. Pirrera, and P. M. Weaver, “Pseudo-bistable self-actuated domes for morphing applications,” *Int. J. Solids Struct.*, vol. 49, no. 9, pp. 1077–1087, 2012.

[18] Dow Corning, “Sylgard ® 182 Silicone Elastomer Datasheet,” *Silicone Elastomer Tech. Data Sheet*, no. 11, pp. 1–5, 2018.

[19] W. Megone, N. Roohpour, and J. E. Gautrot, “Impact of surface adhesion and sample heterogeneity on the multiscale mechanical characterisation of soft biomaterials,” *Sci. Rep.*, vol. 8, no. 1, pp. 1–10, 2018.

[20] A. Müller, M. C. Wapler, and U. Wallrabe, “A quick and accurate method to determine the Poisson’s ratio and the coefficient of thermal expansion of PDMS,” *Soft Matter*, vol. 15, no. 4, pp. 779–784, 2019.

[21] Y. Kwak, Y. Kang, W. Park, E. Jo, and J. Kim, “Fabrication of fine-pored polydimethylsiloxane using an isopropyl alcohol and water mixture for adjustable mechanical, optical, and thermal properties,” *RSC Adv.*, vol. 11, no. 29, pp. 18061–18067, 2021.

[22] S. K. Bhunia, S. Nandi, R. Shikler, and R. Jelinek, “Tuneable light-emitting carbon-dot/polymer flexible films prepared through one-pot synthesis,” *Nanoscale*, vol. 8, no. 6, pp. 3400–3406, 2016.

[23] D. Corning, “Electronics Encapsulants: Sylgard® 170 Silicone Elastomer,” pp. 1–4.

[24] Dow, “Sylgard® 170 SDS.”

[25] H. She and M. K. Chaudhury, “Estimation of adhesion hysteresis using rolling contact

mechanics," *Langmuir*, vol. 16, no. 2, pp. 622–625, 2000.

[26] "Silcoset 105 Technical Data Sheet," *ACC Silicones*, vol. 123, no. May, pp. 98–99, 2005.

[27] CHT, "SILCOSET 105 Safety Data Sheet," no. 21, 2020.

[28] A. Carlson, A. M. Bowen, Y. Huang, R. G. Nuzzo, and J. A. Rogers, "Transfer printing techniques for materials assembly and micro/nanodevice fabrication," *Adv. Mater.*, vol. 24, no. 39, pp. 5284–5318, 2012.

[29] MicroChem, "Su-8 2025-75 Datasheet," pp. 1–5, 2006.

[30] "Kapton Tapes Datasheet." [Online]. Available: https://www.kaptontape.com/1_Mil_Kapton_Tapes_Datasheet.php.

[31] S. Deguchi, J. Hotta, S. Yokoyama, and T. S. Matsui, "Viscoelastic and optical properties of four different PDMS polymers," *J. Micromechanics Microengineering*, vol. 25, no. 9, 2015.

[32] K. Xiang, G. Huang, J. Zheng, X. Wang, G. X. Li, and J. Huang, "Accelerated thermal ageing studies of polydimethylsiloxane (PDMS) rubber," *J. Polym. Res.*, vol. 19, no. 5, 2012.

Chapter 5

Double Casting PDMS Silicones Facilitated by Ultraviolet/Ozone Surface Treatment

This chapter will describe and present a new method for achieving PDMS double casting with a range of commercially available PDMS silicones, Sylgard 184, Sylgard 182 and Sylgard 170. Firstly a review of the current PDMS double casting processes will be discussed, including looking at some potential limitations of various methods. Then details of the casting processes for the different silicones will be presented alongside the ultraviolet/ozone treatment process method.

After that the effects of the UVO treatment process will be reviewed and discussed by using adhesion data and contact angle goniometry to determine what changes the double casting has on the surface of the PDMS surface.

5.1 PDMS Casting Methods

5.1.1 Introduction

As discussed in previous chapters, PDMS is a widely used material in multiple fields and in many of these, structured PDMS surfaces are essential. This could be for a wide range of reasons, from creating microfluidic devices for biological applications, to a rapid and low cost prototyping medium.

One of the key methods for the creation of micro-structured PDMS materials for device applications is through a process called soft lithography. This involves casting liquid PDMS precursors against a solid microstructured mould material and curing the PDMS precursor. Commonly, these solid microstructured moulds are fabricated using a photosensitive polymer called a photoresist and a rigid flat substrate like silicon or glass. A widely used method is to use a layer of SU-8 photoresist (but other photoresists are occasionally used. More information regarding SU-8 processing is included in Chapter 3: Experimental Techniques) and a silicon wafer which are then used as a mould to cast a structured PDMS device. This has been used in a range of fields and for different applications such as for microfluidic devices [1][2][3] and micro electro mechanical systems (MEMS) [4][5] in order to create structured and patterned devices.

By using this method of casting a structured PDMS stamp, multiple stamps can be created quickly as the master mould can be used repeatedly and has a long lifetime, so long as it is handled carefully and avoiding aggressive chemical cleaning processes or mechanical abrasion. However sometimes certain designs of stamps do not lend themselves to being cast in this particular method. This can be due to constraints with the processing method or concern

for the lifetime of the master moulds as these can be expensive and time-consuming to make as to produce a master mould using photoresist and a silicon wafer, cleanroom facilities are required as well as specific pieces of equipment such as mask aligners and spinners. In some cases it might be more suitable to use a direct laser mask writer in order to directly pattern the photoresist, which rapidly increases the processing time for the master mould.

One of the difficulties that can be encountered when spinning large areas of thick photoresist is ensuring that the surface of the photoresist remains flat. This is particularly an issue for fabricating transfer printing stamps where any surface undulations or ripples will be directly transferred to the PDMS stamp during casting which could cause unwanted contact to occur when the stamp is brought into contact with a substrate. In order to minimise these additional steps are required during the processing as well as careful attention to minor details that for thinner photoresists is less of a concern, such as the levelling of the hotplate required to perform the soft and hard bakes. More details about the photolithography process can be found in Chapter 3: Experimental Techniques.

5.1.2 Double Casting

In order to bypass some of the issues discussed in the previous section (section 5.1.1) it is possible to cast uncured mixed PDMS mixture on top of a cured PDMS mould in a process called double casting. This would allow for a photoresist pattern to be inverted ensuring that the majority of the mould surface would be smooth silicon rather than photoresist which can be challenging to make flat. Once the mould is prepared a mixed PDMS mixture can be poured over and cured according to the instructions for each specific PDMS. Once cast and peeled

from the mould, the PDMS sub-master can then be cast upon again which creates an inverse pattern onto a newly cast PDMS stamp. These PDMS sub-master mould can then be used again, depending on the method used to treat the PDMS sub-master, it has been reported that good replicability is achieved even after 7 castings [6]. By creating PDMS sub-master moulds, it is possible to increase the potential lifetime of the original master mould due to reduced use.

The key challenge with double casting is that if a liquid PDMS is poured directly onto another PDMS surface, once cured, the two pieces of PDMS are bonded together permanently. There have been several reports of various methods that attempt to stop the bonding of the liquid PDMS to the PDMS mould, some of which use a chemical treatment to modify the surface of the mould.

5.1.2.1 Surfactant Treatment

In literature, there have been a range of surface treatments used to modify the PDMS sub-master surface to enable PDMS double casting. As an example, Hassanin et al [7] proposed a method of achieving PDMS double casting by treating the surface of a PDMS mould with the surfactants Brij52 (Sigma Aldrich, UK) and D-3005 (Rohm & Haas, USA) dissolved in acetone and DI water respectively. Surfactants are chemicals that reduce the surface tension of a liquid, allowing for an increased wettability of a surface. This method deposits a small quantity of the surfactant on the surface of the PDMS mould as a thin layer, acting as a thin interface between the two materials, often called a release agent, preventing bonding between the mould and the PDMS casting.

To achieve this, firstly a photoresist master mould was created using SU-8 photoresist patterned using UV lithography by spinning a thick layer of SU-8 photoresist over a silicon

wafer to give a 1000μm thick film and exposing selected areas to UV light. Once the pattern had been defined, a mixed PDMS mixture (PDMS base mixed with curing agent but before curing) of 10:1 Sylgard 184 was cast over the mould and cured.

Once the PDMS had been cured and removed from the SU-8 master mould, it was supported by bonding onto a glass slide then placed into a 5-10 wt.% surfactant solution for 15 minutes before being rinsed with deionised water then a fresh PDMS mixture was poured over the treated mould and cured at 90°C for 30 minutes.

The results show little deviation from the original pattern after 2 castings on the PDMS sub-master using both D3005 and Brij52, and show good definition of the high side wall features. As well as the successful castings the process requires very little additional equipment to perform making it an accessible process to those without access to an extensive laboratory or costly equipment. Due to limited availability and challenges of obtaining certain surfactants internationally it might not be possible to use D-3005 meaning for some people wishing to use a surfactant for PDMS double casting, Brij52 is the most viable option. Sylgard 184 in particular has been shown to absorb and swell in the presence of certain solvents, one of which being acetone [8], the solvent Brij52 is dissolved in. This could mean that if Brij52 and acetone were used to treat the surface of a PDMS mould, smaller features may be distorted as well as potentially outgassing of the absorbed acetone at higher temperatures and over time.

5.1.2.2 Thermal Aging

It has been well documented that the properties of PDMS change over time as it ages [9][10][11][12]. Often this is seen as a detrimental effect however Kwapiszewska et al [13]

utilised these changes in characteristics of PDMS to reduce the adhesion of a PDMS mould in order to achieve PDMS double casting. This process accelerated the aging process by leaving the PDMS in a high temperature (100°C) environment for prolonged periods of time (up to 72 hours). By doing so, low molecular weight chains within the bulk polymer became cross-linked, reducing the adhesion of the surface sufficiently to allow for a clean and lossless release of PDMS cast over its surface.

In this report [13], a master mould was created using poly(methyl methacrylate) (PMMA) patterned using CNC micro-milling. A Sylgard PDMS (it was not specified which Sylgard PDMS was used but from the curing times (3 hours at 70°C), mixing ratios (8:1 to 10:1), and popularity of Sylgard 184, it can be assumed that Sylgard 184 was used) was cast over the top of this mould using a 10:1, 9:1, and 8:1 mixture (base to curing agent) and cured at an elevated temperature (70°C) for 3 hours. Once cured the PDMS mould was then thermally aged by being placed in a laboratory oven at 100°C for between 16 hours and 72 hours. Once aged, a fresh PDMS mixture was poured over the PDMS mould and cured under the same conditions as before.

Using this method it was possible to achieve PDMS double casting, with results dependant on the mixing ratios of PDMS. The best results were when both PDMS mould and cast PDMS were both of 9:1 ratio and the mould had been thermally aged for 48 hours as the PDMS was ridged enough yet still flexible enough to not be damaged during the demoulding process. Under optimal conditions, up to 10 castings on one mould were possible.

This process of PDMS double casting required very little specialist equipment once the master PMMA mould had been created, namely a laboratory oven and some form of desiccator or vacuum chamber to outgas the mixed PDMS mixture to remove any bubbles. However, this to thermally age a PDMS mould, specific mixing ratios are necessary and the whole process can take a long time.

5.1.2.3 Oxygen Plasma Treatment

One PDMS double casting method that has shown excellent results with high aspect ratio patterns and structures is a process by Kim et al [14]. By using an oxygen plasma followed by a wash using methanol/ethanol, the PDMS mould surface is modified to reduce adhesion and allow for successful peeling of double cast PDMS.

During the oxygen plasma treatment, the PDMS surface reacts, leaving behind a surface layer that has a lower carbon content and a higher oxygen content [15] with oxygen-containing groups being formed such as Si-Ox, Si-OH, C-OH and COOH [16]. The resulting surface is more similar to a silicon oxide crust than the previously soft and adhesive surface of PDMS. Once the surface had been treated with the plasma, the alcohol treatment removed any un-crosslinked free siloxanes still present in the PDMS that could interfere with the release of the mould from the cast PDMS.

As a demonstration, high aspect ratio castings of objects such as hair and bristles of a toothbrush were performed using a PDMS ratio of 10:1 with Sylgard 184.The solvents used (methanol and ethanol) are both commonly found in laboratories and are relatively inexpensive and unlike some solvents (like acetone as discussed earlier in this chapter) do not swell the PDMS.

While the use of alcohols in this paper is cheap and the process is easily replicable without specific equipment, in order to perform plasma treatment, specific and expensive equipment is required which could limit the feasibility of this process to certain facilities without access to the required equipment.

An oxygen plasma treatment is an aggressive surface treatment which creates a brittle silicon oxide like crust on the surface with a thickness dependant on the oxygen plasma treatment duration [17]. When the underlying soft and flexible PDMS is stretched or curved,

like during peeling of a double cast PDMS stamp with the PDMS mould, the hardened crust can split and produce cracks [18] reducing the lifetime usability of the treated mould. This cracking can even be seen without manipulation and bending of the surface if the oxygen plasma treatment is high enough power or long enough duration [19].

5.1.3 Ultraviolet/Ozone Treatment of PDMS

A method commonly used to reduce the hydrophobic nature of a PDMS surface, often in the microfluidic field, is ultraviolet/ozone treatment (UV/Ozone). Earlier work [20] showed that a UV/ozone treatment was capable of creating SiO_x layers from a PDMS surface which, in this regard, is similar to that of oxygen plasma treatment discussed earlier. This was then used by Berdichevsky et al as a method to treat the surface of a microfluidic patterned PDMS device [21].

An ultraviolet/ozone cleaner uses an ultraviolet lamp to generate high levels of ozone, this is done through a synthetic quartz UV grid lamp that emits UV light at two wavelengths, 185 nm and 254 nm [22]. The 185 nm light is absorbed by the surrounding O_2 in the air and creates O_3 (ozone), then in the presence of the 254 nm UV light, organic components on the target surface react with the O_3 creating CO_2 gas and H_2O. When this is performed on a PDMS surface, as shown in Figure 5.1, the CH_3 methyl group of the PDMS react with the ozone to leave a SiO_x surface behind.

This treated surface has been shown to be more hydrophilic than the original PDMS surface which is more favourable for microfluidic applications. However, this state does not last permanently, as PDMS goes through a process of hydrophobic recovery, whereby free siloxane chains in the bulk PDMS can migrate up to, and pass through, this SiO_x crust that is formed [23]. It is thought that this process of hydrophobic recovery can take differing lengths

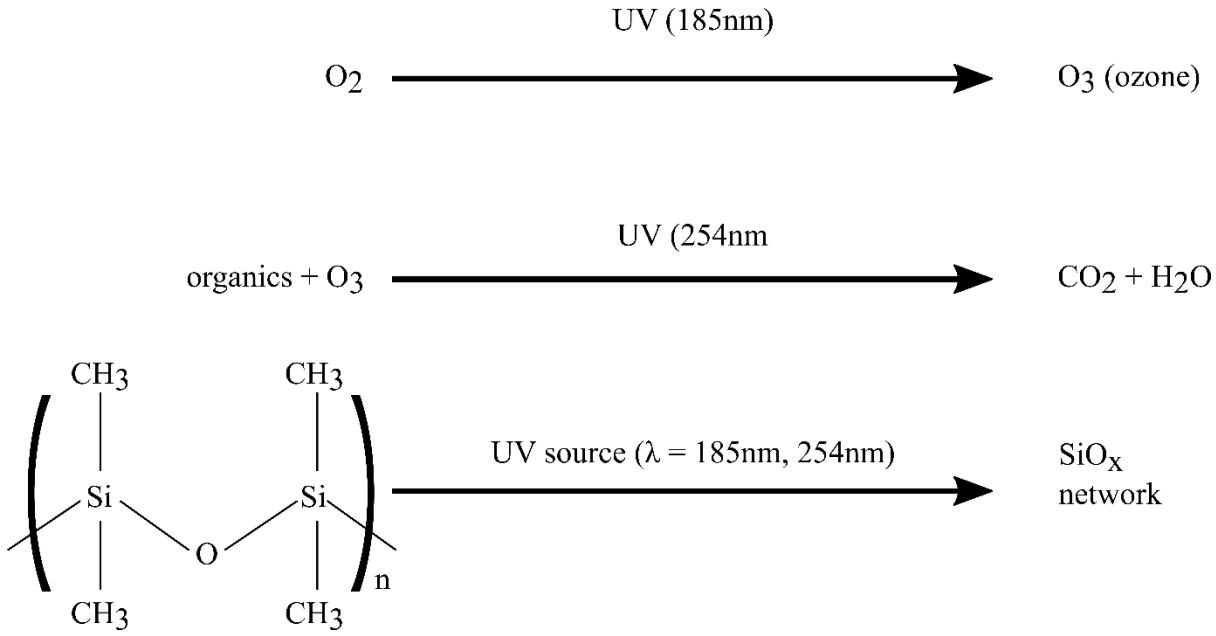

Figure 5.1: Diagram of the proposed chemistry of Ultraviolet/ozone treatment of a PDMS surface. Adapted from [23].

of time to fully achieve, meaning higher thicknesses of the modified PDMS layer increase the time needed to fully recover.

5.1.4 Contact Angle Goniometry

In order to get an understanding of what changes occur to the treated PDMS surface after the UVO process contact angle goniometry can provide some insight. This technique uses a droplet of liquid (in this report de-ionised water was used) placed onto a surface and measuring the angle the liquid droplet forms when in contact with a surface.

Depending on the surface energy of a particular surface when a droplet of a liquid is placed onto a solid surface and the properties of the liquid itself, such as the surface tension, the angle formed by the droplet can provide information about different surfaces and surface

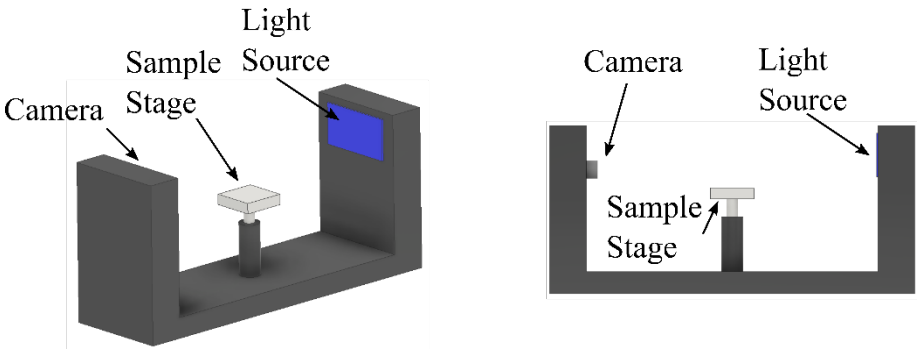

Figure 5.2: Diagram showing the components of a contact angle goniometer including a camera to take images, a sample stage upon which a sample can be placed and raised or lowered according. Finally there is the light source, often this is a large area uniform light source, which helps with providing the camera a uniform background as well as enabling high contrast images to be taken.

energies as well as any changes that might have taken place e.g. after surface treatment. If the surface energy of a surface is much greater than the surface tension of a liquid then the liquid droplet will spread and wet the surface. However, if the surface energy of a surface is much smaller than the surface tension of the droplet, then it will bead on the surface. [24].

The equipment used to perform contact angle goniometry comprises of a flat sample holder between a light source and a high resolution camera, a diagram of which can be seen in Figure 5.2. By taking an image of the droplet on the surface, the angle formed between the droplet and surface can be measured.

5.2 Experimental techniques

This section will outline the techniques and methods undertaken to investigate the ultraviolet/ozone process and fabricate PDMS stamps.

5.2.1 Mould Creation and Casting the Stamp

5.2.1.1 Master Mould

In order to create the master moulds, 100μm thick SU-8 photoresist (SU-8 2050, MicroChem) was spun onto a piece of Si(100) wafer. Due to this being a double casting process, the pattern of the photoresist was inverted which would provide the flat and clean silicon wafer being the main surface across the majority of the mould, with a small $100\mu m^3$ pedestal protruding from that surface.

For these moulds, 1.5 cm by 1.5 cm pieces of Si(100) wafer were cleaved then a 3 solvent clean using n-Butyl acetate (Fisher Chemical), acetone (99% acetone, Fisher Chemical), and isopropyl alcohol (99.8% isopropyl alcohol, Fisher Chemical) was performed. Once the surface of the wafer fragments was free of any dust, particulates, or other surface contaminants the Si(100) substrate was then baked at 100°C for 1 minute on a hot plate in order to perform a dehydration bake, removing any surface water or condensation which might interfere with the photolithography process.

The substrate was then mounted on a programmable spinner and briefly spun while blowing the surface with nitrogen to remove any new potential dust from the surface which may have settled during the dehydration bake. Once this was complete, SU-8 2050 was

deposited onto the surface of the substrate. Due to the viscosity of this particular SU-8 (12900 cSt [25]), it was necessary to manually cover the entire substrate surface with SU-8 first before spinning, without doing so would lead to areas of the Si(100) substrate being left uncovered by the SU-8. The sample was left for between 30 seconds and 60 seconds to enable any bubble that were trapped in the SU-8 during deposition to burst. After this time, larger bubbles that persisted were removed using a pipette, while smaller bubbles were removed in following steps.

The SU-8 covered Si(100) substrate was then spun at 500 rpm for 15 seconds with an acceleration of 100 rpm/s which was then increased to a spin speed of 1700 rpm for 30 seconds with a 300 rpm/s ramp rate. It was found that the edge bead that formed during this process inhibited good contact with the mask during the exposure step, therefore an edge bead removal process was used. In order to perform this, 0.5 ml of an edge bead remover (EBR PG, MicroChem) was sprayed onto the surface of the SU-8 coated Si(100) sample that was placed onto a levelled plate. Once the surface had been sprayed with the edge bead remover, the Si(100) and SU-8 mould was then covered with a plastic cover with a small 1 mm hole drilled into the top which had the effect of restricting the rate at which the edge bead remover would evaporate. This was then left for 24 hours at room temperature before being visually inspected. If the surface was not flat or still had bubbles present, the process was repeated until the SU-8 film was flat and bubble free.

The SU-8 covered Si(100) was then soft baked at 65°C for 5 minutes followed by a 95°C bake for 16 minutes before being aligned to the mask made from quartz glass and titanium using a UV400 mask aligner and exposed for 48 seconds. The SU-8 was then baked at 65°C for 4 minutes then for 9 minutes at 95°C.

In order to remove the unexposed SU-8 the use of an ultrasonic bath (UT8031/EUK Ultrasonic Cleaner, Shesto) was necessary. The sample was submerged in SU-8 developer and

placed into the ultrasonic bath for 6 minutes on delicate mode, but every 2 minutes, the process was paused to visually inspect the SU-8 and Si(100) to check the development progress. Once complete, it was then rinsed and dried using de-ionised water and nitrogen. At this stage, it was common for small crack to appear on the SU-8 surface, to repair these, a short 30 second bake on a hot plate set to 180°C caused the SU-8 to re-flow slightly and 'heal' the cracks. Once the mould was ready, it was flood exposed with the UV400 mask aligner for 5 minutes.

5.2.1.2 Sub-Master PDMS mould

Now that a SU-8 and silicon master mould had been created, the next stage of stamp preparation could be performed. For this, the focus of the experimentation was on 3 different PDMS silicones in order to determine if the process of UVO treating the surface of a PDMS mould was transferrable between different materials. The PDMS silicones that were selected were Sylgard 184 (Sylgard 184, Dow), Sylgard 182 (Sylgard 182, Dow), and Sylgard 170 (Sylgard 170, Dow). This process was very similar to the standard PDMS casting performed throughout this PhD as well as castings performed in many other reports where a measured mass of the PDMS base.

The PDMS base was weighed out in an aluminium tin before an appropriate amount of curing agent was added in a ratio of 10:1 for Sylgard 184 and Sylgard 182 and 1:1 for Sylgard 170 before being thoroughly mixed and outgassed in a desiccator and cured in a laboratory oven at 100°C for 35 minutes for Sylgard 184, 75 minutes for Sylgard 182, and 10 minutes for Sylgard 170.

5.2.1.3 Ultraviolet/Ozone Surface Treatment

Once the PDMS Master mould was cured and ready for use they were first washed with isopropyl alcohol (IPA) (99.8% isopropyl alcohol, Fisher Chemical) to remove any surface contaminants, such as dust or photoresist residue. This was achieved by lowering the moulds into a beaker of IPA and leaving for 1 minute with gentle agitation with tweezers. Due to the adhesive nature of some of the PDMS silicones, the use of an IPA soaked cotton bud to remove any well-adhered contaminants was not possible. Once the moulds had been submerged for 1 minute, they were removed from the beaker and dried with nitrogen.

Now clean and dry, the inverted PDMS moulds were placed onto the loading tray of the Ultraviolet/ozone (UVO) cleaner (UV Ozone Cleaner, Ossila). They were then subjected to the UVO process for 30 minutes. It was found that in order to achieve a successful double casting it was imperative to leave the PDMS Master mould for approximately 24 hours in a vented polystyrene Petri dishes. This was to enable the free siloxanes to migrate to the surface of the PDMS past the oxide crust and to cure. This would ensure that the free siloxanes would not interfere with the peeling of subsequent castings. In order to determine the duration of the waiting times, tests were performed on a UVO treated sub masters of all of the Sylgard PDMS silicones, ranging from only a few minutes, to 48 hours. Only after a minimum of 12 hours had passed was a successful casting achieved but in order to be certain of a successful casting, 24 hours was deemed to be the more appropriate. For the wait times over 24 hours, no noticeable improvement was apparent to the quality of subsequent double castings.

5.2.1.4 Double Casting

To perform the double casting of the various PDMS silicones being investigated, each silicone was mixed in the same way as the inverted PDMS mould as described previously. A 10:1 mixture of PDMS in the case of Sylgard 184 and Sylgard 182, and 1:1 mixture of Sylgard 170, mixed thoroughly and outgassed before being cured at an elevated temperature (100°C) for 75 minutes for Sylgard 182, 35 minutes for Sylgard 184, and 10 minutes for Sylgard 170. In order to determine what effect the UVO treatment of the mould had on the final stamp, repeat castings

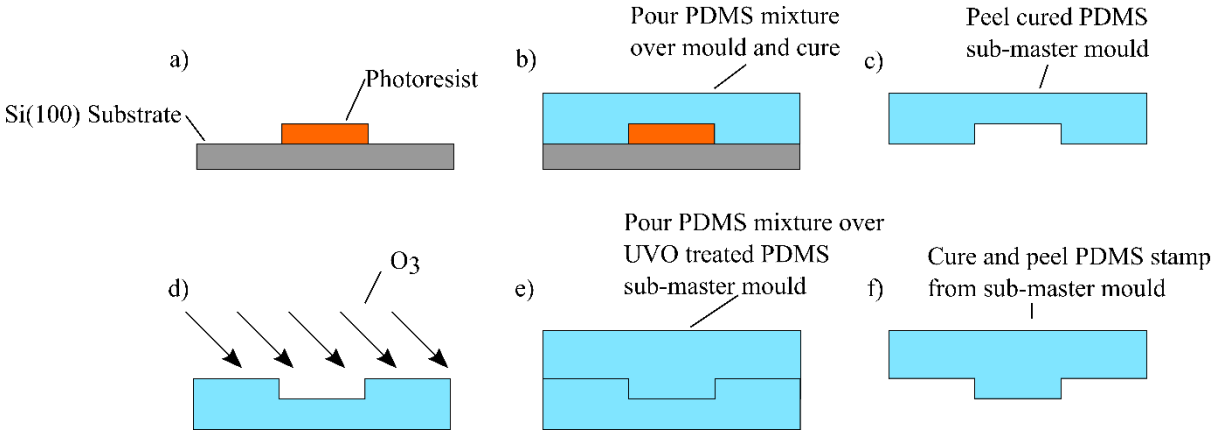

Figure 5.3: Schematic showing the stages involved in casting and treating a PDMS double cast sub-master mould followed by the secondary casting of the PDMS stamp from the sub-master mould. A) the preparation of the photoresist on Si(100) master mould, b) pouring and curing the mixed PDMS mixture that will form the sub-master mould, c) peeling the sub-master mould away from the Si(100) master mould, d) Ultraviolet/ozone (O_3) treatment of the PDMS sub-master after cleaning with isopropyl alcohol, e) After 24 hour wait time, fresh PDMS mixture is poured over the sub-master and cured, f) finally the PDMs stamp is peeled from the PDMS sub-master mould in preparation for use.

were performed to determine if the mould would survive multiple uses. A schematic of the process of UVO double casting can be found in Figure 5.3.

5.2.2 Challenges and Difficulties Overcome in Order to Achieve Ultraviolet/Ozone Double Casting

In order to determine the parameters that would give a successful casting, initially PDMS moulds were treated for a range of different lengths in the UVO cleaner. This led to a window of 30-35 minutes being discovered. This was long enough for the surface to be fully treated and oxidised sufficiently, while ensuring that the surface was still flexible enough to be peeled

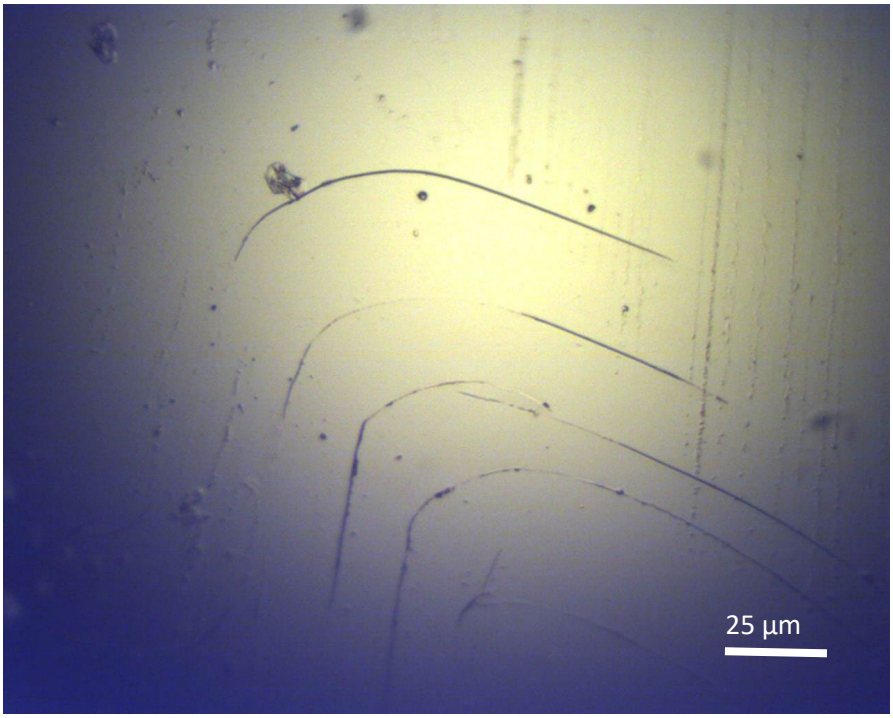

Figure 5.4: Microscope image of cracking on a UVO treated Sylgard 184 surface after 4 castings. These cracks appeared after excessive bending of the UVO treated surface during the peeling of a double cast piece of PDMS from the surface.

away after casting without permanently damaging the surface. Samples left for significantly longer the 35 minutes would form a very thick and brittle glass-like layer which would provide a very good surface to cast off of, yet would be too brittle to reuse. Cracking of the silica-like layer can be seen in Figure 5.4.

5.2.3 Adhesion Testing

In order to investigate in more depth how the UVO double casting process could affect the usability of transfer printing stamp, adhesion tests were performed on each of these double cast stamps. In each case, the stamp surface was patterned with a 100 μm^3 pedestal in order to ensure a repeatable contact area was achieved with each test.

As it has been shown that during UVO treatment, a thin oxide crust is formed and free siloxanes migrate to the surface. These potentially could interfere with the adhesion of the stamp surface during transfer printing so for each PDMS investigated, an identical casting was performed which was gently washed in isopropyl alcohol (99.8% isopropyl alcohol, Fischer Chemical) to remove some of these surface contaminants.

These adhesion tests were performed in the same manner to those mentioned in previous chapters however it will be included here briefly so as to give a more complete picture of the investigation. To perform the adhesion tests for each of these stamps, each stamp was adhered to a clean glass slide and secured in a vertical stage (ANT130LZ Single-Axis z Nanopositioning Stage, Aerotech) using a vacuum chuck. By using the Aerobasic script (more details about this script are included in Chapter 3: Experimental Techniques) the stage could be finely controlled to make contact with the silicon (100) test substrate which was in turn attached to a load cell (GSO-10, Transducer Techniques). Figure 5.5 shows the PDMS stamp

approaching the load cell. Once the pedestal had made contact with the silicon wafer surface, it was carefully partially compressed to ensure good contact had been made, then there was a 5 second relaxation period, before a retraction at a selected speed (between 10 μm^{-1} and 700 $\mu m.s^{-1)}$. By using this code, a greater level of control over the system was achieved including the acceleration profile of the vertical stage, how much the pedestal was compressed, and how slowly the stamp would be brought into contact.

Once this was performed for a selected retraction speed, then this process would be repeated using the same stamp but for a range of retraction speeds to provide a range of data points. When all of the data for a selected stamp was collected, it was then plotted so that the minimum value could be taken. This value was then zeroed using the baseline load cell reading and converted from grams to mN. By plotting each of these minimum values for a range of retraction speeds, a better understanding of the stamp material and surface can be reached.

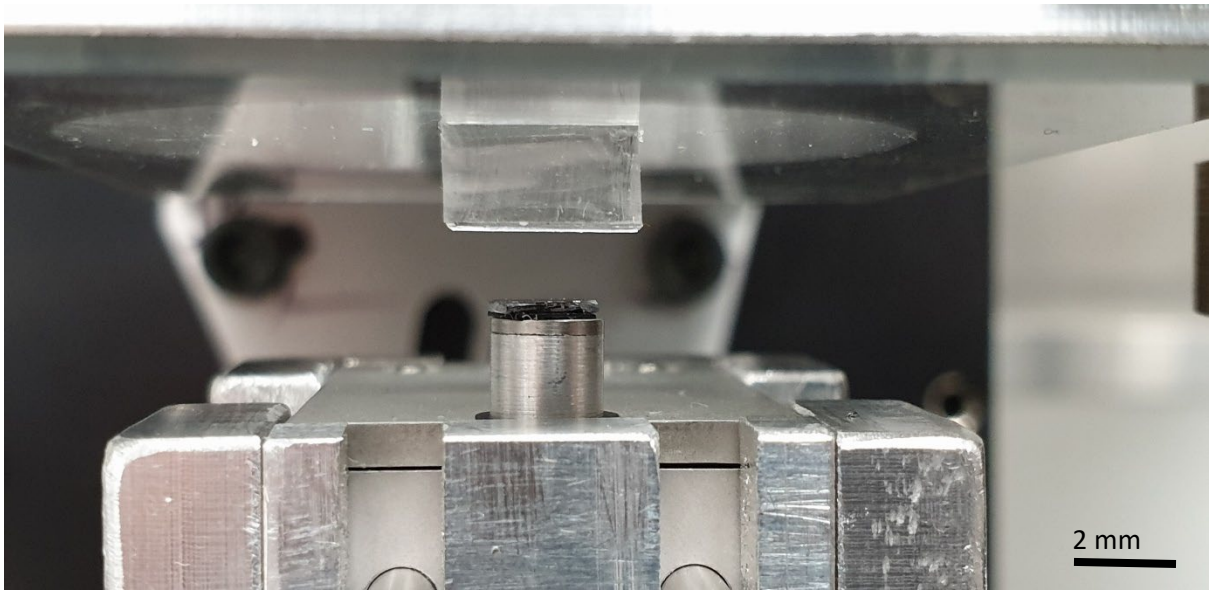

Figure 5.5: Photograph showing a Sylgard 184 PDMS stamp during approach to the load cell. Mounted on the load stem is a fragment of Si(100) .

5.3 Results

This section will cover the results of the adhesion tests and contact angle measurements for the different PDMS types, Sylgard 184, Sylgard 182 and Sylgard 170 as well as the success of multiple castings from one mould.

5.3.1 Casting Replication

In order to achieve a successful PDMS double casting enabled by a UVO treatment a minimum of 30 minutes UVO treatment was necessary. Figure 5.6 shows a successfully double cast PDMS pedestal. At treatment times less than 30 minutes, after casting, sections of the surface bonded permanently to the mould leaving small craters in the surface. This destroys both the stamp and the mould during the first casting attempt.

When treatment times extend beyond 35 minutes, the silicon oxide crust becomes too thick and brittle leading to visible cracking occurring on the surface of the mould. These cracks

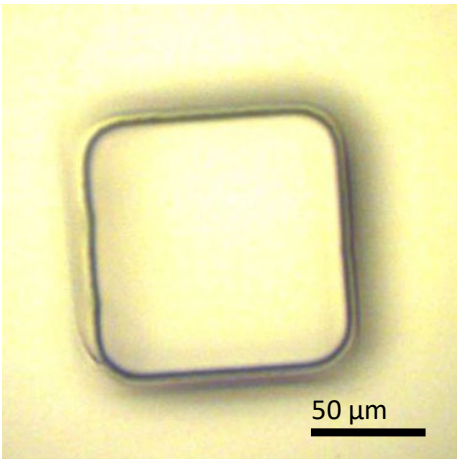

Figure 5.6: Microscope image of double cast Sylgard 184 stamp. Rounding of the corners of the pedestal can be seen which was largely due to the SU-8 patterning process.

are apparent on the surface of the PDMS stamp that is cast onto the mould which distorts and destroys the flat surface as well as any small features. The longer the treatment time, the more apparent the cracks became and the more fragile the mould was. When peeling the cast PDMS stamp from the mould, it is very difficult to not bend either part meaning that for all of these tests, only one successful casting was achieved.

By treating the surface of the mould with a 30-35 minute UVO treatment, there was enough oxidation of the surface to enable to freshly cast PDMS to peel off with no bonding between the stamp and the mould, yet the surface with the oxide crust is still flexible enough to bend while peeling without cracking. With a mould treated for 30 minutes, 4 successful castings were achieved with Sylgard 184 and Sylgard 182. Damage that occurred to the PDMS sub-master mould be seen in Figure 5.7. However, Sylgard 170 has significantly different properties to Sylgard 184 and 182 and is much less flexible. This meant that only 2 successful castings were achieved before the mould suffered damage and was unusable.

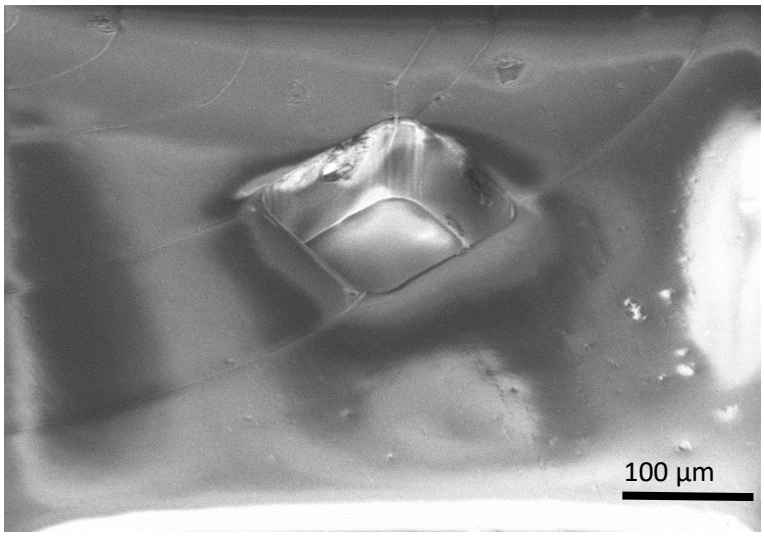

Figure 5.7: SEM image of UVO treated Sylgard 184 sub-master mould after 3 castings. Note some small defects in the surface, possibly caused by small scale bonding between areas of the cast Sylgard 184 and the sub-master surface.

5.3.2 Adhesion Data

In order to determine any long lasting impact or residue left on the surface any PDMS stamp fabricated through the use of PDMS double casting facilitated by UVO treatment, adhesion testing was performed.

5.3.2.1 Sylgard 184

Figure 5.8 shows the energy release rate of a 100 μm^2 pedestal made from Sylgard 184 cast from a UVO treated Sylgard 184 sub-master mould from a clean Si(100) surface. This stamp was not washed or treated in any way before adhesion tests were performed. When compared to the energy release rate curve from Chapter 4: Compatibility of Different PDMS Silicones for Fabrication of Viscoelastic Transfer Printing Stamps, it is obvious that the double casting process has affected the surface of the Sylgard 184 stamp as the stamp displays significantly worse adhesive properties, although the double cast stamp does still display an increase in adhesion as the stamp retraction speed is increased.

The reduction in the adhesiveness of the stamp could have been due to contamination of the cast surface as the UVO process is known to create thin silicon oxide surfaces on treated PDMS. It is possible that during the casting process on a treated PDMS sub-master mould, small pieces or whole thin layers of this glass-like silicon oxide crust could be removed from the mould and become stuck to the surface of the double cast PDMS stamp. On such a small

contact area, such as the 100 μm^2 pedestal face, this could reduce the adhesion of the stamp to the degree that can be seen in Figure 5.8.

Another possibility is that there are still free siloxane chains present on the surface of the treated mould that remain present after the 24 hour waiting period necessary for the double casting process. These free siloxanes could be transferred to the surface of the double cast pedestal surface and, during adhesion testing, might prevent good contact being made between the Sylgard 184 pedestal and the Si(100) surface.

This reduction in the adhesion showed that some mechanism, whether that be the silicon oxide crust or the free siloxanes, was affecting the final double cast Sylgard 184 stamp. In order to determine the effectiveness of UVO treatment of a PDMS sub-master mould for the purpose of double casting an attempt was made to try to return the properties of the double cast Sylgard 184 stamp to how a directly cast Sylgard 184 stamp performed.

In an attempt to achieve create a double cast Sylgard 184 stamp with the same adhesion properties as a directly cast stamp, a Sylgard 184 sub-master that had been treated with UVO and left for the 24 hour wait time, was left to soak in IPA for 1 minute with gentle agitation by swilling before being dried in dry nitrogen. Once the Sylgard 184 sub-master was dry, the rest of the processing took place as described in Section 5.2.1.4. This would help to remove any contaminants that might be present on the surface of the mould and, if there were any free siloxanes present, they would be absorbed and removed.

Figure 5.8 compares the results of adhesion tests performed on a Sylgard 184 stamp cast on an IPA washed Sylgard 184 sub-master with the previous results. By washing the Sylgard 184 sub-master mould post UVO treatment and 24 hour wait time, the adhesion of the stamp improved significantly with the maximum energy release rate being 0.87 mN at 700 $\mu m.s^{-1}$ compared to 1.1 mN for a directly cast Sylgard 184 stamp and 0.7 mN for the double cast stamp from an unwashed mould.

It should be noted that despite the reduction in the adhesion, even with the washed mould, the stamp still displayed velocity dependant adhesive properties and could still have

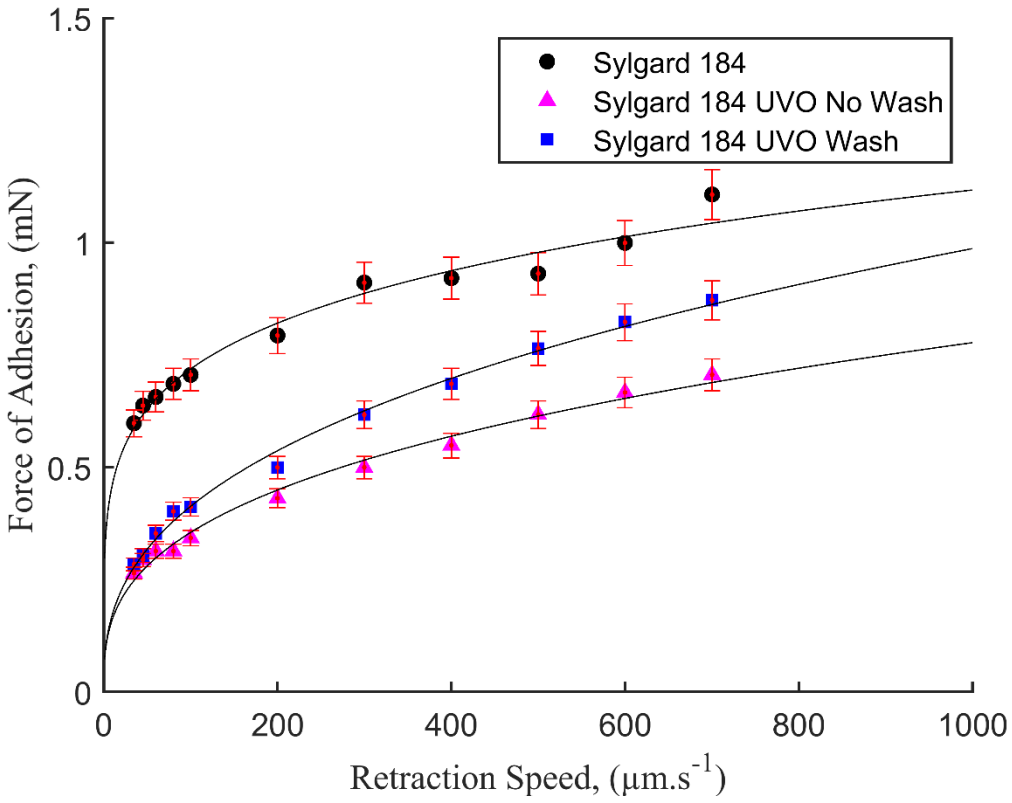

Figure 5.8: Graph showing the force of adhesion achieved by a 100 μm^2 contact area Sylgard 184 pedestal at a range of retraction speeds, ranging from 35 $\mu m.s^{-1}$ to 700 $\mu m.s^{-1}$ for a pristine Sylgard 184 stamp, and double cast Sylgard 184 stamps, one without any washing of the PDMS sub-master mould after UVO treatment, and one with an IPA washed sub-master mould.

successfully be used to selectively pick up and print particular materials, albeit with a narrower operating window.

5.3.2.2 Sylgard 182

Sylgard 182 is a very similar PDMS silicone to Sylgard 184 both in appearance and physical properties but with one major difference. Unlike Sylgard 184, Sylgard 182 cannot be cured at room temperature, has a much longer working time, and a longer high temperature (100°C) curing time. Figure 5.9 shows the energy release rate for a Sylgard 184 stamp with a 100 μm^2 pedestal when retracted from a Si(100) surface without any washing or treatment of the stamp surface after casting. The data for this, when compared to a stamp cast directly from a Si and SU-8 mould using the data from Chapter 4: Compatibility of Different PDMS Silicones for Fabrication of Viscoelastic Transfer Printing Stamps shows that, like with the Sylgard 184, there is a significant drop in adhesion when double casting with the unwashed mould. With the maximum adhesion achieved being 0.8 mN compared to that of the directly cast stamp 1.2 mN.

When the experiment was repeated but the mould was washed with IPA as described in section 5.3.2.2 it can be seen that the adhesion of the stamp cast onto the washed UVO treated mould begins to approach that of the directly cast stamp with the adhesion at 700 $\mu m.s^{-1}$ being 1 mN.

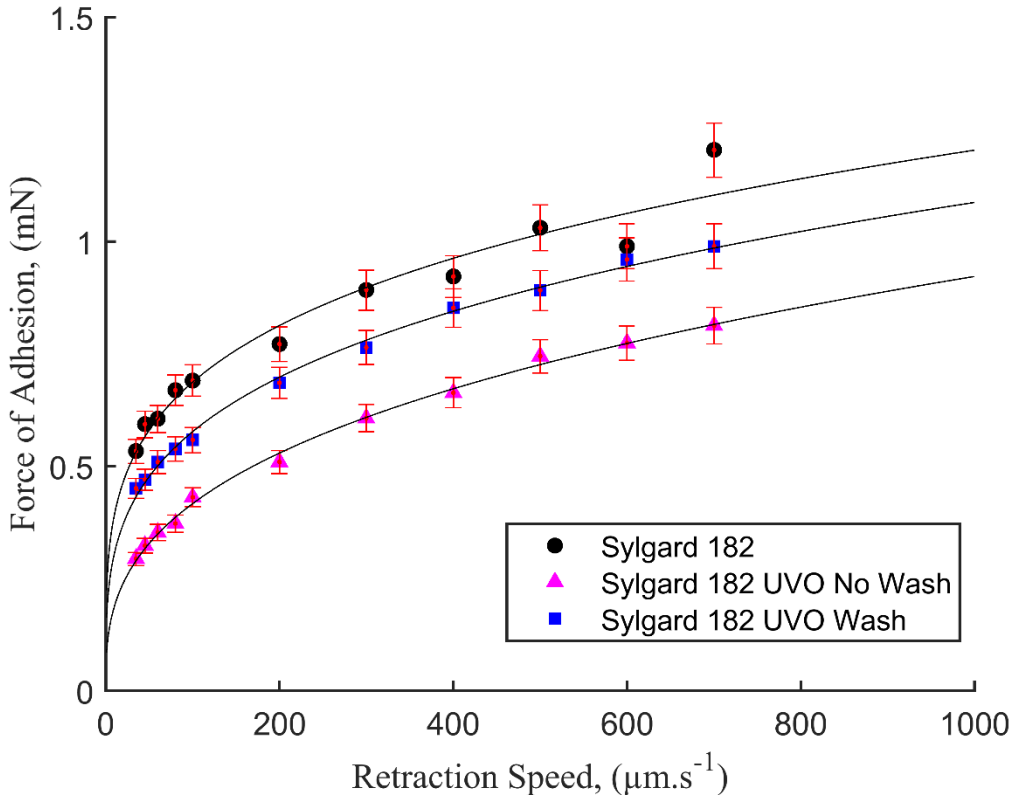

Figure 5.9: Graph showing the force of adhesion achieved by a 100 µm^2 contact area Sylgard 182 pedestal at a range of retraction speeds, ranging from 35 µm.s^{-1} to 700 µm.s^{-1} for a pristine Sylgard 182 stamp, and double cast Sylgard 182 stamps, one without any washing of the PDMS sub-master mould after UVO treatment, and one with an IPA washed sub-master mould.

5.3.2.3 Sylgard 170

Unlike the previous Sylgard PDMS silicones, Sylgard 170 had very different properties both in terms of the appearance, it being an opaque dark grey compared to Sylgard 184 and Sylgard 182 which were clear and transparent, and physical properties such as a smaller Young's modulus (the Young's modulus for Sylgard 184 is 1.32-2.97 Mpa (depending on the curing

conditions) [26], Sylgard 182 has a Young's modulus of 0.935 Mpa [27], Sylgard 170 has a Young's modulus of 0.65 Mpa [28]. However, as has been shown in Chapter 4: Compatibility of Different PDMS Silicones for Fabrication of Viscoelastic Transfer Printing Stamps, Sylgard 170 does still display a velocity dependant adhesion, albeit a smaller adhesion to a Si(100) substrate. As can be seen in Figure 5.10 there is a noticeable reduction in the adhesion achieved by a Sylgard 184 stamp that has been fabricated using a double casting process. This follows the same trend as the results from a Sylgard 184 and Sylgard 182 stamp, however, after a wash of IPA, the stamp does not seem to recover as quickly as can be seen with the other PDMS

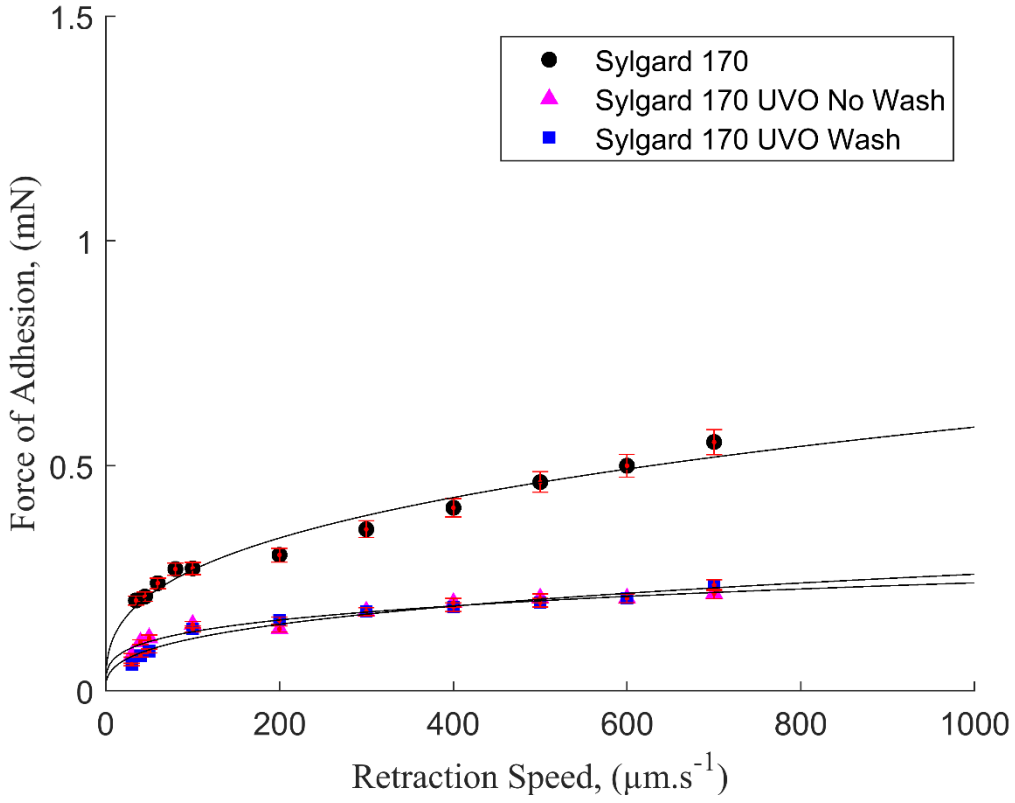

Figure 5.10: Graph showing the force of adhesion achieved by a 100 µm^2 contact area Sylgard 170 pedestal at a range of retraction speeds, ranging from 35 µm.s^{-1} to 700 µm.s^{-1} for a pristine Sylgard 170 stamp, and double cast Sylgard 170 stamps, one without any washing of the PDMS sub-master mould after UVO treatment, and one with an IPA washed sub-master mould.

silicones tested in this report (with the exception of Silcoset 105 which yielded no successful double cast stamps). In fact, after an IPA wash, at 700 μm.s^{-1}, the Sylgard 170 stamp only achieved 0.24 mN, 0.02 mN higher than that achieved by the unwashed stamp.

5.3.3 Contact Angle Measurements

In order to understand what occurs on the surface of PDMS silicones immediately after the UVO treatment, and to try to explain why a 24 hour waiting period is necessary before double castings can be performed. For this experiment, flat pieces of each PDMS silicone were cast and then cleaned thoroughly with isopropyl alcohol and dried with nitrogen. Once clean and dry, the samples were subjected to half an hour of ultraviolet/ozone (UVO) then the contact angle measurements were taken at the following time intervals: immediately after UVO treatment, after 1 hour, 6 hours, 24 hours, 48 hours, and 7 days (168 hours). By analysing the results obtained through contact angle goniometry and using data already published on the process of UVO treatment of PDMS, it was hoped that this would increase our understanding on what mechanism enables the release of a double cast PDMS stamp. Figure 5.14 shows the

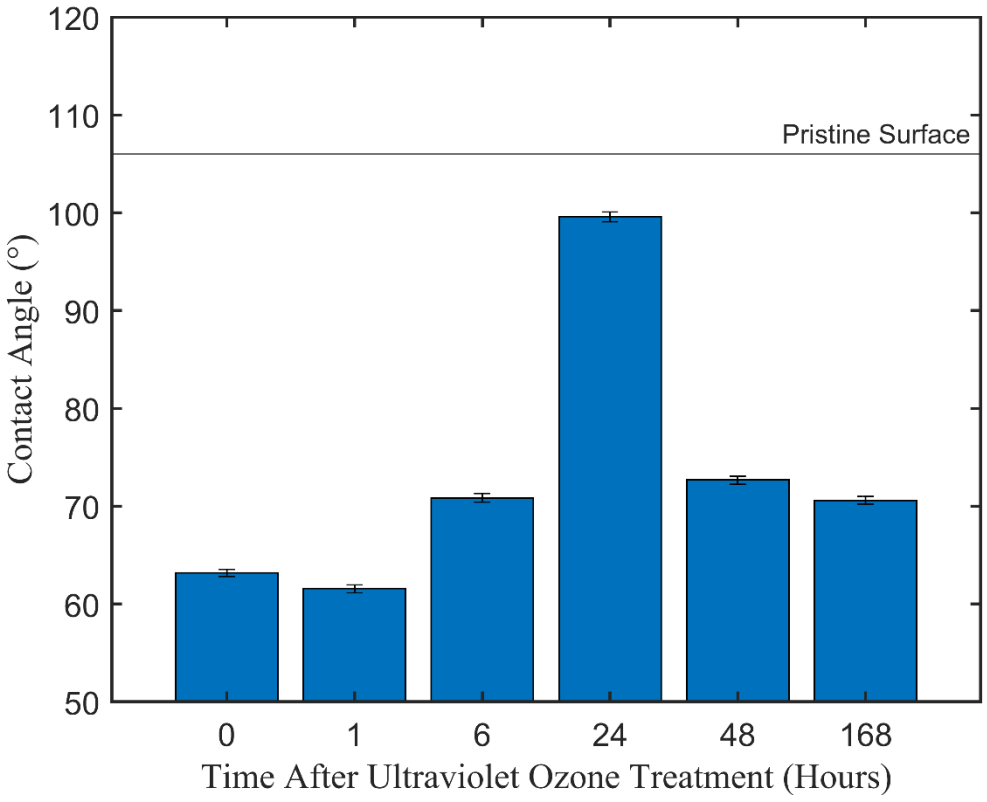

Figure 5.11: Graph showing the contact angle between a droplet of de-ionised water and a Sylgard 184 surface, treated with ultraviolet/ozone for 30 minutes. The horizontal line marks the contact angle of a pristine Sylgard 184 surface.

visible difference in the contact angles made by a droplet of de-ionised water when in contact with an untreated PDMS surface and that of a treated surface.

As can be seen in Figure 5.11, immediately after UVO treatment, a Sylgard 184 surface displays a significantly smaller contact angle (62°) with a DI water droplet than a pristine, untreated Sylgard 184 surface (106°). After 1 hour, the contact angle drops again to 61° before seeing a recovery in the contact angle after 6 hours and again at 24 hours with the contact angle after 24 hours reaching 99°. After 48 hours however, the contact angle drops again down to 72° and again, after 7 days, the contact angle drops further to 70°.

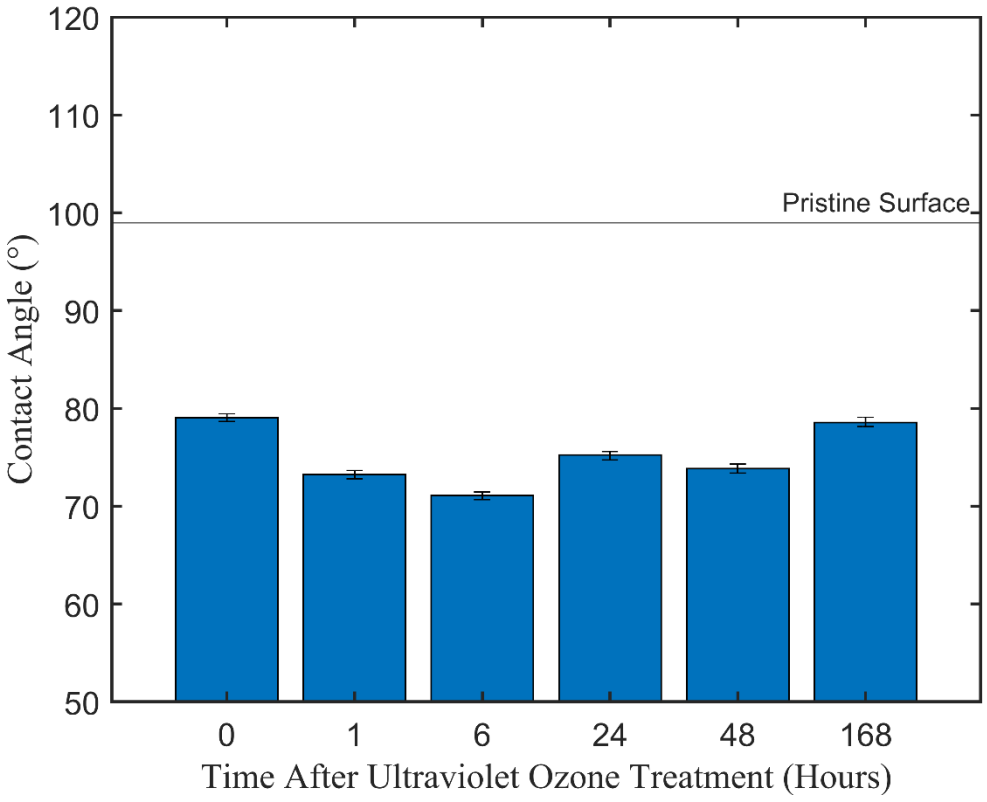

Figure 5.12: Graph showing the contact angle between a droplet of de-ionised water and a Sylgard 182 surface, treated with ultraviolet/ozone for 30 minutes. The horizontal line marks the contact angle of a pristine Sylgard 182 surface.

Figure 5.12 shows the contact angles of Sylgard 182, a PDMS with similar physical properties and, other than having a longer curing time, appears to be very similar to Sylgard 184. Contact angle measurement showed that the UVO treatment process of the surface of Sylgard 182 had a smaller initial impact on the surface energy of the PSMS stamp with the contact angle reducing from 100° for a pristine surface, to 72° immediately after UVO treatment. After an hour the contact angle reduced to 60° but after 6 hours, the contact angle increased to 67°. After 7 days, the contact angle measurements returned to that of a Sylgard 182 surface that was measured immediately after UVO treatment.

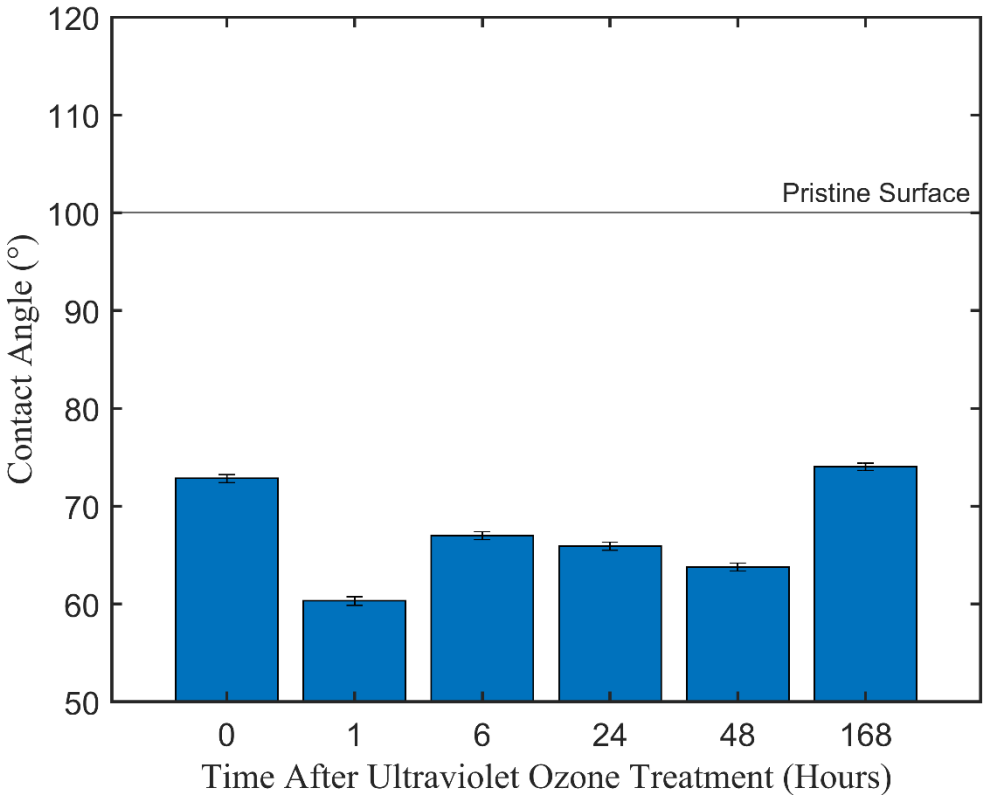

Figure 5.13: Graph showing the contact angle between a droplet of de-ionised water and a Sylgard 170 surface, treated with ultraviolet/ozone for 30 minutes. The horizontal line marks the contact angle of a pristine Sylgard 182 surface.

As can be seen in Figure 5.13, initially after UVO treatment of the PDMS surface, Sylgard 170 seemed to display a less severe change in contact angle with a de-ionised water droplet than that of Sylgard 184 or Sylgard 182, reducing from 99° for a pristine untreated surface to 79° immediately after 30 minutes of UVO treatment. The contact angle continued to reduce, with the contact angle after 6 hours post UVO treatment being 71°. By 24 hours however, the contact angle measurements increased to 75° before once again dropping slightly after 48 hours to 74°. Finally, at 168 hours after UVO treatment, the contact angle measurement had recovered almost back to that of the surface immediately after UVO treatment.

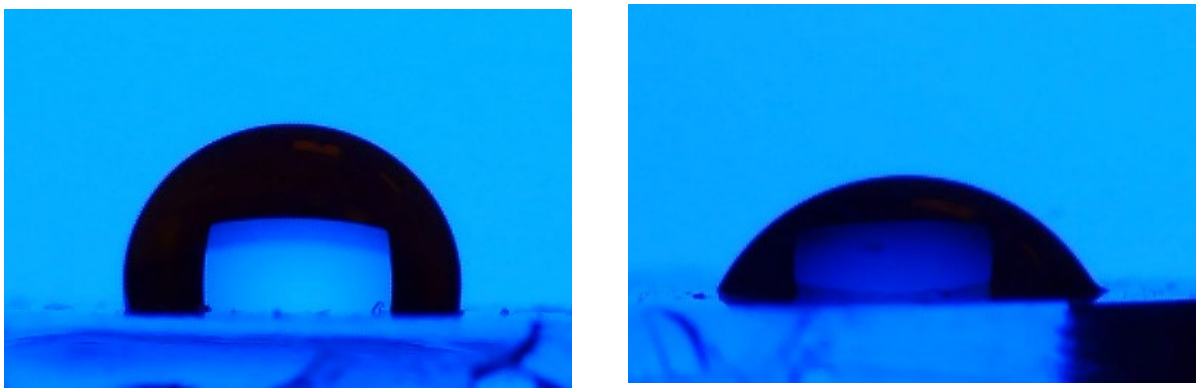

Figure 5.14 Contact angle goniometry images of the contact angle differences between an untreated Sylgard 182 surface (left) and a Sylgard 182 surface that has been treated with UVO and left for 1 hour (right) The contact angle of the untreated Sylgard 182 is 100° and the contact angle of the UVO treated Sylgard 182 surface after 1 hour is 60°.

5.3.4 Comparison

Each of the PDMS stamps, whether made from Sylgard 184, Sylgard 182 or Sylgard 170 each displayed a drastic reduction in the adhesion achieved when retracted from a Si(100) surface. This is particularly noticeable at the higher end of the retraction speed range that was investigated in this report. Sylgard 184 displayed a reduction of 0.4 mN, approximately a 36% reduction, which Sylgard 182, a very similar PDMS silicone saw the same reduction of 0.4 mN, approximately a 33% decrease. Sylgard 170 has a much lower adhesion normally caused by its smaller Young's modulus and potential over curing at high temperate to name but a few, however, like with the previous PDMs silicones, it too saw a reduction in adhesion of 0.33 mN, a 60% reduction in adhesive force.

This reduction in adhesion that is seen across all three PDMS silicones that were successfully created using this double casting process is likely due to contamination of the surface of the PDMS stamp. Any contamination at the interface between the PDMS pedestal surface or the surface of the Si(100) substrate prevents good contact being made and makes it easier for a crack to propagate, leading to a lowered adhesion. In this case, the contamination was most likely either free siloxanes that had migrated to the surface of the UVO treated PDMS sub-master mould or by small pieces of the silica-like crust that is formed during the UVO process break off and become stuck to the surface of the PDMS stamp that is cast.

It appears that for the case of Sylgard 184 and Sylgard 182, if the UVO treated mould is washed with isopropyl alcohol, any subsequent casting has an increased adhesion to the Si(100) substrate. This increase in adhesion is not enough to bring the stamp adhesion back to the levels of a pristine directly cast stamp of the same PDMS material, however Sylgard 184 saw an increase of 0.17 mN meaning an overall of a 20% reduction in adhesion when compared to a pristine direct cast Sylgard 184 stamp. Sylgard 182 saw an increase of 0.2 mN giving a 17% reduction in adhesion compared to maximum adhesion achieved by a direct cast Sylgard 182 stamp. Sylgard 170, although, did not appear to be as affected by the isopropyl alcohol wash with there being only a small increase in adhesion of 0.02 mN which still had a 56% reduction in adhesion compared to the direct cast Sylgard 170 stamp.

The surface energy of a UVO treated PDMS shows that after the UVO process has taken place, the surface energy immediately is increased with the contact angle decreasing overall for each of the PDMS silicone tested. Even after 7 days, this contact angle never fully recovers and the surface energy is increased permanently. For Sylgard 184, it is particularly noticeable that after 24 hours, the contact angle has increased drastically, however after 48 hours, the contact angle had reduced back to previous levels. Each PDMS show the trend of a decreasing contact angle, followed by an increase at somewhere between 6 and 24 hours,

followed by another decrease after that and in the case of Sylgard 182 and Sylgard 170, a slight increase after 7 days. However none of these contact angles, over the course of 7 days, appear to return to the same value that the pristine PDMS surface had. The obvious change in the surface energy around the 24 hour period implies some change in the material surface at this time, which corresponds to the necessary 24 hour wait the PDMS UVO double casting process requires in order to achieve a successful casting.

5.4 Conclusion

In this chapter, a novel method of performing PDMS double casting has been presented. This process, which uses an ultraviolet/ozone (UVO) treatment to modify the surface of a PDMS mould, has been shown to be an effective method of double casting for 3 different PDMs silicones, Sylgard 184, Sylgard 182 and Sylgard 170 which can enable this process

This method of PDMS double casting showed that, after the double casting process has taken place, the double cast stamp displays a reduced adhesion to a Si(100) substrate due to potential contamination of the PDMS surface with either free siloxane chains that have migrated to the surface, or small pieces of the silica like crust that is formed on the surface of a UVO treated mould. By washing the treated mould with isopropyl alcohol, the adhesion of the double cast stamps made from Sylgard 184 and Sylgard 182 show an increased level of adhesion which begins to approach that of a pristine direct cast stamp, however those made from Sylgard 170 only show a very minor recovery.

The PDMS silicones that had the highest number of double castings performed without damaging were Sylgard 184 and Sylgard 182, achieving 4 castings before suffering damage,

while the Sylgard 170 double casting sub-master moulds only survives 2 castings. This is likely due to the flexibility of each PDMS. Sylgard 184 and Sylgard 182 both have higher Young's moduli than Sylgard 170. This could have a twofold impact. Firstly, a sub-master mould of Sylgard 170 would be more likely to suffer cracks or split while being peeled from the Sylgard 170 stamp after casting. Repeated castings could exacerbate this as the sub-master moulds would be heated multiple times during each casting process, causing thermal degradation [9] of the PDMS sub-master, although this may have an impact on Sylgard 184 and Sylgard 182 sub-masters, due to the greater Young's modulus of both of these silicones, any effect is likely to be reduced.

The second impact that the lower Young's modulus of Sylgard 170 may have had on the lifetime of the sub-master mould could have been a reduced number of free siloxane chains in the bulk Sylgard 170 mould. If there were fewer of these free siloxane chains available to migrate to the surface, this could have some impact on the lifetime of the mould.

UVO treatment of moulds made from Silcoset 105 did not produce any usable double cast stamps. This was most likely due to the calcium carbonate additives [29] in the Silcoset 105 PDMS silicone. The presence of these additives could have interfered with the migration of free siloxanes and the formation of the silica-like crust that forms during UVO treatment.

With further development, such as optimising the UVO treatment time and using other methods of cleaning the surface of a double cast PDMS stamp, it would be possible to fabricate UVO double cast PDMS stamps for use in transfer printing with minimal impact on the adhesive properties. Further work could also include experimentation with alternative mixing ratios of PDMS, Sylgard 184 and Sylgard 182 become more flexible when mixed in a ratio of 20:1 (base to curing agent) which could help to prolong the life if the PDMS sub-master.

5.5 References

[1] T. Fujii, "PDMS-based microfluidic devices for biomedical applications," *Microelectron. Eng.*, vol. 61–62, pp. 907–914, 2002.

[2] G. Kaur, M. Tomar, and V. Gupta, "Development of a microfluidic electrochemical biosensor: Prospect for point-of-care cholesterol monitoring," *Sensors Actuators, B Chem.*, vol. 261, pp. 460–466, 2018.

[3] A. Shakeri, S. Khan, and T. F. Didar, "Conventional and emerging strategies for the fabrication and functionalization of PDMS-based microfluidic devices," *Lab Chip*, vol. 21, no. 16, pp. 3053–3075, 2021.

[4] J. Shi, Z. Luo, Z. Dibin, and S. Beeby, "Optimization a structure of MEMS based PDMS ferroelectret for human body energy harvesting and sensing," *Smart Mater. Struct.*, vol. 28, no. 7, 2019.

[5] C. Liu, "Recent developments in polymer MEMS," *Adv. Mater.*, vol. 19, no. 22, pp. 3783–3790, 2007.

[6] L. Gitlin, P. Schulze, and D. Belder, "Rapid replication of master structures by double casting with PDMS," *Lab Chip*, vol. 9, no. 20, pp. 3000–3002, 2009.

[7] H. Hassanin and K. Jiang, "Multiple replication of thick PDMS micropatterns using surfactants as release agents," *Microelectron. Eng.*, vol. 88, no. 11, pp. 3275–3277, 2011.

[8] B. Yang, B. Nagarajan, and P. Mertiny, "Characterization of swelling behavior of carbon nano-filler modified polydimethylsiloxane composites," *J. Elastomers Plast.*,

pp. 1–20, 2021.

[9] K. Xiang, G. Huang, J. Zheng, X. Wang, G. X. Li, and J. Huang, “Accelerated thermal ageing studies of polydimethylsiloxane (PDMS) rubber,” *J. Polym. Res.*, vol. 19, no. 5, 2012.

[10] D. T. Eddington, J. P. Puccinelli, and D. J. Beebe, “Thermal aging and reduced hydrophobic recovery of polydimethylsiloxane,” *Sensors Actuators, B Chem.*, vol. 114, no. 1, pp. 170–172, 2006.

[11] A. P. Munaro *et al.*, “Ageing and structural changes in PDMS rubber investigated by time domain NMR,” *Polym. Degrad. Stab.*, vol. 166, pp. 300–306, 2019.

[12] Z. Brounstein, J. Zhao, D. Geller, N. Gupta, and A. Labouriau, “Long-term thermal aging of modified sylgard 184 formulations,” *Polymers (Basel).*, vol. 13, no. 18, 2021.

[13] K. Kwapiszewska, K. Zukowski, R. Kwapiszewski, and Z. Brzózka, “Double casting prototyping with a thermal aging step for fabrication of 3D microstructures in poly(dimethylsiloxane),” *AIMS Biophys.*, vol. 3, no. 4, pp. 553–562, 2016.

[14] S. H. Kim, S. Lee, D. Ahn, and J. Y. Park, “PDMS double casting method enabled by plasma treatment and alcohol passivation,” *Sensors Actuators, B Chem.*, vol. 293, no. December 2018, pp. 115–121, 2019.

[15] B. A. Langowski and K. E. Uhrich, “Oxygen plasma-treatment effects on Si transfer,” *Langmuir*, vol. 21, no. 14, pp. 6366–6372, 2005.

[16] B. Ruben *et al.*, “Oxygen plasma treatments of polydimethylsiloxane surfaces: Effect of the atomic oxygen on capillary flow in the microchannels,” *Micro Nano Lett.*, vol. 12, no. 10, pp. 754–757, 2017.

[17] Q. Li, X. Han, J. Hou, J. Yin, S. Jiang, and C. Lu, “Patterning Poly(dimethylsiloxane) Microspheres via Combination of Oxygen Plasma Exposure and Solvent Treatment,” *J. Phys. Chem. B*, vol. 119, no. 42, pp. 13450–13461, 2015.

[18] N. Y. Adly *et al.*, “Observation of chemically protected polydimethylsiloxane: Towards crack-free PDMS,” *Soft Matter*, vol. 13, no. 37, pp. 6297–6303, 2017.

[19] J. A. Juárez-Moreno, A. Ávila-Ortega, A. I. Oliva, F. Avilés, and J. V. Cauich-Rodríguez, “Effect of wettability and surface roughness on the adhesion properties of collagen on PDMS films treated by capacitively coupled oxygen plasma,” *Appl. Surf. Sci.*, vol. 349, pp. 763–773, 2015.

[20] C. L. Mirley and J. T. Koberstein, “A Room Temperature Method for the Preparation of Ultrathin SiOx Films from Langmuir-Blodgett Layers,” *Langmuir*, vol. 11, no. 4, pp. 1049–1052, Apr. 1995.

[21] Y. Berdichevsky, J. Khandurina, A. Guttman, and Y. H. Lo, “UV/ozone modification of poly(dimethylsiloxane) microfluidic channels,” *Sensors Actuators, B Chem.*, vol. 97, no. 2–3, pp. 402–408, 2004.

[22] Ossila, “Ossila UV Ozone Cleaner Manual,” pp. 1–22, 2020.

[23] A. Oláh, H. Hillborg, and G. J. Vancso, “Hydrophobic recovery of UV/ozone treated poly(dimethylsiloxane): Adhesion studies by contact mechanics and mechanism of surface modification,” *Appl. Surf. Sci.*, vol. 239, no. 3–4, pp. 410–423, 2005.

[24] M. E. Schrader, “Young-Dupre Revisited,” *Langmuir*, vol. 9, no. 6, pp. 3585–3589, 1995.

[25] MicroChem, “Su-8 2025-75 Datasheet,” pp. 1–5, 2006.

[26] I. D. Johnston, D. K. McCluskey, C. K. L. Tan, and M. C. Tracey, “Mechanical characterization of bulk Sylgard 184 for microfluidics and microengineering,” *J. Micromechanics Microengineering*, vol. 24, no. 3, 2014.

[27] A. Brinkmeyer, M. Santer, A. Pirrera, and P. M. Weaver, “Pseudo-bistable self-actuated domes for morphing applications,” *Int. J. Solids Struct.*, vol. 49, no. 9, pp. 1077–1087, 2012.

[28] H. She and M. K. Chaudhury, “Estimation of adhesion hysteresis using rolling contact mechanics,” *Langmuir*, vol. 16, no. 2, pp. 622–625, 2000.

[29] CHT, “SILCOSET 105 Safety Data Sheet,” no. 21, 2020.

Chapter 6

Thermally Modified PDMS Transfer Printing Stamps Using Embedded Fluidic Channels

In this chapter a novel technique of controlling the temperature of a PDMS transfer printing stamp in order to modify the adhesion to a substrate will be presented. Initially an overview of the field of microfluidics will be presented, as well as the role that PDMS has within this field. A discussion of transfer printing will also be included, looking at what makes PDMS an attractive material from which to fabricate transfer printing stamps. The results of the simulation work performed will be included, as well as how this informed the design of the final PDMS fluidic stamp configuration. This will then be followed by an in depth review of the processes that were undertaken in order to combine the field of microfluidics with that of transfer printing. The design and fabrication methods of the PDMS fluidic stamp will be discussed, as well as how PDMS transfer printing stamps with embedded heated fluidic channels were tested.

Results of adhesion testing will then be presented, along with a discussion as to how these results may widen the operating window for a transfer printing stamp, enabling in-situ modification of the adhesion achieved by a PDMS transfer printing stamp not only through

exploitation of the viscoelastic nature of PDMS, but also the temperature dependant nature of the adhesion of PDMS as well enabling the use of new material/substrate combinations.

6.1 Microfluidics and Transfer Printing

Poly(dimethylsiloxane) (PDMS) is part of a wider category silicones [1] and has become a widely used material in various fields. This has been largely driven by developments in the soft lithography process which is the method of forming silicones into predesigned structures and patterns [2]. One key field that has been one of the driving factors in the development of soft lithography processes for PDMS is microfluidics, where micrometre scale channels are used to manipulate fluids for applications in fields such as chemical analysis [3][4] and mass spectrometry [5][6].

Glass and silicon were initially attractive materials used for creating these micrometre scale channels due to the maturity of the processing methods required in order to fabricate microfluidic channels as well as the rigidity of the materials themselves, providing a more solid microfluidic device [7]. However, microfluidic devices made from these materials were costly to design and make as well as being time consuming to produce. As such, PDMS generated significant interest as a material from which fabrication of microfluidic channels could be achieved, in particular was Sylgard 184 [8].

One of the greatest attributes of PDMS is its ability to be rapidly prototyped and fabricated using processes involving casting the uncured PDMS against a patterned or structured solid surface [9]. To fabricate high quality glass microfluidic devices multiple stages

of development are required. A process for the fabrication of glass microfluidic devices is described by Golozar et al [10] whereby a clean glass substrate had a 200nm thick layer of amorphous silicon deposited onto the surface using low pressure chemical vapour deposition (LPCVD) followed by a standard photolithography process involving spin coating a photoresist layer, exposing certain areas of the photoresist and developing it. Then the exposed amorphous silicon layer on top of the glass, is plasma etched in order to reveal the surface of the glass in selected areas. The exposed glass was then wet etched using 49% hydrofluoric (HF) acid before the remaining photoresist was removed, followed by the removal of the amorphous silicon. The patterned glass was then further processed by thermally bonding this microfluidic channel patterned glass substrate to another patterned glass substrate. This process involves many steps, each requiring expensive and, in some cases, dangerous processes in order to achieve a 30μm deep microfluidic channel.

For silicon devices, channels can be created by using a patterned photoresist layer on the surface of a silicon wafer so that only selected areas of the silicon wafer are exposed, then performing a reactive ion etching (RIE) process to etch away the exposed material [11]. This is a time consuming process that requires the use of expensive equipment and facilities.

The process of fabricating a PDMS microfluidic device by comparison require very little equipment and can be performed quickly. There are many way to create a solid patterned structure onto which the PDMS can be cast such as 3D printing [12] which would be more suitable for larger scale features, or photoresist patterning [13] which can provide greater resolution structures. Once a patterned mould has been created, prepared uncured PDMS mixtures can be cast over the mould, requiring relativity little curing time, often less than 24 hours. PDMS, in particular Sylgard 184, has been shown to have good replicability when cast over a structured mould as shown by Rogers and Nuzzo [14] where a structured mould using 0.5-5nm diameter carbon nanotubes was successfully cast over with Sylgard 184 PDMS and

showed transfer of the pattern onto the PDMS surface. Once the PDMS has been cured, the mould can then be reused multiple times, providing a method of rapidly fabricating microfluidic devices.

The cured and patterned PDMS microfluidic device can then be subjected to further processing if desired, such as oxygen plasma treatment of PDMS microfluidic channels [15] in order to create super-hydrophilic PDMS channels, enabling spontaneous capillary flow of water through the channels. It is clear that PDMS has become a highly useful material for applications in microfluidics and methods of PDMS microfluidic device fabrication will continue to develop. PDMS is not exclusively used for the fabrication of microfluidic devices. It has also been used to fabricate a patterned structure for use in transfer printing. This method has been of particular interest in the semiconductor field as a way of fabricating heterogeneous devices and materials [16].

The process of transfer printing, as already discussed, relies upon the exploitation and control of the kinetically controlled adhesive properties of PDMS, however, this property of PDMS can be modified. PDMS, in particular Sylgard 184, is supplied in two components, a bulk base component, and a curing agent and it can be seen from Kim et al [17] and Carlson et al [18] that by mixing the ratios of base to curing agent, the adhesive properties can be modified further. The manufacturers recommended ratio of Sylgard 184 is 10:1 base to curing agent, however Kim et al [17] used a ratio of 5:1 base to curing agent. This provided a much less adhesive and less flexible PDMS which can be seen in the reported adhesion data. At 750 μms^{-1} the 5:1 PDMS achieved approximately 1 mN, corresponding to an energy release rate of 10 $J.m^{-2}$, a significant reduction from the energy release rate Carlson reported that at an interface made from a 20:1 PDMS, which creates a more adhesive and soft PDMS, at 750 $\mu m.s^{-1}$ the force of adhesion was 7.5 mN for a 100 μm^2 contact area. This corresponds to an energy release rate of 75 $J.m^{-2}$ In these cases, as the PDMS stamps were not entirely comparable due to

differing contact areas which give a different level of adhesion, therefore these values have been converted to energy release rate. The equation relating the adhesive force and the energy release rate is given as [19]:

$$G = \frac{F}{w}$$

Where G is the energy release rate ($J.m^{-2}$), F is the adhesive force (N), and w is the out of plane width. By using energy release rate rather than adhesion, it can allow for stamps of different contact areas to be compared.

It has been reported by Feng et al [19] that the kinetically controlled adhesion of a PDMS stamp can also be modified by changing the interface temperature between the PDMS stamp surface and the substrate surface. It has been shown that the adhesion of a PDMS stamp reduces as the interface temperature increases and likewise as the temperature lowers, the adhesion increases. In this report, 3 temperatures were compared, 4°C, 24°C, and 37°C. The energy release rates for stamps at these temperatures were presented at a range of retraction speeds. At $7.5mm.s^{-1}$ retraction speed, the energy release rates were 16 $J.m^{-2}$ at 4°C, 7.5 $J.m^{-2}$ at 24°C, and 6 $J.m^{-2}$ at 37°C. The full data has been reproduced in Figure 6.1. By controlling the adhesion of a PDMS transfer printing stamp not only through control of the retraction speed, but also through the exploitation of the temperature dependant nature of the adhesion of PDMS too, different combinations of materials and substrates could be achieved.

Saeidpourazar et al [20] developed a process of laser driven transfer printing where a laser was used to heat the transfer printed materials when in contact with the receiving substrate. This report only described how the thermal expansion coefficient difference between PDMS and the heated ink caused bowing of the ink, which facilitated easy printing, however, heating the ink to over 250°C would cause an increase in the temperature of the PDMS in

contact with the ink. Feng et al [19] have already shown that small increases in temperature of PDMS have a notable impact on the adhesion of that PDMS so it is possible that this played a part in facilitating printing of the ink.

By combining the fields of microfluidics and transfer printing it would be possible to create an adhesive PDMS stamp, the surface temperature of which could be modified using embedded heated fluidic channels, which would widen the operating window for the transfer printing process.

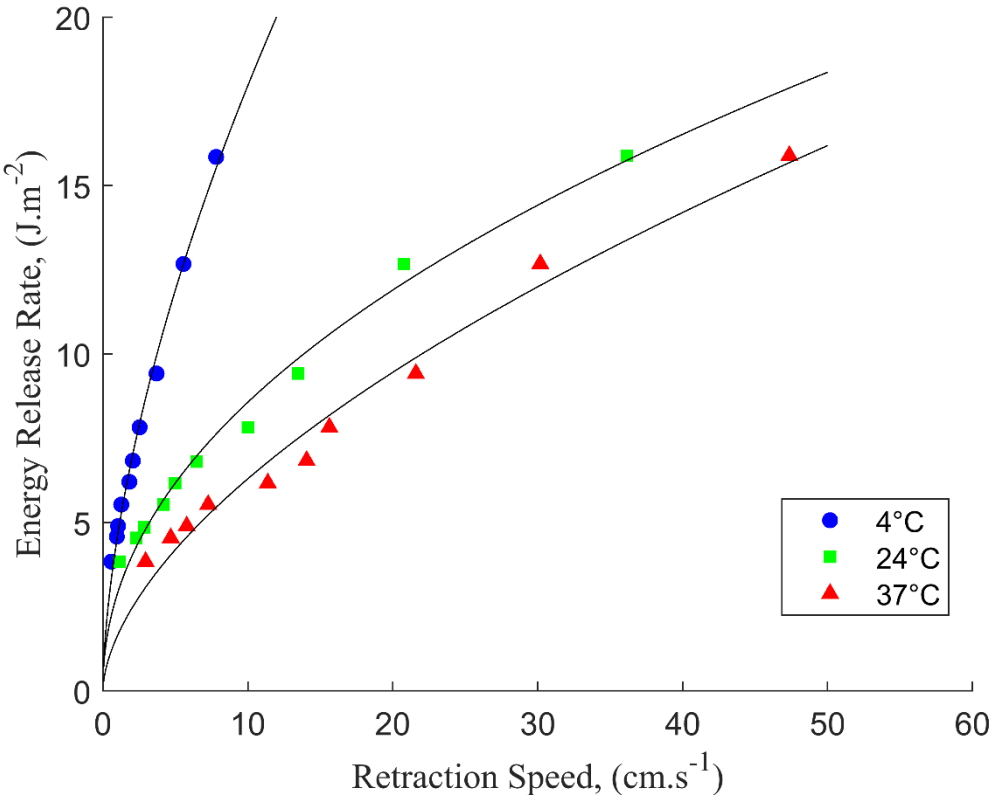

Figure 6.1: Graph showing the impact of changing the temperature of the surface of a PDMS stamp on the velocity dependant adhesion. Reproduced from [19].

6.2 Methods

This section will describe the processes and experimentation that was developed and used in order to achieve a thermally controllable PDMS stamp using heated embedded fluidic channels in order to modify the adhesive nature of PDMS. By controlling the adhesion of a PDMS stamp through surface temperature modification, the operating window for a particular stamp can be widened. Current methods of achieving temperature control of a PDMS stamp have been demonstrated however these are complicated and expensive to implement, and in some cases scalability is not as feasible. Initially simulation work was performed which informed the designing of the PDMS layer structured with fluidic channels of the composite fluidic PDMS stamp, the key aspect of which was the proximity of the fluidic channels to the surface of the PDMS stamp in order to achieve heating within a reasonable time frame. Designing of the fluidic channels then took place followed by fabrication of the fluidic PDMS stamp components as well as experimentation with methods of bonding two PDMS components together. The PDMS stamp design with embedded fluidic channels in shown in Figure 6.2.

6.2.1 Simulations

In order to develop a simple and scalable approach for surface temperature modification of PDMS transfer printing stamp in order to exploit the temperature dependant nature of the

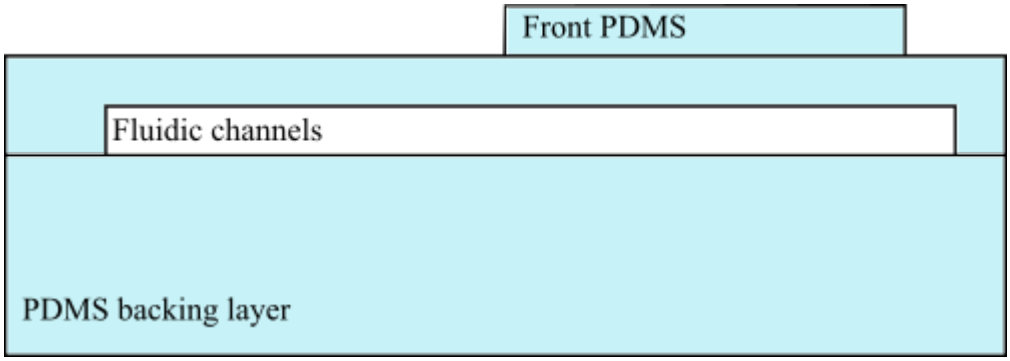

Figure 6.2: Schematic showing the layers of the PDMS stamp with embedded fluidic channels.

adhesive properties of PDMS, a PDMS stamp was designed which contained embedded channels through which heated water could be pumped.

The key factor that needed to be identified before any experimentation could begin was how close to the surface of a PDMS stamp did a channel have to be in order to detect a temperature change on the surface. To do this, COMSOL simulations were performed using the Heat Transfer module. Using a 3D model of a PDMS stamp with two channels running through, time dependant simulated measurements of the surface temperature of the stamp were taken. These results would provide information that would be used when designing mould from which to cast PDMS.

6.2.2 Mould Creation

The technique of using microfluidic systems cast in PDMS has been well documented in numerous reports [8][21][22][13][23] which often involve the use of thick layers of structured SU-8 on a silicon substrate. This process has been mentioned earlier for the use in fabricating posts on PDMS stamps for transfer printing applications [24]. Achieving thick SU-8 of around

100 μm or greater can be challenging, especially when uniform and flat surfaces are required [25]. For microfluidics, channels on the scale of 100 μm are suitable, however, in order to achieve suitable flow of heated water through the PDMS stamp in order to register a temperature increase, fluidic channels of greater dimensions were necessary.

6.2.2.1 Aluminium Moulds

The first design of fluidic moulds in which to cast a PDMS fluidic stamp used a 1 mm wide and 2 mm high channel with two small reservoirs at the inlet and outlet. This was milled into the surface of an aluminium plate which was then polished in order to achieve a flat surface, a photograph of this can be seen in Figure 6.3. Due to the limitations available with fabrication of this mould, only an inverse mould (with the channel material removed from the mould) was achievable. This would then be used as the first stage of a PDMS double casting process as described in Chapter 5.

The initial casting a 10:1 mixture of Sylgard 184 PDMS into mould was met with mixed success. The milling process used to remove material to form the fluidic channels left sharp edges surrounding the channels which cut into the cured PDMS so that when attempts were made to peel the cured PDMS from the mould, often the PDMS would split, leaving the channel material stuck within the mould. Only by very gently removing the stamp from the mould after being curing achieved any success, but still often led to some damage or splitting occurring to the stamp. It was evident that the low success rate of this design, combine with the necessary

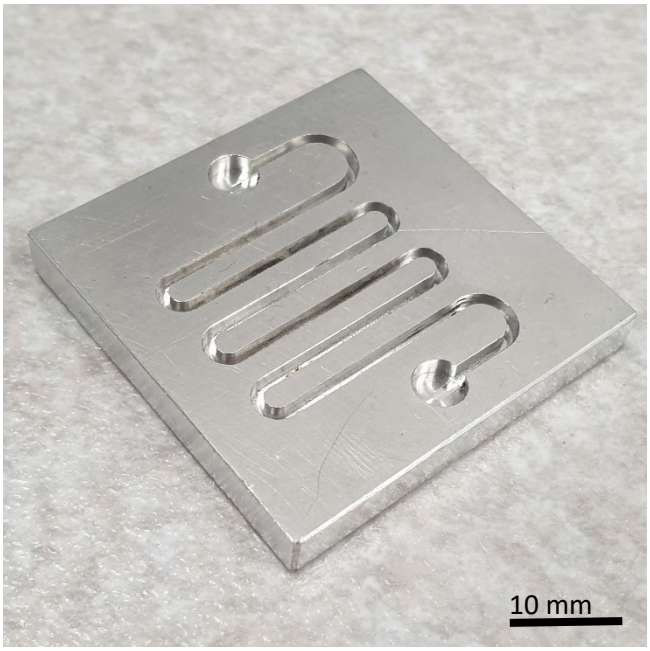

Figure 6.3: Photograph showing the first iteration of the fluidic channel mould. This was an aluminium double casting mould as the PDMS cast from it would have the inverse pattern than was desired. This meant that to use the stamp cast from this mould, it would need to be treated to enable PDMS double casting. Due to the milling process used to make this mould, the edges of the fluidic channels were sharp and were liable to split any PDMS that was cast into it.

further processing of double casting, was too unreliable a method to continue development with.

6.2.2.2 3D Printable Fluidic Channel Moulds

In order to more rapidly create moulds that could be used to cast fluidic channels in PDMS, and remove the necessity for a double casting process, a 3D printing approach was used. By using CAD (computer aided design) software, it was possibly to quickly design a range of

moulds which could then be produced using 3D printing using a PLA (poly-lactic acid) filament.

The first design to be 3D printed used smaller channels, with the intension being to achieve a higher density of channels, producing a more even heating of the PDMS surface. These channels were 1mm by 1mm and had only 1mm spacing between them. However, issues arose from both the design, and the material that was used to create the 3D printed mould. The gap between channels was much too small, leading to the same issue as was encountered with the aluminium mould previously, where the PDMS became stuck between the features and split, rather than releasing easily. Secondly, up until this point, elevated temperatures were used to accelerate the curing time of Sylgard 184 (more information regarding this is included in Chapter 3: Experimental Techniques) however, even at temperatures as low as 100°C, the PLA mould began to soften and warp which became more prominent with repeat castings.

The second design built on observations seen with the previous two moulds and used a larger channel, 2mm x 1mm, which allowed for a higher flow rate, Figure 6.4 shows a photograph of this 3D printed mould. As well as the larger channels, this new mould design had wider gaps separating the channels, reducing the radius of the curves in the channels that were necessary in order to achieve an s-shape channel. The increase in size of these features led to an overall more successful casting which was only performed at room temperature in order to prolong the lifetime of the mould. Due to the process of 3D printing and the nozzle size used to print the mould, the flat underside of the cast PDMS was very rough. Initial attempts to smooth this rough face were met with destruction of the moulds or damaged features.

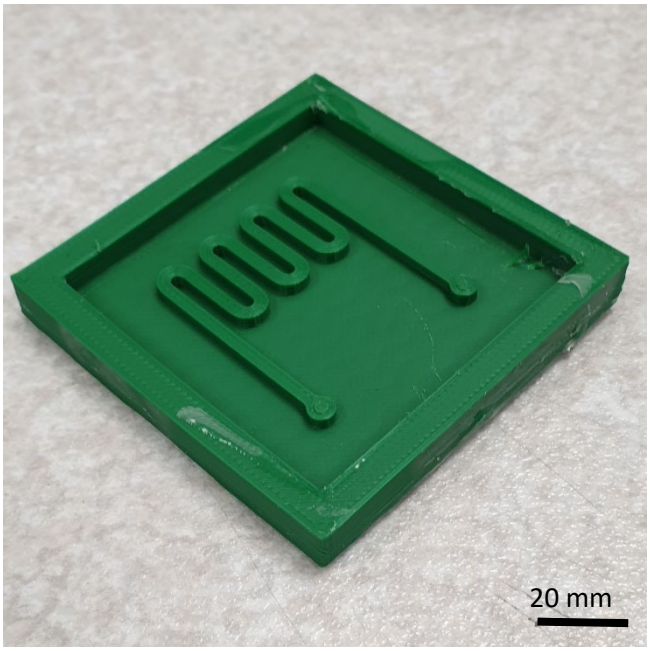

Figure 6.4: Photograph of the final design used for the 3D printed mould. Note the rough face at the base of the mould due to the nozzle size of the 3D printer. This roughness limited which bonding methods were appropriate.

6.2.3 PDMS Casting

In order to achieve a PDMS stamp with embedded fluidic channels, it was necessary to cast PDMS silicone in multiple parts. This section will discuss the preparation of the PDMS silicone as well as how each component of the PDMS stamp was made. The process of bonding the components together is also discussed.

6.2.3.1 PDMS Preparation

Each Fluidic PDMS stamp was composed of three discreet castings that were combined once the casting were completed. Each PDMS casting in this chapter was performed using Sylgard 184 (Dow) and followed the same preparation process. Firstly, the Sylgard 184 base material was deposited into an aluminium tin and weighed, then using a pipette, a corresponding quantity of curing agent was added. The mixing ratio of Sylgard 184 base to curing agent varied depending on application with 10:1 (base to curing agent) being the suppliers recommended ratio, while a 20:1 ratio resulted in a much more adhesive and flexible PDMS.

Once the curing agent had been added to the base silicone, the two components were thoroughly combined using a plastic spoon. Due to both the base and curing agent being a colourless liquid, ensuring that both components were evenly mixed could not easily be observed, so in order to guarantee an even mixing, the two components were vigorously mixed, trapping air within the mixture. When the PDMS mixture, or slurry, became opaque due to the number of bubbles introduced into the mixture, it can be presumed that a complete and even mixture has been achieved.

The mixed PDMS has too much trapped air in to achieve a successful casting, so it was outgassed in a desiccator for 10 minute intervals until any trapped air bubbles are removed. The bubble free mixture was then ready to be poured over whatever mould is required. Sylgard 184 can be cured in 48 hours at room temperature, or for 35 minutes at 100°C.

6.2.3.2 Casting Fluidic Channels

When casting the component with the fluidic channel, Sylgard 184 was mixed in a 20:1 ratio (base to curing agent) according to the process described in the previous section and was poured into the 3D printed PLA mould. The 20:1 mixing ratio for this component of the fluidic stamp was crucial as earlier experimentation with 10:1 castings of the same design experienced leaking around the ports, which connected the fluidic stamp to a larger water loop. A 20:1 mixture of Sylgard 184 gives a much softer and more flexible PDMS which would provide a better seal around the ports. Once the mould had been filled with the PDMS slurry, it was gently agitated for 2 minutes, then left for a further 2 minutes in order to allow any bubbles

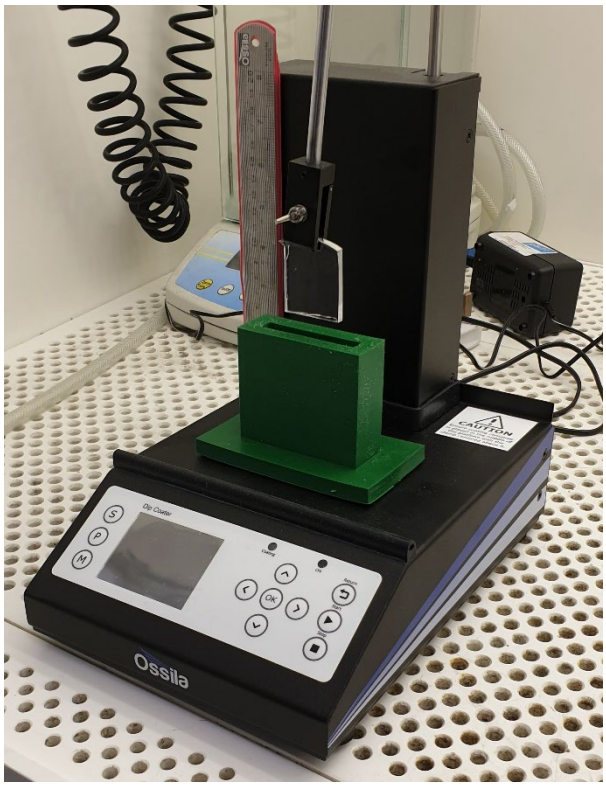

Figure 6.5: Photograph of the Ossila Dip Coater ready to lower the PDMS bulk back piece into a waiting vessel of liquid PDMS. This would then be used to form the back side of a fluidic PDMS stamp.

introduced during the PDMS pouring had time to rise to the surface and burst. After this time, any bubbles that remained were manually removed using a pair of tweezers to manually remove any trapped bubbles. Once bubble free, the mould was left on a flat surface for 48 hours until cured.

To seal the fluidic channels and ensure water tightness, a flat bulk piece of PDMS was cast, onto which the fluidic channel layer could be bonded. In order to cast this, 10:1 PDMS mas mixed as described previously and poured into a flat polystyrene Petri dish which was then left on a flat surface at room temperature for 48 hours. Once cured, the surface of this PDMS backing layer was cut to the same size as that of the fluidic layer, washed with isopropyl alcohol (IPA) (99.8% isopropyl alcohol, Fisher Chemical) and dried with nitrogen. Once prepared, the PDMS backing layer was mounted onto the dip coater (Dip Coater, Ossila), displayed in Figure 6.5, and lowered into a vessel containing premixed and bubble free 10:1 PDMS (Sylgard 184). The dip coated was programmed to retract at 0.3 $mm.s^{-1}$ which provided a thick enough layer of PDMS that the rough underside surface of the fluidic channel layer was evenly coated an a good seal was made, while being thin enough that the fluidic channels would not be filled with the liquid PDMS adhesive. Once the dip coater had retracted the PDMS backing layer from the liquid PDMS vessel, it was laid onto a flat aluminium plate and the fluidic layer was carefully

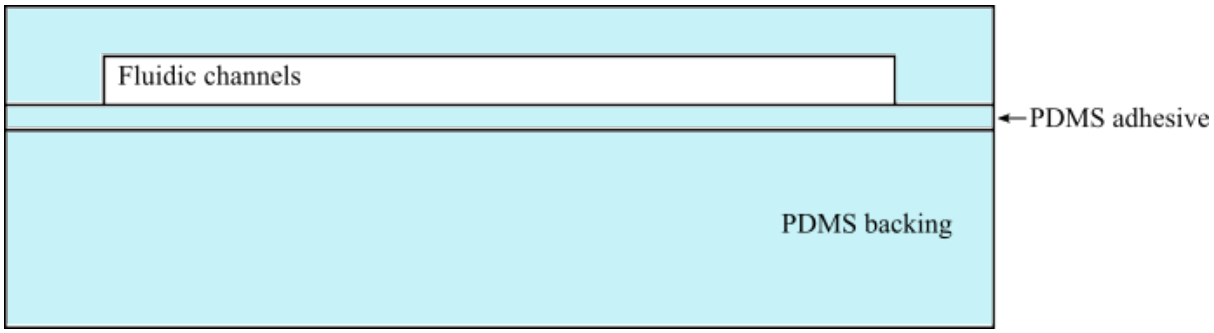

Figure 6.6: Schematic showing the layer of PDMS adhesive sealing the fluidic channels and bonding the PDMS backing component and the PDMS layer structured with the fluidic channels.

lowered onto the surface. Once the fluidic layer was in place, and there were no trapped bubbles between the two layers, the aluminium plate, with the two PDMS stamp components were baked in an oven at 100°C for 35 minutes. Once cooled, the stamp with embedded fluidic channels was peeled from the aluminium plate and any liquid PDMS that had seeped out from between the two layers during casting was trimmed away using a scalpel. This is shown in Figure 6.6.

6.2.3.3 Casting Front Plate

It had been previously noted that a flat surface of 20:1 PDMS had such a high adhesion to a silicon substrate that it risked overloading the load cell on the transfer printing system. As such it was necessary to include an additional layer to the PDMS fluidic stamp that was made from a lower adhesion PDMS, in this case a 10:1 mixing ratio square of PDMS, 2 mm thick, was cast. In order to achieve a flat PDMS suitable for adhesion measurements, a Si(100) wafer fragment was adhered to polyimide tape which was then stretched across the back of an aluminium frame. Once flat and sealed, mixed Sylgard 184 in a 10:1 mixing ratio was added and cured at 100°C for 35 minutes.

Once this had cured and cooled, and the embedded fluidic channel stamp was ready, the back side of the flat square of 10:1 PDMS and the top of the fluidic stamp were cleaned with IPA to remove any potential contaminants from the surface. Once clean and dry, the two cleaned faces were treated with ultraviolet/ozone (UVO) (Ultraviolet Ozone Cleaner, Ossila) for 30 minutes before being immediately contacted with the corresponding treated surface and

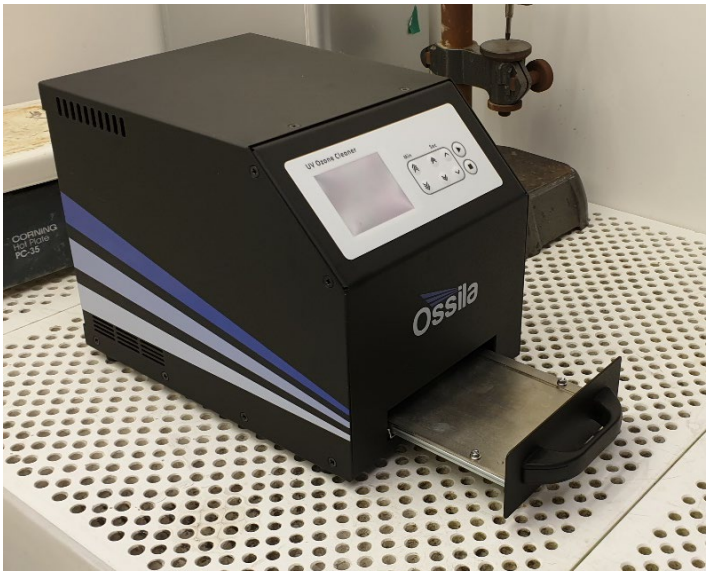

Figure 6.7: Photograph of Ossila ultraviolet/ozone cleaner in preparation for UVO treatment of the 10:1 PDMS front plate and the embedded fluidic stamp in order to bond the two together.

left for 24 hours before being ready to use. A photograph of the UVO cleaner is displayed in Figure 6.7.

6.2.4 Ports

The fluidic channels embedded within the PDMS stamp were just part of a much larger water loop. In order to connect the fluidic PDMS stamp to the rest of the water loop, ports were necessary. Initially a coring punch was used to create a small hole within the PDMS that would allow for small barbed Luer lock adapter to be inserted. While this method did initially provide a water tight seal, small adjustments to the angle of the ports, often caused by movement of the connected water loop, led to leakage around the ports.

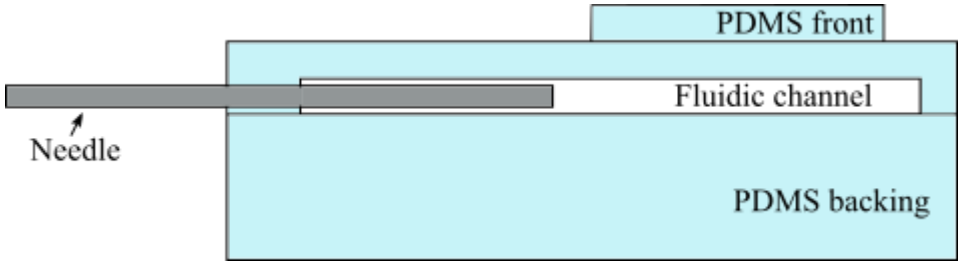

Figure 6.8: Diagram showing how a needle would be inserted into the fluidic channel within the PDMS stamp to connect it to the water loop.

As a replacement to the barbed ports, hypodermic needles were selected. As these were available in much greater lengths, it enabled these ports to sit more firmly within the channel, so they were less likely to slip or fall out. Due to the needles being hypodermic, they were easily inserted into the PDMS stamp without the need to punch a guiding hole as was needed before. These needles were connected to the water loop using Luer lock connections which provided a good water tight connection. Figure 6.8 shows a schematic of a PDMS stamp with a needle inserted.

6.2.5 Pumps and Insulation

To get heated water to flow through the stamp, heating the surface and providing a temperature change at the stamp/substrate interface which would modify the adhesion of the stamp, various pumps were selected, each with different flow rates in order to achieve optimal heating.

Initially a peristaltic pump (Variable-Speed Pump Medium Flow, Cole-Parmer) (60ml/min) was selected, connected to a closed water loop filled with de-ionised water. In order to achieve a temperature change, a water bath (Clifton NE1D-4) was used. This was an

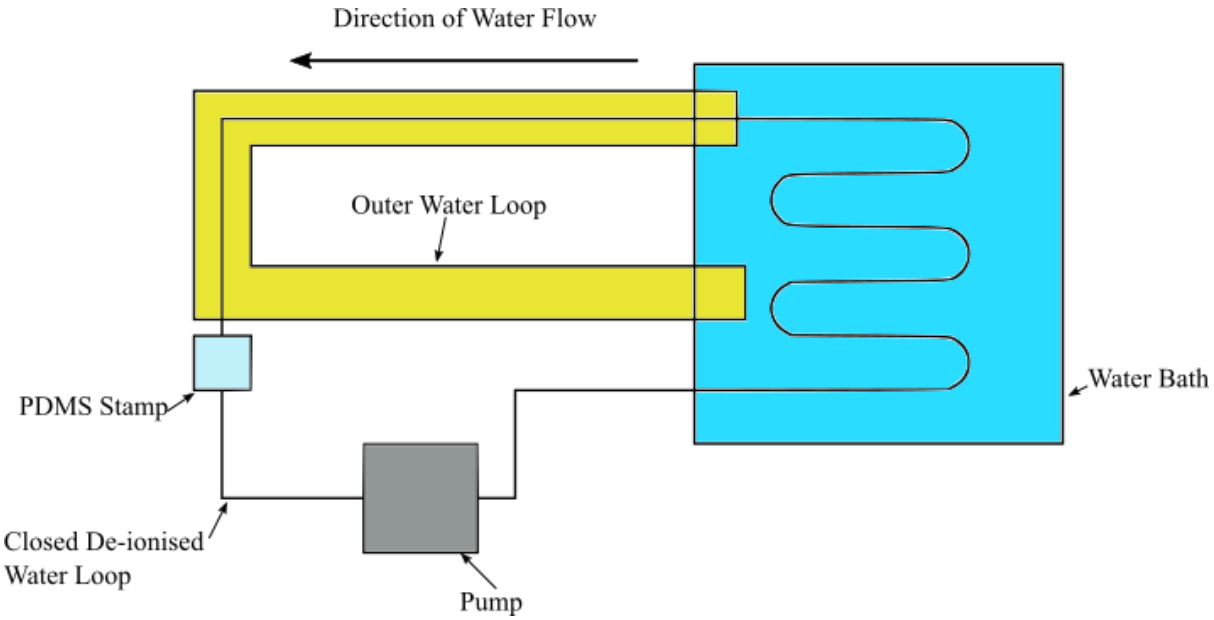

Figure 6.9: Layout of the final water loop used to heat the PDMS stamp with embedded heated fluidic channels.

unstirred water bath, but was initially mixed with manual stirring, then after using a pump to agitate the water achieving even heating of the water. A heat exchanger submersed within the water bath would heat the water in the closed loop system which would then be pumped around the entire water loop. This water loop system can be seen in Figure 6.9.

The low flow rate of the peristaltic pump was beneficial as it reduced the chance of rupturing any of the seals within the loop, such as those made by the ports to the PDMS stamp, or the PDMS adhesive seal that was made between the two components of the PDMS stamp. However, even with the shortest loop possible, the heat loss that occurred in the time it took for the water to flow to the PDMS stamp, no noticeable temperature change was measured on the stamp surface using a thermocouple. As a potential solution, insulation was added to the water loop tubing in the hopes of reducing the heat loss. Even with the insulation, at a water bath temperature of 95°C, there was only a 5°C temperature change at the surface of the PDMS stamp.

Two modifications were made to the water loop in order to further reduce the heat loss that occurred between the water leaving the heat exchanger in the water bath and reaching the PDMS stamp. The first was the use of an actively heated water jacket around the closed water loop tubing. This was created using double walled tubing through which a higher flow rate of heated water could be pumped, further reducing the heat loss. This water pump (GP20/18, Totton Pumps) was used which had a flow rate of 18 litres per minute, much higher than that of the pump used for the water loop. This higher flow rate would help minimise the cooling that would take place. As well as the heated double walled tubing used, a higher flow rate water pump was used (12V 380mbar Direct Coupling Centrifugal Water pump, RS Components) which could feed water to the stamp at a rate of 1150 ml/min. This reduced the time taken for water to flow from the heat exchanger to the PDMS stamp, drastically reducing the heat loss. The combination of the double walled tubing and the higher flow rate pump meant that a stamp temperature of 39°C was achievable at a bath temperature of 70°C.

6.2.6 Adhesion Testing

The process of measuring the kinetically controlled adhesion between a PDMS stamp and a substrate will be described as well additional steps necessary to protect the electrical equipment by minimising the chance of a water leak. As well as this, the automation of the transfer printing process will be covered, looking at methods of how the automation process provided greater control over the z-stage.

6.2.7 Transfer Printing System

In order to collect the adhesion data at a range of retraction speeds in order to get a complete picture of how the temperature of the stamp impacts its adhesive properties a transfer printing system was used. This system uses a vertical z-stage that can be controlled using a connected computer using a script that was written to have a great level of control over the stage. This vertical stage has an arm that ran parallel to the load cell upon which glass slide with the PDMS stamp adhered can be mounted. For these tests, the usual mounting method of using a vacuum

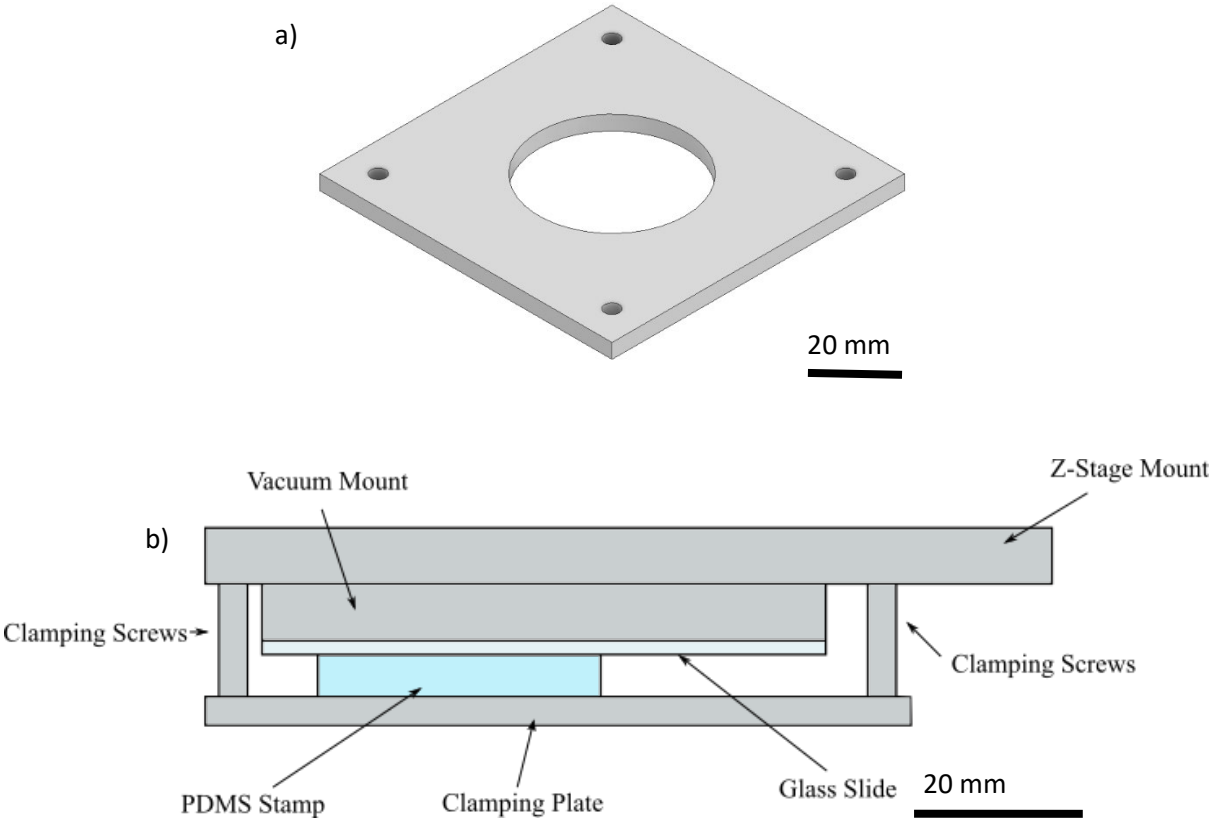

Figure 6.10: a) The clamping plate created to ensure the PDMS stamp would be securely mounted which was especially important due to the additional weight of the ports and water loops connected to the stamp. In b) it can be seen how the clamping plate would hold the PDMS stamp in place by compressing it slightly onto the glass slide.

chuck was insufficient due to the added weight of the water loop, the larger stamp and the added safety measures. So another mount was designed which had an optional front plate that could be screwed into place which can be seen in Figure 6:10. This meant that for regular transfer printing use, the plate was unnecessary and could be removed, using only the vacuum chuck to hold the stamp and the glass slide in place. However should that be insufficient, the plate can be screwed into place, pushing against either the glass slide or the PDMS stamp (depending on the size of the PDMS stamp in use) and locking it in place.

In order to support the water loop and the ports, special clamps were designed which could be secured to the arm of the vertical stage and the front plate with the water loop and port running in between the two section of the clamp. The clamp could then close on the compliant water loop, ensuring that should something catch on the water loop, the hypodermic needle would not come free, risking harm to the users, or that water could leak out, risking damage to electrical equipment.

Below the stamp was an x/y-stage upon which had a load cell (GSO-10, Transducer Techniques) could be attached, providing the adhesion data from the stamp that would be essential for determining the impact of temperature of the stamp on the adhesion as well as the effectiveness of this method of heating the PDMS stamp.

6.2.8 Noise

During initial testing and development of the transfer printing system it was mounted upon a flat optical bench, ensuring the alignment of the system. However it soon became apparent that there were further developments needed to the transfer printing system due to background noise readings from the load cell. It was unclear initially whether these were caused by physical vibrations or electrical interference. It had already been seen that the load cell readings were sensitive enough to be disrupted by the footsteps of other laboratory users as well as the laboratory door being opened and closed. It was decided that the first change to the system would be to move it entirely onto a new bench, the new one being plumbed into the building nitrogen line to provide a floating benchtop to better isolate the system from vibration isolation.

Despite the vibration isolation that the new bench provided, load cell readings were still picking up noise that was masking the load cell output that was of interest. To try to shield the system better from any background electrical inference of EMI a Faraday cage was installed, fully surrounding the transfer printing system except for small holes in the sides through which cables and the nitrogen line could be passed. The Faraday cage reduced the induced EMI slightly however a particular noise artefact still persisted. The Faraday cage also had a secondary impact which was to shield the load cell from any air movement in the laboratory. The transfer printing system was located directly underneath an outlet for the air conditioning system which could not be switched off and caused occasional noise reading on the load cell. The complete enclosure of the system within the Faraday cage helped to protect the load cell from this movement of air.

It was noted that despite the load cell being enclosed within the Faraday cage, sections of the wiring connecting the load cell to the motion controller (which controlled the z-stage,

but also acted as a method of collecting the load cell data) was unshielded. This could be one way that the shielded load cell could still be producing readings with high levels of noise. The cable connecting it to the motion controller was replaced, firstly with a section of twisted pair wire wrapped around a ferrite core, then to a length of shielded cable which would run between the load cell and the motion controller.

All of these modification to the transfer printing system reduced some of the background noise that was masking the load cell data that was needed, however there was still a particular noise artefact that occurred at irregular intervals. A final modification to the transfer printing system was the introduction of an UPS (uninterruptable power supply) through which the motion controller, z-stage, load cell, and connected computer were powered. A UPS is usually used as a method of keeping key equipment powered in case of power cuts or electrical disruption. The UPS charges an internal battery that can supply power should the mains power be switched off. However, due to the constant charging of the battery, it can act as a filter for the mains electricity. The laboratory housing the transfer printing system is located within a building that contains a larger number of pump and chillers that could introduce some noise into the mains power lines within the building.

The end result of all of these added features to the transfer printing system was to reduce the background noise of the load cell considerably, allowing for low adhesion materials and stamps to be tested.

6.3 Results

6.3.1 Simulation Results

The results of the COMSOL simulations which informed the design of the fluidic mould that was fabricated showed that for a PDMS stamp in isolation with 2mm diameter channels embedded 2mm below the surface, perfect thermal equilibrium would take an impractical length of time to reach. An example of the stamp design is shown in Figure 6.11. The simulations performed studied the surface temperature of a PDMS stamp with two fluidic channels for 1 hour at 3 different water temperatures, 50°C, 60°C, and 70°C.

The results are displayed in Figure 6.12 and show that for a water channel temperature of 70°C it would take 4.5 minutes in order to achieve a surface temperature of ~336K (~63°C), however by the time 47.5 minutes had elapsed, the PDMS stamp surface temperature had reached ~342K (~69°C). During this window of 43 minutes, the transfer printing process could have been performed many times as each transfer printing process, either inking or printing, takes less than 30 seconds to perform. During this time, the temperature of the stamp surface would not

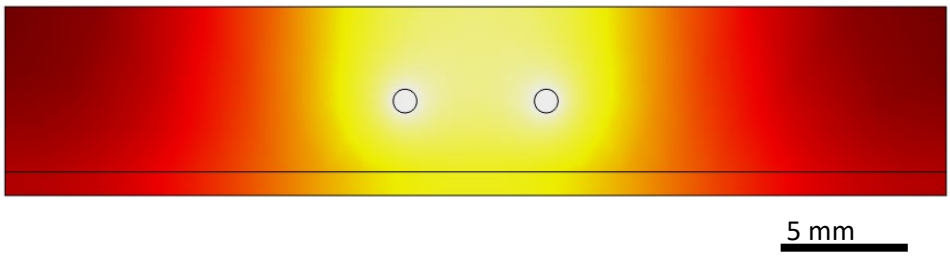

Figure 6.11: Side on view of the COMSOL model for the PDMS stamp.

have changed drastically, so that even if the adhesion of the stamp is heavily dependent on the temperature of the stamp, this minor variation would not impact the adhesion.

In comparison to the channel temperature of 70°C, at channel temperatures of 60°C and 50°C, there is a similar trend, with a rapid initial increase in surface temperature of the PDMS stamp which then levels off over time. After 3.5 minutes the PDMS stamp with a channel temperature of 50°C showed a rapid surface temperature increase from 20°C to ~45°C however after this point the rate of change of temperature reduced and after 46 minutes had elapsed, the PDMS stamp surface temperature was ~49.5°C. This is the same for a 60°C channel temperature where after 4 and a half minutes, the stamp had reached 54°C and only reached

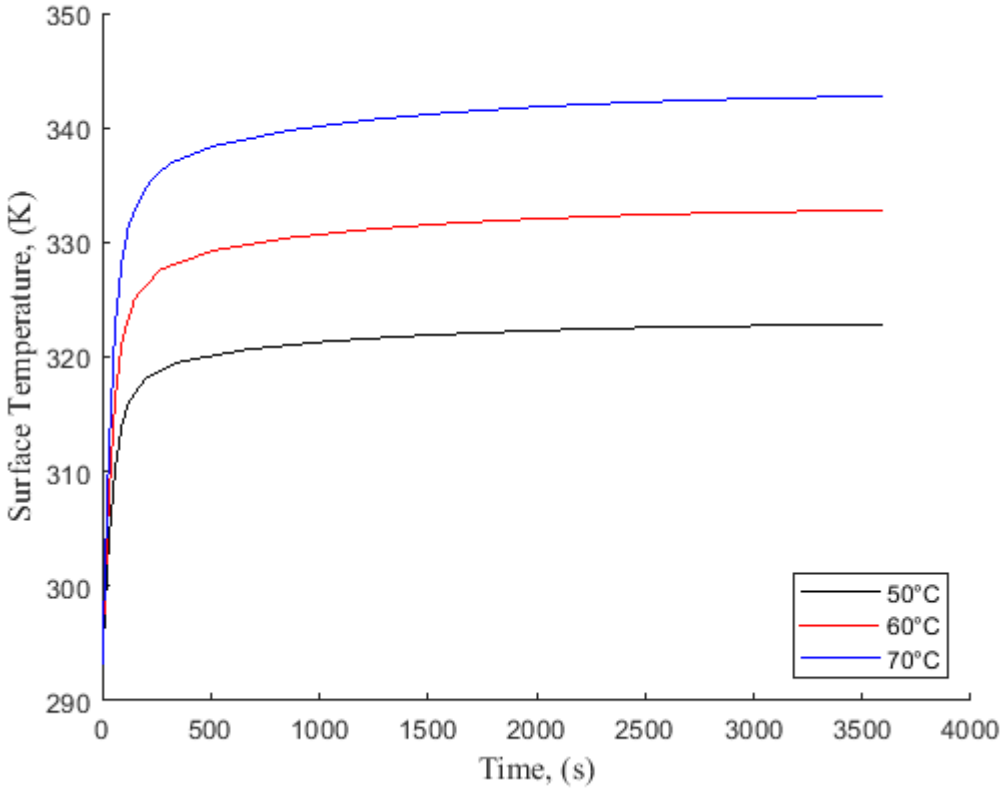

Figure 6.12: Graph showing the results from the COMSOL simulations of PDMS stamp surface temperature against time with heated fluidic channels embedded 2mm below the surface at 3 temperatures: 50°C, 60°C, and 70°C.

99% of the target temperature after 47 minutes. These results are collected in Table 6.1 for easy comparison.

Table 6.1: Table containing the simulation results of the time taken for PDMS stamp with fluidic channels of different temperatures (50°C, 60°C, and 70°C) to achieve 90%, 95%, and 99% of the target surface temperature surface.

	Time taken to reach % of target surface temperature		
Fluidic Channel Temperature	90%	95%	99%
50°C	210s	690s	2760s
60°C	270s	810s	2820s
70°C	270s	840s	2850s

To understand how the addition of components to the PDMS stamp might affect the heating of the surface, simulations were performed of a PDMS stamp with a pair of 2mm diameter fluidic channels 2 mm beneath the surface of the PDMS stamp. Onto the bottom of this 4mm thick PDMS stamp a glass slide was modelled and surface temperature measurements were taken. As well as this, an example piece of transfer printable material, or 'ink' made from silicon were adhered to the surface of the PDMS stamp in order to understand how the addition of inks to the surface of a PDMS stamp might impact the heating. Figure 6.13 shows the simulation data of the surface temperature of the stamp with 70°C channels 2 mm below the

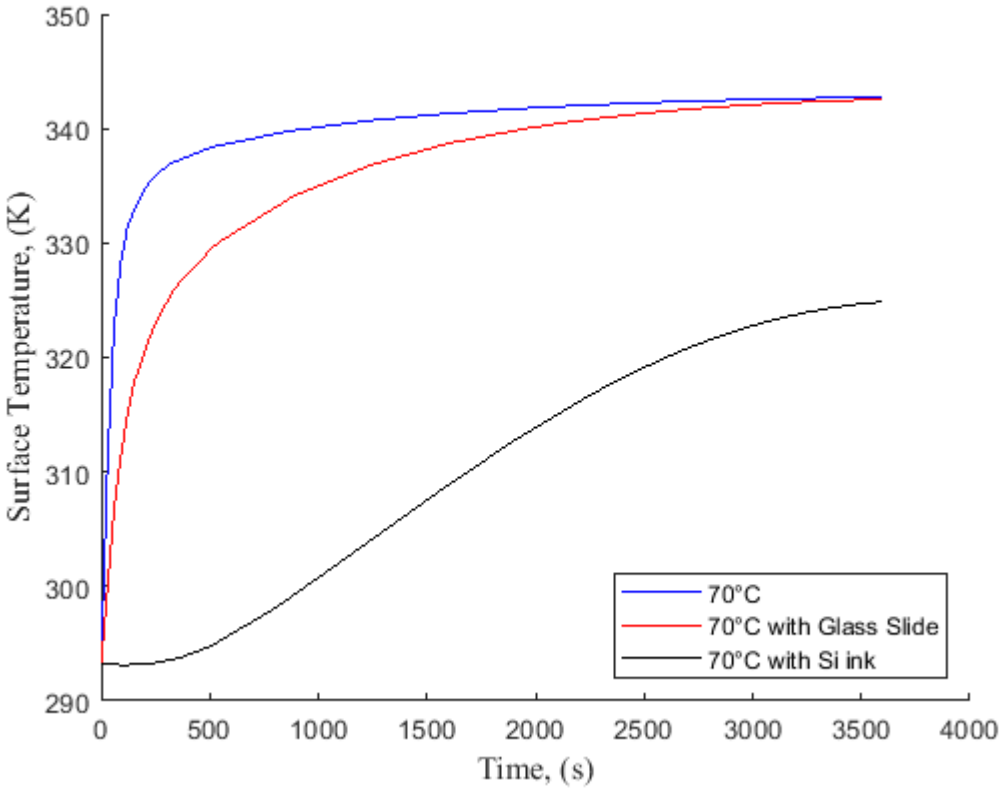

Figure 6.13: Graph showing the results from the COMSOL simulations of PDMS stamp surface temperature against time with heated fluidic channels embedded 2mm below the surface at 70°C. Also shown is the temperature change of a PDMS stamp with a glass slide adhered to the back of the stamp and a PDMS stamp with a piece of silicon ink adhered.

surface as well as with the addition of a glass slide to the underside of the stamp and a stamp with the addition of a silicon ink to the surface.

The addition of a glass slide to the back of the PDMS stamp has the effect of reducing the rate at which the PDMS surface temperature increases. Unlike for a PDMS stamp in isolation, where to achieve 90% of the target temperature it took 4.5 minutes, when a glass slide is attached, this took 19.5 minutes and to achieve 99%, took 57.5 minutes compared to the time taken without the glass slide, which was 47.5 minutes. This clearly shows that for a

PDMS stamp adhered to a glass slide, the time taken to heat the surface and stabilize takes significantly longer.

The addition of a silicon ink to the surface had a significant impact on the heating of the PDMS surface. With the silicon ink (1 mm x 1 mm x 0.2 mm) on the surface, the PDMS stamp temperature never reached 90% of the target surface temperature even after an hour had passed. After 1 hour had passed, the temperature of the surface of the PDMS was ~52°C. Table 6.2 displays the time taken to reach 90%, 95% and 99% of the target temperature for each of these sets of conditions.

Table 6.2: Table containing the simulation results of the time taken for PDMS stamp with fluidic channels at 70°C to achieve 90%, 95%, and 99% of the target surface temperature surface and at 70°C with a glass slide backing, as well as a stamp with silicon ink adhered to the surface.

	Time taken to reach % of target surface temperature		
Simulation conditions	90%	95%	99%
70°C	270s	840s	2850s
70°C with Glass Slide	1170s	1860s	3450s
70°C with Si ink	-	-	-

As there was such a great impact on the surface temperature of the PDMS stamp when a piece silicon ink on the surface of the stamp, a more in depth investigation was carried out. The same simulation was prepared as before, with the PDMS stamp 4mm thick, with a piece of silicon ink adhered to the surface however the temperature of the embedded channels was varied.

As has already been shown, after heating a PDMS with 70°C fluidic channels for 1 hour, the temperature achieved was ~52°C, ~18°C short of the target surface temperature of 70°C. This failure to reach the target surface temperature even after an hour was seen at 50°C and 60°C as well as at 70°C. The results of the surface temperature simulations of a PDMS at these temperatures are presented in Figure 6.14. From these results, a design for the PDMS

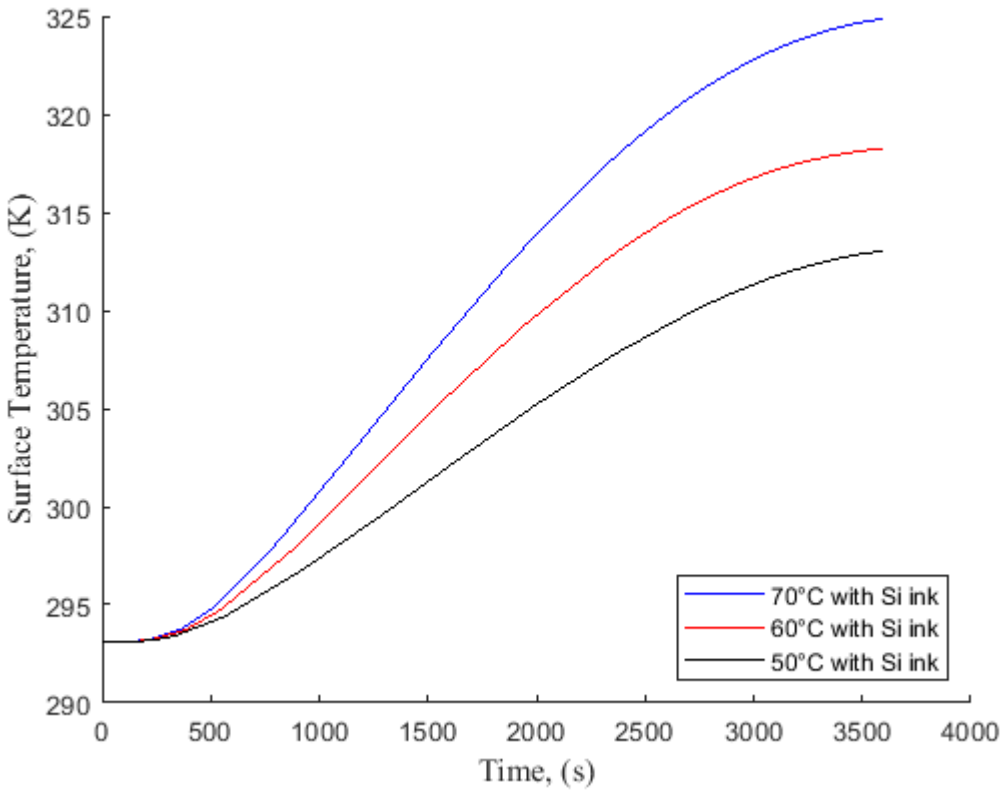

Figure 6.14: Graph showing the results from the COMSOL simulations of PDMS stamp surface temperature against time with heated fluidic channels embedded 2mm below the surface and a silicon ink at 70°C, 60°C, and 50°C.

transfer printing stamp with embedded fluidic channels was developed. The design used a 2 mm wide channel that covered a larger area of the PDMS stamp surface, heating a larger area of the PDMS, minimising the heat loss when in contact with an ink.

6.3.2 Adhesion Testing

The stamp created for adhesion testing using a 3D printed mould to create the fluidic layer and bonded with a PDMS adhesive to a bulk backing sheet and with UVO bonding to a front plate shows that by using existing techniques, it is possible to fabricate a PDMS fluidic channel stamp for use with transfer printing. The use of a water bath and water loop in order to heat the water that would be used to modify the temperature of the PDMS stamp surface again show that by using easily accessible general laboratory equipment, it would be possible to implement this process into any transfer printing system, without the need for the use of expensive equipment or specialist laboratories.

COMSOL simulations showed that for a fluidic channel 2 mm below the surface of the stamp, it would take under 10 minutes for the surface of the stamp to stabilise close to the temperature of the water. In actuality, most of the heat loss in the system came not from the stamp, but from the water loop itself and the time taken to pump water from the heat exchanger to the stamp. With no insulation and a low flow rate peristaltic pump, a water bath temperature of 95°C only achieved a temperature increase of 5°C at the stamp surface. By using an actively heated insulation layer through the use of double walled tubing with water from the water bath pumped around the outside at a high flow rate, this reduced the cooling of the water, giving

greater control over the stamp temperature. Which led to a change in temperature of 19°C with a water bath temperature of 70°C.

Adhesion measurements taken from the fluidic PDMS stamp at room temperature (measured to be 20°C) show a similar trend as has been seen in previous chapters showing that the addition of embedded fluidic channels within the stamp does not impact the velocity dependant adhesion. At elevated temperatures the adhesive nature of PDMS is reduced, leading to an overall reduction in adhesion. This can be seen in Figure 6.15. Even at low retraction speeds, a difference in the adhesion is noticeable with larger temperature changes with the adhesion at a stamp surface temperature of 20°C at 100 µm.s^{-1} being 1.28 mN while when the surface of the PDMS stamp is raised to 39°C the adhesion at 100 µm.s^{-1} drops to 0.562 mN, a

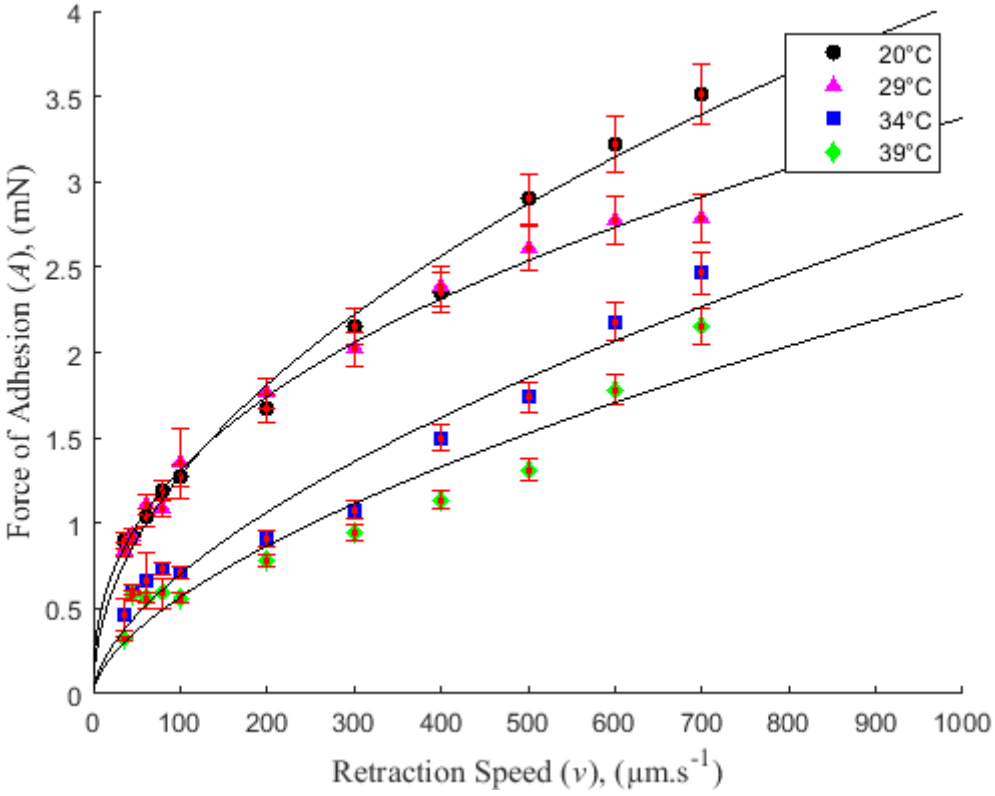

Figure 6.15: Graph showing the adhesion force achieved for a fluidic PDMS stamp from a range of velocities between 35 µm.s^{-1} and 700 µm.s^{-1} at 4 stamp surface temperatures, 20°C, 29°C, 34°C, and 39°C.

reduction of approximately 56% (0.72 mN). This difference in the magnitude of the adhesion becomes more pronounced as the retraction speed increases, leading to a difference of 1.36 mN at 700 $\mu m.s^{-1}$.

This also suggests the importance of a controllable environment when performing a standard transfer printing process, as can be seen in Figure 6.9, at higher retraction speeds, even a 9°C increase in temperature can lead to over 20% reduction of the adhesion of the stamp at 700$\mu m.s^{-1}$ which for some applications, could be the difference between achieving a successful pick-up or being unable to do so.

Figure 6.16 shows how the maximum measured adhesion of a PDMS stamp changes with temperature. As can be seen, across the data range collected in this report, there is a linear

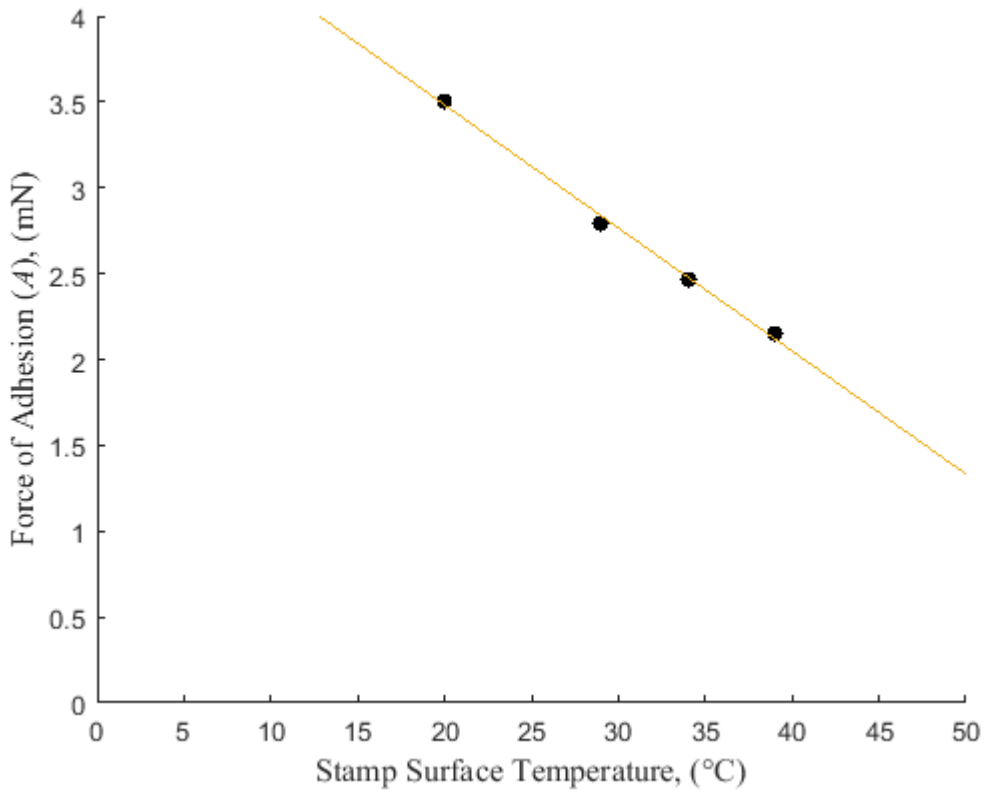

Figure 6.16: Graph showing the maximum adhesion force achieved by a heated fluidic PDMS stamp at 4 temperatures; 20°C, 29°C, 34°C, and 39°C at a retraction speed of 700 $\mu m.s^{-1}$.

relationship between the maximum adhesion achieved and the temperature of the stamp and the interface with the substrate. This relationship means that, depending on the application purpose of the PDMS stamp, using the same retraction speed but varying only the surface temperature of the stamp, it would be possible to achieve successful pick-up and print cycles.

6.4 Conclusion

In this chapter a simple method of modifying the adhesion of a PDMS stamp further than control over the retraction speed alone. To achieve this, the surface temperature of the stamp was increased through the use of embedded fluidic channels within the stamp through which heated water could be pumped.

This method used 2 mm x 1 mm channels embedded 2mm below the surface of the stamp fabricated from a layer of 20:1 Sylgard 184. These channels are sealed onto a flat piece of 10:1 Sylgard 184 using dip coating and a PDMS adhesive. As the increased adhesive properties of 20:1 PDMS compared to 10:1 were at risk of overloading and damaging the load cell used for adhesion measurements, a 10:1 flat plate of Sylgard 184 was bonded to the front side of the stamp using an ultraviolet/ozone treatment.

The closed water loop which supplied the stamp with heated water ran through a heated water bath, which then fed through a double walled section of tubing with heated water pumped through the outer tubing, reducing heat loss between the water bath and the stamp to provide greater control over the temperature modification.

It has been shown that for applications where precise control over the adhesion of a PDMS stamp is required, the introduction of some climate control might be necessary as even small temperature changes (such as the ambient temperature in summer and winter) can have a measureable impact on the adhesion.

At a stamp temperature of 20°C (room temperature) the introduction of embedded fluidic channels beneath the surface has no impact on the velocity dependant adhesive nature of the PDMS stamp, implying that a fluidic stamp would be able to be integrated into any stamp design without needed for major changes to be made to the stamp structure. And as the temperature increases, the adhesion of the stamp reduces in line with the results shown by Feng et al [19].

The significant benefit of using a method such as is that the temperature of the PDMS stamp surface can be modified in situ, while the stamp is in contact with the ink, and to a greater degree of control than other methods of heating a stamp surface. A transfer printing process that uses a fluidic stamp could pick-up while using a room temperature stamp, obtaining the highest possible adhesion improving the success rate of pick-up. However when it comes to printing the picked up ink, the temperature could be increase, as well as using a lower retraction speed, further reducing the adhesion of the stamp to the ink, and increasing the printing success rate. This might also allow ink materials and substrates that were previously unavailable to a transfer printing process, such as a very low adhesion receiving substrate.

6.5 References

[1] S. Wang, D. Feng, C. Hu, and P. Rezai, "The simple two-step polydimethylsiloxane transferring process for high aspect ratio microstructures," *J. Semicond.*, vol. 39, no. 8, p. 086001, 2018.

[2] Y. Y. Huang *et al.*, "Stamp collapse in soft lithography," *Langmuir*, vol. 21, no. 17, pp. 8058–8068, 2005.

[3] E. Y. u. Basova and F. Foret, "Droplet microfluidics in (bio)chemical analysis," *Analyst*, vol. 140, no. 1, pp. 22–38, 2015.

[4] V. J. Sieben, C. F. A. Floquet, I. R. G. Ogilvie, M. C. Mowlem, and H. Morgan, "Microfluidic colourimetric chemical analysis system: Application to nitrite detection," *Anal. Methods*, vol. 2, no. 5, pp. 484–491, 2010.

[5] E. E. Kempa *et al.*, "Coupling Droplet Microfluidics with Mass Spectrometry for Ultrahigh-Throughput Analysis of Complex Mixtures up to and above 30 Hz," *Anal. Chem.*, vol. 92, no. 18, pp. 12605–12612, 2020.

[6] R. D. Pedde, H. Li, C. H. Borchers, and M. Akbari, "Microfluidic-Mass Spectrometry Interfaces for Translational Proteomics," *Trends Biotechnol.*, vol. 35, no. 10, pp. 954–970, 2017.

[7] C. Iliescu, H. Taylor, M. Avram, J. Miao, and S. Franssila, "A practical guide for the fabrication of microfluidic devices using glass and silicon," *Biomicrofluidics*, vol. 6, no. 1, 2012.

[8] L. J. Millet, M. E. Stewart, J. V. Sweedler, R. G. Nuzzo, and M. U. Gillette,

"Microfluidic devices for culturing primary mammalian neurons at low densities," *Lab Chip*, vol. 7, no. 8, pp. 987–994, 2007.

[9] A. Bonyár, H. Sántha, M. Varga, B. Ring, A. Vitéz, and G. Harsányi, "Characterization of rapid PDMS casting technique utilizing molding forms fabricated by 3D rapid prototyping technology (RPT)," *Int. J. Mater. Form.*, vol. 7, no. 2, pp. 189–196, 2014.

[10] M. Golozar, W. K. Chu, L. D. Casto, J. McCauley, A. L. Butterworth, and R. A. Mathies, "Fabrication of high-quality glass microfluidic devices for bioanalytical and space flight applications," *MethodsX*, vol. 7, p. 101043, 2020.

[11] Z. B. Qi *et al.*, "Disposable silicon-glass microfluidic devices: Precise, robust and cheap," *Lab Chip*, vol. 18, no. 24, pp. 3872–3880, 2018.

[12] M. de Almeida Monteiro Melo Ferraz, J. B. Nagashima, B. Venzac, S. Le Gac, and N. Songsasen, "3D printed mold leachates in PDMS microfluidic devices," *Sci. Rep.*, vol. 10, no. 1, pp. 1–9, 2020.

[13] J. C. McDonald and G. M. Whitesides, "Poly(dimethylsiloxane) as a material for fabricating microfluidic devices," *Acc. Chem. Res.*, vol. 35, no. 7, pp. 491–499, 2002.

[14] J. A. Rogers and R. G. Nuzzo, "Recent progress in soft lithography," *Mater. Today*, vol. 8, no. 2, pp. 50–56, 2005.

[15] B. Ruben *et al.*, "Oxygen plasma treatments of polydimethylsiloxane surfaces: Effect of the atomic oxygen on capillary flow in the microchannels," *Micro Nano Lett.*, vol. 12, no. 10, pp. 754–757, 2017.

[16] R. Lerner *et al.*, "Flexible and Scalable Heterogeneous Integration of GaN HEMTs on

Si-CMOS by Micro-Transfer-Printing," *Phys. Status Solidi Appl. Mater. Sci.*, vol. 215, no. 8, pp. 1–7, 2018.

[17] S. Kim *et al.*, "Enhanced adhesion with pedestal-shaped elastomeric stamps for transfer printing," *Appl. Phys. Lett.*, vol. 100, no. 17, 2012.

[18] A. Carlson, S. Wang, P. Elvikis, P. M. Ferreira, Y. Huang, and J. A. Rogers, "Active, programmable elastomeric surfaces with tunable adhesion for deterministic assembly by transfer printing," *Adv. Funct. Mater.*, vol. 22, no. 21, pp. 4476–4484, 2012.

[19] X. Feng, M. A. Meitl, A. M. Bowen, Y. Huang, R. G. Nuzzo, and J. A. Rogers, "Competing fracture in kinetically controlled transfer printing," *Langmuir*, vol. 23, no. 25, pp. 12555–12560, 2007.

[20] R. Saeidpourazar *et al.*, "Laser-driven micro transfer placement of prefabricated microstructures," *J. Microelectromechanical Syst.*, vol. 21, no. 5, pp. 1049–1058, 2012.

[21] M. Srisa-Art, S. D. Noblitt, A. T. Krummel, and C. S. Henry, "IR-Compatible PDMS microfluidic devices for monitoring of enzyme kinetics," *Anal. Chim. Acta*, vol. 1021, pp. 95–102, 2018.

[22] R. W. R. L. Gajasinghe *et al.*, "Experimental study of PDMS bonding to various substrates for monolithic microfluidic applications," *J. Micromechanics Microengineering*, vol. 24, no. 7, 2014.

[23] J. C. McDonald *et al.*, "Fabrication of microfluidic systems in poly(dimethylsiloxane).," *Electrophoresis*, vol. 21, no. 1, pp. 27–40, 2000.

[24] H. Keum *et al.*, "Silicon micro-masonry using elastomeric stamps for three-

dimensional microfabrication," *J. Micromechanics Microengineering*, vol. 22, no. 5, p. 055018, 2012.

[25] S. Iezekiel, "Accurate layer thickness control and planarization for multilayer SU-8 structures," *J. Micro/Nanolithography, MEMS, MOEMS*, vol. 10, no. 1, p. 013019, 2011.

Chapter 7

Enhanced Controllable Adhesion of Carbon Nanotube Embedded PDMS Transfer Printing Stamps

In this chapter a method of enhancing the adhesion of a PDMS stamp will be detailed through the use of embedded carbon nanotubes to create a conductive PDMS stamp which will enable the surface of the stamp to be electrostatically charged.

Initially existing methods of creating electrically conductive PDMS materials will be detailed as well as a look at how the properties of PDMS are utilised in a transfer printing process. This will be followed by a detailed report of how a carbon nanotube embedded PDMS stamp was fabricated.

Initial results will then be displayed discussing the impact electrostatically charging of the CNT stamp surface on two substrates, Si(100) and GaN on sapphire, has on the adhesion of the stamp.

7.1 Conductive PDMS

Poly(dimethylsiloxane) is a silicone material which has been used in a wide range of applications such as a material to make microfluidic devices from [1], stretchable electronics [2] and adhesive stamps for the transfer printing of semiconductor devices [3]. This section will include and discuss different methods of turning PDMS from an electrically insulating material into a conductive material. Sylgard 182, a very similar PDMS silicone to Sylgard 184 except for variations in the curing conditions, has a conductivity of 2.53e-05 $S.m^{-1}$ [4].

7.1.1 Methods of Creating Conductive PDMS

There are some applications for PDMS which rely on the physical and mechanical properties that this material has for applications, such as its biocompatibility [5] or flexibility [6], however there are certain applications whereby having an electrically conductive material would be beneficial [7] as well as having the appealing mechanical properties of PDMS as well. In these such situations, there have been reports of addition of certain materials which can reduce the resistivity of a PDMS material.

One such method of creating an electrically conductive PDMS is that by Feng et al [8] who, in order to create stretchable conductive PDMS, drop casted Au nanowires (AuNW) onto a silicon substrate followed by casting PDMS (Sylgard 184) over the silicon and AuNWs. Once cured and peeled from the silicon substrate, the result was a piece of bulk PDMS, which remained flexible and had the same mechanical properties of a regular piece of PDMS, but with a thin conductive layer of PDMS/AuNW at the surface. This PDMS/AuNW layer

displayed an almost linear relationship between the resistance measured and the strain percentage. At 0% strain (no elongation) the conductivity measured in this film was measured to be ~8,130 $S.cm^{-1}$. When that strain was released however, there was only a partial recovery of the resistance. By the 4^{th} elongation, the resistance of the PDMS/AuNW film appeared to have stabilised and only a small change in the resistance was seen during elongation and after the release of the strain.

There have been other attempts to create electrically conductive PDMS such as by Ao et al [9] where a matrix of graphene tubes are grown around a 3D network of nickel fibres. These nickel fibres were then etched away, leaving the matrix of hollow graphene, around which PDMS was cast. The resulting conductivity of the PDMS with the graphene matric was 6100 $S.m^{-1}$ but with a reduced elongation before failure.

These are not the only methods of creating a PDMS that has increased electrical conductivity. Another method has been to use carbon nanotubes embedded within the PDMS, in a similar way as the AuNWs were introduced previously. Kim et al [10] used an ultrasonic bath to disperse multi-walled carbon nanotubes (MWCNT) in isopropyl alcohol (IPA) (>99.9% isopropyl alcohol, Sigma Aldrich) before adding PDMS oil and dispersing that evenly using the ultrasonic bath. Once prepared, the Sylgard 184 base was added to the IPA/MWCNT/PDMS oil base. This ensured even distribution of the MWCNTs within the PDMS. The PDMS base with the added IPA, PDMS oil, and MWCNT was then heated at a low temperature to remove the IPA from the mixture before adding the Sylgard 184 curing agent and curing. This has shown to create a PDMS which has a sheet resistance of <20 Ω/sq.

7.1.2 Transfer Printing

While PDMS has many applications where it has become a key material, the one of greatest interest in this report is transfer printing. Transfer printing is a process which selectively picks up material or pre-fabricated devices from a donor substrate and prints them onto a receiving substrate [11]. One of most appealing applications for this process is the use of unusual substrates, such as those used as flexible substrates [12].

In order to achieve a successful transfer printing process, a PDMS stamp is used which often has a patterned surface, which is brought into contact with selected coupons of material or devices, often referred to as ink. It has been shown that PDMS has a kinetically dependant adhesion to a surface [13] whereby at high retraction speeds, a PDMS stamp displays a greater level of adhesion, while low retraction speeds put the PDMS stamp into a low adhesion state.

By modifying the adhesion of the stamp by controlling the retraction speed of the stamp from the surface, it would be possible to put a stamp into a high adhesion state when picking up the material, also known as stamp inking, increasing the success rate of pick-up, then during printing, low retraction speeds can be used, reducing the adhesion to the ink and making it easier to selectively print onto a substrate. This also has the potential to allow for the use of more unusual substrate materials as receiving substrates that previously were not possible due to low adhesion surfaces.

One of the benefits of using PDMS as a material from which to fabricate transfer printing stamps from is that, due to the ease at which PDMS can be patterned through soft lithographic processes, for each process using PDMS stamps, each stamp can be bespoke, made to suit that particular device or material, and with an adhesion to suit the substrates being used. As such most of the developments in transfer printing have been modifications to the PDMS

stamp structure itself [14] [15], as well as the introduction of other techniques as well to widen the operating window [16].

7.1.3 Soft Nanocomposite Electroadhesives (SNEs)

There are a number of pick and place techniques for semiconductor devices [17][18][19]. One such technique, demonstrated by Kim et al, uses arrays or "forests" of vertical carbon nanotubes (CNT), with a uniform ultrathin (1 nm) dielectric coating to create soft nanocomposite electroadhesives (SNEs) [20]. The result of the application of a bias of 30V to these SNEs have shown a >100-fold increase in adhesive force to (sub). The adhesion of an SNE to a Pt-coated spherical AFM tip was approximately 0.02 μN without any applied voltage which increased to ~2.3 μN when 30V was applied.

The application of a bias voltage causes an electrostatic charge to build up on the CNTs that are in contact, or near to, the target material surface. Various aspects of the design of an SNE impact the adhesion achieved for a given bias voltage. Primarily these are dielectric coating and CNT density, with thinner dielectric coatings giving an increased change in adhesion when a bias voltage is applied, while a higher density of CNTs can also increase the adhesion.

In this study, it was stated that for conductive materials, in this case microspheres were used, when a SNE with a bias voltage is in contact, polarization occurs within the microsphere which causes the increase in adhesion when a bias voltage is applied to be greater than for dielectric materials. Pull-off forces showed that a bias of approximately 50V was necessary to

achieve the same pull-off force for a dielectric microsphere that a 10V bias achieved for a microsphere that can conductive.

By combining the principles of using carbon nanotubes coated in a dielectric material to electrostatically charge the surface of an SNE to increase the adhesion to a material as shown by Kim et al, with that of transfer printing, where adhesion modification comes from the exploitation of the viscoelastic properties of the PDMS stamp, it would be possible to create a PDMS transfer printing stamp that could be switched between a high and low adhesion state by controlling the separation speed between the stamp and the target material while also be able to be switched to a high or low adhesion state by applying a bias voltage if the PDMS stamp were embedded with carbon nanotubes.

7.2 Methods

In this section, the process undertaken in order to achieve successful castings of MWCNT embedded PDMS stamps for transfer printing will be detailed. After this, the process of applying a voltage bias to the PDMS stamp surface in order to achieve electrostatic charging of the surface will be included followed by a discussion about how adhesion measurements were taken.

7.2.1 Carbon Nanotube Embedded PDMS Stamps for Transfer Printing

In order to achieve a successful casting a process similar to that described by Kim et al [10] previously. To begin with, 200mg of multiwalled carbon nanotubes (>99.9% multiwalled carbon nanotubes, 10-30um length, 25nm outer diameter, Ossila) were weighed into an aluminium tin before 20ml of IPA (99.8% isopropyl alcohol, Fisher Scientific) was added. This was then placed into an ultrasonic bath to be sonicated for 30 minutes to separate the CNTs. After 30 minutes, 0.5g of PDMS oil (Silicone oil 100 cSt, Sigma Aldrich) was added and manually stirred to combine before being sonicated for a further 10 minutes to disperse the CNTs. After 10 minutes had elapsed, 2g of the base PDMS (Sylgard 184) was added, mixed roughly with a plastic spoon and sonicated again for 10 minutes.

The mixture was then placed onto a hotplate set to 55°C and the mass was measured regularly. Once the mixture measured 2.7g, it was known that the added IPA had been removed. Previous attempts had shown that there was still some trapped IPA within the mixture even once this mass had been reached, therefore in order to remove any final trapped gasses in the PDMS/CNT mixture an additional outgassing stage was added. The mixture was outgassed for 20 minutes which also gave the mixture time to cool, before 0.27g of Sylgard 184 curing agent was added, mixed thoroughly using a spoon and desiccated for 10 minutes.

Once bubble free, the PDMS slurry with the CNTs was poured into a mould comprised of an aluminium frame and polyimide tape across the back. To this a flat Si(100) wafer was adhered which would provide a flat surface that the PDMS would be cast against. This was then placed into an oven at 100°C for 35 minutes, then peeled from the mould.

7.2.2 Creating CNT Composite Stamp

With the carbon nanotube embedded PDMS prepared, a step of bonding it to a larger PDMS stamp was necessary. To avoid wastage of the costly carbon nanotubes, the quantity of CNT embedded PDMS was kept to a minimum, namely the area that would make contact with the substrates that were mounted onto the load cell. To make up the rest of the bulk of the PDMS stamp, Sylgard 184 was mixed in a ratio of 10:1 first by measuring out the required quantity of base into an aluminium tin, then adding the appropriate quantity of curing agent. Once thoroughly mixed with a plastic spoon, the mixture was outgassed for in 10 minute intervals until bubble free. Once bubble free, the CNT PDMS was placed into an aluminium frame backed with polyimide tape. The PDMS slurry was then poured over the CNT PDMS in the mould and cured at 100°C for 35 minutes.

7.2.3 Transfer Printing

In order to determine whether applying a bias to the CNT PDMS would change the adhesion of the stamp to a substrate, a transfer printing system was used. This system comprised of a vertical z-stage (ANT130LZ Single-Axis z Nanopositioning Stage, Aerotech) controlled by a motion controller (Ensemble HLe Controller and Linear Digital Drive, Aerotech). This stage has a transfer printing PDMS stamp mount, where a PDMS stamp, attached to a glass slide backing can be adhered to the stage using a vacuum chuck. Below the z-stage is an x/y-stage with a load cell (GSO-10, Transducer Techniques), able to measure forces up at an accuracy of ±0.005g [21]. Onto the load cell, sample substrate could be loaded, adhered to the load stem using adhesive carbon pads.

By using the vertical stage, the PDMS stamp could be lowered into contact with the surface of the mounted substrate and retracted at a preselected retraction speed, giving greater control over the retraction speed, and in turn, control over the adhesion between the stamp and the substrate.

For the substrates investigated in this report, 2 substrates were selected, Si(100) and GaN on sapphire. These would give a greater understanding of the applicability of this process for different materials and substrates. Each sample was mounted onto the load stem using an adhesive carbon pad, commonly used for mounting samples in an SEM.

The transfer printing system had multiple modifications to it since it was initially established. At lower retraction speeds, or for very low adhesion PDMS stamps, the adhesion became so low that background noise measured on the load cell was great enough to mask any measurements. It was noticed that the load cell was sensitive enough to pick up and be disrupted by physical vibrations such as those caused by other laboratory users walking nearby or by the laboratory door opening or closing. As such, the first change made to the transfer printing system was to move it to a floating optical bench plumbed into a nitrogen gas line. This would help to isolate the transfer printing system from any vibrations through the floor.

This reduced some of the background noise, however this did not remove a particular noise artefact that was picked up by the load cell. It was thought that this could have been caused by induced EMI so to try to shield the transfer printing system a Faraday cage was built surrounding the whole system. This Faraday cage has a twofold effect, firstly it shielded the transfer printing system from a large amount of background noise and EMI, but it also protected the load cell from the movement of air around the laboratory from the air conditioning system, which could also be detected on the load cell.

The introduction of the Faraday cage further reduced the background noise present on load cell readings, however it did not remove the noise artefact that was recorded previously. To further protect the system, the cable connecting the load cell to the motion controller, which also collected the load cell data, was replaced with a twisted pair cable, wrapped around a ferrite core. This was then connected to a shielded cable which ran out of the Faraday cage to the motion controller. Again, this reduced the background noise, but still a particular noise artefact that appeared in previous measurements persistent.

The final modification made to the transfer printing system was the use of a UPS (uninterruptable power supply) to power the motion controller, and therefore the vertical stage and the load cell. The computer which operates the motion controller was also connected. A UPS is often used to power critical pieces of equipment and protect them from power outages. This is achieved by having a battery contained within the power supply which is constantly being charged during every day operation. If there is a power outage then the battery kicks in and supplies power to the equipment for a short time. As the UPS has a power supply, this acts as a filter for the mains power supply. As the laboratory housing the transfer printing system is located within a building that has a large number of pumps and chiller, there was a high possibility that these were introducing some noise into the building mains power lines, so the use of a UPS helped to filter this out. The result of all of the modifications to the transfer printing system was a reduction in noise sufficient enough to allow for small adhesion measurements to be taken.

7.2.4 Adhesion Measurements

In order to have the greatest control over the retraction speed of the z-stage, a script was written within the Aerotech Ensemble Motion Composer software. This software provided a user interface to the motion controller, and through that, the z-stage. The full script is included in the Appendix section of this thesis and a more detailed breakdown of the code and its different sections is included in Chapter 3: Experimental Techniques. In summary, the code reads the load cell and lowers the stage in small steps, taking new load cell measurements at each step, once the load cell reading increases above a set value, the stamp has made contact and the stage stops moving.

There was a 5 second wait time while the stamp relaxes and makes good contact to the substrate surface, before the stage retracts at a pre-set velocity, and with a pre-set acceleration and acceleration profile. The load cell records the adhesion achieved by the stamp at a set velocity and in this case too, at a set voltage bias.

7.3 Results

This section will look at the initial results of adhesion tests performed with a carbon nanotube embedded PDMS stamp against two different substrates and at a range of voltage biases. Figure 7.1 displays the adhesion achieved by a Sylgard 184 stamp embedded with 7% carbon nanotubes at bias voltages of 0V, 1V, 5V, 10V, and 20V when retracted from a Si(100) wafer at 700 $\mu m.s^{-1}$. When a voltage bias is applied when retracting from a Si(100) substrate, as can be seen that the adhesion is modified by a voltage bias of 1V increasing the adhesion to the Si(100) substrate by 8 µN. When a 5V bias is applied, this increases the adhesion further, achieving an increase of ~12 µN to the Si(100) substrate. With a voltage bias of 20V, the CNT stamps adhesion to the Si(100) substrate increased to ~0.32 mN, an increase of ~25 µN.

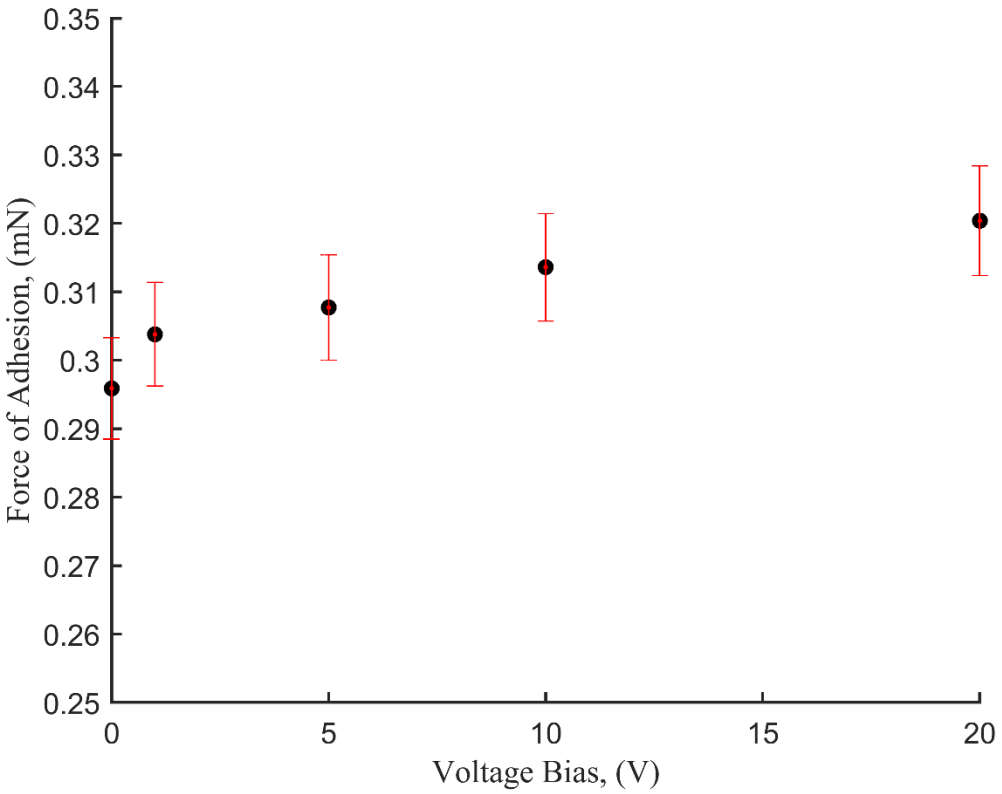

Figure 7.1: Graph showing the adhesion between a CNT PDMS stamp and a Si(100) substrate at 700 $\mu m.s^{-1}$ for a range of bias voltages between 0V and 20V.

The second substrate that was tested was GaN on a sapphire substrate, which, The CNT PDMS stamp still displayed a velocity dependant nature of the adhesion to the GaN surface with the adhesion achieving 0.245 mN at 700um.s-1. Unlike with the previous two substrates however, there was no adhesion change at all with the application of a bias even up to 20V which can be seen in Figure 7.2. The reason that no adhesion change was observed is probably down to the sapphire substrate the GaN was grown onto.

In order to gain a better understanding of the characteristics of the CNT PDMS stamp, current/voltage measurements were taken using a probe station and a source measurement unit. The results are presented in Figure 7.3. Measurements were performed between 0V and 20V, the same range of voltages as was applied as a voltage bias to the CNT PDMS. It was found

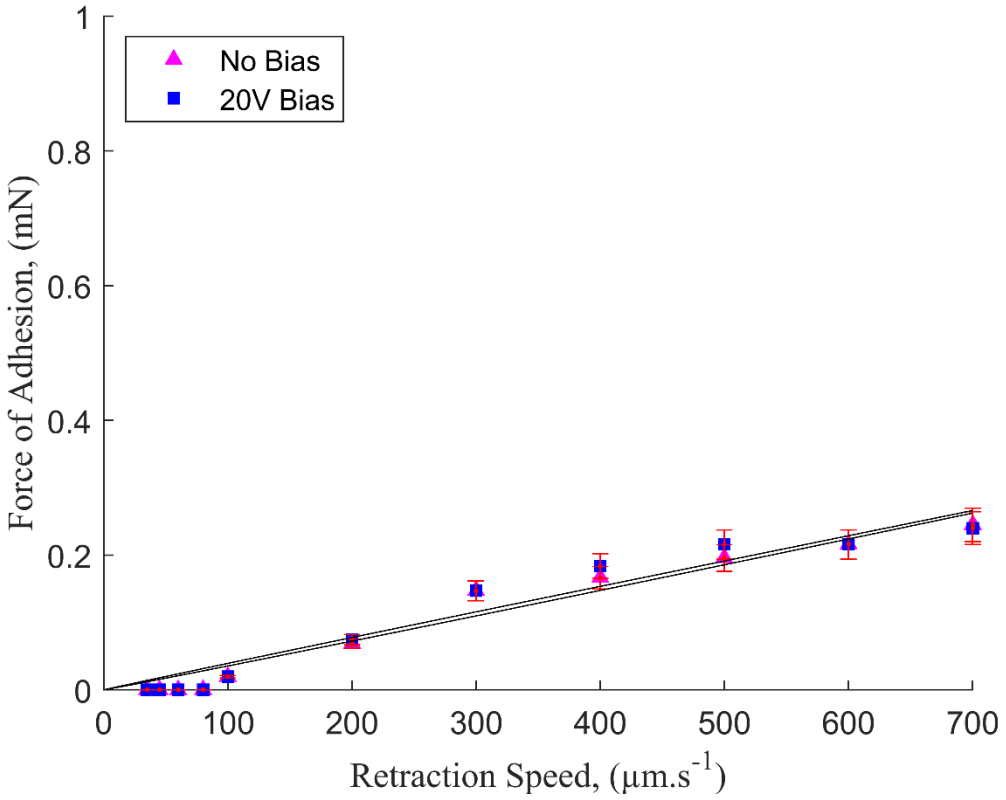

Figure 7.2: Graph showing the force of adhesion to a GaN on sapphire substrate achieved by a carbon nanotube embedded PDMS stamp for retractions speeds up to 700 µm.s^{-1} at 2 bias voltages, 0V bias and 20V bias.

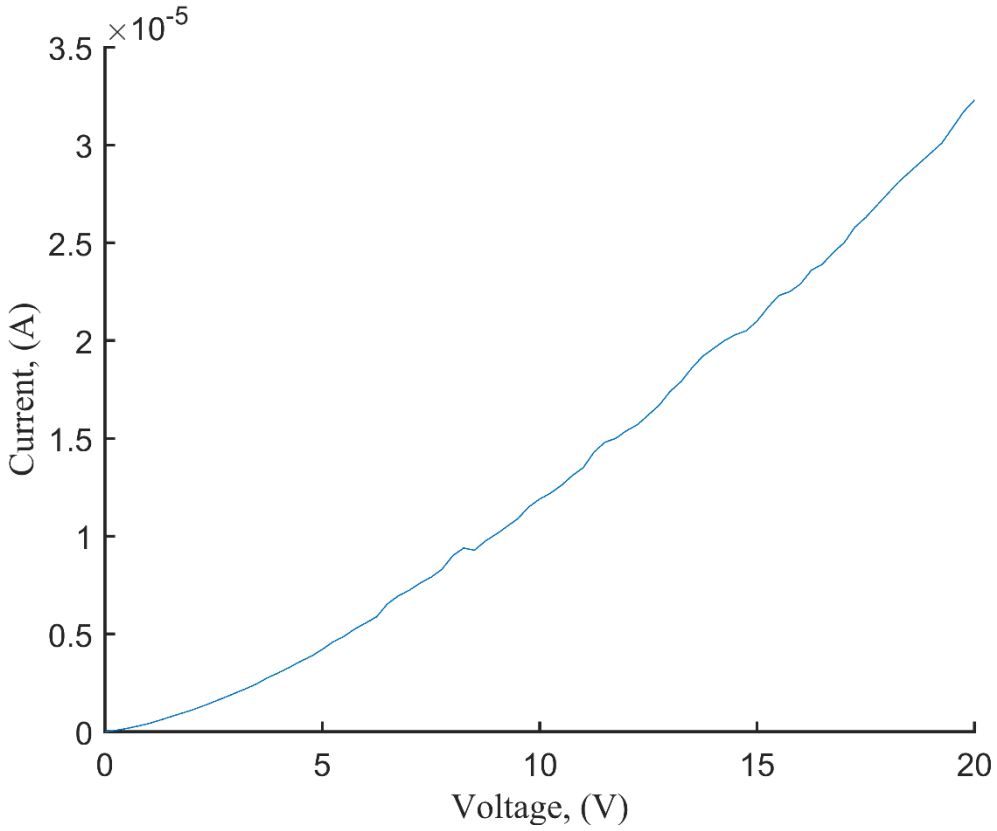

Figure 7.3: Graph of the current against voltage results of a CNT PDMS stamp with a 1.5 mm separation.

that, for a probe separation of 1.5 mm, a similar separation to that between the connection of the CNT PDMS stamp and the contact face of the stamp, the current increases as the voltage increases. For a PDMS stamp embedded with 7% carbon nanotubes the resistance at 1V was 2.41 MΩ however at 5V, the resistance reduces to 1.19 MΩ. As the voltage increase, this same trend is seen, with the resistance decreasing to 0.62 MΩ at 20V.

7.4 Discussion and Conclusion

This chapter presents a novel method of modifying the adhesion of a PDMS transfer printing stamp through electrostatic charging of embedded CNTs within the stamp that would provide control over the adhesion of the stamp through both the kinetically controlled adhesion as well as widening the process window through the application of a voltage bias. In order to achieve electrostatic charging, a conductive PDMS stamp was fabricated using CNTs embedded within the PDMS stamp. The adhesion between the CNT PDMS stamp and a Si(100) substrate was increased from 0.296 mN at 700 $\mu m.s^{-1}$ to 0.304 mN at 700 $\mu m.s^{-1}$ by applying a 1V bias to the CNT PDMS stamp. Further increases in voltage bias resulted in further increases in the adhesion achieving 0.32 mN at 20V. The second tested substrate was GaN on sapphire, however this substrate was unchanged by the application of any bias voltage up to 20V.

As with the results published by Kim et al [20], the electrostatic changing of carbon nanotubes coated by a dielectric coating, in this case PDMS, increased the adhesion to a conductive material like Si(100). The results obtained for the CNT PDMS stamp adhesion to a GaN on sapphire substrate are in line with this too, as sapphire is a non-conductive material [22], therefore the polarisation which Kim suggests enables the increase in adhesion, does not take place.

The introduction of a CNT embedded PDMS stamp that can be electrostatically charged in order to increase the adhesion to certain substrates and materials into a transfer printing process opens up the possibility of using more unusual substrates and materials through a greater level of control over the switchablility between a high adhesion state and a low adhesion state. When attempting to selectively pick up an ink, the highest adhesion possible is preferable as it ensures a greater chance of a successful pickup. This could be enhanced through the use

of a CNT PDMS stamp. The benefit of a CNT PDMS stamp is that, unlike with a PDMS stamp that has undergone surface treatments or has been structured with a pedestal design that increases the adhesion [14], the voltage bias can be switched off when the increased adhesion is no longer necessary. This still enables the same stamp to achieve low levels of adhesion that are necessary to successfully print the pinked up material onto the receiving substrate.

The next stage for this technique could be to test the adhesion of a CNT PDMS stamp over a wider bias voltage range to determine whether, at higher voltages, there is a greater increase in adhesion than that already seen in this report. Future work could also include adjusting the concentration of carbon nanotubes within the PDMS, or the type of carbon nanotubes used, such as testing the use of functionalised carbon nanotubes. Any of these future works could help to widen the operating window that is possible using a carbon nanotube PDMS stamp.

7.5 References

[1] J. C. McDonald *et al.*, “Fabrication of microfluidic systems in poly(dimethylsiloxane).,” *Electrophoresis*, vol. 21, no. 1, pp. 27–40, 2000.

[2] D. Qi, K. Zhang, G. Tian, B. Jiang, and Y. Huang, “Stretchable Electronics Based on PDMS Substrates,” *Adv. Mater.*, vol. 33, no. 6, pp. 1–25, 2021.

[3] C. Prevatte *et al.*, “Pressure activated interconnection of micro transfer printed components,” *Appl. Phys. Lett.*, vol. 108, no. 20, 2016.

[4] K. T. S. Kong, M. Mariatti, A. A. Rashid, and J. J. C. Busfield, “Enhanced conductivity behavior of polydimethylsiloxane (PDMS) hybrid composites containing exfoliated graphite nanoplatelets and carbon nanotubes,” *Compos. Part B Eng.*, vol. 58, pp. 457–462, 2014.

[5] M. Ionescu *et al.*, “Enhanced biocompatibility of PDMS (polydimethylsiloxane) polymer films by ion irradiation,” *Nucl. Instruments Methods Phys. Res. Sect. B Beam Interact. with Mater. Atoms*, vol. 273, pp. 161–163, 2012.

[6] W. Y. Wu, X. Zhong, W. Wang, Q. Miao, and J. J. Zhu, “Flexible PDMS-based three-electrode sensor,” *Electrochem. commun.*, vol. 12, no. 11, pp. 1600–1604, 2010.

[7] X. Gao *et al.*, “Mechanically enhanced electrical conductivity of polydimethylsiloxane-based composites by a hot embossing process,” *Polymers (Basel).*, vol. 11, no. 1, 2019.

[8] F. Xu and Y. Zhu, “Highly conductive and stretchable silver nanowire conductors,” *Adv. Mater.*, vol. 24, no. 37, pp. 5117–5122, 2012.

[9] D. Ao *et al.*, “Highly conductive PDMS composite mechanically enhanced with 3d-graphene network for high-performance EMI shielding application,” *Nanomaterials*, vol. 10, no. 4, 2020.

[10] J. H. Kim *et al.*, “Simple and cost-effective method of highly conductive and elastic carbon nanotube/polydimethylsiloxane composite for wearable electronics,” *Sci. Rep.*, vol. 8, no. 1, pp. 1–11, 2018.

[11] M. A. Meitl *et al.*, “Transfer printing by kinetic control of adhesion to an elastomeric stamp,” *Nat. Mater.*, vol. 5, no. 1, pp. 33–38, 2006.

[12] C. Linghu, S. Zhang, C. Wang, and J. Song, “Transfer printing techniques for flexible and stretchable inorganic electronics,” *npj Flex. Electron.*, vol. 2, no. 1, 2018.

[13] X. Feng, M. A. Meitl, A. M. Bowen, Y. Huang, R. G. Nuzzo, and J. A. Rogers, “Competing fracture in kinetically controlled transfer printing,” *Langmuir*, vol. 23, no. 25, pp. 12555–12560, 2007.

[14] S. Kim *et al.*, “Enhanced adhesion with pedestal-shaped elastomeric stamps for transfer printing,” *Appl. Phys. Lett.*, vol. 100, no. 17, 2012.

[15] A. Carlson, S. Wang, P. Elvikis, P. M. Ferreira, Y. Huang, and J. A. Rogers, “Active, programmable elastomeric surfaces with tunable adhesion for deterministic assembly by transfer printing,” *Adv. Funct. Mater.*, vol. 22, no. 21, pp. 4476–4484, 2012.

[16] R. Saeidpourazar *et al.*, “Laser-driven micro transfer placement of prefabricated microstructures,” *J. Microelectromechanical Syst.*, vol. 21, no. 5, pp. 1049–1058, 2012.

[17] Y. Mengüç, S. Y. Yang, S. Kim, J. A. Rogers, and M. Sitti, “Gecko-inspired

controllable adhesive structures applied to micromanipulation," *Adv. Funct. Mater.*, vol. 22, no. 6, pp. 1246–1254, 2012.

[18] J. B. Park *et al.*, "Stable and efficient transfer-printing including repair using a GaN-based microscale light-emitting diode array for deformable displays," *Sci. Rep.*, vol. 9, no. 1, pp. 1–7, 2019.

[19] T. H. Kim *et al.*, "Heterogeneous stacking of nanodot monolayers by dry pick-and-place transfer and its applications in quantum dot light-emitting diodes," *Nat. Commun.*, vol. 4, 2013.

[20] S. Kim *et al.*, "Soft nanocomposite electroadhesives for digital micro- And nanotransfer printing," *Sci. Adv.*, vol. 5, no. 10, pp. 1–9, 2019.

[21] Transducer Techniques, "GSO-10 Specification." [Online]. Available: https://www.transducertechniques.com/gso-load-cell.aspx. [Accessed: 23-Mar-2022].

[22] M. A. Bouchiat, J. Guéna, P. Jacquier, M. Lintz, and A. V. Papoyan, "Electrical conductivity of glass and sapphire cells exposed to dry cesium vapor," *Appl. Phys. B Lasers Opt.*, vol. 68, no. 6, pp. 1109–1116, 1999.

Chapter 8

Conclusions and Further Work

8.1 Conclusion

This thesis presents developments of transfer printing, the process by which semiconductor materials and devices can be transferred from their as-grown state on a donor substrate to a receiving substrate using an adhesive PDMS stamp to selectively pick and print devices and materials. This involved developing novel methods of widening the operating window of an adhesive PDMS stamp not only by exploiting the viscoelastic nature of PDMS, but through the use of heated fluidic channels to exploit the temperature dependant nature of PDMS as well as the viscoelastic nature, and then through the use of carbon nanotubes embedded within a PDMS stamp in order to create an electrically conductive stamp enabling the electrostatic charging the stamp surface. As well as this, an investigation was undertaken to establish if other PDMS silicones were suitable alternatives to Sylgard 184, the most widely used PDMS for transfer printing stamps. A novel method of double casting PDMS silicones through the use of ultraviolet/ozone treatment on a PDMS sub-master mould was also developed.

Three PDMS silicones were investigated as alternative materials to Sylgard 184 from which adhesive stamps for transfer printing could be made. Structured stamps were made using a soft lithography casting process using the following PDMS silicones: Sylgard 182, Sylgard 170, and Silcoset 105. The velocity dependant adhesion of Sylgard 182 was seen to be

comparable to that of Sylgard 184. However Sylgard 170 displayed a velocity dependant adhesion which was 50% lower than that of Sylgard 184 at a retraction speed of 700 $\mu m.s^{-1}$ Silcoset 105 however displayed no adhesion to a Si(100) wafer fragment. As such Sylgard 182 and Sylgard 170 would be suitable alternatives to Sylgard 184 as materials to make transfer printing stamps. This would enable tailoring of the transfer printing stamp adhesive properties, providing the option to have greater control over lower adhesion transfer printing using Sylgard 170, or greater control over greater adhesion levels using Sylgard 184 and Sylgard 182. Sylgard 182 has a much longer working time, which could be advantageous when performing complex PDMS castings, such as injection moulding.

A novel method of achieving PDMS double casting was presented. Double casting is the process of casting an uncured PDMS over a structured mould made from the same material. Without a surface treatment, release of the cast PDMS from the mould is impossible. By treating the surface of a PDMS sub-master with ultraviolet/ozone (UVO) for 30 minutes, 4 successful double castings were performed using Sylgard 184 and Sylgard 182 and 2 successful castings were achieved using Sylgard 170. Attempted to perform double casting with Silcoset 105 were unsuccessful. Adhesion testing was performed using transfer printing stamps to determine if the UVO double casting process had any impact on the final stamps. It was found that the adhesion of a PDMS stamp that had been fabricated using a UVO double casting process had a ~36% lower adhesion force at 700 $\mu m.s^{-1}$ than a stamp that had not been double cast. This was true for Sylgard 182 as well, with a ~33% reduction in adhesive force for a stamp that had been fabricated using a double casting process. However, if the UVO treated PDMS sub-master mould was washed with isopropyl alcohol then there was a lesser impact on the adhesive force of the PDMS stamp. The exception to this was Sylgard 170, which saw a reduction in adhesion at 700 $\mu m.s^{-1}$ of ~50% compared to a stamp that was not double cast and only saw a slight recovery in adhesion if the mould was washed.

Widening the operating window of a PDMS stamp in-situ is an important aspect for achieving new device and substrate combinations. A novel method of widening the operating window for transfer printing has been demonstrated. Through the use of embedded heated fluidic channels within a PDMS transfer printing stamp it was possible to modify the stamper surface temperature which impacted the adhesion of the stamp. This method enabled the PDMS stamp to be heated using a simple heated water loop and pump, achieving a stamp temperature of up to 39°C. At this temperature, the adhesion of the stamp was reduced by 1.36 mN at 700 $\mu m.s^{-1}$.

Another novel method for widening the operating window of a PDMS stamp in-situ was demonstrated. Using a PDMS stamp with carbon nanotubes embedded, electrostatic charging of the stamp surface was achieved. Through applying a bias voltage of 20V to the PDMS stamp, the adhesion to a Si(100) substrate was increased by ~25 μN. For non-conductive substrates such as a GaN on sapphire however, it was found that there was no noticeable increase in adhesion when a voltage bias of 20V was applied.

8.2 Future Works

While there are many different PDMS silicones available, three were investigated as potential alternatives to Sylgard 184 as a material from which transfer printing stamps can be fabricated. Future work could include the study of more of these alternative PDMS silicones. By understanding the adhesive properties different PDMS silicones have, it could allow for greater tuning of the adhesive properties of a transfer printing stamp where the user could fabricate a

transfer printing stamp with precise adhesive properties to suit the particular combination of device and substrate.

Sylgard 184 has been shown to be able to be mixed and cast in a range of mixing ratios of base to curing agent which would impact the adhesive nature of the stamp. Future work may include investigation into how the adhesive properties of Sylgard 182 and Sylgard 170 vary when ratios of components are adjusted. It would be expected that a 20:1 ratio of Sylgard 182 would be significantly more adhesive than 10:1, and 5:1 much less adhesive, but it is currently uncertain by how much this would impact the adhesion.

Ultraviolet/ozone treatment of a PDMS sub-master mould has been shown in this report to enable a double casting process to be performed up to 4 times for a Sylgard 184 and Sylgard 182 sub-master mould. Most of the damage that occurred while separating the UVO treated sub-master from the double cast PDMS stamp did so due to bending of the PDMS mould, which caused cracks to form on the SiO_x crust that was created during the UVO process. Future work could investigate a range of curing ratios of Sylgard 184 and Sylgard 182, to determine if a less flexible sub-master (i.e. a 5:1 ratio of base to curing agent) increased the lifetime of the sub-master moulds by reducing the chance of damage occurring due to bending of the mould.

It was found in this report that the adhesion of a PDMS transfer printing stamp that was cast using a double casting process had a lower adhesion than a stamp made using a normal single casting process. This was partially rectified by washing the treated sub-master mould with isopropyl alcohol, however further investigation into methods of minimising the impact UVO double casting has on the adhesive nature of the stamp.

In this report a novel method of widening the operating window of a PDMS stamp was presented using embedded fluidic channels in order to heat the surface of a PDMS stamp which would modify the adhesion of the stamp. The presented method is simple and easily scalable. Future work could include heating of arrays of microstructured pedestals in order to transfer print arrays of devices by inking the stamp at room temperature and printing at an elevated temperature.

Other future work could include investigation into other fluidic channel designs where specific areas of a stamp are heated where low adhesion is desired, while other areas remain at room temperature or are actively cooled used a cold water loop, providing greater adhesion in these cooler areas. A technique like this could enable a microstructured stamp to be brought into contact with entire arrays of devices but upon retraction, only the desired devices are picked up. By using a method like this, careful alignment could be made to device arrays across an entire wafer and by pumping heated or cooled water to particular areas of the stamp, the desired devices could be picked up.

A second method has been presented in this report which widens the operating window of a PDMS transfer printing stamp. By using carbon nanotubes embedded within a PDMS stamp, the surface of the stamp can be electrostatically charged, increasing the adhesion of the stamp. Future developments of this process may include the study of other substrate materials, to determine what considerations are required when designing a CNT PDMS stamp for transfer printing of particular device materials. As well as this, testing the adhesion of a CNT PDMS stamp at greater bias voltages than 20V may also be beneficial, especially for non-conductive substrates where the increase in adhesion due to electrostatic charging is very small.

There are also potential avenues of research that could be conducted by tuning the PDMS stamp. This report used a PDMS stamp with 7% carbon nanotube concentration. By increasing the concentration of carbon nanotubes within the PDMS stamp, there may be a greater change in the adhesive nature of the stamp when a bias voltage is applied.

Appendix

Full Aerobasic Code for Transfer Printing

Included in this appendix is the entire code written to control the transfer printing system in the approach to and retraction from the load cell.

```
' Approach and Retract Using Current Feedback

' To set up , adhere the desired stamp to the glass slide
' and use the vacuum pump to secure the glass slide to the
' stage. Secure the target substrate for pick up material
' to the vacuum chuck. Slowly lower the stage manually
' (using jog stage controls) and position the substrate
' under the stamp so that the pedestal is in line with the
' material features. Then run program. NOTE: the digital
' scope must be open and connected to the controller for
' this to work.

      ' The HEADER is to allow the AeroBasicInclude file to be
      ' included in the code. This has various commands and
      ' variables that are used by the SCOPEDATA function uses.
      ' It does not work without it, do not remove.
      HEADER

            INCLUDE "AeroBasicInclude.abi"

      END HEADER



      PROGRAM

            ' VARIABLE DEFINITIONS

                  ' Defining different variables within the code.
                  ' This should not need to be changed.
                        DIM RetractionDistance AS DOUBLE
                        DIM RetractionSpeed AS DOUBLE
                        DIM LoadCellOutput AS DOUBLE



Setting LoadCellOutput Variable
```

```
Setting the baseline reading for the StageCurrent value. The scope triggers
and collects a small set of data which is then used to update the
StageCurrent value. Without this, the StageCurrent value would be the last
used value (usually the cut off current).

Setting the number of data points that are collected.
      SCOPEBUFFER 1
      SCOPETRIGPERIOD 1
Triggering the scope to collect data.
      SCOPETRIG

Pauses the code for a given time in seconds. This gives the software time
to collect the data points from the scope.
      DWELL 0.2

Cancels the scope data collection.
      SCOPETRIG STOP

Pauses the code to give the digital scope time to process the data.
      DWELL 2

Defines the variable LoadCellOutput using the SCOPEDATA function.
<return> = SCOPEDATA (<DataType>, <DataIndex>)
DataIndex refers to the data point that is returned.
      LoadCellOutput = SCOPEDATA (AnalogInput0, 1)



Defining RetractionDistance and Retraction Speed


Setting the distance (mm) that the stage will retract once the approach has
been completed and the stamp has been compressed.

      RetractionDistance = -0.2


Setting the speed at which the stage will retract (mm/s).

      RetractionSpeed = 0.7


ACCELERATION PROFILE SETUP


Set the curve factor.
This value ranges anywhere from 0 to 100. Any value outside this range is a
runtime error. If the S-curve is zero, the ramp up and ramp down is linear.
If the value is 100, the ramp up and ramp down is parabolic. Any value
between these values is the percentage of the ramp up and ramp down that is
parabolic.
      SCURVE 0

Declares that the acceleration desired will be set by the user.
      RAMP MODE RATE
```

```
Setting acceleration (mm/s^2) (1000 mm/s^2 = 1 m/s^2)
      RAMP RATE 3000



LOWERING THE STAGE


ENABLING THE X AXIS. This must be done to activate the stage.
      ENABLE X

Creating a WHILE loop stating that while the load cell reading is less than
a given value (in volts (which is equivalent to grams with the GSO-10 load
cell) the stage is to lower by 0.01 mm at 0.1 mm/s.

      WHILE LoadCellOutput < 0.56

Triggers the digital scope to start collecting data.
      SCOPETRIG

Commands the stage to move down at 0.01 mm at a speed of 0.1 mm/s.
LINEAR <Axis> <Distance> F <CoordinateSpeed)
      Linear X 0.001 F 0.1

Cancels the digital scope data collection.
      SCOPETRIG STOP

Updates the value of the LoadCellOutput variable which will be used in the
next iteration of the WHILE loop.
      LoadCellOutput = SCOPEDATA (AnalogInput0, 1)

Ends the WHILE loop
      WEND



RELAXATION PERIOD

Relaxation Part 1
Relaxation time for PDMS stamp. 5 seconds standard.
                              DWELL 5



RETRACTION


Scope Setup
      SCOPEBUFFER 32000
Setting the data collection rate. This is separate from the previous data
collections as this will provide the data needed to analyse what has
happened during pick up or placement. Be aware that at higher sample rates
(-20 max) the collection period will be shorter.
      SCOPETRIGPERIOD -2
```

```
Scope Trigger

Scope trigger for data collection.
      SCOPETRIG


Relaxation Part 2

This is a second short relaxation time. This line of code will happen
immediately after the previous relaxation dwell.

      DWELL 0.1


Retracting the Stage

Retract stage the distance defined in RetractionDistance at the speed
defined by RetractionSpeed.
LINEAR <Axis> <Distance> F <CoordinateSpeed>
      LINEAR X RetractionDistance F RetractionSpeed

      DWELL 0.1
Cancelling Data Collection
Cancels the digital scope data collection.
      SCOPETRIG STOP



      END PROGRAM
```